Enfermedades fúngicas de la madera de la vid en materiales de vivero y viñedos de Uruguay

TESIS DOCTORAL

Programa de Desarrollo de las Ciencias Básicas

Ciencias Biológicas, Opción Microbiología

UdelaR

Por

María Julia Carbone Marichal

Directora: Dra. Ing. Agr. Sandra Alaniz

Co-director: Dr. Ing. Agr. Pedro Mondino

Montevideo

2023

Esta tesis se presenta bajo el formato de compilación de artículos. El documento incluye una introducción general, la presentación de cuatro artículos científicos, una discusión general y, por último, las conclusiones.

Los artículos científicos compilados son los siguientes:

Artículo 1- Grapevine nursery propagation material as source of fungal trunk disease pathogens in Uruguay. (2022) Publicado en: *Frontiers in Fungal Biology*, 3:958466. https://doi.org/10.3389/ffunb.2022.958466

Artículo 2- Black foot in nursery grapevines in Uruguay caused by *Dactylonectria* and *Ilyonectria*. (2023) Publicado en: *Phytopathologia Mediterranea*, 62(2):199-211. https://doi.org/10.36253/phyto-14498

Artículo 3- Drought influences fungal community dynamics in the grapevine rhizosphere and root microbiome. (2021) Publicado en: *Journal of Fungi*, 7:686 https://doi.org/10.3390/jof7090686

Artículo 4- Four *Diaporthe* species associated with grapevine wood in nursery plants and commercial vineyards in Uruguay. (2023) A enviar a: Plant Pathology.

AGRADECIMIENTOS

Este documento de tesis es el resultado de seis años de trabajo como estudiante de posgrado. El trabajo ha sido en equipo y he tenido la fortuna de estar muy bien acompañada.

Es a mis tutores, Sandra Alaniz y Pedro Mondino, a quienes agradezco en primer lugar. A Sandra por su compromiso y dedicación para con este trabajo, así como por su valiosa orientación y disposición constante a ayudarme a resolver y corregir lo que fuera que se haya presentado en el camino. A Pedro por su valiosa crítica constructiva durante todo el proceso y absoluta disposición a colaborar cada vez que lo necesité. Agradezco especialmente a ambos por siempre dejarme las puertas abiertas.

En segundo lugar, expreso mi agradecimiento a los compañeros del Laboratorio de Fitopatología, quienes me han acompañado en este camino de formación. En especial a Victoria Moreira, quien ha sido mi par desde el primer día de tesis, y a Matías Gelabert y Rossana Reyna, por su valiosa colaboración en los experimentos.

Expreso también mi agradecimiento a David Gramaje y su equipo de BioVitis, quienes me recibieron en su laboratorio en España y dedicaron su valioso tiempo a brindarme su conocimiento y experiencia, y, sobre todo, por su generosidad.

Por último, agradezco a mis padres por alentarme a este camino y sostenerme incondicionalmente. A ellos les dedico mis logros.

TABLA DE CONTENIDOS

RESUMEN

Las enfermedades de madera (EM) de la vid constituyen un complejo de enfermedades causadas por múltiples patógenos fúngicos, que infectan y colonizan los tejidos leñosos desde temprana edad ocasionando pérdidas de rendimiento, decaimiento de plantas y menor longevidad de los viñedos. Prospecciones realizadas en la década del 2000 en Uruguay permitieron constatar la presencia de alguna de estas EM en los viñedos comerciales de diferentes regiones vitícolas, no obstante, no se disponía de mucha información acerca del estado sanitario de las plantas de vivero producidas en el país. En este contexto surge este trabajo con el fin de ampliar los conocimientos sobre la incidencia, etiología y biología de las EM en plantas de vivero y viñedos comerciales de Uruguay. Se constató que las plantas de vid producidas en el país presentan altos niveles de incidencia de EM. Las enfermedades encontradas fueron Enfermedad de Petri, Pie Negro, Decaimiento por Botryosphaeria y Decaimiento por Diaporthe, causadas por más de 20 patógenos diferentes. Asimismo, se demostró que durante el proceso de propagación ocurren infecciones, siendo las etapas de injertación y encallado, y el enraizamiento en el suelo del vivero los momentos en los cuales suceden la mayoría. Particularmente la fase de enraizamiento es cuando ocurren infecciones por los patógenos causantes de Pie Negro, una de las principales enfermedades encontradas afectando plantas terminadas. Se definieron con precisión los agentes causales de esta enfermedad. *Dactylonectria macrodidyma* fue encontrada como especie prevalente, seguida por *D. novozelandica*, *D. torresensis*, *D. palmicola* e *Ilyonectria liriodendri*, mientras que un grupo de aislados del género *Ilyonectria* no se agrupó con ninguna especie conocida. Los hongos causantes de Pie Negro son patógenos que habitan en el suelo y su desarrollo y/o supervivencia puede verse afectada por el contenido hídrico del mismo. Mediante estudios de la composición del microbioma asociado a las raíces y rizósfera de la vid bajo diferentes escenarios de riego, se constató que los patógenos de Pie Negro son favorecidos por condiciones de buena irrigación, mientras que condiciones de déficit hídrico severo resultan desfavorables para ellos. Por otra parte, en base al hallazgo de patógenos causantes de Decaimiento por Diaporthe en los materiales de propagación, se realizó una prospección exhaustiva para dilucidar si la enfermedad también estaba presente en los viñedos comerciales. Se constató la presencia de esta enfermedad afectando vides adultas, aunque su incidencia en los viñedos fue baja. *Diaporthe ampelina* fue encontrada como especie prevalente dentro del grupo, mientras que las otras especies identificadas fueron

D. foeniculina, *D. eres* y *D. terebinthifolii*. Los resultados obtenidos sugieren la necesidad de diseñar en el corto plazo medidas de manejo que permitan disminuir la incidencia de las EM en las plantas de vivero, ya que éstas comprometen, desde el inicio, la productividad y longevidad del viñedo. La utilización de materiales de vivero con bajos niveles de incidencia y la implementación de medidas para prevenir nuevas infecciones en el viñedo, así como de prácticas de manejo que fomenten su crecimiento y desarrollo equilibrado, probablemente sean las claves para que la producción de uva siga siendo una actividad sostenible en el país.

INTRODUCCIÓN GENERAL

El cultivo de la vid

La vid (*Vitis vinifera* L.), cuyo centro de origen se sitúa entre el Mar Negro y el Mar Caspio en Asia Menor, fue introducida en Uruguay a mediados del siglo XVII de la mano de colonizadores españoles. Más adelante, a mediados del silgo XIX con la llegada de inmigrantes principalmente italianos, la viticultura comenzó a experimentar un gran impulso en el país. Los primeros dos viñedos establecidos, en los cuales se ensayó con éxito la adaptabilidad de diferentes cepas europeas a las condiciones locales, datan de mediados de la década del 1870. Desde entonces el sector experimentó un fuerte dinamismo hasta alcanzar las casi 3000 hectáreas cultivadas a principios de la década de 1890, cuando el insecto plaga "filoxera" afectó las plantaciones nacionales (Baptista y Berreta, 2005). La adopción de la técnica del injerto de la vid europea (*V. vinifera*) sobre portainjertos de vides americanas resistentes a este insecto (*V. rupestris*, *V. riparia* y *V. berlandieri*) permitió subsanar este suceso.

Superada la crisis de la filoxera, el sector vitícola uruguayo transitó una nueva fase de fuerte reconversión y crecimiento desde comienzos del siglo XX (Baptista y Berreta, 2005). Actualmente, la superficie vitícola nacional ocupa 5848 hectáreas, distribuidas en 1129 viñedos, lo cual posiciona a este rubro como uno de los principales cultivos frutícolas del país. La producción total en el año 2022 fue de 106.000 toneladas de uva, las cuales fueron mayoritariamente destinadas a la elaboración de vino (96%) (INAVI, 2022; MGAP, 2023). En cuanto a la extensión de los viñedos, el 71% del área se distribuye entre viñedos de menos de cinco hectáreas de superficie, lo que demuestra el fuerte componente de producción familiar que tiene esta actividad agropecuaria en el país. Además, la viticultura uruguaya se caracteriza por ser altamente tecnificada e intensiva en el uso de recursos y mano de obra.

La distribución geográfica de los viñedos muestra una fuerte concentración en la región centro-sur del país, en los departamentos de Canelones (66% de la superficie total de viñedos) y Montevideo (12%), como ha sido tradicionalmente desde los comienzos de la viticultura en el país. En la región suroeste, los departamentos de Colonia y San José aportan el 10% de la superficie vitícola nacional, mientras que, en el este, en el departamento de Maldonado es donde ha ocurrido un destacado crecimiento del sector en los últimos años, aportando el 7% de la superficie total de viñedos. En cuanto a las

variedades cultivadas, Tannat se destaca con el 27% de la superficie total de viñedos, seguida de Moscatel de Hamburgo (18%), Merlot (11%), Ugni Blanc (10%), Cabernet Sauvignon (6%) y otras variedades con menor escala de producción. Con relación a los portainjertos, el más utilizado es el SO4 (63% de la superficie total de viñedos), seguido de 3309 (12%), P 1103 (8%), R 110 (5%) y Gravesac (4%) (INAVI, 2022). Respecto al origen de las plantas, el 65% de la superficie está cultivada con plantas importadas mayoritariamente desde Europa, el 18% con plantas de origen nacional, y el 17% restante con plantas producidas localmente a partir de materiales de origen importado (INAVI, 2022).

Enfermedades fúngicas de la madera de la vid

El cultivo de la vid es susceptible a numerosas enfermedades, entre las cuales se encuentran aquellas que afectan tejidos verdes (flores, hojas, pámpanos), otras que ocasionan podredumbre de racimos y otras que afectan las partes leñosas. Estas últimas constituyen un complejo de enfermedades de madera (EM) causadas por múltiples patógenos fúngicos, que en las últimas décadas se han convertido en una de las principales limitantes sanitarias del cultivo en todas las regiones vitícolas del mundo (Martín y Cobos, 2007; Bruez et al., 2013; Úrbez-Torres et al., 2014, Gramaje et al., 2018). Los patógenos causantes de estas enfermedades infectan y colonizan los tejidos leñosos generando necrosis vasculares y/o sectoriales en el tronco principal, ramas secundarias y/o raíces. Las vides afectadas manifiestan vigor reducido, menor desarrollo foliar, acortamiento de entrenudos, hojas cloróticas con margen necrótico, brotación retardada, decaimiento, menor productividad, muerte de ramas y eventualmente muerte de toda la planta (Bertsch et al., 2013; Gramaje et al., 2018).

Las primeras referencias y descripciones sobre EM afectando la vid datan de épocas medievales e incluso anteriores. Sin embargo, las investigaciones y reportes formales sobre la etiología de estas enfermedades comenzaron a finales del siglo XIX y principio del siglo XX, en Francia y Estados Unidos (Mugnai et al., 1999; Úrbez-Torres et al., 2013). Históricamente las EM se asociaban mayoritariamente a plantaciones adultas y presentaban bajos niveles de incidencia. Sin embargo, en la década del 1990 comenzó a registrarse un sostenido incremento en la incidencia de estas enfermedades, tanto en viñedos adultos como en viñedos jóvenes (Mugnai et al., 1999; Gramaje et al., 2018). Dicho incremento coincidió con la expansión de la industria vitivinícola a nivel mundial, durante la cual ocurrió un importante intercambio de materiales de propagación entre

países y continentes (Gramaje et al., 2018). Además, se sucedieron cambios en el sistema de manejo del cultivo, como el incremento de las densidades de plantación y de las intervenciones de poda y conducción, dando lugar a mayor número de heridas, las cuales constituyen la principal vía de entradas para estos patógenos (Mondello et al., 2018). Otro hecho relevante que contribuyó al incremento de la incidencia de las EM fue la prohibición del uso de arsenito de sodio, benzimidazoles y bromuro de metilo en algunos países a principios de los 2000, los cuales eran hasta entonces los productos químicos más efectivos disponibles contra las EM (Gramaje et al., 2018).

El impacto de esta problemática es preocupante en varios países. A modo de ejemplo, en Italia se estima que la incidencia de EM en viñedos adultos de entre 15 y 18 años alcanza valores desde 8 a 19% dependiendo del cultivar (Mondello et al., 2018). En Canadá, en la provincia de Columbia Británica, se observó que el 90% de los viñedos presentaban algún síntoma de EM, y en algunos de ellos la incidencia alcanzaba el 54% del cultivo (Úrbez-Torres et al., 2014). En España se estima un 10% de incidencia en los viñedos, mientras que en Francia aproximadamente el 13% de los viñedos se encuentran improductivos por causa de estas enfermedades (De la Fuente et al., 2016). Actualmente y debido a la creciente incidencia de estas enfermedades, la longevidad de los viñedos está muy comprometida, al punto de que, en España, por ejemplo, preocupa que algunos viñedos no superen los 5 años de vida (Armengol, 2017).

Las EM se pueden clasificar según su preferencia en cuanto a la edad de la planta que suelen afectar. Aquellas que se asocian principalmente a plantaciones jóvenes (de menos de 5 años) son la Enfermedad de Petri y el Pie Negro. La Enfermedad de Petri es ocasionada por los ascomicetes *Phaeomoniella chlamydospora*, *Cadophora* spp. (principalmente *C. luteo-olivacea*) y numerosas especies pertenecientes al género *Phaeoacremonium* (Mostert et al., 2006; Halleen et al., 2007). El Pie Negro es causado por una gran diversidad de hongos conocidos como "tipo *Cylindrocarpon*" (Agustí-Brisach y Armengol, 2013), quienes recientemente han sido sometidos a una profunda revisión taxonómica (Chaverri et al., 2011; Cabral et al., 2012a, 2012b; Lombard et al., 2014). Hoy en día se conocen más de 30 especies pertenecientes a los géneros *Campylocarpon*, *Cylindrocladiella*, *Dactylonectria*, *Ilyonectria*, *Neonectria*, *Pleiocarpon* y *Thelonectria* asociadas al Pie Negro (Agustí-Brisach y Armengol, 2013; Lombard et al., 2014; Carlucci et al., 2017; Aigoun-Mouhous et al., 2019). Las enfermedades Decaimiento por Botryosphaeria, ocasionada por numerosas especies pertenecientes a la

familia Botryosphaeriaceae, y Decaimiento por Diaporthe, causada por especies del género *Diaporthe* (syn. *Phomopsis*), han sido encontradas con mayor frecuencia en vides adultas (más de 5 años), aunque también se han encontrado en plantas jóvenes (Giménez-Jaime et al., 2006; Úrbez-Torres et al., 2006; Martin y Cobos, 2007; Moreno-Sanz et al., 2013; Whitelaw-Weckert et al., 2013; Larignon et al., 2015; Carlucci et al., 2017). Por último, la Esca, ocasionada por diversos basidiomicetes y por los ascomicetes *Ph. chlamydospora* y *Phaeoacremonium* spp. (Mugnai et al., 1999), y la Eutipiosis, ocasionada por especies pertenecientes a la familia Diatrypaceae (Luque et al., 2012), se asocian exclusivamente a plantas adultas.

Numerosas investigaciones han confirmado que las EM también afectan a las plantas de vivero y que, por lo tanto, el material de propagación constituye una de las principales vías para su diseminación (Gramaje y Armengol, 2011). El proceso de producción de plantas de vid es un proceso muy conservado mundialmente, aunque puede presentar variantes en determinados países o regiones de acuerdo con la cultura y tradición local. En términos generales, durante el invierno, época de poda de la vid, se colecta el material vegetal madre de portainjertos y variedades a propagar y se almacena en cámara de frío. A inicios de la primavera los materiales madre se retiran gradualmente de la cámara de frío y se hidratan en agua durante 24 a 48 horas para seguidamente realizar la injertación. La etapa de injertación implica en primer lugar acondicionar los materiales de portainjerto y variedad, es decir, cortar las estacas de portainjerto del tamaño requerido y quitarle las yemas, y preparar las yemas de las variedades a injertar.

Una vez acondicionado el material, el injerto se realiza mediante el sistema omega (tipo de injerto de mesa) y la zona del injerto se cubre con cera derretida. Inmediatamente los materiales injertados pasan a la etapa de forzadura y encallado. Para esto, la base de los portainjertos se coloca en agua o en turba humedecida y se mantienen a una temperatura de 28-30°C con alta humedad relativa en el ambiente durante 10 a 15 días hasta que se forme el callo en la zona del injerto y se induzca el enraizamiento. La etapa siguiente es la de aclimatación en lugares semiabiertos durante una o dos semanas, hasta su traslado al suelo del vivero donde completarán el desarrollo de raíces y la brotación de la variedad. Allí permanecen durante toda la estación de crecimiento de la vid hasta el invierno siguiente, cuando son arrancadas y acondicionadas para ser comercializadas en estado durmiente (Gramaje y Armengol, 2011).

Numerosos trabajos han constatado que las infecciones por estos patógenos pueden ocurrir en varias etapas del proceso de producción, lo que da lugar a altos niveles de incidencia de EM en las plantas terminadas (Halleen et al., 2003, 2006; Aroca et al., 2006; Giménez-Jaime et al., 2006; Rego et al., 2009; Spagnolo et al., 2011; Agustí-Brisach et al., 2013a; Carlucci et al., 2017; Pintos et al., 2018; Guarnaccia et al., 2018; Berlanas et al., 2020; Maldonado-González et al., 2020). Por otra parte, existen determinadas etapas del proceso de vivero que son especialmente propicias para que ocurran las infecciones por algunos de estos patógenos. Por ejemplo, la etapa de enraizamiento en el suelo de los viveros ha sido señalada como una etapa clave en la que ocurren infecciones de Pie Negro (Halleen et al., 2003; Agustí-Brisach et al., 2013a).

Particularmente el Pie Negro es una de las principales enfermedades responsables del decaimiento en plantas jóvenes y ocurre en prácticamente todos los países productores de uva (Gramaje y Armengol, 2011). Las plantas afectadas por esta enfermedad presentan menor desarrollo radicular, lesiones necróticas en las raíces, estrías necróticas que se desarrollan desde la base de la planta y necrosis en la base del portainjerto. Los síntomas foliares suelen presentarse durante los primeros 3 a 5 años luego de la plantación, y en general implican pérdida de vigor, decaimiento y muerte de la planta (Halleen et al., 2006; Agustí-Brisach y Armengol, 2013). Si bien la epidemiología de esta enfermedad no ha sido del todo esclarecida, es sabido que estos patógenos forman parte de la microbiota del suelo, en donde producen abundantes conidios que se dispersan con ayuda del agua libre (Petit et al., 2011). Además, algunas especies son capaces de producir clamidosporas que les permiten sobrevivir por largos períodos de tiempo en el suelo (Halleen et al., 2004), así como también son capaces de infectar malezas las cuales pueden actuar como fuente de inóculo para las infecciones a la vid (Agustí-Brisach et al., 2011).

Suelos de textura pesada, alto contenido de humedad y malas condiciones de drenaje se señalan como favorables para los patógenos causantes de Pie Negro (Halleen et al., 2006). Es esperable que alteraciones en el contenido de humedad en el suelo afecten a las poblaciones de estos patógenos, así como también al resto de la microbiota presente. De hecho, la sequía, cuya frecuencia e intensidad se espera que aumente en algunas regiones debido al cambio climático (Santillán et al., 2019), influye sobre la estructura de las comunidades microbianas del suelo (Barnard et al., 2013; Bouskill et al., 2013), aunque su efecto sobre las comunidades fúngicas asociadas a las raíces de las plantas ha sido poco explorado (Bouasria et al., 2012; Barnard et al., 2013; Naylor et al., 2017, 2018;

Fuchslueger et al., 2016). Las plantas se relacionan estrechamente con los microorganismos que habitan el continuo suelo-rizosfera-raíz (Santos-Medellín et al., 2017; Trivedi et al., 2020). Algunos de estos microorganismos proveen beneficios a la planta contribuyendo con la movilización y transporte de nutrientes, protección contra patógenos y plagas, y reducción del estrés (Trivedi et al., 2020). Particularmente en la vid se han estudiado las respuestas fisiológicas de la planta frente al estrés hídrico (Lovisolo et al., 2010), sin embargo, la información disponible sobre cómo influye el estrés hídrico en la comunidad fúngica asociada a las raíces y suelo circundante, en donde habitan los patógenos del Pie Negro, aún es escaza.

Situación de las enfermedades fúngicas de la madera de la vid en Uruguay

La preocupación del sector vitícola uruguayo por las EM comenzó en la década del 2000. Prospecciones realizadas en viñedos jóvenes y adultos en esa época permitieron constatar la presencia de Decaimiento por Botryosphaeria, Eutipiosis, Esca, Enfermedad de Petri y Pie Negro afectando las plantaciones nacionales (Abreo, 2011; Abreo et al., 2010, 2011, 2013a). Los patógenos encontrados fueron *Botryosphaeria dothidea*, *Diplodia seriata*, *Neofusicoccum luteum*, *N. australe*, *N. kwambonambiense*, *N. parvum* y *Lasiodiplodia theobromae* asociados al Decaimiento por Botryosphaeria (Abreo et al. 2013a), *Eutypella vitis* como causante de la Eutipiosis (Abreo, 2011), *Ph. chlamydospora*, *Pm. aleophilum*, *Pm. australiense, Cadophora luteo-olivacea* y *C. melinni* asociadas a la Enfermedad de Petri, y junto con *Inocutis jamaicensis* a la Esca (Abreo, 2011; Abreo et al., 2011), y *Ca. pseudofasciculare*, *Cylindrocarpon destructans* var. *crassum*, *C. liriodendri*, *C. macrodidyma*, *C. olidum* var. *crassum* como causantes del Pie Negro (Abreo et al., 2010). Además, en dichas prospecciones también se aisló a *D. ampelina* (syn. *Phomopsis viticola*) de plantas adultas con síntomas, aunque su participación en el desarrollo de los síntomas de cancro y necrosis sectoriales fue descartada (Abreo, 2011). Asimismo, se realizaron algunas prospecciones puntuales en plantas madre y en plantas de vivero y se constató la presencia de *Ph. chlamydospora*, *Pm. aleophilum, C. luteo-olivacea*, *C. liriodendri*, *C. macrodidyma*, especies de la familia Botryosphaeriaceae y *Diaporthe* spp. en el interior de la madera (Abreo et al., 2011; Abreo et al., 2013a, 2013b).

La presencia de estas enfermedades en viñedos jóvenes es un indicio de que al menos una parte de esas plantas enfermas pueden haber sido infectadas en la etapa de vivero. Más aún, el hecho de haberse detectado estos patógenos en plantas madre y plantines sugiere que los materiales de propagación producidos en Uruguay constituyen

una vía de diseminación de estas enfermedades. No obstante, no existen antecedentes de prospecciones exhaustivas durante el proceso de producción de plantas que permitan confirmar la ocurrencia de EM en materiales en las diferentes etapas del proceso de vivero, conocer los niveles de incidencia, las enfermedades presentes y los patógenos involucrados.

Por otra parte, si bien el hallazgo de *D. ampelina* en plantas adultas fue irrelevante en las prospecciones llevadas a cabo por Abreo (2011), actualmente se conoce que esta es una de las especies más virulenta causante del Decaimiento por Diaporthe en varias regiones vitícolas del mundo (Kaliterna et al., 2012; Baumgartner et al., 2013; Úrbez-Torres et al., 2013; Lawrence et al., 2015; Lesuthu et al., 2019). Si bien existen antecedentes de esta enfermedad desde principios del siglo XX, su inclusión dentro del complejo de EM fue propuesto recientemente luego de que en diversas prospecciones realizadas en Estados Unidos y Canadá se encontrara una alta incidencia de especies del género *Diaporthe* asociadas a los síntomas de cancros de la madera, falta de brotación y muerte de plantas (Úrbez-Torres et al., 2013).

Este trabajo de tesis doctoral se propuso con el objetivo de ampliar los conocimientos sobre la incidencia, etiología y biología de las EM en materiales de vivero y viñedos de Uruguay. Por un lado, se planteó determinar la incidencia y etiología de las EM presentes en materiales de propagación durante las diferentes etapas del proceso de vivero, con el fin de generar información que permita diseñar en el futuro medidas de manejo que mejoren la calidad sanitaria de las plantas de vid producidas en el país. Por otra parte, y en el entendido de que la identificación precisa de los patógenos es crucial para llevar a cabo estudios sobre la epidemiología y para el desarrollo e implementación de medidas de manejo efectivas, y considerando que es una de las enfermedades más importantes que afecta a las plantas jóvenes, se propuso caracterizar la población de patógenos causantes de Pie Negro asociada a las plantas de vivero. Asimismo, se propuso evaluar el efecto de diferentes condiciones de estrés hídrico sobre la comunidad fúngica asociada a las raíces de la vid, en particular sobre los patógenos de Pie Negro. Por último, y dado que no disponemos de información precisa sobre la presencia, incidencia y etiología de la enfermedad Decaimiento por Diaporthe en el país, se propuso determinar con mayor detalle el rol de *Diaporthe* spp. como causante de EM en las plantas de vivero y en vides adultas.

HIPÓTESIS

1. Las plantas de vid producidas en viveros nacionales están afectadas por enfermedades fúngicas de la madera.
2. Las infecciones de los patógenos causantes de las enfermedades de madera ocurren durante las diferentes etapas del proceso de producción de plantas en el vivero.
3. El Pie Negro es una de las enfermedades de mayor incidencia que afecta a las plantas de vivero producidas en Uruguay y es causada por diversas especies de hongos conocidos como “tipo *Cylindrocarpon*”.
4. Condiciones de estrés hídrico provocan alteraciones en la composición y estructura de la comunidad fúngica asociada a las raíces, rizosfera y suelo circundante de la vid, y afectan a los patógenos causantes de Pie Negro.
5. La enfermedad Decaimiento por Diaporthe se encuentra presente en Uruguay afectando plantas de vivero y vides adultas.

OBJETIVOS

Objetivo general

Ampliar los conocimientos sobre la incidencia, etiología y biología de las enfermedades fúngicas de la madera de la vid que afectan materiales de vivero y viñedos adultos de Uruguay.

Objetivos específicos

1. Determinar la incidencia y etiología de las enfermedades fúngicas de la madera de la vid en materiales de vivero en las diferentes etapas del proceso de producción, desde planta madre a planta terminada.
2. Caracterizar las especies causantes de Pie Negro asociadas a plantas de vivero producidas en Uruguay, mediante estudios morfológicos, análisis filogenéticos y evaluación de su patogenicidad.
3. Conocer el efecto de diferentes condiciones de estrés hídrico sobre la comunidad fúngica asociada a la raíz, rizosfera y suelo circundante de la vid, con especial atención a lo que ocurre con los patógenos causantes de Pie Negro.
4. Evaluar la presencia de la enfermedad Decaimiento por Diaporthe en plantas de vivero y viñedos adultos de Uruguay, y determinar su etiología en base a la caracterización de las especies mediante estudios morfológicos, filogenéticos y de patogenicidad.

ARTÍCULO 1

Grapevine nursery propagation material as source of fungal trunk disease pathogens in Uruguay

MARÍA JULIA CARBONE, MATÍAS GELABERT, VICTORIA MOREIRA, PEDRO MONDINO, SANDRA ALANIZ

Departamento de Protección Vegetal, Facultad de Agronomía, Universidad de la República

Publicado en: *Frontiers in Fungal Biology* (2022) 3:958466.
https://doi.org/10.3389/ffunb.2022.958466

Grapevine nursery propagation material as source of fungal trunk disease pathogens in Uruguay

ABSTRACT

Grapevine fungal trunk diseases (GTDs) have become a serious problem for grapevines worldwide. Nursery vines infected during the propagation process are considered one of the main ways of dissemination of GTD pathogens. In this study, we examined the status of GTDs in grapevine planting material, from rootstocks and scion mother cuttings to grafted rooted vines ready to plant, according to the local nursery propagation process. During 2018-2019, internal symptoms of GTDs were examined in 2400 propagation materials and fungal isolations were carried out from a subsample of 1026 selected materials. Our results revealed that nursery grapevine plants produced in Uruguay have a high incidence of GTDs, regardless of the scion/rootstock combination. Typical brown to black streaks and sectorial wood necrosis were observed in materials on all propagation stages, with a markedly increasing incidence throughout the nursery process, reaching almost 100% in grafted rooted vines ready to plant. Botryosphaeria dieback, Petri disease and black-foot disease were the main GTDs found. The results showed that Botryosphaeria dieback and Petri disease pathogens infect materials from the early stages of the process, with a marked increase towards the end of the plant production process, whereas black-foot disease pathogens were found exclusively in vines ready to plant. Diaporthe dieback pathogens were also detected in materials in all stages but in a low proportion (less than 10% of infected material). Based on single locus analysis, the 180 isolates selected were placed into eight genera and 89% identified within 22 fungal species associated with GTDs, with *Phaeoacremonium oleae* and *Diaporthe terebinthifolii* as new records on grapevine worldwide. Our results have concluded that locally produced vines are one of the main ways of dissemination of GTD pathogens and showed that a nursery sanitation programme is required to reduce the incidence of these diseases.

Keywords: *Vitis vinifera*, propagation material, black-foot disease, Petri disease, Botryosphaeria dieback, Diaporthe dieback

1. INTRODUCTION

Grapevine fungal trunk diseases (GTDs) have become a serious problem for grapevine growers around the world (Martín and Cobos, 2007; Romanazzi et al., 2009; Bruez et al., 2013; Yan et al., 2013; Ridgway et al., 2014; Úrbez-Torres et al., 2014). The significant increment of decline symptoms in grapevines during the last decades causes loss of productivity and reduction in longevity, especially in young vineyards (Gramaje and Armengol, 2011). This situation makes growers replant vast areas, resulting in important economic losses in viticulture worldwide (Gramaje et al., 2018). External decline symptoms on young vineyards include reduced vigour, retarded or absent sprouting, shortened internodes, reduced foliage, chlorotic foliage with necrotic margins, reduced leaf size, failure of the graft unions, wilting and often leading to death of affected plants (Scheck et al., 1998a; Rego et al., 2000; Fourie and Halleen, 2001).

Petri disease (PD), caused mostly by *Phaeomoniella chlamydospora*, *Cadophora luteo-olivacea* and numerous species of *Phaeoacremonium* (Scheck et al., 1998b; Mugnai et al., 1999; Crous and Gams, 2000; Mostert et al., 2006a; Halleen et al., 2007; Gramaje et al., 2011; Navarrete et al., 2011), and black-foot disease (BFD), caused by species of *Cylindrocarpon*-like asexual morphs, *Campylocarpon* and *Cylindrocladiella* genera (Mohammadi et al., 2009; Agustí-Brisach and Armengol, 2013; Lombard et al., 2014; Carlucci et al., 2017) are the main GTDs associated with young decline symptoms (Rego et al., 2000; Gramaje and Armengol, 2011; Carlucci et al., 2017; Gramaje et al., 2018).

In addition, Botryosphaeria dieback (BD) caused by species belonging to *Botryosphaeriaceae*, as well as, though less frequently, Diaporthe dieback (DD) caused by species of *Diaporthe*, have been isolated from young vines showing decline symptoms (Giménez-Jaime et al., 2006; Úrbez-Torres et al., 2006; Martin and Cobos, 2007; Moreno-Sanz et al., 2013; Whitelaw-Weckert et al., 2013; Larignon et al., 2015; Carlucci et al., 2017).

External symptoms do not allow an easy distinction among GTDs because they can overlap (Gramaje et al., 2018; Mondello et al., 2018). However, internally, vines affected by PD show black discoloration of the xylem vessels because of the accumulation of phenolic compounds. These discolorations are seen as dark brown to black spots and dark streaks, in cross and longitudinal section, respectively (Mugnai et al., 1999; Mostert et al., 2006a). Vines affected by BFD present brown to dark streaks that develop from the

base of the rootstock, wood necrosis at the base of the trunk, sunken necrotic root lesions and reduced root biomass (Rego et al., 2000; Halleen et al., 2006; Alaniz et al., 2007). Internal symptoms of Botryosphaeria dieback include typical trunk cankers or sectorial wood necrosis as well as vascular streaking (Larignon and Dubos, 2001; Phillips, 2002; van Niekerk et al., 2004), symptoms which are also observed in DD infected vines (Úrbez-Torres et al., 2013; Guarnaccia et al., 2018).

Many studies have highlighted the role of infected propagation material as a major source of spread of GTD pathogens (Gramaje and Armengol, 2011). Several researchers have concluded that a high percentage of the plants ready to plant are infected by PD, BFD, BD and DD fungal pathogens, acting alone or simultaneously, even when plants are externally apparently healthy (Halleen et al., 2003; Aroca et al., 2006; Halleen et al., 2006; Giménez-Jaime et al., 2006; Rego et al., 2009; Spagnolo et al., 2011; Agustí-Brisach et al., 2013a; Carlucci et al., 2017; Pintos et al., 2018; Guarnaccia et al., 2018; Berlanas et al., 2020; Maldonado-González et al., 2020).

Traditional grapevine propagation techniques were analysed and described by Gramaje and Armengol (2011). Briefly, dormant cuttings are taken from rootstock and scion mother vines for bench grafting, rooting or field budding. The propagation process includes cold storage, hydration, disbudding, grafting, callusing, and rooting of grafted plants in the nursery field (Gramaje and Armengol, 2011). Most of these steps have been identified as an opportunity for GTD pathogens to cause new infections. Firstly, several authors have reported that rootstocks and scion mother used to propagate vines are infected by PD, BFD, BD and DD pathogens with varying incidence, and constitute a primary inoculum source for GTD pathogens (Rego et al., 2001; Fourie and Halleen, 2002, 2004; Edwards and Pascoe, 2004; Retief et al., 2006; Whiteman et al., 2007; Zanzotto et al., 2007; Aroca et al., 2010; Serra et al., 2011; Billones-Baaijens et al., 2013). Additionally, GTD pathogens have been detected in water of hydration tanks, washings of scissors used in the grafting process, washings of grafting machines, and in the peat used for the callusing stage (Retief et al., 2006; Aroca et al., 2010; Gramaje et al., 2011; Agustí-Brisach et al., 2013a). Finally, the nursery soil where the rooting phase of the grafted plants occurs, constitutes the main inoculum source of BFD pathogens, which are known to be soil-borne pathogens (Rego et al., 2001; Halleen et al., 2006; Agustí-Brisach et al., 2013b, 2014; Berlanas et al., 2017). Furthermore, the soil is also a reservoir for PD pathogens (Retief et al., 2006; Agustí-Brisach et al., 2013b).

In Uruguay, BFD and PD pathogens have been reported to cause decline symptoms in young vines (Abreo et al., 2010, 2011). Also, the analysis of asymptomatic canes of rootstocks and scions mother plants detected the presence of *Ph. chlamydospora* and *Phaeoacremonium* spp., as well as *Botryosphaeriaceae* pathogens (Abreo et al., 2011, 2013). However, to the best of our knowledge, the occurrence of infections of GTD pathogens during the propagation process and the health status of the nursery plants produced in local nurseries has not been extensively explored. Thus, the aim of this study was: 1) to identify the GTDs and associated pathogens affecting nursery grapevine plants produced in Uruguay and quantify their incidence and 2) to find out the steps in which the incidence of GTDs increases during the local nursery propagation process.

2. MATERIAL AND METHODS

2.1 Sampling of grapevine propagation material

During 2018-2019, a total of 2400 grapevine propagation materials were sampled from the main grapevine commercial nursery in Uruguay, located in Las Violetas, Canelones (34°34′48.45″ S and 56°17′50.17″ W). Samples were taken randomly at the following four stages of the standard propagation process in the nursery: (1) rootstock and scion cuttings just after they were collected from mother plants in winter (1.1 m long), (2) rootstock and scion cuttings after storage during 2-3 months at 5-6°C and hydration for 24-48 hours in water before grafting (1.1 m long), (3) grafted plants after callusing stage (the callusing boxes contained water, according to standard practice in the nursery) and (4) dormant rooted grafted plants ready to plant. The rootstocks cuttings derived from nursery-grown mother plants, whereas scion cuttings were collected from commercial vineyards, according to the usual process implemented in the nursery. The rootstock and scion cultivars and rootstock-scion combinations sampled are listed in Table 1.

2.2 Internal disease symptoms

The occurrence of internal symptoms resembling GTDs, such as dark spots or streaks and sectorial wood necrosis, was examined in all samples collected. Propagation materials in stages 1 and 2 were examined as follows: cross-sectional and longitudinal sections were made in the first 0.15 m from the bottom part of the cutting (the portion of the cutting nearest to the mother trunk), and at 0.95-1.10 m, the top of the cutting (the portion of the cutting furthest from the mother trunk). Callused grafted plants and rooted grafted plants, stages 3 and 4 respectively, were analysed performing cross and

longitudinal cuts in the grafted union section including the scion, and at the basal part of the plant (=foot). Additionally, materials in stage 4 were examined in the middle part of the rootstock between the graft union and the foot. The incidence of internal wood symptoms was calculated for each portion of rootstock, scion cultivar and rootstock-scion combination evaluated.

Table 1. Grapevine propagation materials sampled from four stages of the nursery process in 2018 and 2019: scion cultivars, rootstocks, and combination cultivar-rootstocks.

Grapevine propagation materials	2018		2019	
	Grapevine cultivar/Rootstock	Samples collected	Grapevine cultivar/ Rootstock	Samples collected
Stage 1- rootstock and scion cuttings from mother plants				
Rootstock	Gravesac, 1103P, SO4, 101-14, 3309C	250	Gravesac, SO4, 3309C	150
Scion	Albariño, Tannat, Marselan, Merlot, Lácrima-Christi	250	Albariño, Tannat, Marselan	150
Stage 2- rootstock and scion cuttings after cold storage and hydration				
Rootstock	Gravesac, 1103P, SO4, 101-14, 3309C	250	Gravesac, SO4, 3309C	150
Scion	Albariño, Tannat, Marselan, Merlot, Lácrima-Christi	250	Albariño, Tannat, Marselan	150
Stage 3- grafted plants after callusing				
Cultivar/ Rootstock	Albariño/Gravesac, Albariño/101-14, Lácrima Christi/SO4, Tannat/1103P, Moscatel de Hamburgo/SO4	250	Marselan/3309C, Tannat/Gravesac, Albariño/SO4	150
Stage 4- rooted grafted plants				
Cultivar/ Rootstock	Merlot/101-14, Lácrima Christi/1103P, Cabernet Franc/3309C, Tannat/Gravesac, Chardonnay/SO4	250	Albariño/Gravesac, Albariño/101-14, Tannat/1103P	150

2.3 Fungal isolation and morphological identification

A subsample of 1026 materials was selected to perform fungal isolations. To do this, samples with typical internal symptoms of GTDs were picked up, but also asymptomatic samples were selected for isolations. All samples were first surface sterilized by soaking each portion in 95% ethanol for 1 s followed by flaming (Delgado et al., 2016). Then, the bark was removed with a sterile scalpel and seven thin pieces of

wood, 0.5 cm long, of each section were taken from the margin between necrotic and apparently healthy wood tissue and plated onto potato dextrose agar (PDA) (Oxoid Ltd., Hampshire, England) supplemented with 0.4 g L^{-1} of streptomycin sulphate (Sigma-Aldrich, China). From the asymptomatic materials, pieces of wood were taken from each section at random and processed as indicated above. Additionally, root sections were included in the isolations from the basal part of the plants in stage 4.

Plates were incubated for 5 to 21 days at 25°C in darkness and were examined daily to check for fungal growth. Based on phenotypical characteristics such as growth rate, colour, texture and shape of colonies, and microscopic examination of fruiting structures, conidiophores, and conidia (Crous and Gams, 2000; van Niekerk et al., 2004; Mostert et al., 2006b; Chaverri et al. 2011; Agustí-Brisach and Armengol, 2013; Úrbez-Torres et al., 2013), cultures resembling species within GTD causal agents were selected and sub-cultured on PDA and incubated at the same conditions. Subsequently, isolates were sub-cultured by hyphal tipping on PDA to purify the culture (Úrbez-Torres et al., 2006) and then stored in colonized sterile filter papers at -20°C (Peever et al., 1999).

Based on the phenotypical characteristics indicated above, fungal isolates were grouped into four categories according to the GTDs expected to be associated with the grapevine propagation material: *i*) Petri disease (PD); *ii*) black-foot disease (BFD); *iii*) Botryosphaeria dieback (BD) and *iv*) Diaporthe dieback (DD). Petri disease fungi were further divided into *Phaeomoniella chlamydospora*-like isolates and *Phaeoacremonium* spp. isolates. To induce the production of reproductive structures, isolates belonging to *Botryosphaeriaceae* and *Diaporthe* genus were plated onto water agar with sterilized pine needles on the agar surface and onto PDA, respectively, and incubated under near-UV light with a 12-hr photoperiod at 25°C (Úrbez-Torres et al., 2006; Guarnaccia et al., 2018). A representative subsample of each group, attempting to include as much diversity as possible, was selected for subsequent molecular identification.

2.4 Molecular identification

Total DNA was extracted from pure cultures grown on PDA at 25 °C in darkness for 7 to 14 days using the commercial kit Quick-DNA™ Fungal/Bacterial Miniprep Kit (ZymoResearch, USA) following the manufacturer´s instructions. All DNA suspensions were stored at -20 °C for further studies.

Sequences were generated from internal transcribed spacer region and 5.8S rRNA (ITS) with ITS1/ITS4 primers (White et al., 1990) for *Phaeomoniella chlamydospora*-like isolates, beta-tubulin (TUB2) with T1/BT2b primers (O'Donnell and Cigelnik, 1997) for *Phaeoacremonium* isolates, histone 3 (HIS3) with CYLH3F/CYLH3R primers (Crous et al., 2004) for BFD isolates and elongation factor 1-α (TEF) with EF1-728F/EF1-986R primers (Carbone and Kohn, 1999) for *Botryosphaeriaceae* and *Diaporthe* isolates. These loci were proposed to be the most informative for each pathogen group (Tegli et al., 2000; Cabral et al., 2012a; Phillips et al., 2013; Santos et al., 2017; Marin-Felix et al., 2019).

Polymerase chain reaction (PCR) amplifications were performed on a MultiGene™ Mini (Labnet International, Inc., USA). Each PCR reaction contained 1x PCR buffer, 2.5 mM MgCl2, 0.4 mM of each dNTP, 0.4 µM of each primer, 1 U of DNA polymerase (Bioron, Germany) and 1 µL of template DNA. The PCR reaction was adjusted to a final volume of 20 µl with MQ water. The PCR conditions consist of an initial step of 94 °C for 3 min followed by 34 cycles for ITS, TUB2 and TEF regions and 40 cycles for HIS3 gene of denaturation at 94°C for 30 s, annealing at 57°C for ITS and TUB2 and 55°C for HIS3 and TEF for 30 s, and elongation at 72°C for 45 s. A final extension was performed at 72°C for 10 min. PCR products were analysed in 1.5% agarose gels stained with GelRed™ and visualized in a transilluminator under UV light. A GeneRuler 100-bp DNA ladder plus was used as a molecular weight marker (Thermo, Lithuania).

PCR products were purified and sequenced in Macrogen Inc., Seoul, Korea. Preliminary identifications were obtained by comparing the sequences with those deposited in the GenBank using the BLAST source (https://blast.ncbi.nlm.nih.gov/Blast.cgi). The BLAST identifications were confirmed by phylogenetic analysis using Bayesian inference (BI) and Maximum Likelihood (ML) methods. For this, alignments were constructed using ClustalW program, available within MEGA 11.0.11 program (https://www.megasoftware.net/). Alignments were manually edited when necessary. Related sequences as well as sequences of the phylogenetically closest species obtained from the GenBank, including ex-type isolates, were incorporated to the alignments (Supplementary Table 1). BI and ML analyses were inferred with MrBayes v3.2.7a and RAxML v8.2.12 programs, respectively, implemented in CIPRES Science Gateway v3.3 (http://www.phylo.org/). For BI analysis, best-fit models of nucleotide substitution were selected for each genus according to the Akaike information

criterion (AIC), using the jModelTest2 v2.1.6 tool (Darriba et al., 2012) implemented in CIPRES Science Gateway v3.3 (Supplementary Table 2). Four Markov chain Monte Carlo (MCMC) chains were run simultaneously starting from a random tree to 10 million of generations. Trees were sampled every 1000 generations, and the first 2500 were discarded as the burn-in phase of each analysis. Posterior probabilities were determined from a majority-rule consensus tree generated from the remaining 7500 trees. For the ML analysis, generalized time-reversible with gamma correction (GTR + GAMMA) nucleotide substitution model and 1000 bootstrap iterations were indicated. The other parameters were used as default settings. The sequences generated in this study were deposited in GenBank database (Supplementary Table 3).

2.5 Fungal trunk disease incidence

The GTD incidence, alone or in combination, was calculated based on the incidence of fungal pathogens in propagation materials at the four stages of the nursery process, for each portion of wood analysed. The incidence was determined as follows: (number of materials infected by each GTD or specific combination of GTDs, divided by the total number of materials processed) x 100.

3. RESULTS

3.1 Internal disease symptoms

All grapevine cultivars and rootstocks presented typical internal wood symptoms of GTDs in the four stages of the nursery propagation process in both years of evaluation, except from the rootstock 101-14. This rootstock showed no internal wood symptoms in stages 1 and 2 in 2018 (the only year of evaluation of this rootstock). Around the 80% of materials with symptoms presented black discoloration of xylem vessels. This symptom was observed in materials from all stages of the propagation process analysed. Sectorial wood necrosis was the other symptom observed, also present in all stages, but with a markedly less incidence (around the 20% of materials with this symptoms). Additionally, grafted rooted plants (stage 4) also presented brown to black discolouration and necrosis from the base and necrotic lesions in the roots (Figure 1).

The incidence of symptoms increased throughout the nursery propagation process with a markedly increment in stage 4 (grafted rooted plants) (Figure 2). Considering all cultivars, in 2018 rootstock cuttings from stage 1 presented in average an incidence of

symptoms of 5% at the top and 10% at the bottom, whereas the incidence on scion cuttings was 2% at the top and 10% at the bottom. In stage 2, rootstocks cuttings presented an average incidence of 13% and 15%, whereas scion cuttings showed 18% and 27% of incidence, at the top and at the bottom of the cuttings, respectively. Grafted plants in stage 3 had on average 44% of incidence in the grafted union and 35% in the basal part of the plant. Finally, plants in stage 4 showed on average 97%, 97% and 98% of incidence in the grafted union, middle part of the rootstock and in the foot, respectively. In 2019, the average incidence of symptoms in rootstock cuttings in stage 1 was 2% and 6%, whereas in scion cuttings was 12% and 21%, at the top and the bottom, respectively. Rootstock cuttings in stage 2 showed an incidence of 3% and 5%, whereas scion cuttings showed an incidence of 24% and 13%, at the top and at the bottom of the cuttings, respectively. Materials in stage 3 showed an average incidence of internal symptoms in the grafted union of 54% and 55% in the foot. Finally, plants in stage 4 had an average incidence of almost 100%, in all the three plant portions analysed (Figure 2).

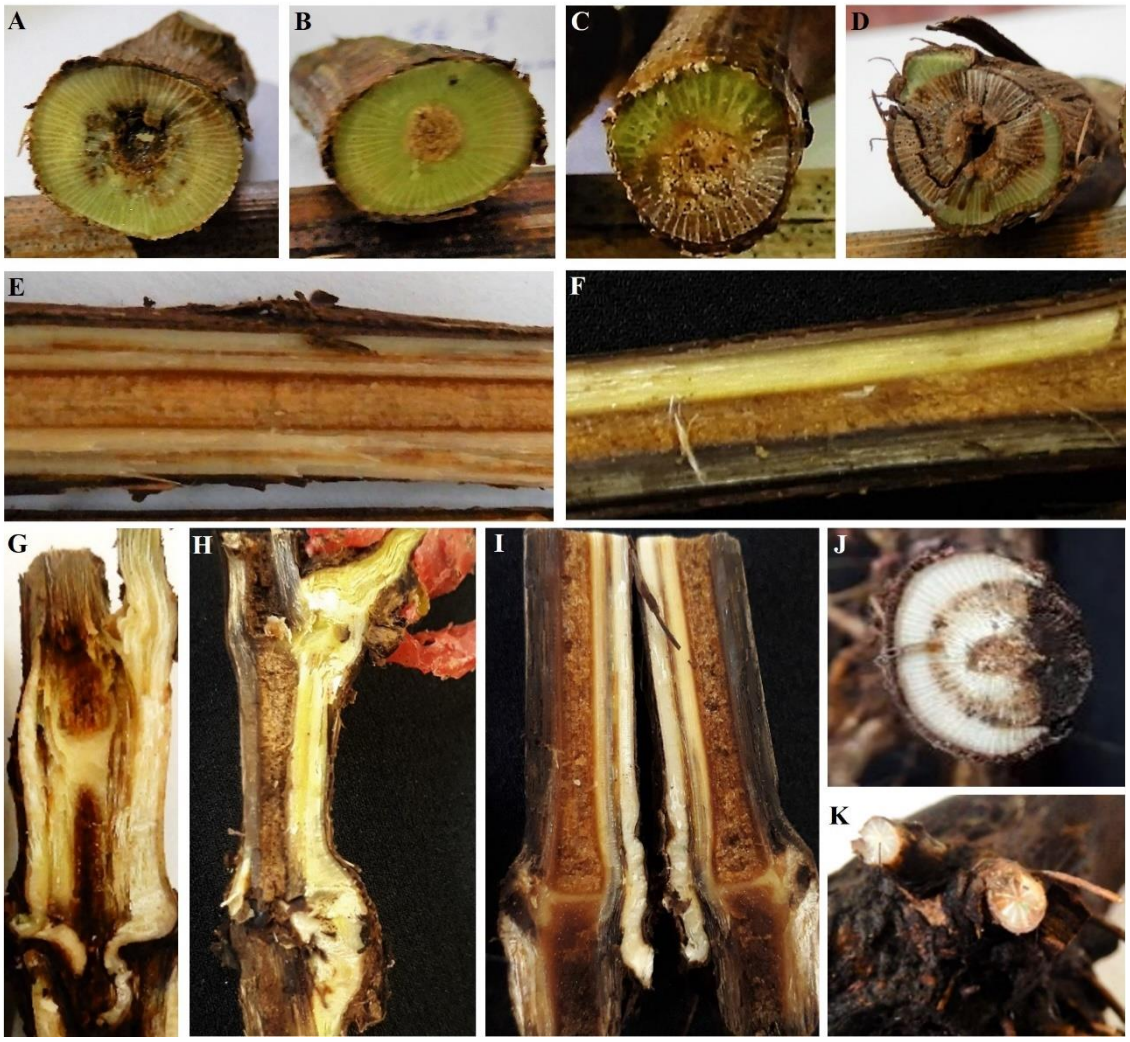

Figure 1. Internal symptoms caused by fungal pathogens associated with grapevine trunk diseases. Cross section of cuttings showing (A-B) black discoloration of the xylem vessels seen as black spots and (C-D) sectorial wood necrosis. Longitudinal section of cuttings showing (E) black discoloration of the xylem vessels seen as dark streaks and (F) sectorial wood necrosis. Longitudinal section of the graft union area showing (G) dark streaks and (H) sectorial wood necrosis. Longitudinal section of the base of the rootstock showing (I) dark streaks that develops from the base and sectorial wood necrosis. Cross section of the base of the rootstocks showing (J) a half-ring of black spots and sectorial wood necrosis. Cross section of roots showing (K) sectorial wood necrosis.

3.2 Fungal isolation and morphological identification

A total of 495 fungal isolates were obtained from grapevine, of which 236 were classified associated with BD, 181 to PD, 52 to BFD and 26 to DD.

Fungal isolates associated with BD were obtained from brown to dark streaks and sectorial wood necrosis. These isolates presented fast-growing, cottony aerial mycelium with white colour at the beginning turning to grey, dark grey or olive-green few days later. Approximately 80% of these isolates produced hyaline, aseptate and fusiform conidia resembling those produced by genera such as *Botryosphaeria* and *Neofusicoccum*, whereas the remaining 20% of isolates produced dark, aseptate and oblong to rounded apex conidia, which characterize *Diplodia* genus (Delgado et al., 2016). Fungal isolates of PD pathogens were obtained from brown to dark streaks and characterized by slow mycelial growth. The first sub-group formed by 100 *Ph. chlamydospora*-like isolates, presented sparse aerial mycelium, with colours ranging from green-olivaceous to olivaceous-black, abundant straight and pigmented conidia and dark green-brown conidiophores, characteristic of *Ph. chlamydospora* (Crous and Gamms, 2000). The other sub-group was formed by 81 *Phaeoacremonium* spp. isolates, which showed a flat, pale to medium brown mycelium, abundant sporulation of hyaline and aseptate conidia and different types, sizes, and shapes of phialides, morphological characteristics of this genus (Mostert et al., 2006b). Isolates associated with BFD were obtained from brown to dark streaks and necrosis from the foot and from roots. These strains showed aerial and cottony mycelia ranging in colours from white to dark-yellow or slightly brown and produced macroconidia, microconidia and chlamydospores, resembling *Cylindrocarpon*-like asexual morphs (Chaverri et al., 2011; Agustí-Brisach and Armengol, 2013). Finally, isolates associated with DD were isolated predominantly

from brown to dark streaks and characterized by moderate aerial mycelium white at first becoming light cream later and usually forming concentric rings with visible conidiomata at maturity containing alfa and beta conidia, morphologically resembling members of *Diaporthe* genus (Úrbez-Torres et al., 2013).

Considering both years of sampling, 18.2% of the total fungal isolates were obtained from asymptomatic wood tissues (90 strains). The 80% of these were associated with BD, 10% to PD and the remaining 10% to DD, whereas no isolates associated with BFD were obtained from asymptomatic tissues. Fungal isolates from asymptomatic tissues associated with BD and DD diseases accounted for 31% and 35% of total BD and DD isolates, respectively, whereas isolates associated with PD from asymptomatic tissues accounted for 5% of total PD isolates. Regarding the propagation stages from which they were isolated, 84.3% and 100% were obtained from materials at the first three stages (stages 1, 2 and 3) in 2018 and 2019, respectively.

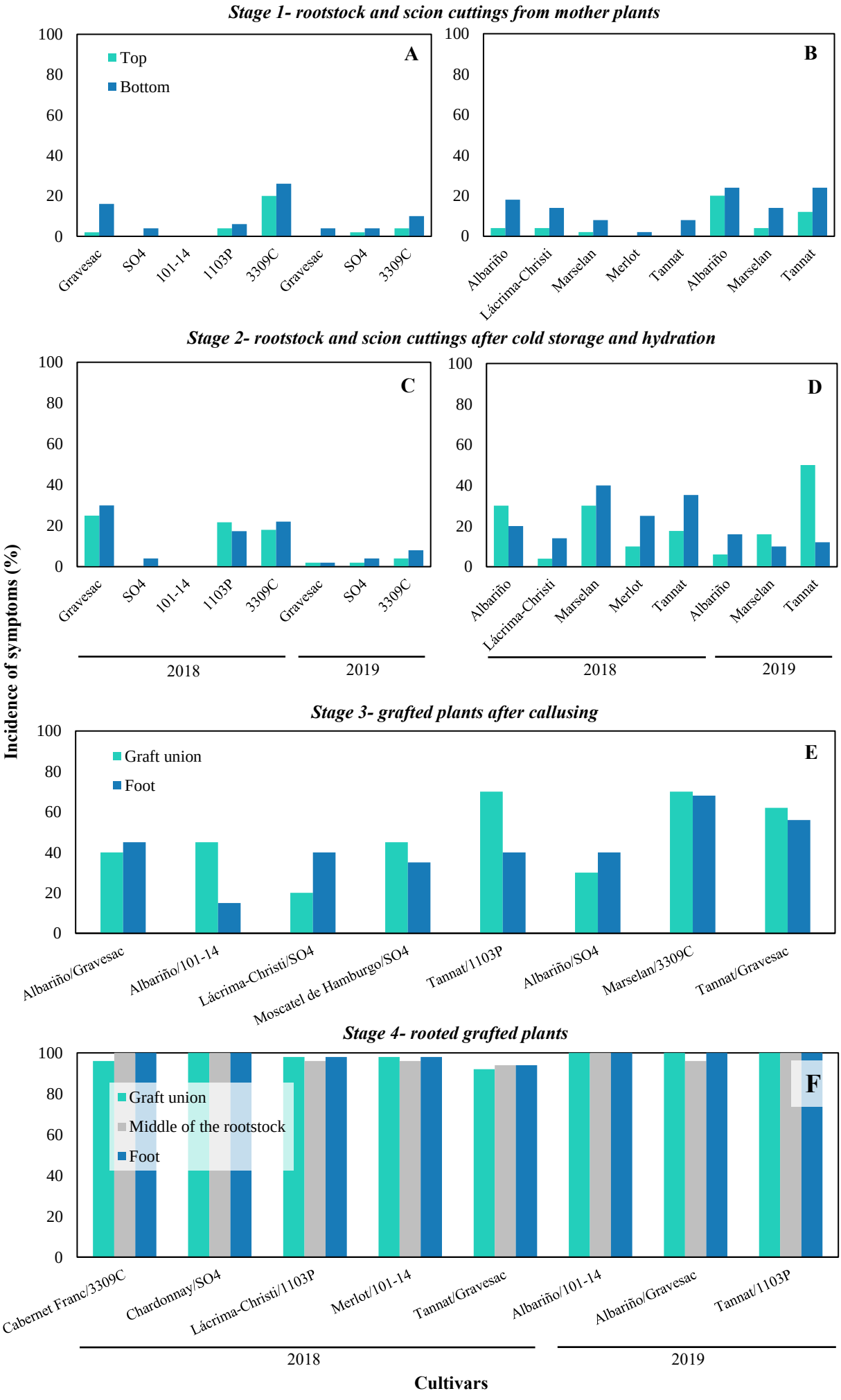
Stage 1- rootstock and scion cuttings from mother plants
A
Top
Bottom
100
80
60
40
20
0
Gravesac
SO4
101-14
1103P
3309C
Gravesac
SO4
3309C
B
Albariño
Lácrima-Christi
Marselan
Merlot
Tannat
Albariño
Marselan
Tannat
Stage 2- rootstock and scion cuttings after cold storage and hydration
C
D
2018
2019
Incidence of symptoms (%)
Stage 3- grafted plants after callusing
E
Graft union
Foot
Albariño/Gravesac
Albariño/101-14
Lácrima-Christi/SO4
Moscatel de Hamburgo/SO4
Tannat/1103P
Albariño/SO4
Marselan/3309C
Tannat/Gravesac
Stage 4- rooted grafted plants
F
Graft union
Middle of the rootstock
Foot
Cabernet Franc/3309C
Chardonnay/SO4
Lácrima-Christi/1103P
Merlot/101-14
Tannat/Gravesac
Albariño/101-14
Albariño/Gravesac
Tannat/1103P
2018
2019
Cultivars

Figure 2. Incidence of grapevine trunk diseases symptoms in propagation materials of different cultivars, rootstocks, and combination cultivar-rootstocks throughout four stages of the nursery process in 2018 and 2019: (A) rootstocks and (B) scion cuttings from mother plants (stage 1); (C) rootstocks and (D) scion cuttings after cold storage and hydration (stage 2); (E) grafted plants after callusing (stage 3); (F) rooted grafted plants ready to plant (stage 4).

3.3 Molecular identification

A representative subsample of 180 strains isolated from symptomatic and asymptomatic materials was selected for molecular identification, attempting to include as much morphological diversity as possible within each group of fungi (Supplementary Table 3). BLAST comparisons grouped the isolates into eight fungal genera: *Botryosphaeria* (n=16), *Neofusicoccum* (n=21) and *Diplodia* (n=9) associated with BD, *Phaeoacremonium* (n=43) and *Phaeomoniella* (n=23) associated with PD, *Dactylonectria* (n=36) and *Ilyonectria* (n=6) associated with BFD, and *Diaporthe* (n=26) associated with DD.

The *Botryosphaeriaceae* phylogenetic analyses based on TEF sequences allowed the identification of seven species: *B. dothidea* (n=16), *N. parvum* (n=13), *D. pseudoseriata* (n=7), *N. cryptoaustrale* (n=3), *N. luteum* (n=3), *D. seriata* (n=2) and *N. australe* (n=1) (Supplementary Figures 1-3). The *Dactylonectria* and *Ilyonectria* phylogenetic analyses using HIS3 sequences, enabled us to identify seven species including *Da. novozelandica* (n=15), *Da. macrodidyma* (n=11), *Da. torresensis* (n=6), *Da. pauciseptata* (n=3), *Da. valentina* (n=1), *I. liriodendri* (n=4), *I. robusta* (n=1), whereas one strain was identified as *Ilyonectria* sp. (n=1) (Supplementary Figures 4 and 5).

The *Phaeoacremonium* phylogenetic analysis based on TUB2 sequences allowed us to identify three species, *P. minimum* (n=41), *P. austroafricanum* (n=1) and *P. oleae* (n=1). Regarding *Phaeomoniella chlamydospora*-like isolates, phylogenetic analysis based on ITS sequences grouped all our isolates (n=23) with *Ph. chlamyd*ospora ex-type strain (Supplementary Figures 6 and 7).

Finally, the *Diaporthe* phylogenetic analysis, based on TEF sequences, allowed the identification of *Di. baccae* (n=2), *Di. eres* (n=2), *Di. foeniculina* (n=2) and *Di. terebinthifolii* (n=1), while the remaining 19 strains of this group, could not be

distinguished by this single locus. These 19 strains fell within a *Di. ampelina*/*hungariae*/*hispaniae* clade with high bootstrap support (1 Bayesian posterior probability and 97% Maximum likelihood) (Supplementary Figure 8).

3.4 Fungal trunk disease incidence

In both sampling years, the incidence of GTDs increased noticeably as the grapevine propagation process progressed. BD pathogens were found in materials from the four stages analysed. The total incidence of BD in 2018 was 2.9% and 6.4% in rootstock and scion cuttings, respectively, from stage 1, whereas in 2019 it was 15% in rootstock and 27.4% in scion cuttings (Table 2). In materials from stage 2, the total incidence in rootstock was 2.7% and 8.3%, in 2018 and 2019, respectively, and 15% in scion cuttings from both sampling years. In propagation materials from stage 3, the total incidence of BD was 41% in 2018 and 28% in 2019, being the incidence remarkably higher at the graft union compared with the base of the plant. In stage 4, BD showed an incidence of 55.1% in 2018 and 36.7% in 2019, being these pathogens isolated from all plant portions tested (Table 3).

Regarding PD, in 2018 rootstock cuttings from stage 1 showed a total incidence of 2.9%, whereas scion cuttings presented a total incidence of 0.8%. In 2019, scion cuttings from stage 1 showed a total PD incidence of 2.7%, whereas no isolates associated with PD were obtained from rootstock cuttings (Table 2). Also, no PD isolates were obtained from analysed materials at the stage 2 in neither of the two years of evaluation. At the stage 3, the total incidence was 1% in 2018 and 6.7% in 2019, whereas in plants from stage 4, the incidence of PD was 56.1% and 58.3%, in 2018 and 2019, respectively, considering all the portions of the plant analysed. Pathogens associated with this disease were isolated from all plant portions tested in stage 4 (Table 3).

Table 2. Incidence of fungal grapevine trunk diseases in rootstock and scion cuttings from mother plants (stage 1) and rootstock and scion cuttings after cold storage and hydration (stage 2).

		Disease incidence % (number of infected samples/total samples)											
		Stage 1						**Stage 2**					
		Rootstock			**Scion**			**Rootstock**			**Scion**		
Year	**Fungal disease[1]**	**Top[2]**	**Bottom**	**Total**	**Top**	**Bottom**	**Total**	**Top**	**Bottom**	**Total**	**Top**	**Bottom**	**Total**
2018	PD	1.9 (2/104)	1.0 (1/104)	2.9 (3/104)	-	0.8 (1/125)	0.8 (1/125)	-	-	-	-	-	-
	BFD	-	-	-	-	-	-	-	-	-	-	-	-
	BD	1.0 (1/104)	1.9 (2/104)	2.9 (3/104)	1.6 (2/125)	4.8 (6/125)	6.4 (8/125)	1.8 (2/111)	0.9 (1/111)	2.7 (3/111)	7.0 (7/100)	8.0 (8/100)	15.0 (15/100)
	DD	-	1.0 (1/104)	1.0 (1/104)	-	0.8 (1/125)	0.8 (1/125)	0.9 (1/111)	-	0.9 (1/111)	1.0 (1/100)	4.0 (4/100)	5.0 (5/100)
2019	PD	-	-	-	1.4 (1/73)	1.4 (1/73)	2.7 (2/73)	-	-	-	-	-	-
	BFD	-	-	-	-	-	-	-	-	-	-	-	-
	BD	6.7 (4/60)	8.3 (5/60)	15.0 (9/60)	8.2 (6/73)	19.2 (14/73)	27.4 (20/73)	5.0 (3/60)	3.3 (2/60)	8.3 (5/60)	11.7 (7/60)	3.3 (2/60)	15.0 (9/60)
	DD	-	-	-	1.4 (1/73)	5.5 (4/73)	6.8 (5/73)	-	-	-	-	-	-

[1] PD, Petri disease; BFD, Black-foot disease; BD, Botryosphaeria dieback; DD, Diaporthe dieback.
[2] The "top" margin of rootstock and scion cuttings was the part of the 1.1m long cutting furthest from the mother trunk (at 0.95-1.1 m from the mother trunk), whereas the "bottom" margin was the part of the cutting nearest to the mother trunk (the first 0.15 m of the cutting).

Table 3. Incidence of fungal grapevine trunk diseases in grafted plants after callusing (stage 3) and in rooted grafted plants (stage 4).

		Disease incidence % (number infected of samples/total samples)						
		Stage 3			Stage 4			
Year	Fungal disease[1]	Graft union[2]	Foot	Total	Graft union	Middle part of the rootstock	Foot and roots[3]	Total
2018	PD	1.0 (1/100)	-	1.0 (1/100)	45.9 (45/98)	18.4 (18/98)	38.8 (38/98)	56.1 (55/98)
	BFD	-	-	-	-	-	14.3 (14/98)	14.3 (14/98)
	BD	38.0 (38/100)	4.0 (4/100)	41.0 (41/100)	24.5 (24/98)	39.8 (39/98)	8.2 (8/98)	55.1 (54/98)
	DD	2.0 (2/100)	-	2.0 (2/100)	3.1 (3/98)	4.1 (4/98)	1.0 (1/98)	8.2 (8/98)
2019	PD	2.7 (2/75)	4.0 (3/75)	6.7 (5/75)	40.0 (24/60)	31.7 (19/60)	40.0 (24/60)	58.3 (35/60)
	BFD	-	-	-	3.3 (2/60)	-	60.0 (36/60)	60.0 (36/60)
	BD	25.3 (19/75)	4.0 (3/75)	28.0 (21/75)	21.7 (13/60)	15.0 (9/60)	11.7 (7/60)	36.7 (22/60)
	DD	1.3 (1/75)	-	1.3 (1/75)	1.7 (1/60)	1.7 (1/60)	-	3.3 (2/60)

[1] PD, Petri disease; BFD, Black-foot disease; BD, Botryosphaeria dieback; DD, Diaporthe dieback.
[2] The "Graft union" section includes the portion above the graft union (scion) and the "Foot" is the basal part of the plant. In stage 4, the "Middle part of the rootstock" refers to the portion of the plant between the graft union and the foot.
[3] Only isolates associated with BFD and PD were obtained from roots.

The total incidence of DD in 2018 was 1.0% and 0.8% in rootstock and scion cuttings from stage 1, respectively, whereas in stage 2, the incidence was 0.9% and 5.0%, in rootstock and scion cuttings, respectively. In 2019, isolates of *Diaporthe* from stage 1 were only obtained from scion cuttings, with a total incidence of 6.8%, while no isolates were obtained from materials in stage 2 (Table 2). In propagation materials from stage 3, DD showed an incidence of 2% in 2018 and 1.3% in 2019, whereas in stage 4 the incidence was 8.2% in 2018 and 3.3% in 2019 (Table 3).

Regarding BFD, these pathogens were isolated only from stage 4. The incidence was 14.3% in 2018 and 60% in 2019 and were isolated from the foot and roots of the plants, except from two strains that were isolated from the graft union in 2019 (Table 3). From roots, only pathogens associated with BFD and PD were isolated.

Infected materials in stages 1, 2 and 3 had only one disease. However, in grafted rooted plants in stage 4, combinations of up to four diseases were found to affect the same plant simultaneously in 2019. From the results of isolations, the total incidence of GTDs in materials from stage 4 was 84.7% in 2018 and 83.3% in 2019. The most prevalent GTD combination was BD with PD in 2018 (26.5% of the plants) and PD with BFD in 2019 (18.3% of the plants) (Table 4).

Table 4. Incidence of grapevine trunk diseases on grafted rooted vines ready to plant (stage 4) based on fungal isolations.

	Frequency of infected plants (% disease incidence)	
Fungal disease[1]	**2018**	**2019**
Alone		
Petri disease (PD)	21.4 (21/98)	16.7 (10/60)
Black-foot disease (BFD)	4.1 (4/98)	10.0 (6/60)
Botryosphaeria dieback (BD)	15.3 (15/98)	1.7 (1/60)
Diaporthe dieback (DD)	-	-
In combination		
PD + BFD	3.1 (3/98)	18.3 (11/60)
PD + BD	26.5 (26/98)	5.0 (3/60)
PD + DD	-	-
BD + BFD	5.1 (5/98)	13.3 (8/60)
BD + DD	3.1 (3/98)	-
PD + BFD + BD	1.0 (1/98)	15.0 (9/60)
PD + BD + DD	4.1 (4/98)	-
PD + BFD + DD	1.0 (1/98)	1.7 (1/60)
PD + BFD + BD + DD	-	1.7 (1/60)
Total	84.7 (83/98)	83.3 (50/60)

4. DISCUSSION

In this study, we have examined the incidence of GTDs in grapevine planting material, throughout the four stages of the local nursery propagation process, based on the presence of internal wood symptoms and GTD pathogens. We have been particularly interested in understanding the health status of the vines produced, which GTD pathogens affect the planting material and the steps of the local nursery process in which vines are infected. To the best of our knowledge, this is the first comprehensive study in South America showing the role of infected planting material in the dissemination of GTDs.

Our results show that there is a high incidence of GTDs in nursery grapevines produced in Uruguay, regardless of the scion/rootstock combination. The 84.7% and 83.3% of the examined finished nursery vines were affected by at least one GTD-associated fungus, in 2018 and 2019, respectively. These results highlight the role of infected locally produced vines as one of the main ways of dissemination of GTD pathogens. Several studies have also confirmed GTDs affecting nursery vines with varying incidence in Spain (Aroca et al., 2006; Giménez-Jaime et al., 2006; Agustí-Brisach et al., 2013a; Pintos et al., 2018; Berlanas et al., 2020; Maldonado-González et al., 2020), Portugal (Rego et al., 2009), Italy (Spagnolo et al., 2011; Carlucci et al., 2017), South Africa (Halleen et al., 2003, 2006) and France (Spagnolo et al., 2011). Furthermore, noticeable incidence of GTDs in nursery grapevines was also observed by Pintos et al. (2018) in Spain, who found that the incidence of at least one GTD-associated fungus affecting grafted rooted vines was 93%.

Incidence of symptoms and GTD-associated fungi increased throughout the four stages evaluated, suggesting that fungal infections occurred during the propagation process, which is consistent with previous studies (Gramaje and Armengol, 2011; Gramaje et al., 2022). Firstly, typical internal wood symptoms of GTDs were observed and pathogens associated with PD, BD and DD diseases were isolated in low frequency from scion and rootstocks cuttings from mother plants, as it has been described in other grapevine world regions (Pascoe and Cottral, 2000; Rego et al., 2001; Ridgway et al., 2002; Edwards and Pascoe, 2004; Fourie and Halleen, 2004; Zanzotto et al., 2007; Whiteman et al., 2007; Aroca et al., 2010; Billones-Baaijens et al., 2013). Therefore, our results also provided evidence that scion and rootstocks cuttings used for propagation are a primary source of GTD pathogens. Then, after cold storage and hydration for 24-48 hours in water, the scion and rootstocks cuttings generally showed a slight increase in the

incidence of GTDs internal symptoms. Several studies have detected the presence of PD and BD pathogens in the water of hydration tanks using both, molecular detection, and culture dependent approaches, suggesting that during soaking step infections can occur (Retief et al., 2006; Edwards et al., 2007; Pollastro et al., 2009; Vigues et al., 2009; Aroca et al., 2010; Gramaje et al., 2011). Moreover, Waite et al. (2013) confirmed that soaking cuttings is a potential source of cross contamination of field-acquired microorganisms and found that this can occur after relatively short periods of soaking. Therefore, it is likely that some infections occurred during the hydration stage, but they were not visible at the time of sampling due to the slow development of GTDs symptoms in the host.

Grafting and callusing stages have been widely identified as key steps of the propagation process in which new infections occur (Gramaje and Armengol, 2011). Our results also showed an increment of GTDs symptoms and isolated pathogens after grafting and callusing, suggesting that new infections may have occurred at this stage. These steps involve many cuts and wounds, as a consequence of the disbudding, grafting and improperly matched graft unions, which make the material susceptible to be infected by GTD-associated fungi (Giménez-Jaime et al., 2006; Gramaje and Armengol, 2011). In addition, several investigations detected the presence of PD pathogens in washings of scissors used to cut buds and grafting machines (Whiteman et al., 2004; Retief et al., 2006; Pollastro et al., 2009; Aroca et al., 2010; Gramaje et al., 2011), indicating that pathogen dissemination also occurs during this stage. Moreover, the environmental conditions of high temperature and humidity in callusing rooms, are favorable for the growth and wood colonization of pathogens (Gramaje and Armengol, 2011).

The main GTDs found affecting nursery vines ready to plant were PD, BFD and BD, alone or in combination. The prevalence of PD and BFD was expected, as a big amount of research indicated that these are the main GTDs affecting nursery and young vines in the world (Rego et al., 2000; Halleen et al., 2003; Gramaje and Armengol, 2011, Gramaje et al., 2018), and in Uruguay (Abreo et al., 2010, 2011). As well as this, the high incidence of BD was unsurprising, as *Botryosphaeriaceae* species were recently the most frequently detected GTD-associated fungi affecting nursery vines in Spain (Pintos et al., 2018) and Italy (Carlucci et al., 2017). The simultaneous presence of these diseases in vines ready to plant is especially worrisome because any stress factor may trigger more rapidly the symptoms of decline in the vineyard (Hyrcan et al., 2020).

Black-foot pathogens were exclusively isolated from vines after the stage of rooting in the nursery field. This result agrees with several studies that have indicated that BFD pathogens rarely occur in the propagation material prior to the rooting stage in nursery fields (Rego et al., 2001; Fourie and Halleen, 2002, 2004; Halleen et al., 2003, 2006, 2007; Agustí-Brisach et al., 2013a). Based on our culture-dependent approach, results make emphasis on the fact that the nursery field is the primary source of inoculum of BFD, as it was also previously demonstrated (Rego et al., 2001; Halleen et al., 2006; Agustí-Brisach et al., 2013b, 2014; Berlanas et al., 2017). However, some research based on molecular techniques also detected BFD inoculum in the water of hydration tanks, washings of cutting and grafting tools, callusing media, and grafted plants after callusing, suggesting that infections of BFD-associated fungi can also occur during these earlier stages or at least may spread (Cardoso et al., 2013; Agustí-Brisach et al., 2013a). On the other hand, a marked increase in PD incidence was also observed in rooted grafted vines, compared with materials from earlier stages. Several researchers have been reported the presence of PD inoculum in nursery and vineyards soil (Rooney et al., 2001; Mostert et al., 2006a; Retief et al., 2006; Agustí-Brisach et al., 2013b; Maldonado-González et al., 2020), which, together with the wounds generated during the rooting process and the probable incomplete callusing of the basal end of the rootstock (Gramaje and Armengol, 2011), could explain the registered increment.

The increment of internal symptoms and GTD-associated fungi isolated after the rooting stage could be mainly explained by the occurrence of new infections throughout the growing season in the nursery field. However, it is also necessary to emphasize that GTD pathogens can appear as endophytes or latent pathogens and grow over a larger area within the nursery stock as the material ages before symptoms develop (Halleen et al., 2003; Aroca et al., 2010; Abreo et al., 2013; Úrbez-Torres et al., 2015; Berlanas et al., 2020; Hrycan et al., 2020). In fact, although culture-dependent approaches require a high level of colonization of the pathogen in the host to be detected by isolation (Agustí-Brisach et al., 2013a), we also isolated GTD pathogens from asymptomatic material earlier in the propagation process, mainly BD pathogens, confirming that these pathogens can occur as latent or endophytes in nursery material. Therefore, in stage 4 we observed an accumulation of infections that occurred during the propagation process, including those that were not previously visible.

Based on the phylogenetic analysis of a single locus, the 180 isolates selected were placed into eight genera and 89% identified within 22 fungal species associated with GTDs in the nursery grapevine material. Within the *Botryosphaeriaceae* group we found *N. cryptoaustrale* and *D. pseudoseriata* as new records on grapevine in Uruguay. Regarding BFD pathogens, *Da. novozelandica*, *Da. torresensis*, *Da. valentina* and *I. robusta* are new records on grapevine in this country. It should be noted that the etiology of BFD has been subjected to taxonomic revision in recent years (Chaverri et al., 2011; Cabral et al., 2012a; Cabral et al., 2012b; Lombard et al., 2014). Thus, the main causal agents of BFD identified previously as *Cylindrocarpon*-like asexual morphs, are now identified as belonging to the genera *Ilyonectria* and *Dactylonectria*. Therefore, the additional fungal species detected in this work, *Da. macrodidyma*, *Da. pauciseptata* and *I. liriodendri*, do not represent new records as they were previously reported associated with BFD in Uruguay like *Cylindrocarpon macrodidymum*, *C. pauciseptatum* and *C. liriodendri* by Abreo et al. (2010). Regarding PD pathogens, *P. austroafricanum* is a new record on grapevine in Uruguay and, to the best of our knowledge, this is the first report of *P. oleae* associated with PD on grapevine worldwide. *Phaeoacremonium oleae* was isolated from a symptomatic grafted rooted plant. The species was described by Spies et al. (2018) and has been reported associated with olive trunk diseases in South Africa (Spies et al., 2018) and Italy (Raimondo et al. 2021). Finally, within the *Diaporthe* genus, *Di. baccae*, *Di. eres*, *Di. foeniculina* are new records on grapevine in Uruguay, and as far as we know, this is the first record of *Di. terebinthifolii* on grapevine worldwide. *Diaporthe terebinthifolii* was described by Gomes et al. (2013) and was isolated for first time as an endophytic specie from the leaf of *Schinus terebinthifolius* in Brazil. In this work, it was isolated from an asymptomatic scion cutting, thus, it would be necessary to test the pathogenicity on grapevine. For *Diaporthe* strains that could not be identified based on the phylogeny of the single TEF locus, it will be essential to develop a multi-locus phylogeny analysis for their identification. In recent works, three and up to seven loci have been employed to accurately identified *Diaporthe* species (Guarnaccia et al., 2018; Manawasinghe et al., 2019; León et al., 2020; Dong et al., 2021; Jimenez et al., 2022).

In conclusion, our results showed that the current health status of nursery vines produced in Uruguay may endanger the longevity of the vineyard from the start. Further research is needed to assess how many of these infected nursery vines develop foliar

symptoms in the vineyard. Nevertheless, our results suggested that a sanitation programme is required to reduce the incidence of GTDs on nursery vines. It has been proposed that an integrated and holistic management program, including biological, physical, chemical, and other strategies, is the most effective way to reduce GTD pathogens infections in the nursery (Halleen and Fourie, 2016; Gramaje et al., 2018). Currently, GTD pathogens are not included in the grapevine nursery certification program of Uruguay (INASE, 2006). The establishment of tolerance limits for the presence of fungal trunk pathogens in nursery vines could help to attempt to control these diseases.

5. REFERENCES

Abreo, E., Martínez, S., Bettucci, L., Lupo, S. (2010). Morphological and molecular characterization of *Campylocarpon* and *Cylindrocarpon* spp. associated with black foot disease of grapevines in Uruguay. *Australas. Plant Pathol.* 39, 446–452. doi:10.1071/AP10021

Abreo, E., Martínez, S., Bettucci, L., Lupo, S. (2011). *Phaeomoniella chlamydospora* and *Phaeoacremonium* spp. in grapevines from Uruguay. *Phytopathol. Mediterr.* 50, 77–85.

Abreo, E., Martínez, S., Bettucci, L., Lupo, S. (2013) Characterization of *Botryosphaeriaceae* species associated with grapevines in Uruguay. *Australas. Plant Pathol.* 42, 241–249. doi:10.1007/s13313-013-0200-8

Agustí-Brisach, C., Armengol, J. (2013). Black-foot disease of grapevine: an update on taxonomy, epidemiology and management strategies. *Phytopathol. Mediterr.* 52, 245–261. doi:10.14601/Phytopathol_Mediterr-12662

Agustí-Brisach, C., Gramaje, D., García-Jiménez, J., Armengol, J. (2013a). Detection of black-foot disease pathogens in the grapevine nursery propagation process in Spain. *Eur. J. Plant Pathol.* 137: 103–112. doi:10.1007/s10658-013-0221-8

Agustí-Brisach, C., Gramaje, D., García-Jiménez, J., Armengol, J. (2013b). Detection of black-foot and Petri disease pathogens in soils of grapevine nurseries and vineyards using bait plants. *Plant Soil* 364, 5–13. doi:10.1007/s11104-012-1333-1

Agustí-Brisach, C., Mostert, L., Armengol, J. (2014). Detection and quantification of *Ilyonectria* spp. associated with black-foot disease of grapevine in nursery soils using multiplex nested PCR and quantitative PCR. *Plant Pathol.* 63, 316–322. doi:10.1111/ppa.12093

Alaniz, S., León, M., Vicent, A., García-Jiménez, J., Abad-Campos P., Armengol J. (2007). Characterization of *Cylindrocarpon* species associated with black foot disease of grapevine in Spain. *Plant Dis.* 91, 1187–1193. doi:10.1094/PDIS-91-9-1187

Aroca, A., García-Figueres, F., Bracamonte, L., Luque, J., Raposos, R. (2006). A survey of trunk disease pathogens within rootstocks of grapevines in Spain. *Eur. J. Plant Pathol.* 115, 195–202. doi:10.1007/s10658-006-9008-5

Aroca, A., Gramaje, D., Armengol, J., García-Jiménez, J., Raposo, R. (2010). Evaluation of the grapevine nursery propagation process as a source of *Phaeoacremonium* spp. and *Phaeomoniella chlamydospora* and occurrence of trunk disease pathogens in rootstocks mother vines in Spain. *Eur. J. Plant Pathol.* 126, 165–174. doi:10.1007/s10658-009-9530-3

Berlanas, C., López-Manzanares, B., Gramaje, D. (2017). Estimation of viable propagules of black-foot disease pathogens in grapevine cultivated soils and their relation to production systems and soil properties. *Plant Soil* 417, 467–479. doi:10.1007/s11104-017-3272-3

Berlanas, C., Ojeda, S., López-Manzanares, B., Andrés-Sodupe, M., Bujanda, R., Martínez-Diz, M. P., et al. (2020). Occurrence and diversity of black-foot disease fungi in symptomless grapevine nursery stock in Spain. *Plant Dis.* 104, 94–104. doi:10.1094/PDIS-03-19-0484-RE

Billones-Baaijens, R., Ridgway, H. J., Jones, E. E., Jaspers, M. V. (2013). Inoculum sources of Botryosphaeriaceae species in New Zealand grapevine nurseries. *Eur. J. Plant Pathol.* 135, 159–174. doi:10.1007/s10658-012-0075-5

Bruez, E., Lecomte, P., Grosman, J., Doublet, B., Bertsch, C., Fontaine, F., et al. (2013). Overview of grapevine trunk diseases in France in the 2000s. *Phytopathol. Mediterr.* 52, 262–275. doi:10.14601/Phytopathol_Mediterr-11578

Cabral, A., Rego, C., Nascimento, T., Oliveira, H., Johannes, Z., Crous, P. W. (2012a). Multi-gene analysis and morphology reveal novel Ilyonectria species associated with black foot disease of grapevines. *Fungal Biol.* 116, 62–80. doi:10.1016/j.funbio.2011.09.010

Cabral, A., Groenewald, J. Z., Rego, C., Oliveira, H., Crous, P. W. (2012b). Cylindrocarpon root rot: multi-gene analysis reveals novel species within the *Ilyonectria radicicola* species complex. *Mycol. Prog.* 11, 655–688. doi:10.1007/s11557-011-0777-7

Carbone, I., and Kohn, L. M. (1999). A method for designing primer sets for speciation studies in filamentous ascomycetes. *Mycologia* 91, 553–6. doi:10.1080/00275514.1999.12061051

Cardoso, M., Diniz, I., Cabral, A., Rego, C., Oliveira, H. (2013). Unveiling inoculum sources of black foot pathogens in a commercial grapevine nursery. *Phytopathol. Mediterr.* 52, 298–312. doi:10.14601/Phytopathol_Mediterr-11593

Carlucci, A., Lops, F., Mostert, L., Halleen, F., Raimondo, M. (2017). Occurrence fungi causing black foot on young grapevines and nursery rootstock plants in Italy. *Phytopathol. Mediterr.* 56, 10–39. doi:10.14601/Phytopathol_Mediterr-18769

Chaverri, P., Salgado, C., Hirooka, Y., Rossman, A. Y., Samuels, G. J. (2011). Delimitation of *Neonectria* and *Cylindrocarpon* (*Nectriceae*, *Hypocreales*, *Ascomycota*) and related genera *Cylindrocarpon*-like anamorphs. *Stud. Mycol.* 68, 57–78. doi:10.3114/sim.2011.68.03

Crous, P. W., and Gams, W. (2000). *Phaeomoniella chlamydospora* gen. et comb. nov., a causal organism of Petri grapevine decline and esca. *Phytopathol. Mediterr.* 39, 112–118.

Crous, P. W., Groenewald, J. Z., Risede J. M., Hywel-Jones N. L. (2004). *Calonectria* species and their *Cylindrocladium* anamorphs: Species with sphaeropedunculate vesicles. *Stud. Mycol.* 50, 415–429.

Darriba, D., Taboada G. L., Doallo, R., Posada, D. (2012). jModelTest 2: more models, new heuristics and parallel computing. *Nat. Methods* 9, 772. doi:10.1038/nmeth.2109

Delgado, L., Mondino, P., Alaniz, S. (2016). Botryosphariaceae species associated with stem canker, die-back and fruit rot on apple in Uruguay. *Eur. J. Plant Pathol.* 146, 637–655. doi:10.1007/s10658-016-0949-z

Dong, Z., Manawasinghe, I. S., Huang, Y., Shu, Y., Phillips, A. J. L., Dissanayake, A. J., et al. (2021). Endophytic *Diaporthe* associated with *Citrus grandis* cv. Tomentosa in China. *Front. Microbiol.* 11, 609387. doi:10.3389/fmicb.2020.609387

Edwards, J., and Pascoe, I. G. (2004). Ocurrence of *Phaeomoniella chlamydospora* and *Phaeoacremonium aleophilum* associated with Petri disease and esca en Australian grapevines. *Australas. Plant Pathol.* 33, 273–279. doi:10.1071/AP04016

Edwards, J., Constable, F., Wiechel, T., Salib, S. (2007). Comparison of the molecular tests - single PCR, nested PCR and quantitative PCR (SYBR®Green and TaqMan®) - for detection of *Phaeomoniella chlamydospora* during grapevine nursery propagation. *Phytopathol. Mediterr.* 46, 58–72. doi:10.1400/68072

Fourie, P. H., and Halleen, F. (2001). Diagnosis of fungal diseases and their involvement in dieback disease of young vines. *Wynboer* 149, 19–23.

Fourie, P. H., and Halleen, F. (2002). Investigation on the occurrence of *Phaeomoniella chlamydospora* in canes of rootstock mother vines. *Australas. Plant Pathol.* 31, 425–426. doi:10.1071/AP02049

Fourie, P. H., and Halleen, F. (2004). Occurrence of grapevine trunk disease pathogens in rootstock mother plants in South Africa. *Australas. Plant Pathol.* 33, 313–315. doi:10.1071/AP04005

Giménez-Jaime, J., Aroca A., Raposo, R., García-Jiménez, J., Armengol, J. (2006). Occurrence of fungal pathogens associated with grapevine nurseries and the decline of young vines in Spain. *J Phytopathol.* 154, 598–602. doi:10.1111/j.1439-0434.2006.01153.x

Gomes, R. R., Glienke, C., Videira, S. I. R., Lombard, L., Groenewald, J. Z., Crous, P. W. (2013). *Diaporthe*: a genus of endophytic, saprobic and plant pathogenic fungi. *Persoonia* 31, 1–41. doi:10.3767/003158513X666844

Gramaje, D., and Armengol, J. (2011). Fungal trunk pathogens in the grapevine propagation process: potential inoculum sources, detection, identification, and management strategies. *Plant Dis.* 95, 1040–1055. doi:10.1094/PDIS-01-11-0025

Gramaje, D., Mostert, L., Armengol, J. (2011). Characterization of *Cadophora luteo-olivacea* and *C. melinii* isolates obtained from grapevines and environmental samples from grapevine nurseries in Spain. *Phytopathol. Mediterr.* 50, 112–126.

Gramaje, D., Úrbez-Torres, J. R., Sosnowski, M. (2018). Managing grapevine trunk diseases with respect to etiology and epidemiology: current strategies and future prospects. *Plant Dis.* 102, 12–39. doi:10.1094/PDIS-04-17-0512-FE

Gramaje, D., Eichmeier, A., Spetik, M., Carbone, M. J., Bujanda, R., Vallance, J., et al. (2022). Exploring the temporal dynamics of the fungal microbiome in rootstocks, the lesser-known half of the grapevine crop. *J. Fungi* 4, 821. doi:10.3390/jof8050421

Guarnaccia, V., Groenewald, J. Z., Woodhall, J., Armengol, J., Cinelli I.T., Eichmeier, A. (2018). *Diaphorte* diversity and pathogenicity revealed from a broad survey of grapevine diseases in Europe. *Persoonia* 40, 135–153. doi:10.3767/persoonia.2018.40.06

Halleen, F., Crous, P. W., Petrini, O. (2003). Fungi associated with healthy grapevine cuttings in nurseries, with special reference to pathogens involved in the decline of young vines. *Australas. Plant Pathol.* 32, 47–52. doi:10.1071/AP02062

Halleen, F., Fourie, P. H., Crous, P. W. (2006). A review of black foot disease of grapevine. *Phytopathol. Mediterr.* 45, 55–67. doi:10.1400/52261

Halleen, F., Mostert, L., Crous, P. W. (2007). Pathogenicity testing of lesser-known vascular fungi of grapevines. *Australas. Plant Pathol.* 36, 277–285. doi:10.1071/AP07019

Halleen, F., Fourie, P. H. (2016). An integrated strategy for the proactive management of grapevine trunk disease pathogen infections in grapevine nurseries. *South African J. Enol. Vitic.* 37, 104–114.

Hrycan, J., Hart, M., Bowen, P., Forge, T., Úrbez-Torres, J. R. (2020). Grapevine trunk disease fungi: their roles as latent pathogens and stress factors that favour disease development and symptom expression. *Phytopathol. Mediterr.* 59, 395–424. doi:10.14601/Phyto-11275

INASE. (2006). Producción de materiales de propagación de vid de clase certificada, resolución No. 692, July 14, 2006 actualization. Uruguay: Instituto Nacional de Semillas (INASE). Available at: https://www.inase.uy/Files/Docs/BA4FCB8DF2561CFC.pdf [Accessed April 15, 2022].

Jimenez, I., Besoain, X., Saa, S., Peach-Fine, E., Cadiz, F., Riquelme, N., et al. (2022). Identity and pathogenicity of Botryosphaeriaceae and Diaporthaceae from Juglans regia in Chile. *Phytopathol. Mediterr.* 61, 79–94. doi:10.36253/phyto-12832

Larignon, P., and Dubos, B. (2001). Le Black Dead Arm: Maladie nouvelle ane pas confondre avec l'Esca. *Phytoma* 5, 30–31.

Larignon, P., Spagnolo, A.; Bertsch, C., Fontaine, F. (2015). First report of young grapevine decline caused by *Neofusicoccum parvum* in France. *Plant Dis*. 99, 1859. doi:10.1094/PDIS-03-15-0280-PDN

León, M., Berbegal, M., Rodríguez-Reina, J. M., Elena, G., Abad-Campos, P., Ramó-Albalat, A., et al. (2020). Identification and characterization of *Diaporthe* spp. associated with twig cankers and shoot blight of almonds in Spain. *Agronomy* 10, 1062. doi:10.3390/agronomy10081062

Lombard, L., Van der Merwe, N. A., Groenewald, J. Z., Crous, P. W. (2014). Lineages in *Nectriaceae*: Re-evaluating the generic status of *Ilyonectria* and allied genera. *Phytopathol. Mediterr*. 53, 515–532. doi:10.14601/Phytopathol_Mediterr-14976

Maldonado-González, M. M., Martínez-Diz, M. P., Andrés-Sodupe, M., Bujanda, R., Díaz-Losada, E., Gramaje, D. (2020). Quantification of *Cadophora luteo-olivacea* from grapevine nursery stock and vineyard soil using droplet digital PCR. *Plant Dis.* 104, 2269–2274. doi:10.1094/PDIS-09-19-2035-RE

Manawasinghe, I. S., Dissanayake, A. J., Li X., Liu M., Wanasinghe, D. N., Xu, J., et al. (2019). High genetic diversity and species complexity of *Diaporthe* associated with grapevine dieback in China. *Front. Microbiol.* 10, 1936. doi:10.3389/fmicb.2019.01936

Marin-Felix, Y., Hernández-Restrepo, M., Wingfield M. J., Akulov, A., Carnegie, A. J., Cheewangkoon, R., et al. (2019). Genera of phytopathogenic fungi: GOPHY 2. *Stud. Mycol.* 92, 47–133. doi:10.1016/j.simyco.2018.04.002

Martin, M. T., and Cobos, R. (2007). ldentification of fungi associated with grape vine decline in Castilla y León (Spain). *Phytopathol. Mediterr.* 46, 18–25. doi:10.1400/68063

Mohammadi, H., Alaniz, S., Banihashemi, Z., Armengol, J. (2009). Characterization of *Cylindrocarpon liriodendri* associated with black foot disease of grapevine in Iran. *J Phytopathol*. 157, 642–645. doi:10.1111/j.1439-0434.2009.01555.x

Mondello, V., Songy, A., Battiston, E., Pinto, C., Coppin, C., Trotel-Aziz, P., et al. (2018). Grapevine Trunk Diseases: a review of fifteen years of trials for their control with chemicals and biocontrol agents. *Plant Dis*. 102, 1189–1217. doi:10.1094/PDIS-08-17-1181-FE

Moreno-Sanz, P., Lucchetta, G., Zanzotto, A., Loureiro, M. D., Suarez, B., Angelini, E. (2013). Fungi associated to grapevine trunk diseases in young plants in Asturias (Northern Spain). *Hortic. Sci.* 40, 138–144. doi:1017221/9/2013-HORTSCI

Mostert, L., Halleen, F., Fourie, P., Crous, P. W. (2006a). A review of *Phaeoacremonium* species involved in Petri disease and esca of grapevines. *Phytopathol. Mediterr.* 45, 12–29. doi:10.1400/52258

Mostert, L., Groenewald, J. Z., Summerbell, R. C., Gams, W., Crous, P. W. (2006b). Taxonomy and pathology of *Togninia* (*Diaporthales*) and its *Phaeoacremonium* anamorphs. *Stud. Mycol.* 54, 1–115. doi:103114/sim.54.1.1

Mugnai, L., Graniti, A., Surico, G. (1999). Esca (black measles) and brown wood-streaking: two old and elusive disease of grapevine. *Plant Dis.* 83, 404–418. doi:10.1094/PDIS.1999.83.5.404

Navarrete, F., Abreo, E., Martínez, S., Bettucci, L., Lupo, S. (2011). Pathogenicity and molecular detection of Uruguayan isolates of *Greeneria uvicola* and *Cadophora luteo-olivacea* associated with grapevine trunk diseases. *Phytopathol. Mediterr.* 50, 166–175. doi:10.14601/Phytopathol_Mediterr-9188

O'Donnell, K., and Cigelnik, E. (1997). Two divergent intragenomic rDNA ITS2 types within a monophyletic lineage of the fungus *Fusarium* are nonorthologous. *Mol. Phylogenet. Evol.* 7, 103–116. doi:10.1006/mpev.1996.0376

Pascoe, I., and Cottral, E. (2000). Developments in grapevine trunk diseases research in Australia. *Phytopathol. Mediterr.* 39, 68–75. doi:10.1400/57813

Peever, T. L., Canihos, Y., Olsen, L., Ibañez, A., Liu, Y. C. Timmer, L. W. (1999). Population genetic structure and host specificity of *Alternaria* spp. causing Brown Spot of Minneola Tangelo and Rough Lemon in Florida. *Phytopathology* 89, 851–860. doi:10.1094/PHYTO.1999.89.10.851

Phillips, A. J. L. (2002). *Botryosphaeria* species associated with diseases of grapevines in Portugal. *Phytopathol. Mediterr.* 41, 3–18. doi:10.1400/14484

Phillips, A. J. L., Alves, A., Abdollahzadeh, J., Slippers, B., Wingfield, M., Groenewald, J. Z., et al. (2013). The *Botryosphaeriaceae*: genera and species known from culture. *Stud. Mycol.* 76, 51–167. doi:10.3114/sim0021

Pintos, C., Redondo, V., Costas, D., Aguín, O., Mansilla, P. (2018). Fungi associated with grapevine trunk diseases in nursery-produced *Vitis vinifera* plants. *Phytopathol. Mediterr.* 57, 407–424. doi:10.14601/Phytopathol_Mediterr-22964

Pollastro, S., Habib, W., Pichierri, A., Masiello, N., Faretra, F. (2009). Potential sources of Phaeomoniella chlamydospora inoculum in grapevine nurseries in southern Italy. *Phytopathol. Mediterr.* 48, 174.

Raimondo, M. L., Lops, F., Carlucci, A. (2021). First report of *Phaeoacremonium oleae* and *P. viticola* associated with olive trunk diseases in Italy. *Plant Dis.* 106, 331. doi:10.1094/PDIS-06-21-1198-PDN

Rego, C., Oliveira, H., Carvalho, A., Phillips, A. J. L. (2000). Involvement of *Phaeoacremonium* spp. and *Cylindrocarpon destructans* with grapevine decline in Portugal. *Phytopathol. Mediterr.* 39, 76–79. doi:10.1400/57814

Rego, C., Carvalho, A., Nascimento, T., Oliveira, H. (2001). First approach on the understanding of inoculum sources of *Cylindrocarpon destructans* and *Phaeomoniella chlamydospora* concerning grapevine rootstocks in Portugal. *IOBC wprs Bulletin* 24, 67–72.

Rego, C., Nascimento, T., Cabral A., Silva, M. J., Oliveira, H. (2009). Control of grapevine wood fungi in commercial nurseries. *Phytopathol. Mediterr.* 48, 128–135. doi:1014601/Phytopathol_Mediterr-2881

Retief, E., McLeod, A., Fourie, P. H. (2006). Potential inoculum sources of *Phaeomoniella chlamydospora* in South African grapevine nurseries. *Eur. J. Plant Pathol.* 115, 331–339. doi:10.1007/s10658-006-9025-4

Ridgway, H. J., Sleight, B. E., Stewart, A. (2002). Molecular evidence for the presence of Phaeomoniella chlamydospora in New Zealand nurseries, and its detection in rootstock

mothervines using species-specific PCR. *Australas. Plant Pathol.* 31, 267–271. doi:10.1071/AP02021

Ridgway, H. J., Baskarathevan, J., Amponsah, N., Jaspers, M. V., Jones, E. E. (2014). The identity, distribution and diversity of botryosphaeriaceous species in New Zealand vineyards – a national perspective. *Phytopathol. Mediterr.* 53, 565. doi:10.14601/Phytopathol_Mediterr-15167

Romanazzi, G., Murolo, S., Pizzichini, L., Nardi, S. (2009). Esca in young and mature vineyards, and molecular diagnosis of the associated fungi. *Eur. J. Plant Pathol.* 125, 277–290. doi:10.1007/s10658-009-9481-8Rooney, S. N., Eskalen, A., Gubler, W. D. (2001). Recovery of *Phaeomoniella chlamydospora* and *Phaeoacremonium inflatipes* from soil and grapevine tissues. *Phytopathol. Mediterr.* 40, 351–356. doi:10.1400/14649

Santos, L., Alves, A., Alves, R. (2017). Evaluating multi-locus phylogenies for species boundaries determination in the genus *Diaporthe*. *PeerJ* 5, e3120. doi:10.7717/peerj.3120

Scheck, H. J., Vasquez, S. J., Fogle, D., Gubler, W. D. (1998a). Grape growers report losses to black-foot and grapevine decline. *Calif. Agric.* 52, 19–23. doi:10.3733/ca.v052n04p19

Scheck, H. J., Vasquez, S. J., Gubler, W. D. (1998b). First report of three *Phaeoacremonium* spp. causing young grapevine decline in California. *Plant Dis.* 82, 590. doi:10.1094/PDIS.1998.82.5.590C

Serra, S., Mannoni, M. A., Ligios, V., Fiori, P. P. (2011). Occurrence of *Phaeomoniella chlamydospora* on grapevine planting material in Sardinia and its control with combined hot water and cyproconazole treatments. *Phytopathol. Mediterr.* 50, 61–76. doi:10.14601/Phytopathol_Mediterr-2753

Spagnolo, A., Marchi, G., Peduto, F., Phillips, A. J. L., Surico, G. (2011). Detection of Botryosphaeriaceae species within grapevine woody tissues by nested PCR, with particular emphasis on the *Neofusicoccum parvum*/*N. ribis* complex. *Eur. J. Plant Pathol.* 129, 485–500. doi:10.1007/s10658-010-9715-9

Spies, C. F. J., Moyo, P., Halleen, F., Mostert, L. (2018). *Phaeoacremonium* species diversity on woody hosts in the Western Cape Province of South Africa. *Persoonia* 40, 26–62. doi:10.3767/persoonia.2018.40.02

Tegli, S., Bertelli, E., Surico, G. (2000). Sequence analysis of ITS ribosomal DNA in five *Phaeoacremonium* species and development of a PCR-based assay for the detection of *P. chlamydosporum* and *P. aleophilum* in grapevine tissue. *Phytopathol. Mediterr.* 39, 134–149. doi:10.1400/57833

Úrbez-Torres, J. R., Leavitt, G. M., Voegel, T. M., Gubler, W. D. (2006). Identification and distribution of *Botryosphaeria* spp. associated with grapevine cankers in California. *Plant Dis.* 90, 1490–1503. doi:10.1094/PD-90-1490

Úrbez-Torres, J. R., Peduto, F., Smith, R., Gubler, W. (2013). Phomopsis dieback: A grapevine trunk disease caused by *Phomopsis viticola* in California. *Plant Dis.* 97, 1571–1579. doi:10.1094/PDIS-11-12-1072-RE

Úrbez-Torres, J. R., Haag, P., Bowen, P., O'Gorman, D. T. (2014). Grapevine trunk diseases in British Columbia: incidence and characterization of the fungal pathogens associated with Esca and Petri diseases of grapevine. *Plant Dis*. 98, 469-482. doi:10.1094/PDIS-05-13-0523-RE

Úrbez-Torres, J. R., O'Gorman, D. T., Haag, P., Bowen, P., Lowery, T. (2015). Development of a DNA microarray for the detection and identification of fungal pathogens causing decline of young grapevines. *Phytopathology* 105, 1373–1388. doi:10.1094/PHYTO-03-15-0069-R

van Niekerk, J. M., Crous, P. W., Groenewald, J. Z., Fourie, P. H., Halleen, F. (2004). DNA phylogeny, morphology and pathogenicity of *Botryosphaeria* species on grapevines. *Mycologia* 96, 781–798. doi:10.1080/15572536.2005.11832926

van Niekerk, J. M., Groenewald, J. Z., Farr, D. F., Fourie, P. H., Halleen, F., Crous, P. W. (2005). Reassessment of *Phomopsis* species on grapevines. *Australas. Plant Pathol.* 34, 27–39. doi:10.1071/AP04072

Vigues, V., Yobregat, O., Barthélémy, B., Dias, F., Coarer, M., Larignon, P. (2009). Fungi associated with wood decay diseases: Identification of the steps involving risk in French nursery. *Phytopathol. Mediterr*. 48, 177–178.

Waite, H., Gramaje, D., Whitelaw-Weckert, M., Torley, P., Hardie, W. J. (2013). Soaking grapevine cuttings in water: a potential source of cross contamination by micro-organisms. *Phytopathol. Mediterr.* 52, 359–368. doi:10.14601/Phytopathol_Mediterr-11555

White, T. J., Bruns, T. D., Lee, S., Taylor, J. W. (1990). Amplification and direct sequencing of fungal ribosomal RNA genes for phylogenetics. In: PCR *Protocols: A guide to Methods and Applications* (M.A. Innes, D.H. Gelfand, J.J. Sninsky and T.J. White, ed.), Academic Press Inc., New York, NY, USA, 315–322.

Whitelaw-Weckert, M. A., Rahman, L., Appleby, L. M., Hall, A., Clark, A.C., Waite, H., et al. (2013). Co-infection by Botryosphaeriaceae and *Ilyonectria* spp. fungi during propagation causes decline of young grafted grapevines. *Plant Pathol*. 62, 1226–1237. doi:10.1111/ppa.12059

Whiteman, S. A., Jaspers, M. V., Stewart, A., Ridgway, H. J. (2004). *Phaeomoniella chlamydospora* detection in the grapevine propagation process by species-specific PCR. *Phytopathol. Mediterr*. 43, 156. doi:10.14601/Phytopathol_Mediterr-11820

Whiteman, S. A., Steward, A., Ridgway, H. J., Jaspers, M. V. (2007). Infection of rootstock mother-vines by *Phaeomoniella chlamydospora* results in infected young grapevines. *Australas. Plant Pathol.* 36, 198–203. doi:10.1071/AP07012

Yan, J. Y., Xie, Y., Zhang, W., Wang, Y., Liu, J. K., Hyde, K. D. et al. (2013) Species of Botryosphaeriaceae involved in grapevine dieback in China. *Fungal Divers.* 61, 221–236. doi:10.1007/s13225-013-0251-8

Zanzotto, A., Autiero, F., Bellotto, D., Dal Cortivo, G., Lucchetta, G., Borgo, M. (2007). Ocurrence of *Phaeoacremonium* spp. and *Phaeomoniella chlamydospora* in grape propagation materials and young grapevines. *Eur. J. Plant Pathol.* 119, 183–192. doi:10.1007/s10658-007-9160-6

6. SUPPLEMENTARY MATERIAL

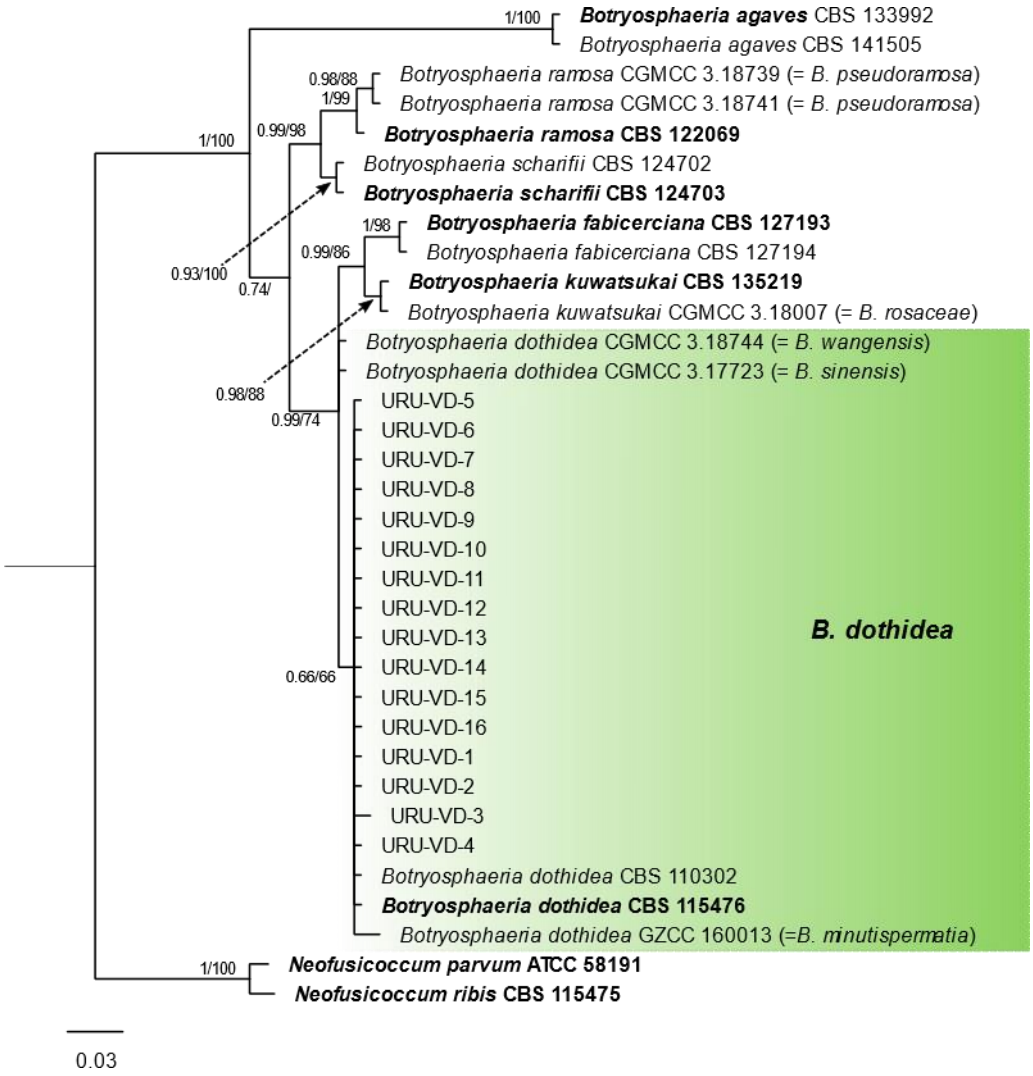

Supplementary Figure 1. Bayesian inference phylogenetic tree inferred from the elongation factor region (TEF) of 16 *Botryosphaeria* strains isolated from grapevine propagation materials and sequences obtained from the GenBank (ex-type indicated in bold). *Neofusicoccum parvum* ATCC58191 and *Neofusicoccum ribis* CBS 115475 were used as outgroup. Bootstrap support values of posterior probability and maximum likelihood higher than 0.50 and 50 are shown at the nodes before and after the bar, respectively. The scripts indicate that the nodes do not exist in the maximum likelihood tree. Scale bar represents the estimated number of substitutions per site.

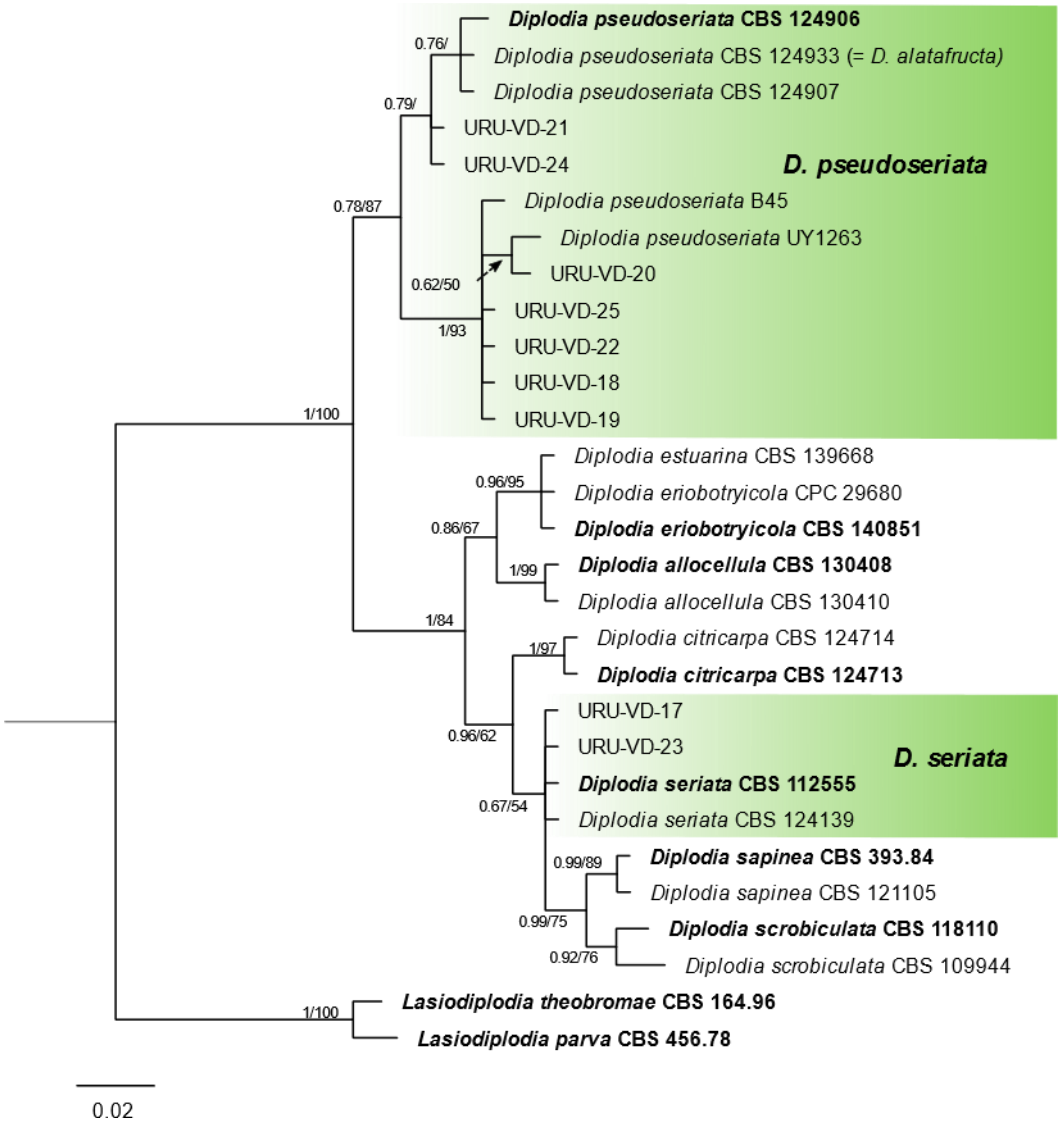

Supplementary Figure 2. Bayesian inference phylogenetic tree inferred from the elongation factor region (TEF) of 9 *Diplodia* strains isolated from grapevine propagation materials and sequences obtained from the GenBank (ex-type indicated in bold). *Lasiodiplodia theobromae* CBS 164.96 and *Lasiodiplodia parva* CBS 456.78 were used as outgroup. Bootstrap support values of posterior probability and maximum likelihood higher than 0.50 and 50 are shown at the nodes before and after the bar, respectively. The scripts indicate that the nodes do not exist in the maximum likelihood tree. Scale bar represents the estimated number of substitutions per site.

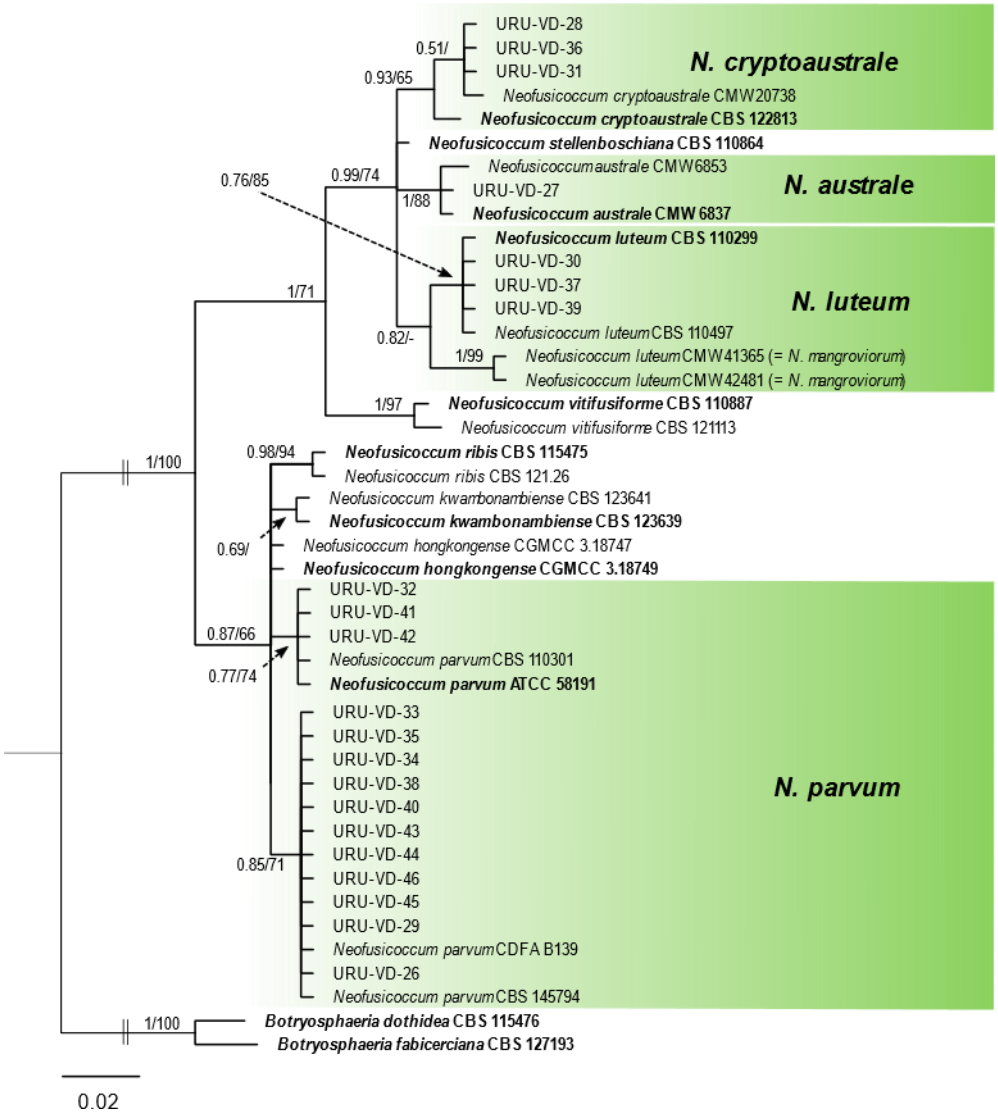

Supplementary Figure 3. Bayesian inference phylogenetic tree inferred from the elongation factor region (TEF) of 21 *Neofusicoccum* strains isolated from grapevine propagation materials and sequences obtained from the GenBank (ex-type indicated in bold). *Botryosphaeria dothidea* CBS 115476 and *Botryosphaeria fabicerciana* CBS 127193 were used as outgroup. Bootstrap support values of posterior probability and maximum likelihood higher than 0.50 and 50 are shown at the nodes before and after the bar, respectively. The scripts indicate that the nodes do not exist in the maximum likelihood tree. Double hash marks indicate branch lengths shortened at least 2-fold to facilitate visualization. Scale bar represents the estimated number of substitutions per site.

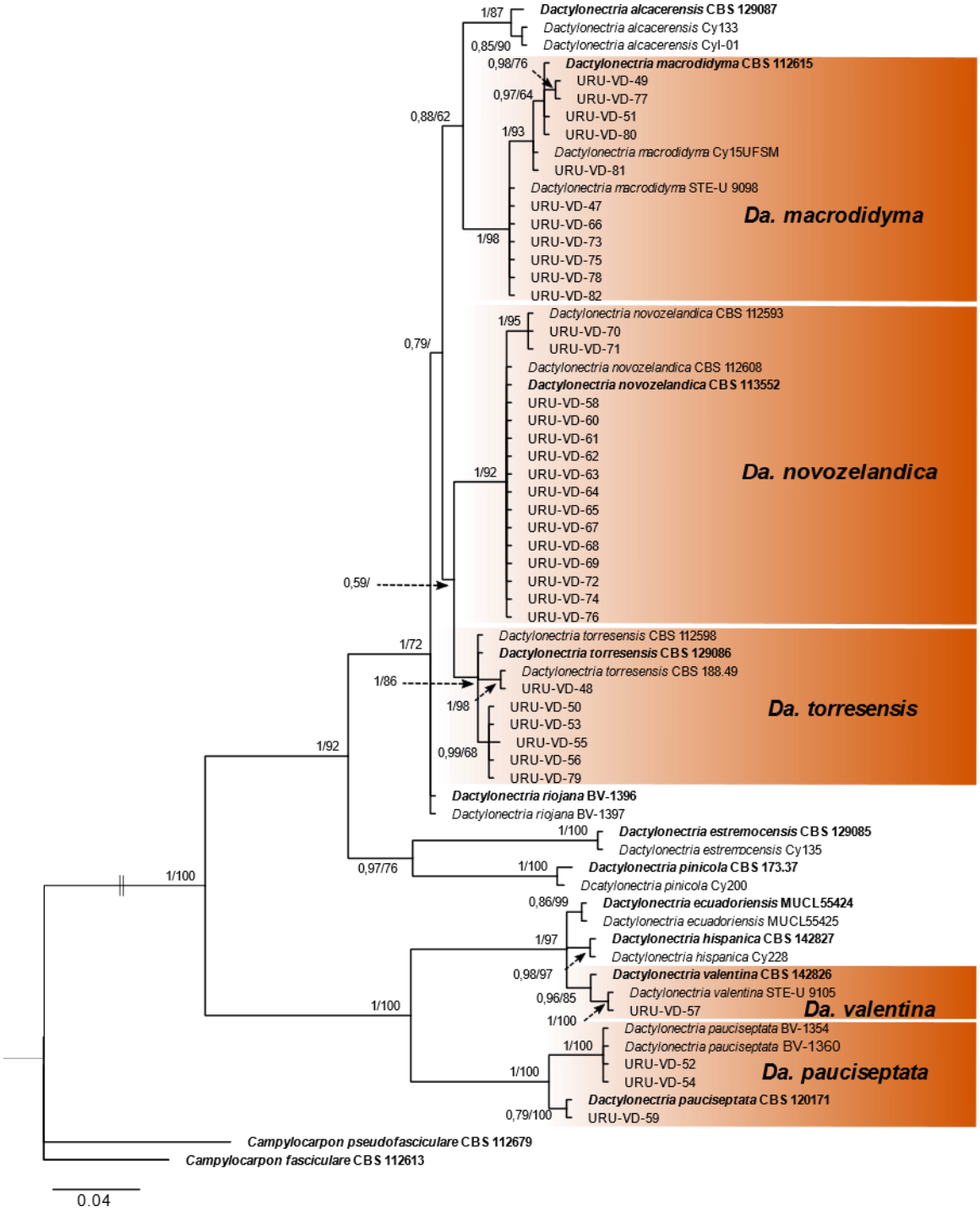

Supplementary Figure 4. Bayesian inference phylogenetic tree inferred from the histone 3 gene region (HIS3) of 36 *Dactylonectria* strains isolated from grapevine propagation materials and sequences obtained from the GenBank (ex-type indicated in bold). *Campylocarpon fasciculare* CBS 112613 and *Campylocarpon pseudofasciculare* CBS 112679 were used as outgroup. Bootstrap support values of posterior probability and maximum likelihood higher than 0.50 and 50 are shown at the nodes before and after the bar, respectively. The scripts indicate that the nodes do not exist in the maximum

likelihood tree. Double hash marks indicate branch lengths shortened at least 2-fold to facilitate visualization. Scale bar represents the estimated number of substitutions per site.

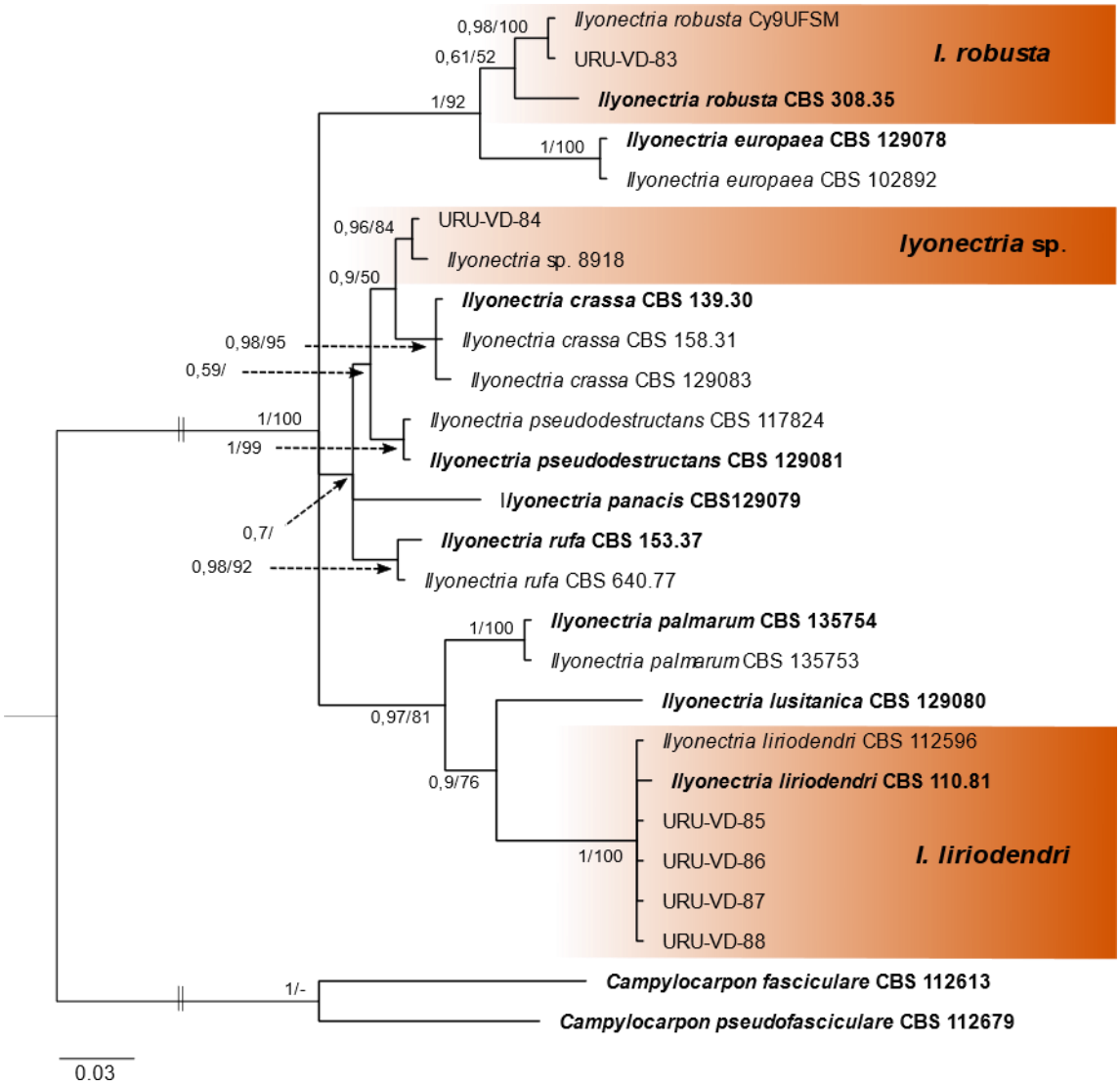

Supplementary Figure 5. Bayesian inference phylogenetic tree inferred from the histone 3 gene region (HIS3) of 6 *Ilyonectria* strains isolated from grapevine propagation materials and sequences obtained from the GenBank (ex-type indicated in bold). *Campylocarpon fasciculare* CBS 112613 and *Campylocarpon pseudofasciculare* CBS 112679 were used as outgroup. Bootstrap support values of posterior probability and maximum likelihood higher than 0.50 and 50 are shown at the nodes before and after the bar, respectively. The scripts indicate that the nodes do not exist in the maximum likelihood tree. Double hash marks indicate branch lengths shortened at least 2-fold to facilitate visualization. Scale bar represents the estimated number of substitutions per site.

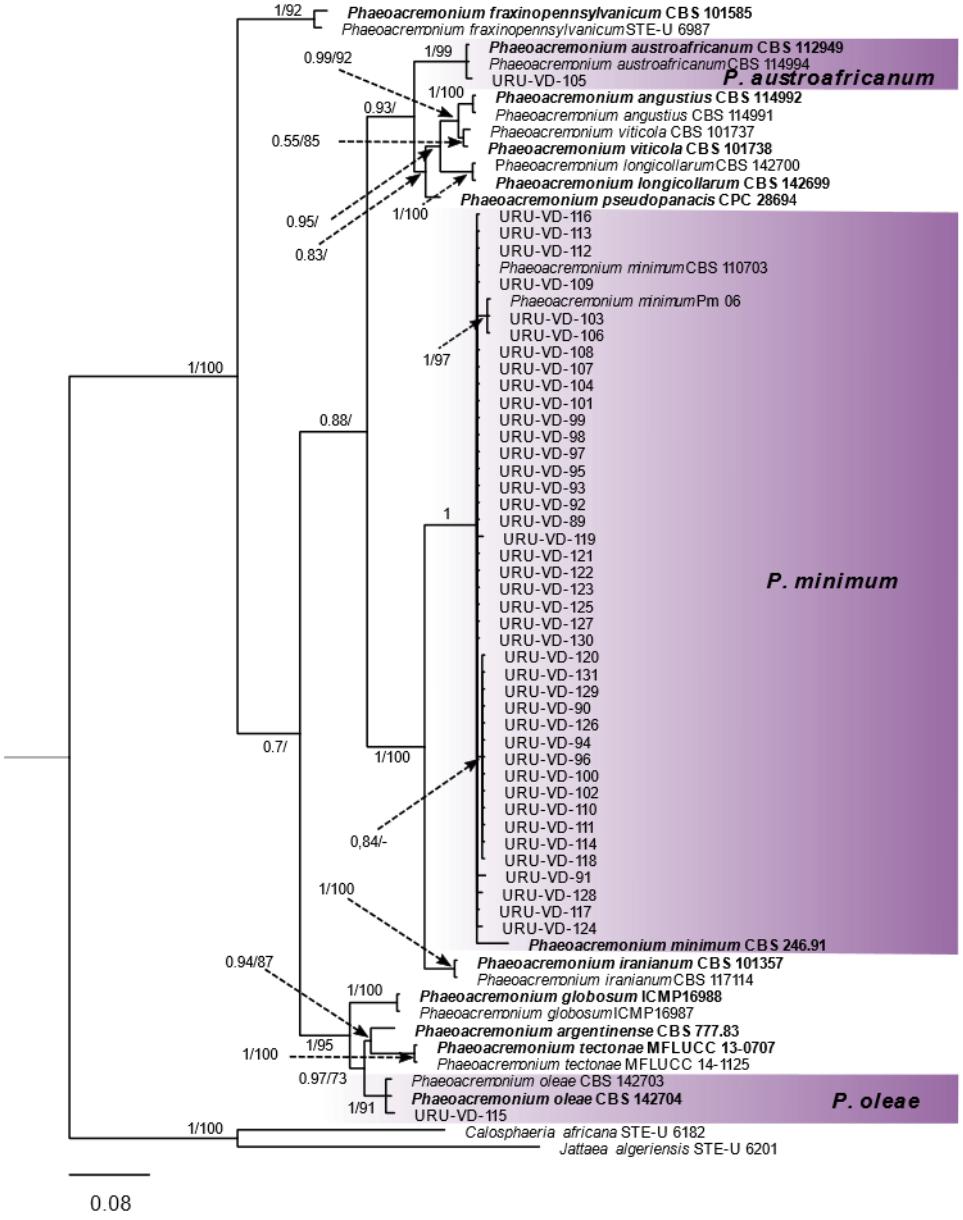

Supplementary Figure 6. Bayesian inference phylogenetic tree inferred from the beta-tubulin gene region (TUB2) of 43 *Phaeoacremonium* strains isolated from grapevine propagation materials and sequences obtained from the GenBank (ex-type indicated in bold). *Calosphaeria africana* STE-U 6182 and *Jattaea algeriensis* STE-U 6201 were used as outgroup. Bootstrap support values of posterior probability and maximum likelihood higher than 0.50 and 50 are shown at the nodes before and after the bar, respectively. The scripts indicate that the nodes do not exist in the maximum likelihood tree. Scale bar represents the estimated number of substitutions per site.

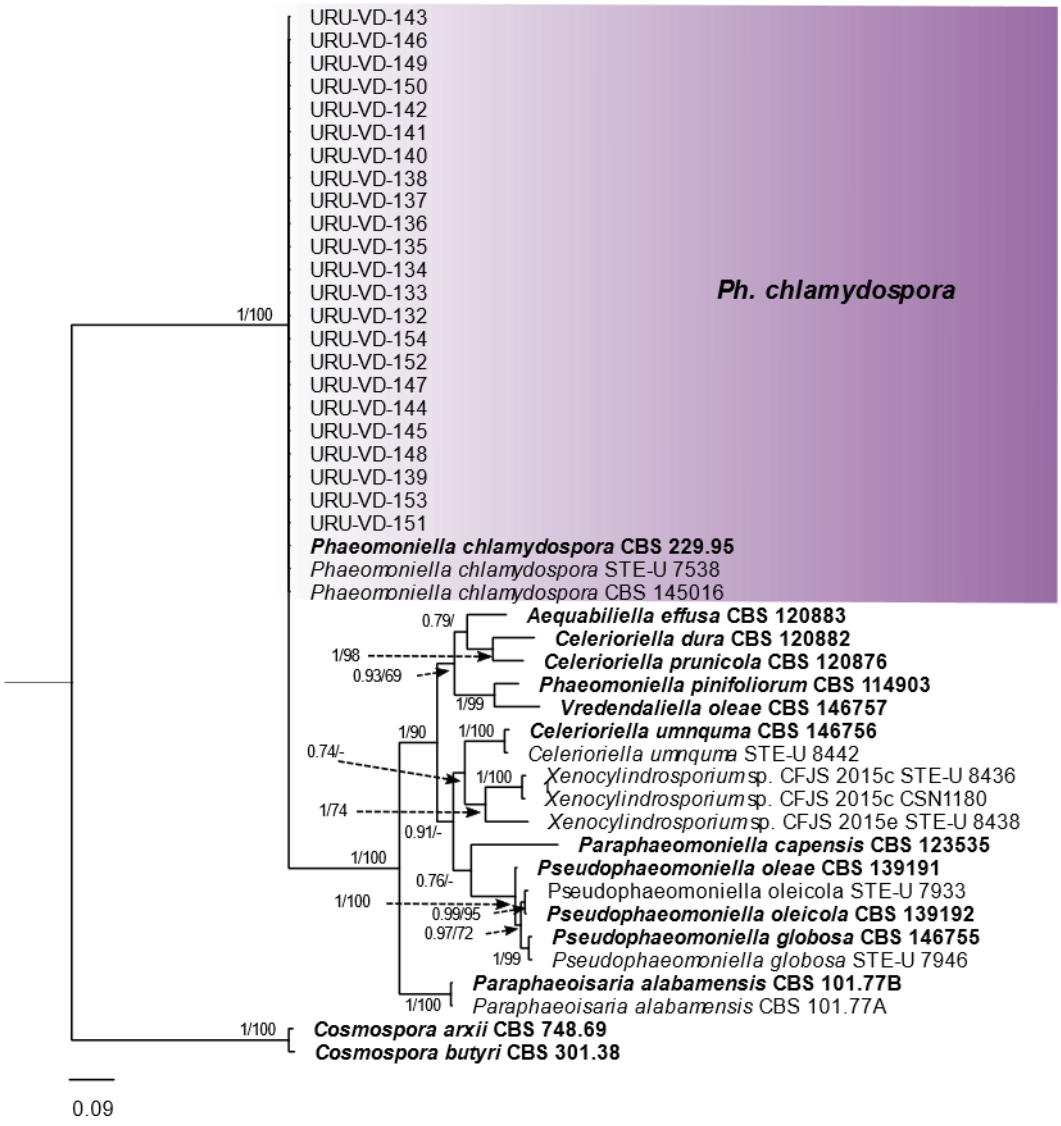

Supplementary Figure 7. Bayesian inference phylogenetic tree inferred from the internal transcribed spacer region and 5.8S rRNA (ITS) of 23 *Phaeomoniella chlamydospora* strains isolated from grapevine propagation materials and sequences obtained from the GenBank (ex-type indicated in bold). *Cosmospora arxii* CBS 748.69 and *Cosmospora butyri* CBS 301.38 were used as outgroup. Bootstrap support values of posterior probability and maximum likelihood higher than 0.50 and 50 are shown at the nodes before and after the bar, respectively. The scripts indicate that the nodes do not exist in the maximum likelihood tree. Scale bar represents the estimated number of substitutions per site.

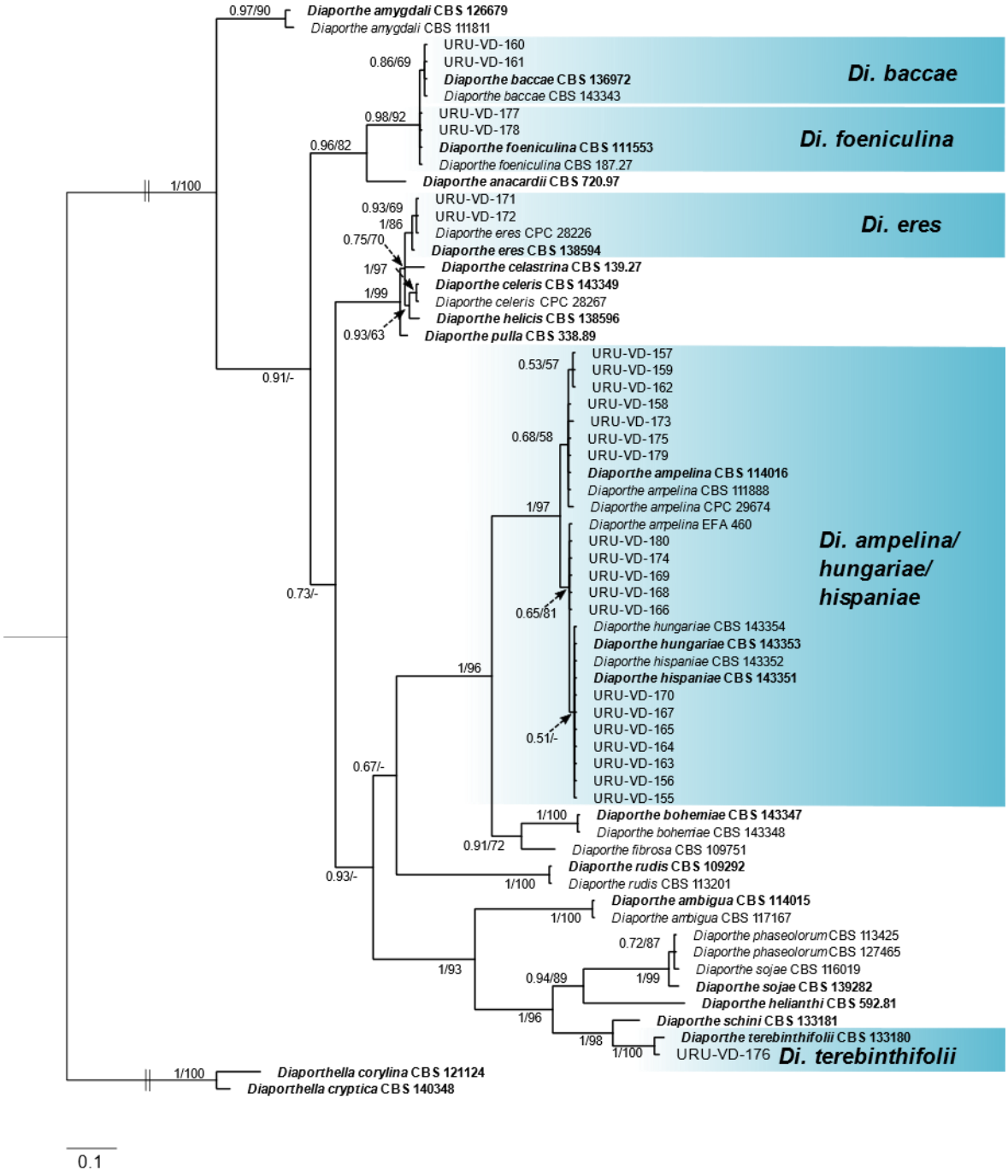

Supplementary Figure 8. Bayesian inference phylogenetic tree inferred from the elongation factor region (TEF) of 26 *Diaporthe* strains isolated from grapevine propagation materials and sequences obtained from the GenBank (ex-type indicated in bold). *Diaporthella corylina* CBS 121124 and *Diaporthella cryptica* CBS 140348 were used as outgroup. Bootstrap support values of posterior probability and maximum likelihood higher than 0.50 and 50 are shown at the nodes before and after the bar, respectively. The scripts indicate that the nodes do not exist in the maximum likelihood

tree. Double hash marks indicate branch lengths shortened at least 2-fold to facilitate visualization. Scale bar represents the estimated number of substitutions per site.

Supplementary Table 1. Accession numbers of DNA sequences obtained from the GenBank and used for the phylogenetic analyses.

Taxon	Fungal species	Strain number	Host	GenBank accesion no.			
				TEF	HIS3	TUB2	ITS
Botryosphaeria	***Botryosphaeria agaves***	**CBS 133992**	*Agave* sp.	JX646856	-	-	-
	Botryosphaeria agaves	CBS 141505	*Agave* sp.	MT592030	-	-	-
	Botryosphaeria dothidea	**CBS 115476**	*Prunus sp.*	AY236898	-	-	-
	Botryosphaeria dothidea	CBS 110302	*Vitis vinifera*	AY573218	-	-	-
	Botryosphaeria dothidea	GZCC 160013	Dead wood	KX447678	-	-	-
	Botryosphaeria dothidea	CGMCC 3.17723	*Morus* sp.	KU221233	-	-	-
	Botryosphaeria dothidea	CGMCC 3.18744	*Cedrus deodara*	KX278107	-	-	-
	Botryosphaeria fabicerciana	**CBS 127193**	*Eucalyptus* sp.	HQ332213	-	-	-
	Botryosphaeria fabicerciana	CBS 127194	*Eucalyptus* sp.	HQ332214	-	-	-
	Botryosphaeria kuwatsukai	**CBS 135219**	*Malus domestica*	KJ433410	-	-	-
	Botryosphaeria kuwatsukai	CGMCC 3.18007	*Malus* sp.	KX197094	-	-	-
	Botryosphaeria ramosa	**CBS 122069**	*Eucalyptus camaldulensis*	EU144070	-	-	-
	Botryosphaeria ramosa	CGMCC 3.18739	*Eucalyptus* hybrid	KX278094	-	-	-
	Botryosphaeria ramosa	CGMCC 3.18741	*Melastoma sanguineum*	KX278102	-	-	-
	Botryosphaeria scharifii	**CBS 124703**	*Mangifera indica*	JQ772057	-	-	-
	Botryosphaeria scharifii	CBS 124702	*Mangifera indica*	JQ772056	-	-	-
Diplodia	***Diplodia allocellula***	**CBS 130408**	*Acacia karroo*	JQ239384	-	-	-
	Diplodia allocellula	CBS 130410	*Acacia karroo*	JQ239386	-	-	-
	Diplodia citricarpa	**CBS 124715**	*Citrus sp.*	KF890189	-	-	-
	Diplodia citricarpa	CBS 124714	*Citrus sp.*	MT592039	-	-	-
	Diplodia eriobotrycola	**CBS 140851**	*Eriobotryia japonica*	MT592047	-	-	-
	Diplodia eriobotrycola	CPC 29680	*Eriobotryia japonica*	KT240193	-	-	-
	Diplodia estuarina	CBS 139668	*Aviccenia marina*	KP860676	-	-	-
	Diplodia pseudoseriata	**CBS 124906**	*Blepharocalyx salicifolius*	EU863181	-	-	-
	Diplodia pseudoseriata	UY1263	*Myrciaria tenella*	EU863182	-	-	-
	Diplodia pseudoseriata	CBS 124933	*Pterocarpus angolensis*	MT592065	-	-	-

	Diplodia pseudoseriata	CBS 124907	*Hexachhlamis edulis*	MT592064	-	-	-
	Diplodia pseudoseriata	B45	*Malus domestica*	KJ499680	-	-	-
	Diplodia sapinea	**CBS 393.84**	*Pinus nigra*	DQ458880	-	-	-
	Diplodia sapinea	CBS 121105	*Prunus persica*	EF445377	-	-	-
	Diplodia scrobiculata	**CBS 118110**	*Pinus banksiana*	AY624253	-	-	-
	Diplodia scrobiculata	CBS 109944	*Pinus greggii*	DQ458884	-	-	-
	Diplodia seriata	**CBS 112555**	*Quercus* sp.	AY573220	-	-	-
	Diplodia seriata	CBS 124139	*Vitis vinifera*	GQ923848	-	-	-
Neofusicoccum	***Neofusicoccum australe***	**CMW 6837**	*Acacia* sp.	AY339270	-	-	-
	Neofusicoccum australe	CMW 6853	*Sequoiadendron giganteum*	AY339271	-	-	-
	Neofusicoccum cryptoaustrale	**CBS 122813**	*Eucalyptus* sp.	FJ752713	-	-	-
	Neofusicoccum cryptoaustrale	CMW 20738	*Eeucalyptus citriodora*	FJ752710	-	-	-
	Neofusicoccum hongkongense	**CGMCC 3.18749**	*Araucaria cunninghamii*	KX278157	-	-	-
	Neofusicoccum hongkongense	CGMCC 3.18747	*Araucaria cunninghamii*	KX278155	-	-	-
	Neofusicoccum kwambonambiense	**CBS 123639**	*Syzygium cordatum*	EU821870	-	-	-
	Neofusicoccum kwambonambiense	CBS 123641	*Syzygium cordatum*	EU821889	-	-	-
	Neofusicoccum luteum	**CBS 110299**	*Vitis vinifera*	AY573217	-	-	-
	Neofusicoccum luteum	CBS 110497	*Vitis vinifera*	EU673277	-	-	-
	Neofusicoccum luteum	**CMW 41365**	*Avicennia marina*	KP860702	-	-	-
	Neofusicoccum luteum	CMW 42481	*Avicennia marina*	KP860692	-	-	-
	Neofusicoccum parvum	**ATCC 58191**	*Populus nigra*	AY236888	-	-	-
	Neofusicoccum parvum	CBS 110301	*Vitis vinifera*	AY573221	-	-	-
	Neofusicoccum parvum	CDFA B139	*Vaccinium corymbosum*	KJ126847	-	-	-
	Neofusicoccum parvum	CBS 145794	*Rhaphiolepis indica*	MN175951	-	-	-
	Neofusicoccum ribis	**CBS 115475**	*Ribes* sp.	AY236877	-	-	-
	Neofusicoccum ribis	CBS 121.26	*Ribes* sp.	AY236879	-	-	-
	Neofusicoccum stellenboschiana	**CBS 110864**	*Vitis vinifera*	AY343348	-	-	-
	Neofusicoccum vitifusiforme	**CBS 110887**	*Vitis vinifera*	AY343343	-	-	-
	Neofusicoccum vitifusiforme	CBS 121113	*Prunus persica*	MT592254	-	-	-
Dactylonectria	***Dactylonectria alcacerensis***	**CBS 129087**	*Vitis vinifera*	-	JF735630	-	-

	Dactylonectria alcacerensis	Cyl-01	*Vitis vinifera*	-	MG745823	-	-
	Dactylonectria alcacerensis	Cy133	*Vitis vinifera*	-	JF735628	-	-
	Dactylonectria ecuadoriensis	**MUCL55424**	*Piper* sp.	-	MF683683	-	-
	Dactylonectria ecuadoriensis	MUCL55425	*Piper* sp.	-	MF683684	-	-
	Dactylonectria estremocencsis	**CBS 129085**	*Vitis vinifera*	-	JF735617	-	-
	Dactylonectria estremocencsis	Cy135	*Vitis vinifera*	-	JF735615	-	-
	Dactylonectria hispanica	**CBS 142827**	*Pinus halepensis*	-	KY676864	-	-
	Dactylonectria hispanica	Cy228	*Ficus* sp.	-	JF735578	-	-
	Dactylonectria macrodidyma	**CBS 112615**	*Vitis vinifera*	-	JF735647	-	-
	Dactylonectria macrodidyma	STE-U 9098	*Olea europaea* subsp. *europaea*	-	MT309058	-	-
	Dactylonectria macrodidyma	Cy15UFSM	*Vitis vinifera*	-	KF633159	-	-
	Dactylonectria novozelandica	**CBS 113552**	*Vitis* sp.	-	JF735633	-	-
	Dactylonectria novozelandica	CBS 112608	*Vitis vinifera*	-	JF735632	-	-
	Dactylonectria novozelandica	CBS 112593	*Vitis vinifera*	-	JF735631	-	-
	Dactylonectria pauciseptata	**CBS 120171**	*Vitis* sp.	-	JF735587	-	-
	Dactylonectria pauciseptata	BV-1354	*Vitis vinifera*	-	MK579256	-	-
	Dactylonectria pauciseptata	BV-1360	*Vitis vinifera*	-	MK579258	-	-
	Dactylonectria pinicola	**CBS 173.37**	*Pinus laricio*	-	JF735614	-	-
	Dactylonectria pinicola	Cy200	*Vitis vinifera*	-	JF735612	-	-
	Dactylonectria riojana	**BV-1396**	*Vitis* sp.	-	MK602831	-	-
	Dactylonectria riojana	BV-1397	*Vitis* sp.	-	MK602832	-	-
	Dactylonectria torresensis	**CBS 129086**	*Vitis vinifera*	-	JF735681	-	-
	Dactylonectria torresensis	CBS 112598	*Vitis vinifera*	-	JF735662	-	-
	Dactylonectria torresensis	CBS 188.49	*Abies nordmanniana*	-	JF735658	-	-
	Dactylonectria valentina	**CBS 142826**	*Ilex aquifolium*	-	KY676863	-	-
	Dactylonectria valentina	STE-U 9105	*Olea europaea* subsp. *europaea*	-	MT309072	-	-
Ilyonectria	***Ilyonectria crassa***	**CBS 139.30**	*Lilium* sp.	-	JF735534	-	-
	Ilyonectria crassa	CBS 158.31	*Narcissus* sp.	-	JF735535	-	-
	Ilyonectria crassa	CBS 129083	*Panax quinquefolium*	-	JF735536	-	-

	Ilyonectria europea	**CBS 129078**	*Vitis vinifera*	-	JF735567	-	-
	Ilyonectria europea	CBS 102892	Stem	-	JF735569	-	-
	Ilyonectria liriodendri	**CBS 110.81**	*Liriodedron tulipifera*	-	JF735507	-	-
	Ilyonectria liriodendri	CBS 112596	*Vitis vinifera*	-	JF735511	-	-
	Ilyonectria lusitanica	**CBS 129080**	*Vitis vinifera*	-	JF735570	-	-
	Ilyonectria palmarum	**CBS 135754**	*Howea forsteriana*	-	HF922620	-	-
	Ilyonectria palmarum	CBS 135753	*Howea forsteriana*	-	HF922621	-	-
	Ilyonectria panacis	**CBS 129079**	*Panax quinquefolium*	-	JF735572	-	-
	Ilyonectria pseudodestructans	**CBS 129081**	*Vitis vinifera*	-	JF735563	-	-
	Ilyonectria pseudodestructans	CBS 117824	*Quercus* sp.	-	JF735562	-	-
	Ilyonectria rufa	**CBS 153.37**	*Dune sand*	-	JF735540	-	-
	Ilyonectria rufa	CBS 640.77	*Abies alba*	-	JF735542	-	-
	Ilyonectria robusta	**CBS 308.35**	*Panax quinquefolium*	-	JF735518	-	-
	Ilyonectria robusta	Cy9UFSM	*Vitis vinifera*	-	KF633172	-	-
	***Ilyonectria* sp.**	**8918**	*Prunus persica* sp.	-	MK765799	-	-
Phaeoacremonium	***Phaeoacremonium angustius***	**CBS 114992**	*Vitis vinifera*	-	-	DQ173104	-
	Phaeoacremonium angustius	CBS 114991	*Vitis vinifera*	-	-	DQ173103	-
	Phaeoacremonium argentinense	**CBS 777.83**	Soil	-	-	DQ173108	-
	Phaeoacremonium austroafricanum	**CBS 112949**	*Vitis vinifera*	-	-	DQ173099	-
	Phaeoacremonium austroafricanum	CBS 114994	*Vitis vinifera*	-	-	DQ173102	-
	Phaeoacremonium fraxinopennsylvanicum	**CBS 101585**	*Vitis vinifera*	-	-	KF764684	-
	Phaeoacremonium fraxinopennsylvanicum	STE-U 6987	*Vitis vinifera*	-	-	JQ038913	-
	Phaeoacremonium globosum	**ICMP16988**	*Vitis berlandieri* × *Vitis riparia*	-	-	EU596525	-
	Phaeoacremonium globosum	ICMP16987	*Vitis berlandieri* × *Vitis riparia*	-	-	EU596527	-
	Phaeoacremonium iranium	**CBS 101357**	*Vitis vinifera*	-	-	DQ173097	-
	Phaeoacremonium iranium	CBS 117114	*Vitis vinifera*	-	-	DQ173098	-
	Phaeoacremonium longicollarum	**CBS 142699**	*Prunus armeniaca*	-	-	KY906689	-
	Phaeoacremonium longicollarum	CBS 142700	*Psidium guajava*	-	-	KY906879	-
	Phaeoacremonium minimum	**CBS 246.91**	*Vitis vinifera*	-	-	AF246811	-

	Phaeoacremonium minimum	CBS 110703	*Vitis vinifera*	-	-	DQ173094	-
	Phaeoacremonium minimum	Pm-06	*Vitis vinifera*	-	-	MG745808	-
	Phaeoacremonium oleae	**CBS 142704**	*Olea europaea*	-	-	KY906937	-
	Phaeoacremonium oleae	CBS 142703	*Olea europaea*	-	-	KY906891	-
	Phaeoacremonium pseudopanacis	CBS 142101	*Pseudopanax crassifolius*	-	-	KY173609	-
	Phaeoacremonium tectonae	**MFLUCC 13-0707**	*Tectona grandis*	-	-	KT285563	-
	Phaeoacremonium tectonae	MFLUCC 14-1125	*Tectona grandis*	-	-	KT285565	-
	Phaeoacremonium viticola	**CBS 101738**	*Vitis vinifera*	-	-	AF192391	-
	Phaeoacremonium viticola	CBS 101737	*Vitis vinifera*	-	-	AF246817	-
Phaeomoniellales	***Aequabiliella effusa***	**CBS 120883**	*Prunus salicina*	-	-	-	NR132005
	Celeriorella umnqumae	STE-U 8442	*Olea europaea*	-	-	-	MT791052
	Celerioriella dura	**CBS 120882**	*Prunus salicina*	-	-	-	NR132004
	Celerioriella prunicola	**CBS 120876**	*Prunus salicina*	-	-	-	NR132003
	Celerioriella umnqumae	**CBS 146756**	*Olea europaea*	-	-	-	MT791051
	Celerioriella umnqumae	STE-U 8442	*Olea europaea*	-	-	-	MT791052
	Paraphaeoisaria alabamensis	**CBS 101.77B**	*Cronartium quercuum*	-	-	-	MH861029
	Paraphaeoisaria alabamensis	CBS 101.77A	*Cronartium quercuum*	-	-	-	MH861028
	Paraphaeomoniella capensis	**CBS 123535**	*Encephalartos altensteinii*	-	-	-	NR137711
	Paraphaeomoniella pinifoliorum	**CBS 114903**	*Vitis vinifera*	-	-	-	NR160218
	Phaeomoniella chlamydospora	**CBS 229.95**	*Vitis vinifera*	-	-	-	NR155612
	Phaeomoniella chlamydospora	STEU7538	*Vitis vinifera*	-	-	-	KU244284
	Phaeomoniella chlamydospora	CBS 145016	*Vitis vinifera*	-	-	-	MH999525
	Pseudophaeomoniella globosa	**CBS 146755**	*Olea europaea*	-	-	-	MT791056
	Pseudophaeomoniella globosa	STE-U 7946	*Olea europaea*	-	-	-	MT791062
	Pseudophaeomoniella oleae	**CBS 139191**	*Olea europaea*	-	-	-	NR137966
	Pseudophaeomoniella oleicola	**CBS 139192**	*Olea europaea*	-	-	-	NR137965
	Pseudophaeomoniella oleicola	STE-U 7933	*Olea europaea*	-	-	-	MW008603
	Vredendaliella oleae	**CBS 146757**	*Olea europaea*	-	-	-	MT791073
	Xenocylindrosporium sp. CFJS2015c	STE-U 8436	*Olea europaea*	-	-	-	MT791080

	Xenocylindrosporium sp. CFJS2015c	CSN 1180	*Olea europaea*	-	-	-	MT791077
	Xenocylindrosporium sp. CFJS2015e	STE-U 8438	*Olea europaea*	-	-	-	MT791079
Diaporthe	***Diaporthe ambigua***	**CBS 114015**	*Pyrus communis*	KC343736	-	-	-
	Diaporthe ambigua	CBS 117167	*Aspalathus linearis*	KC343737	-	-	-
	Diaporthe ampelina	**CBS 114016**	*Vitis vinifera*	GQ250351	-	-	-
	Diaporthe ampelina	CBS 111888	*Vitis vinifera*	KC343742	-	-	-
	Diaporthe ampelina	CPC 29674	*Vitis vinifera*	MG281514	-	-	-
	Diaporthe ampelina	EFA 460	*Vitis vinifera*	MH051278	-	-	-
	Diaporthe amygdali	**CBS 126679**	*Prunus dulcis*	KC343748	-	-	-
	Diaporthe amygdali	CBS 111811	*Vitis vinifera*	KC343745	-	-	-
	Diaporthe anacardii	**CBS 720.97**	*Anacardium occidentale*	KC343750	-	-	-
	Diaporthe baccae	**CBS 136972**	*Vaccinium corymbosum*	KJ160597	-	-	-
	Diaporthe baccae	CBS 143343	*Vitis vinifera*	MG281522	-	-	-
	Diaporthe bohemiae	**CBS 143347**	*Vitis* spp.	MG281536	-	-	-
	Diaporthe bohemiae	CBS 143348	*Vitis* spp.	MG281537	-	-	-
	Diaporthe celastrina	**CBS 139.27**	*Celastrus* sp.	KC343773	-	-	-
	Diaporthe celeris	**CBS 143349**	*Vitis vinifera*	MG281538	-	-	-
	Diaporthe celeris	CPC 28267	*Vitis vinifera*	MG281540	-	-	-
	Diaporthe eres	**CBS 138594**	*Ulmus laevis*	KJ210550	-	-	-
	Diaporthe eres	CPC 28226	*Vitis vinifera*	MG281546	-	-	-
	Diaporthe fibrosa	CBS 109751	*Rhamnus cathartica*	KC343825	-	-	-
	Diaporthe foeniculina	**CBS 111553**	*Foeniculum vulgare*	KC343827	-	-	-
	Diaporthe foeniculina	CBS 187.27	*Camellia sinensis*	KC343833	-	-	-
	Diaporthe helianthi	**CBS 592.81**	*Helianthus annuus*	KC343841	-	-	-
	Diaporthe helicis	**CBS 138596**	*Hedera helix*	KJ210559	-	-	-
	Diaporthe hispaniae	**CBS 143351**	*Vitis vinifera*	MG281644	-	-	-
	Diaporthe hispaniae	CBS 143352	*Vitis vinifera*	MG281645	-	-	-
	Diaporthe hungariae	**CBS 143353**	*Vitis vinifera*	MG281647	-	-	-
	Diaporthe hungariae	CBS 143354	*Vitis vinifera*	MG281648	-	-	-

	Diaporthe phaseolorum	CBS 113425	*Olearia* cf. *rani*	KC343900	-	-	-
	Diaporthe phaseolorum	CBS 127465	*Actinidia chinensis*	KC343903	-	-	-
	Diaporthe pulla	**CBS 338.89**	*Hedera helix*	KC343878	-	-	-
	Diaporthe rudis	**CBS 109292**	*Laburnum anagyroides*	KC843090	-	-	-
	Diaporthe rudis	CBS 113201	*Vitis vinifera*	KC343960	-	-	-
	Diaporthe schini	**CBS 133181**	*Schinus terebinthifolius*	KC343917	-	-	-
	Diaporthe sojae	**CBS 139282**	*Glycine max*	KJ590762	-	-	-
	Diaporthe sojae	CBS 116019	*Caperonia palustris*	KC343901	-	-	-
	Diaporthe terebinthifolii	**CBS 133180**	*Schinus terebinthifolius*	KC343942	-	-	-
Outgroups	*Calosphaeria africana*	CBS 120870	*Prunus armeniaca*	-	-	EU367464	-
	Campylocarpon fasciculare	**CBS 112613**	*Vitis vinifera*	-	JF735502	-	-
	Campylocarpon pseudofasciculare	**CBS 112679**	*Vitis vinifera*	-	JF735503	-	-
	Cosmospora arxii	**CBS 748.69**	*Hypoxylon* sp.	-	-	-	NR145062
	Cosmospora butry	CBS 301.308	Butter	-	-	-	MW827605
	Diaporthella corylina	CBS 121124	*Corylus* sp.	KC343730	-	-	-
	Diaporthella cryptica	**CBS 140348**	*Corylus avellana*	MN271854	-	-	-
	Jattaea algeriensis	CBS 120871	*Prunus salicina*	-	-	EU367466	-
	Lasiodiplodia theobromae	**CBS 164.96**	Fruit along coral reef coast	AY640258	-	-	-
	Lasiodiploida parva	**CBS 456.78**	Cassava-field-soil	EF622063	-	-	-

Supplementary Table 2. Evolutionary models of nucleotide substitution used for the Bayesian Inference analysis, suggested by jModelTest2 according to the Akaike information criterion (AIC).

Taxon	**AIC**[1]
Botryosphaeria	GTR + G
Diplodia	GTR + G
Neofusicoccum	HKY85 + I + G
Dactylonectria	GTR + G
Ilyonectria	GTR + G
Phaeoacremonium	GTR + G
Phaeomoniella	GTR + I
Diaporthe	HKY85 + I + G

[1] GTR = Generalised Time Reversible model
HKY85 = Hasegawa-Kishino-Yano 85 model
I = refers to proportion of invariable sites estimated
G = refers to gamma distribution parameter estimated

Supplementary Table 3. Uruguayan isolates of grapevine trunk diseases pathogens obtained from nursery propagation materials of different grapevine cultivars and rootstocks.

Fungal species	Isolate	Cultivar/Rootstock	Symptomatic or asymptomatic material	Nursery propagation stage[1]	Year of collection	Gene region[2]	GenBank accesion no.
Botryosphaeria dothidea	URU-VD-1	Gravesac	symptomatic	2	2018	TEF	ON573060
	URU-VD-2	Merlot	asymptomatic	1	2018	TEF	ON573061
	URU-VD-3	3309C	symptomatic	1	2018	TEF	ON573062
	URU-VD-4	Albariño	symptomatic	1	2018	TEF	ON573063
	URU-VD-5	Tannat/Gravesac	symptomatic	4	2018	TEF	ON573064
	URU-VD-6	Cabernet Franc/3309C	symptomatic	4	2018	TEF	ON573065
	URU-VD-7	Chardonnay/SO4	symptomatic	4	2018	TEF	ON573066
	URU-VD-8	Marselan	asymptomatic	1	2019	TEF	ON573067
	URU-VD-9	Gravesac	asymptomatic	1	2019	TEF	ON573068
	URU-VD-10	3309C	asymptomatic	1	2019	TEF	ON573069
	URU-VD-11	Albariño/Gravesac	symptomatic	4	2019	TEF	ON573070
	URU-VD-12	Albariño/Gravesac	symptomatic	4	2019	TEF	ON573071
	URU-VD-13	Tannat/1103P	symptomatic	4	2019	TEF	ON573072
	URU-VD-14	Tannat/1103P	symptomatic	4	2019	TEF	ON573073
	URU-VD-15	Tannat	symptomatic	2	2019	TEF	ON573074
	URU-VD-16	Albariño/SO4	symptomatic	3	2019	TEF	ON573075
Diplodia pseudoseriata	URU-VD-18	Merlot	asymptomatic	2	2018	TEF	ON573076
	URU-VD-19	Merlot	symptomatic	2	2018	TEF	ON573077
	URU-VD-20	Gravesac	asymptomatic	2	2018	TEF	ON573078
	URU-VD-21	1103P	symptomatic	2	2018	TEF	ON573079
	URU-VD-22	101-14	asymptomatic	1	2018	TEF	ON573080
	URU-VD-24	101-14	asymptomatic	2	2018	TEF	ON573081

	URU-VD-25	Tannat	asymptomatic	1	2019	TEF	ON573082
Diplodia seriata	URU-VD-17	Merlot	asymptomatic	2	2018	TEF	ON573083
	URU-VD-23	Lácrima-Christi	asymptomatic	2	2018	TEF	ON573084
Neofusicoccum australe	URU-VD-27	Merlot	symptomatic	2	2018	TEF	ON573085
Neofusicoccum cryptoaustrale	URU-VD-28	Gravesac	asymptomatic	1	2018	TEF	ON573086
	URU-VD-31	Albariño	asymptomatic	2	2018	TEF	ON573087
	URU-VD-36	Albariño/Gravesac	symptomatic	3	2018	TEF	ON573088
Neofusicoccum luteum	URU-VD-30	Albariño	asymptomatic	1	2018	TEF	ON573089
	URU-VD-37	Lácrima/1103P	asymptomatic	4	2019	TEF	ON573090
	URU-VD-39	Tannat/1103P	symptomatic	4	2019	TEF	ON573091
Neofusicoccum parvum	URU-VD-26	1103P	asymptomatic	2	2018	TEF	ON573092
	URU-VD-29	Lácrima-Christi	symptomatic	1	2018	TEF	ON573093
	URU-VD-32	Moscatel de Hamburgo/SO4	asymptomatic	3	2018	TEF	ON573094
	URU-VD-33	Lácrima-Christi/SO4	asymptomatic	3	2018	TEF	ON573095
	URU-VD-34	Merlot/101-14	symptomatic	4	2018	TEF	ON573096
	URU-VD-35	Albariño/101-14	asymptomatic	3	2019	TEF	ON573097
	URU-VD-38	Albariño/101-14	symptomatic	4	2019	TEF	ON573098
	URU-VD-40	3309C	symptomatic	2	2019	TEF	ON573099
	URU-VD-41	Albariño/SO4	asymptomatic	3	2019	TEF	ON573100
	URU-VD-42	Tannat/Gravesac	symptomatic	3	2019	TEF	ON573101
	URU-VD-43	Tannat/Gravesac	symptomatic	3	2019	TEF	ON573102
	URU-VD-44	Marselan/3309C	symptomatic	3	2019	TEF	ON573103
	URU-VD-45	Albariño/101-14	symptomatic	4	2019	TEF	ON573104
	URU-VD-46	Tannat	symptomatic	2	2019	TEF	ON573105
Dactylonectria macrodidyma	URU-VD-47	Merlot/101-14	symptomatic	4	2018	HIS3	ON573132
	URU-VD-49	Merlot/101-14	symptomatic	4	2018	HIS3	ON573133
	URU-VD-51	Merlot/101-14	symptomatic	4	2018	HIS3	ON573134
	URU-VD-66	Tannat/1103P	symptomatic	4	2019	HIS3	ON573135

	URU-VD-73	Albariño/101-14	symptomatic	4	2019	HIS3	ON573136
	URU-VD-75	Albariño/Gravesac	symptomatic	4	2019	HIS3	ON573137
	URU-VD-77	Albariño/Gravesac	symptomatic	4	2019	HIS3	ON573138
	URU-VD-78	Albariño/Gravesac	symptomatic	4	2019	HIS3	ON573139
	URU-VD-80	Tannat/1103P	symptomatic	4	2019	HIS3	ON573140
	URU-VD-81	Tannat/1103P	symptomatic	4	2019	HIS3	ON573141
	URU-VD-82	Tannat/1103P	symptomatic	4	2019	HIS3	ON573142
Dactylonectria novozelandica	URU-VD-58	Albariño/101-14	symptomatic	4	2019	HIS3	ON573143
	URU-VD-60	Albariño/101-14	symptomatic	4	2019	HIS3	ON573144
	URU-VD-61	Albariño/101-14	symptomatic	4	2019	HIS3	ON573145
	URU-VD-62	Albariño/101-14	symptomatic	4	2019	HIS3	ON573146
	URU-VD-63	Albariño/101-14	symptomatic	4	2019	HIS3	ON573147
	URU-VD-64	Albariño/Gravesac	symptomatic	4	2019	HIS3	ON573148
	URU-VD-65	Albariño/Gravesac	symptomatic	4	2019	HIS3	ON573149
	URU-VD-67	Tannat/1103P	symptomatic	4	2019	HIS3	ON573150
	URU-VD-68	Tannat/1103P	symptomatic	4	2019	HIS3	ON573151
	URU-VD-69	Tannat/1103P	symptomatic	4	2019	HIS3	ON573152
	URU-VD-70	Albariño/101-14	symptomatic	4	2019	HIS3	ON573153
	URU-VD-71	Albariño/101-14	symptomatic	4	2019	HIS3	ON573154
	URU-VD-72	Albariño/101-14	symptomatic	4	2019	HIS3	ON573155
	URU-VD-74	Albariño/101-14	symptomatic	4	2019	HIS3	ON573156
	URU-VD-76	Albariño/Gravesac	symptomatic	4	2019	HIS3	ON573157
Dactylonectria pauciseptata	URU-VD-52	Tannat/Gravesac	symptomatic	4	2018	HIS3	ON573158
	URU-VD-54	Chardonnay/SO4	symptomatic	4	2018	HIS3	ON573159
	URU-VD-59	Tannat/1103P	symptomatic	4	2019	HIS3	ON573160
Dactylonectria torresensis	URU-VD-48	Merlot/101-14	symptomatic	4	2018	HIS3	ON573161
	URU-VD-50	Merlot/101-14	symptomatic	4	2018	HIS3	ON573162
	URU-VD-53	Tannat/Gravesac	symptomatic	4	2018	HIS3	ON573163

	URU-VD-55	Chardonnay/SO4	symptomatic	4	2018	HIS3	ON573164
	URU-VD-56	Lácrima/1103P	symptomatic	4	2018	HIS3	ON573165
	URU-VD-79	Albariño/Gravesac	symptomatic	4	2019	HIS3	ON573166
Dactylonectria valentina	URU-VD-57	Lácrima/1103P	symptomatic	4	2018	HIS3	ON573167
Ilyonectria liriodendri	URU-VD-85	Tannat/Gravesac	symptomatic	4	2018	HIS3	ON573168
	URU-VD-86	Albariño/Gravesac	symptomatic	4	2019	HIS3	ON573169
	URU-VD-87	Albariño/Gravesac	symptomatic	4	2019	HIS3	ON573170
	URU-VD-88	Tannat/1103P	symptomatic	4	2019	HIS3	ON573171
Ilyonectria robusta	URU-VD-83	Tannat/Gravesac	symptomatic	4	2018	HIS3	ON573172
Ilyonectria sp.	URU-VD-84	Tannat/Gravesac	symptomatic	4	2018	HIS3	ON573173
Phaeoacremonium minimum	URU-VD-89	Merlot/101-14	symptomatic	4	2018	TUB2	ON573174
	URU-VD-90	Merlot/101-14	symptomatic	4	2018	TUB2	ON573175
	URU-VD-91	Tannat/Gravesac	symptomatic	4	2018	TUB2	ON573176
	URU-VD-92	Tannat/Gravesac	symptomatic	4	2018	TUB2	ON573177
	URU-VD-93	Tannat/Gravesac	symptomatic	4	2018	TUB2	ON573178
	URU-VD-94	Tannat/Gravesac	symptomatic	4	2018	TUB2	ON573179
	URU-VD-95	Tannat/Gravesac	symptomatic	4	2018	TUB2	ON573180
	URU-VD-96	Tannat/Gravesac	symptomatic	4	2018	TUB2	ON573181
	URU-VD-97	Tannat/Gravesac	symptomatic	4	2018	TUB2	ON573182
	URU-VD-98	Tannat/Gravesac	symptomatic	4	2018	TUB2	ON573183
	URU-VD-99	Chardonnay/SO4	symptomatic	4	2018	TUB2	ON573184
	URU-VD-100	Chardonnay/SO4	symptomatic	4	2018	TUB2	ON573185
	URU-VD-101	Tannat/Gravesac	symptomatic	4	2018	TUB2	ON573186
	URU-VD-102	Tannat/Gravesac	symptomatic	4	2018	TUB2	ON573187
	URU-VD-103	Chardonnay/SO4	symptomatic	4	2018	TUB2	ON573188
	URU-VD-104	Chardonnay/SO4	symptomatic	4	2018	TUB2	ON573189
	URU-VD-106	Chardonnay/SO4	symptomatic	4	2018	TUB2	ON573190
	URU-VD-107	Chardonnay/SO4	symptomatic	4	2018	TUB2	ON573191

	URU-VD-108	Chardonnay/SO4	symptomatic	4	2018	TUB2	ON573192
	URU-VD-109	Chardonnay/SO4	symptomatic	4	2018	TUB2	ON573193
	URU-VD-110	Lácrima Christi/1103P	symptomatic	4	2018	TUB2	ON573194
	URU-VD-111	Lácrima Christi/1103P	symptomatic	4	2018	TUB2	ON573195
	URU-VD-112	Lácrima Christi/1103P	symptomatic	4	2018	TUB2	ON573196
	URU-VD-113	Lácrima Christi/1103P	symptomatic	4	2018	TUB2	ON573197
	URU-VD-114	Lácrima Christi/1103P	symptomatic	4	2018	TUB2	ON573198
	URU-VD-116	Lácrima Christi/1103P	symptomatic	4	2018	TUB2	ON573199
	URU-VD-117	Albariño/101-14	symptomatic	4	2019	TUB2	ON573200
	URU-VD-118	Albariño/101-14	symptomatic	4	2019	TUB2	ON573201
	URU-VD-119	Albariño/101-14	symptomatic	4	2019	TUB2	ON573202
	URU-VD-120	Albariño/101-14	symptomatic	4	2019	TUB2	ON573203
	URU-VD-121	Albariño/Gravesac	symptomatic	4	2019	TUB2	ON573204
	URU-VD-122	Tannat/1103P	symptomatic	4	2019	TUB2	ON573205
	URU-VD-123	Tannat/1103P	symptomatic	4	2019	TUB2	ON573206
	URU-VD-124	Tannat/1103P	symptomatic	4	2019	TUB2	ON573207
	URU-VD-125	Tannat/1103P	symptomatic	4	2019	TUB2	ON573208
	URU-VD-126	Tannat/1103P	symptomatic	4	2019	TUB2	ON573209
	URU-VD-127	Tannat/1103P	symptomatic	4	2019	TUB2	ON573210
	URU-VD-128	Tannat/1103P	symptomatic	4	2019	TUB2	ON573211
	URU-VD-129	Tannat/1103P	symptomatic	4	2019	TUB2	ON573212
	URU-VD-130	Tannat/Gravesac	symptomatic	3	2019	TUB2	ON573213
	URU-VD-131	Marselan/3309C	symptomatic	3	2019	TUB2	ON573214
Phaeoacremonium austroafricanum	URU-VD-105	Chardonnay/SO4	symptomatic	4	2018	TUB2	ON573215
Phaeoacremonium oleae	URU-VD-115	Lácrima Christi/1103P	asymptomatic	4	2018	TUB2	ON573216
Phaeomoniella chlamydospora	URU-VD-132	Gravesac	symptomatic	1	2018	ITS	ON584361
	URU-VD-133	1103P	asymptomatic	1	2018	ITS	ON584362
	URU-VD-134	Marselan	symptomatic	1	2018	ITS	ON584363

	URU-VD-135	Moscatel de Hamburgo/SO4	asymptomatic	3	2018	ITS	ON584364
	URU-VD-136	Cabernet Franc/3309C	symptomatic	4	2018	ITS	ON584365
	URU-VD-137	Cabernet Franc/3309C	symptomatic	4	2018	ITS	ON584366
	URU-VD-138	Cabernet Franc/3309C	symptomatic	4	2018	ITS	ON584367
	URU-VD-139	3309C	asymptomatic	1	2018	ITS	ON584368
	URU-VD-140	Tannat/Gravesac	symptomatic	4	2018	ITS	ON584369
	URU-VD-141	Chardonnay/SO4	symptomatic	4	2018	ITS	ON584370
	URU-VD-142	Chardonnay/SO4	symptomatic	4	2018	ITS	ON584371
	URU-VD-143	Marselan	symptomatic	1	2019	ITS	ON584372
	URU-VD-144	Albariño/101-14	symptomatic	4	2019	ITS	ON584373
	URU-VD-145	Albariño/101-14	symptomatic	4	2019	ITS	ON584374
	URU-VD-146	Albariño/101-14	symptomatic	4	2019	ITS	ON584375
	URU-VD-147	Albariño/101-14	symptomatic	4	2019	ITS	ON584376
	URU-VD-148	Albariño/101-14	symptomatic	4	2019	ITS	ON584377
	URU-VD-149	Albariño/101-14	symptomatic	4	2019	ITS	ON584378
	URU-VD-150	Albariño/Gravesac	symptomatic	4	2019	ITS	ON584379
	URU-VD-151	Albariño/Gravesac	symptomatic	4	2019	ITS	ON584380
	URU-VD-152	Tannat/1103P	symptomatic	4	2019	ITS	ON584381
	URU-VD-153	Tannat/1103P	symptomatic	4	2019	ITS	ON584382
	URU-VD-154	Marselan/3309C	symptomatic	3	2019	ITS	ON584383
Diaporthe baccae	URU-VD-160	Albariño	asymptomatic	2	2018	TEF	ON573106
	URU-VD-161	Albariño	symptomatic	2	2018	TEF	ON573107
Diaporthe eres	URU-VD-171	Chardonnay/SO4	symptomatic	4	2018	TEF	ON573108
	URU-VD-172	Chardonnay/SO4	symptomatic	4	2018	TEF	ON573109
Diaporthe foeniculina	URU-VD-177	Tannat	symptomatic	1	2019	TEF	ON573110
	URU-VD-178	Albariño/101-14	symptomatic	4	2019	TEF	ON573111
Diaporthe sp.	URU-VD-155	3309C	symptomatic	1	2018	TEF	ON573112
	URU-VD-156	Tannat	asymptomatic	1	2018	TEF	ON573113

	URU-VD-157	Marselan	asymptomatic	2	2018	TEF	ON573114
	URU-VD-158	Marselan	asymptomatic	2	2018	TEF	ON573115
	URU-VD-159	Marselan	symptomatic	2	2018	TEF	ON573116
	URU-VD-162	Moscatel de Hamburgo/SO4	asymptomatic	3	2018	TEF	ON573117
	URU-VD-163	Tannat/Gravesac	symptomatic	4	2018	TEF	ON573118
	URU-VD-164	Moscatel de Hamburgo/SO4	asymptomatic	3	2018	TEF	ON573119
	URU-VD-165	Cabernet Franc/3309C	symptomatic	4	2018	TEF	ON573120
	URU-VD-166	Merlot/101-14	symptomatic	4	2018	TEF	ON573121
	URU-VD-167	Merlot/101-14	symptomatic	4	2018	TEF	ON573122
	URU-VD-168	Tannat/Gravesac	symptomatic	4	2018	TEF	ON573123
	URU-VD-169	Tannat/Gravesac	symptomatic	4	2018	TEF	ON573124
	URU-VD-170	Tannat/Gravesac	symptomatic	4	2018	TEF	ON573125
	URU-VD-173	Tannat	asymptomatic	1	2019	TEF	ON573126
	URU-VD-174	Marselan	asymptomatic	1	2019	TEF	ON573127
	URU-VD-175	Marselan	symptomatic	1	2019	TEF	ON573128
	URU-VD-179	Albariño/101-14	symptomatic	4	2019	TEF	ON573130
	URU-VD-180	Tannat/Gravesac	symptomatic	3	2019	TEF	ON573131
Diaporthe terebinthifolii	URU-VD-176	Marselan	asymptomatic	1	2019	TEF	ON573129

[1] Stage 1 = rootstocks and scion cuttings from mother plants; Stage 2 = rootstocks and scion cuttings after cold storage and hydration; Stage 3 = grafted plants after callusing; Stage 4= rooted grafted plants ready to plant

ARTÍCULO 2

Black foot in nursery grapevines in Uruguay caused by *Dactylonectria* and *Ilyonectria*

MARÍA JULIA CARBONE, ROSSANA REYNA, PEDRO MONDINO, SANDRA ALANIZ

Departamento de Protección Vegetal, Facultad de Agronomía, Universidad de la República

Publicado en: *Phytopathologia Mediterranea* (2023) 62(2):199-211.
https://doi.org/10.36253/phyto-14498

Black foot in nursery grapevines in Uruguay caused by *Dactylonectria* and *Ilyonectria*

ABSTRACT

Black foot is a serious soilborne fungal disease causing decline of young grapevines. Affected plants show brown to dark streaks developing from the rootstock bases, wood necroses at trunk bases, sunken necrotic lesions on roots, and reduced root biomass. Several fungi, commonly known as *Cylindrocarpon*-like asexual morphs, have been associated with black foot. Nursery vines are infected during rooting in propagation processes, which is important for dissemination of the pathogens. Species associated with black foot in nursery vines produced in Uruguay were characterized by molecular, phenotypical and pathogenicity studies. From 2017 to 2019, 181 rooted vines grafted onto '1103P', 'SO4', '101-14', '3309C' or 'Gravesac' rootstocks were sampled, and 71 *Cylindrocarpon*-like fungal isolates were recovered from rootstock tissues (basal ends and roots). Based on multi-gene phylogenetic analyses of HIS3, TEF and TUB2, and supported by phenotypical characterization, five species of *Dactylonectria* and *Ilyonoectria* were identified, with *D. macrodidyma* being the most prevalent followed by *D. novozelandica*, *D. torresensis*, *D. palmicola* and *I. liriodendri*. Four *Ilyonectria* isolates could not be identified to species level. Isolate pathogenicity was assessed using healthy rooted 'Gravesac' plants. After three months, isolates of all species infected the plants, causing necrotic lesions on roots and reducing root biomass. On average, 39% of ready-to-plant nursery vines were affected by black foot, emphasizing the need to develop integrated management to reduce black foot incidence in Uruguayan grapevine nurseries, based on studies under local conditions.

Keywords: *Cylindrocarpon*-like fungi, grapevine trunk disease, *Vitis vinifera*

1. INTRODUCTION

Black foot is a serious soilborne fungal disease affecting nursery grapevine plants and young vineyards (Halleen *et al*., 2006a; Alaniz *et al*., 2007; Gramaje and Armengol, 2011; Agustí-Brisach and Armengol, 2013). This disease, considered a major cause of young vine decline (Gramaje and Armengol, 2011), occurs in the main grape-growing countries worldwide, including Portugal (Rego *et al*., 2000), South Africa (Fourie and Halleen, 2001), New Zealand (Halleen *et al*., 2004), France (Halleen *et al*., 2004), United States (Petit and Gubler, 2005), Spain (Alaniz *et al*., 2007), Australia (Whitelaw-Weckert *et al*., 2007), Uruguay (Abreo *et al*., 2010), Canada (Petit *et al*., 2011), Turkey (Özben *et al*., 2012), Iran (Mohammadi *et al*., 2013), Brazil (dos Santos *et al*., 2014), Italy (Carlucci *et al*., 2017), Czech Republic (Pečenka *et al*., 2018), Algeria (Aigoun-Mouhous *et al*., 2019), China (Ye *et al*., 2021), and Argentina (Longone *et al*., 2022).

Grapevines affected by black foot pathogens show reduced root biomass, sunken necrotic root lesions, dark brown to black streaks that develop from rootstock bases, and wood necroses at trunk bases (Rego *et al*., 2000; Halleen *et al*., 2006a; Alaniz *et al*., 2007; Agustí-Brisach and Armengol, 2013). Foliar symptoms usually appear during the first 3 to 5 years after planting, and involve delayed and failed bud-break, reduced vigour, shortened internodes, chlorotic foliage with necrotic margins, wilting and usually plant death (Halleen *et al*., 2006a; Agustí-Brisach and Armengol, 2013). Death occurs quickly when young vines are infected, while as vines age, a more gradual decline occurs (Gubler *et al*., 2004).

Black foot was first known to be caused by "*Cylindrocarpon*" species, but in the last decade, this genus has undergone extensive taxonomic revision (Chaverri *et al*., 2011; Cabral *et al*., 2012a, 2012b; Lombard *et al*., 2014). Currently, more than 30 fungal species of *Campylocarpon*, *Cylindrocladiella*, *Dactylonectria*, *Ilyonectria*, *Neonectria*, *Pleiocarpon*, and *Thelonectria*, commonly known as *Cylindrocarpon*-like asexual morphs, are associated with black foot (Agustí-Brisach and Armengol, 2013; Lombard *et al*., 2014; Carlucci *et al*., 2017; Aigoun-Mouhous *et al*., 2019). Among these, *D. torresensis* has been reported as the prevalent species in several countries (Reis *et al*., 2013; Berlanas *et al*., 2017; Carlucci *et al*., 2017; Aigoun-Mouhous *et al*., 2019; Akgül *et al*., 2022).

Although the epidemiology of black foot has not been completely clarified, it is well known that black foot pathogens can produce abundant conidia which are dispersed by free water in the soil (Petit *et al*., 2011) and can infect grapevines through natural openings or wounds in trunk bases and roots (Agustí-Brisach and Armengol, 2013). Some species are also able to produce chlamydospores which allow long-term survival in soil (Halleen *et al*., 2004). In addition, several weeds are hosts of black foot pathogens, and these hosts can be inoculum sources for grapevine infections (Agustí-Brisach *et al*., 2011).

Black foot pathogens have been frequently isolated from nursery grapevine plants, indicating that these plants play important roles in the spread of this disease (Halleen *et al*., 2006a; Abreo *et al*., 2010; Agustí-Brisach *et al*., 2013; Cardoso *et al*., 2013; Carlucci *et al*., 2017; Pintos *et al*., 2018; Aigoun-Mouhous *et al*., 2019; Berlanas *et al*., 2020; Akgül *et al*., 2022). Several studies have focused on determining when infection occurs during propagation processes, and there is consensus that the nursery rooting phase is where black foot pathogen infections increase significantly (Halleen *et al*., 2003; Agustí-Brisach *et al*., 2013; Carbone *et al*., 2022). These pathogens can infect nursery plants from the incomplete callus zones or from wounds on roots during rooting in soil, as demonstrated by Probst *et al*. (2019).

A recent study in Uruguay revealed that many plants produced at a local nursery were infected with black foot pathogens (Carbone *et al*., 2022). The present study focused on molecular and phenotypic characterization of the pathogens associated with black foot in nursery vines and assessed the pathogenicity of identified species after inoculation of rooted grapevine rootstocks.

2. MATERIALS AND METHODS

2.1 Sampling material and fungal isolations

During 2017, 2018 and 2019, a total of 181 1-year-old ready-to-plant grapevine plants, grafted onto rootstocks of '1103P' (*Vitis berlandieri* × *V. rupestris*), 'SO4' (*V. riparia* × *V. berlandieri*), '101-14' (*V. riparia* × *V. rupestris*), '3309C' (*V. riparia* × *V. rupestris*), or 'Gravesac' ('161-49' (*V. berlandieri* × *V. riparia*) × '3309C'), were randomly selected from the main commercial grapevine nursery in Uruguay. Fifty-two plants were sampled in 2017, 83 in 2018, and 46 were sampled in 2019. The nursery is located in Canelones (34° 34′ 48.45″ S; 56° 17′ 50.17″ W), the traditional grape-growing

region of Uruguay. To isolate black foot pathogens, the basal part and roots of each plant were separated and then surface sterilized by soaking each portion in 95% ethanol for 1 s followed by flaming (Delgado *et al*., 2016). Cross and longitudinal cuts were then made at the basal portion of the rootstock to reveal internal black foot symptoms. Seven pieces of wood, approx. 5 mm in length, were taken from the margin between necrotic and apparently healthy tissues, using a sterile scalpel, including the basal part of the rootstock and roots. In 2017 and 2019, the wood pieces were selected equally from the basal parts of the rootstocks and roots, while in 2018, the pieces were selected predominantly from the basal parts of the rootstocks. The small pieces of wood were plated onto potato dextrose agar (PDA) (Oxoid Ltd.) supplemented with 0.4 g L^{-1} of streptomycin sulphate (PDAS) (Sigma-Aldrich). The plates were incubated for 5 to 21 d at 25°C in the dark and examined daily for fungal growth. Fungal colonies resembling black foot pathogens, i.e., with aerial and cottony mycelia ranging from white to yellow or light to dark brown, and with macroconidia and microconidia (Halleen *et al*., 2004; 2006b; Cabral *et al*., 2012a), were subculture onto fresh PDA plates to obtain pure cultures. Single conidium isolates were obtained (Carlucci *et al*., 2017), and were stored in colonized sterile filter papers at -20°C. Representative isolates were deposited in the fungal culture collection of the Department of Plant Protection, Faculty of Agronomy, University of the Republic, Uruguay.

2.2 Molecular identification of isolates

Total genomic DNA was extracted from 1-week old pure cultures grown on PDA at 25°C in the dark, using the commercial Quick-DNA™ Fungal/Bacterial Miniprep Kit (ZymoResearch), following the manufacturer´s instructions. Primary identification of black foot pathogens was conducted by sequencing part of the histone H3 gene (HIS3) and comparing the sequences with those deposited in the GenBank, using the BLAST source (https://blast.ncbi.nlm.nih.gov/Blast.cgi). To confirm the isolate identity, partial regions of the translation elongation factor 1-α (TEF) and the beta-tubulin (TUB2) genes were also sequenced, and a multilocus phylogenetic analysis was performed on the three combined gene regions (Cabral *et al*., 2012a; 2012b; Berlanas *et al*., 2020). The primers used were CYLH3F and CYLH3R for HIS3 (Crous *et al*., 2004), CylEF-1 (5'-ATGGGTAAGGAVGAVAAG AC-3'; J. Z. Groenewald, unpublished) and CylEF-R2 (Crous *et al*., 2004) for TEF, and T1 (O'Donnell and Cigelnik, 1997) and BT2b (Glass and Donaldson, 1995) for TUB2.

Polymerase chain reaction (PCR) amplifications were performed on a MultiGene™ Mini (Labnet International Inc.). Each PCR reaction contained 1× PCR buffer, 2.5 mM $MgCl_2$, 0.4 mM of each dNTP, 0.4 µM of each primer, 1 U of DNA polymerase (Bioron), and 1 µL of template DNA. The PCR reaction was adjusted to a final volume of 20 µL with MQ water. The PCR conditions consist of an initial step at 94°C for 3 min followed by 34 cycles for TUB2 and TEF regions, and 40 cycles for HIS3 gene, of denaturation at 94°C for 30 s, annealing at 58°C for TUB2 and TEF and 55°C for HIS3, for 30 s, and elongation at 72°C for 45 s. A final extension was performed at 72°C for 10 min. PCR products were visualized in 1.5% agarose gels stained with GelRedTM, through a transilluminator under UV light. A GeneRuler 100-bp DNA ladder plus (Thermo) was used as a molecular weight marker. PCR products were purified and sequenced by Macrogen Inc., Seoul, Korea.

For each fungus genus, sequences of each gene region were aligned using the ClustalW program, available within MEGA 11.0.11 (https://www.megasoftware.net/), and were manually edited when necessary. Related sequences and sequences of the phylogenetically closest species obtained from GenBank, including ex-type isolates, were incorporated to the alignments (Supplementary Table 1). Multilocus alignments were carried out using Sequence Matrix v.1.8 (http://www.ggvaidya.com/taxondna/). Multilocus phylogenetic analyses were constructed using Bayesian inference (BI) and Maximum likelihood (ML) methods. BI and ML analyses were inferred with, respectively, MrBayes v3.2.7a and RAxML v8.2.12 programs, implemented in CIPRES Science Gateway v3.3 (http://www.phylo.org/). For BI analysis, best-fit models of nucleotide substitution were selected for each gene according to the Akaike information criterion (AIC), using the jModelTest2 v2.1.6 tool (Darriba *et al*., 2012) implemented in CIPRES Science Gateway v3.3. Four Markov chain Monte Carlo (MCMC) chains were run simultaneously, starting from a random tree to 10 million of generations. Trees were sampled every 1000 generations, and the first 2500 were discarded as the burn-in phase of each analysis. Posterior probabilities were determined from a majority-rule consensus tree generated from the remaining 7500 trees. For the ML analysis, the Generalized Time Reversible (GTR) model, with gamma correction (G) nucleotide substitution, and 1000 bootstrap iterations, were indicated. The other parameters were used as default settings. Sequences obtained in this study were submitted to the GenBank database (Supplementary Table 2).

2.3 Morphological characterization of isolates

A sub-sample of nine representative isolates belonging to *Dactylonectria* and *Ilyonectria*, identified in this study using molecular analyses, was selected for phenotypical characterization (Supplementary Table 2). Cultures were grown on PDA and incubated at 25°C in darkness. Ten days later, colony morphological characteristics were observed, and colony colour (Rayner, 1970) was determined. Lengths and widths of 50 conidia per isolate, including macro- and microconidia, were measured at 400× magnification, using a digital camera (Microscope eye-piece camera, AM-4023X, Taiwan) incorporated into the microscope. Conidium colour, shape, and number of septate, and presence of chlamydospores, were recorded.

2.4 Pathogenicity tests

The nine isolates selected for morphological characterization were used to determine their pathogenicity on rooted grapevine plants. Dormant cuttings (0.3 m long) of 'Gravesac' rootstock were surface disinfected according to Akgül *et al*. (2022), placed in a plastic box containing sterilized growth substrate, irrigated, and kept in an acclimatized room (25°C, 85% relative humidity, 12 h photoperiod) for 1 month to induce root formation. The isolates were grown on PDA at 25°C in the dark for 2 weeks and were then liquefied in distilled water (one plate in 150 mL of distilled water). Root tips of the rooted cuttings were slightly cut and were then inoculated by immersing the roots in the culture suspension for 30 s (one liquified plate of one isolate per plant). The inoculated plants were then individually planted in a 2 L capacity pot containing commercial plant growth substrate. Six plants per isolate were inoculated, and six plants were treated with distilled water as controls. The plants were irrigated with tap water and maintained in greenhouse conditions (at 20°C±2ºC), in a completely randomized experimental design.

Three months after inoculation the plants were uprooted, and their roots were carefully washed with tap water and dried in an air-circulated oven at 65°C for 48 h to constant weight, and root dry weights were recorded. Root dry weight data were analysed for normality using the Shapiro-Wilk test and for homogeneity of variance using Levene's test. Data were subjected to statistical analyses by performing analysis of variance (ANOVA) and means comparison by Duncan test at $P = 0.05$, using InfoStat/E version 2020 (http://www.infostat.com.ar). In addition, Koch´s postulates were completed by re-

isolation of the inoculated fungi. For this, roots were separated, washed with tap water, and surface sterilized (as above). Small pieces of the roots were then cut, plated onto PDAS, and incubated in the same conditions as indicated above. Isolates identity was determined by morphological characteristics.

3. RESULTS

3.1 Fungal isolations

A total of 71 isolates resembling *Cylindrocarpon*-like asexual morphs were obtained from ready-to-plant grafted vines with characteristic black foot vascular symptoms. The symptoms consisted of wood necroses at the trunk bases, dark brown streaks developing from the bases of the plants, and sunken necrotic lesions on the roots (Figure 1). Based on the isolation frequency, incidence of black foot was 60% in 2017, 15% in 2018 and 61% in 2019.

Figure 1. Internal symptoms of black foot in ready-to-plant nursery grapevine plants. Wood necrosis and dark brown streaks developing from the base of the plant (**a**) and necrosis in roots (**b**).

3.2 Molecular identification of isolates

BLAST search of the partial HIS3 gene region placed 58 isolates in *Dactylonectria* and 13 within *Ilyonectria*. Subsequently, phylogeny of the individual data sets from the HIS3, TUB2 and TEF gene regions showed no significant conflicts in tree

topology, so the trees were combined. The *Dactylonectria* dataset contained 96 taxa (58 from this study and the two outgroups) and 1856 characters including gaps (TUB2 = 1-579; TEF = 580-1387; HIS3 = 1388-1856), of which 564 were parsimony informative. The *Ilyonectria* dataset consisted of 52 taxa (13 from this study and the two outgroups) and 1882 characters including gaps (TUB2 = 1-567; HIS3 = 568-1038; TEF = 1039-1882), of which 526 were parsimony informative.

The AIC best-fit evolutionary models of nucleotide substitution used for the Bayesian Inference analysis for the *Dactylonectria* dataset were GTR with gamma distributed with invariant sites rates (G+I) for HIS3, and GTR+G for TUB2 and TEF. For *Ilyonectria*, the best-fit nucleotide substitution models were GTR+G+I for HIS3, Hasegawa-Kishino-Yano (HKY) model +G for TUB2, and GTR+G for TEF. In both genera, the topologies of the BI and ML consensus trees were similar, so only the BI trees with posterior probability values and bootstrap support values are presented.

Phylogenetic analyses allowed identification of four species among the 58 *Dactylonectria* isolates, with *D. macrodidyma* being the prevalent species (n = 31), followed by *D. novozelandica* (n = 14), *D. torresensis* (n = 10), and *D. palmicola* (n = 3) (Figure 2). Within the *Ilyonectria* group, the analyses identified nine isolates as *I. liriodendri*, and the remaining four isolates were grouped in a separate clade with the unidentified *Ilyonectria* strain STEU 8918 from South Africa. The node support value for this clade was 0.75 according to the BI method, while with ML method this node was not formed (Figure 3).

Figure 2. Bayesian inference phylogenetic tree built using the concatenated sequences of the HIS3, TEF and TUB2 genomic regions of 58 *Dactylonectria* isolates from Uruguayan nursery grapevines, and sequences retrieved from the GenBank (ex-type indicated in bold font). *Campylocarpon fasciculare* CBS 112613 and *Campylocarpon pseudofasciculare* CBS 112679 were used as the outgroups. Posterior probability and maximum likelihood bootstrap support values greater than, respectively, 0.70 and 70 are shown at the nodes before and after each branch. The scripts indicate that the nodes do not exist in the maximum likelihood tree. Double hash marks indicate branch lengths shortened at least 2-fold to facilitate visualization. The scale bar represents the estimated number of substitutions per site.

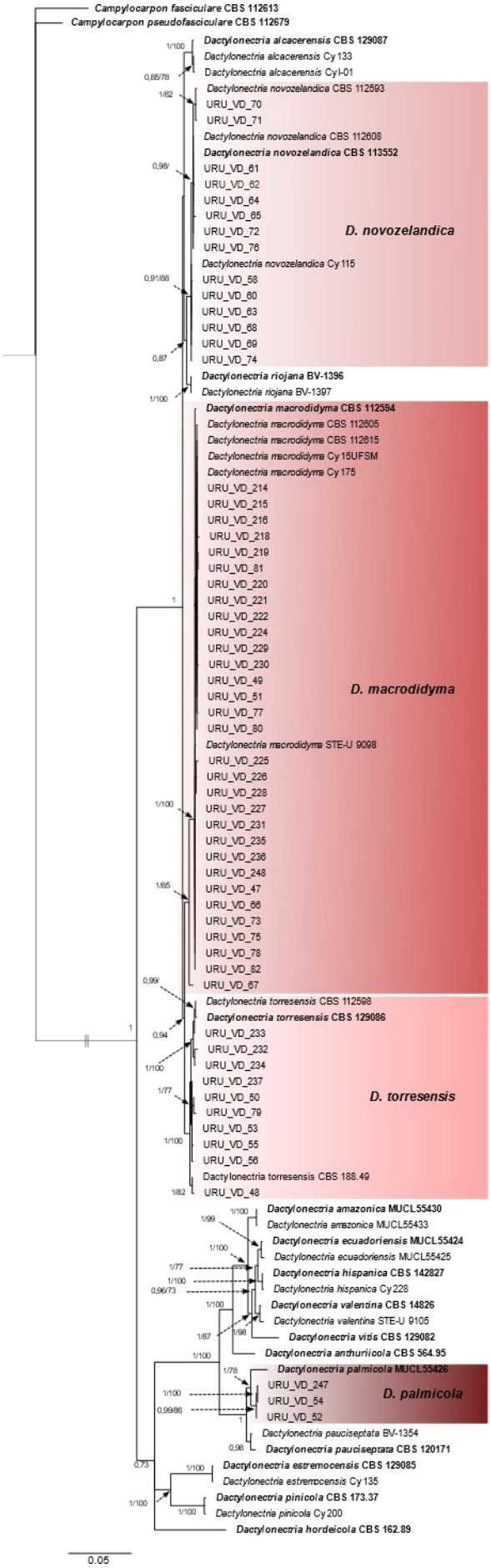

Figure 3. Bayesian inference phylogenetic tree built using the concatenated sequences of the HIS3, TEF and TUB2 genomic regions of 13 *Ilyonectria* isolates obtained from Uruguayan nursery grapevines, and sequences retrieved from the GenBank (ex-type indicated in bold font). *Campylocarpon fasciculare* CBS 112613 and *Campylocarpon pseudofasciculare* CBS 112679 were used as outgroups. Posterior probability and maximum likelihood bootstrap support values greater than 0.70 and 70 are shown at the nodes, respectively, before and after each bar. The scripts indicate that the nodes do not exist in the maximum likelihood tree. Double hash marks indicate branch lengths shortened at least 2-fold to facilitate visualization. The scale bar represents the estimated number of substitutions per site.

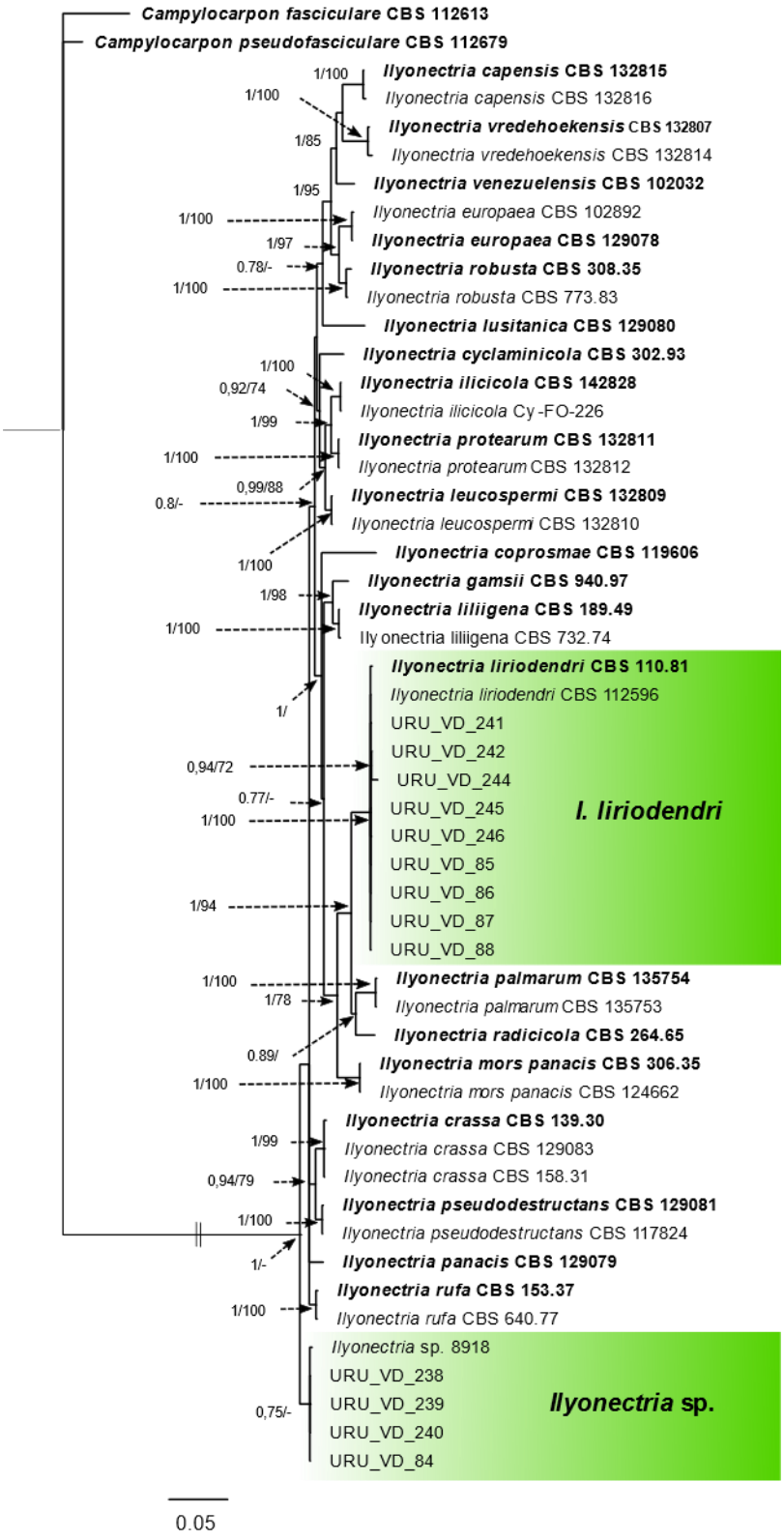

3.3 Morphological characterization of isolates

All the *Dactylonectria* and *Ilyonectria* isolates had aerial and cottony mycelia, and their colonies were white to yellow or light to dark brown on PDA. Conidiophores were simple or complex, sporodochial, and produced microconidia and macroconidia (Figure 4, Table 1). Macroconidia were predominantly straight, occasionally slightly curved and typically cylindrical, for the *D. macrodidyma*, *D. novozelandica*, *D. torresensis*, *D. palmicola*, and *I. liriodendri* isolates. Microconidia were generally ellipsoidal to ovoidal and straight. In addition, the isolates URU-VD-80 and URU-VD-242 produced chlamydospores, which is consistent with the characteristics expected for *D. macrodidyma* and *I. liriodendri* (Halleen *et al*., 2006b). The isolate URU-VD-84, identified as *Ilyonectria* sp., also had simple or complex conidiophores, produced sporodochia, and microconidia that were 0-1 septate, ellipsoidal to ovoidal and slightly curved, and macroconidia that were 1-3 septate (predominantly 1-septate), cylindrical and usually slightly curved, and produced chlamydospores (Figure 4, Table 1)

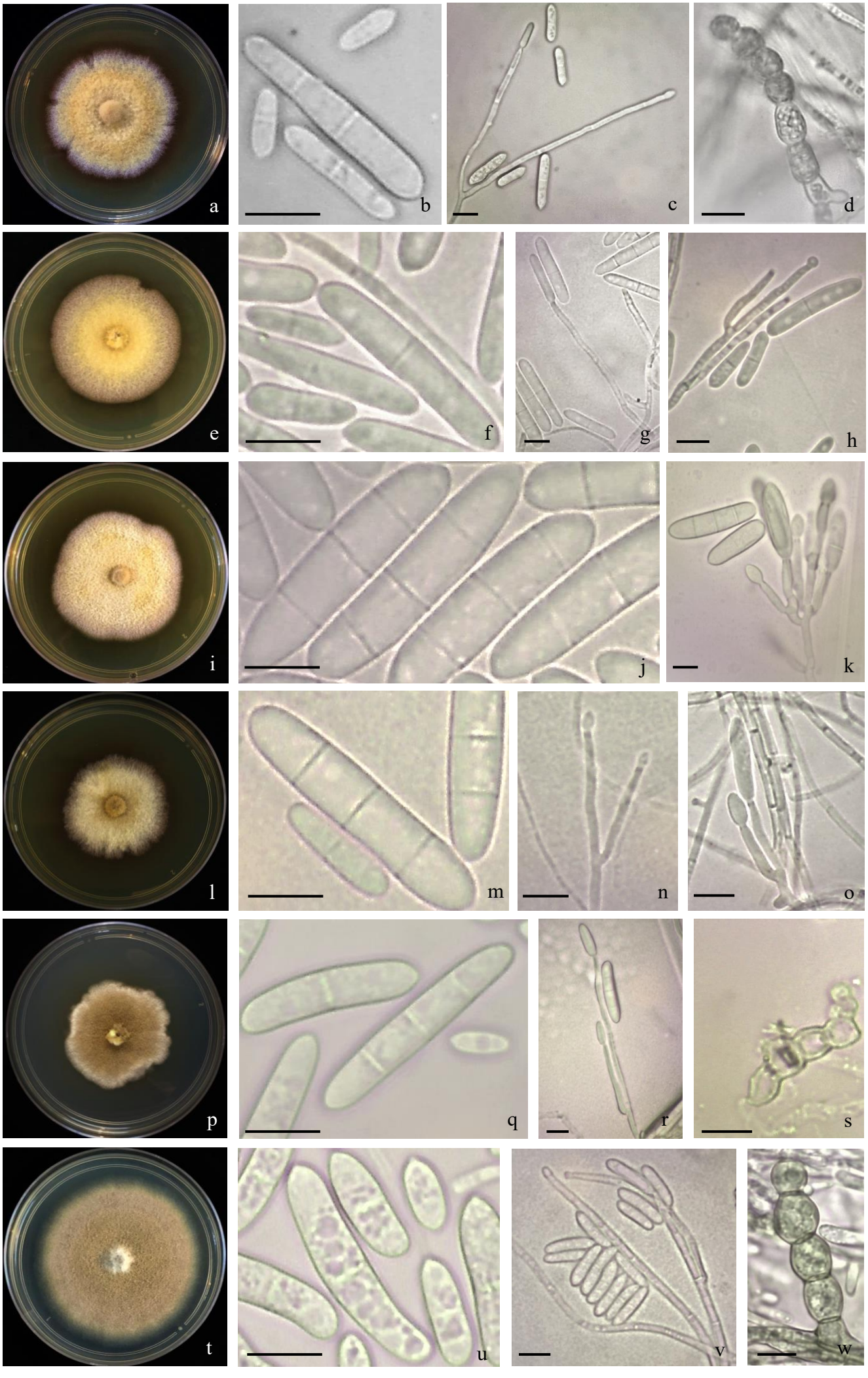
a
b
c
d
e
f
g
h
i
j
k
l
m
n
o
p
q
r
s
t
u
v
w

Figure 4. Morphological characteristics of *Dactylonectria* and *Ilyonectria* species isolated from grapevine nursery plants in Uruguay. Ten-days-old colonies on PDA at 25°C of *D. macrodidyma* (**a**), *D. novozelandica* (**e**), *D. palmicola* (**i**), *D. torresensis* (**l**), *I. liriodendri* (**p**) and *Ilyonectria* sp. (**t**). Macro- and microconidia (**b**), simple conidiophore (**c**) and chlamydospores in chain (**d**) of *D. macrodidyma*. Macro- and microconidia (**f**) and simple conidiophores (**g and h**) of *D. novozelandica*. Macroconidia (**j**) and complex, sporodochial conidiophore (**k**) of *D. palmicola*. Macro- and microconidia (**m**) and simple conidiophores (**n and o**) of *D. torresensis*. Macro- and microconidia (**q**), simple conidiophore (**r**) and chlamydospores in chain (**s**) of *I. liriodendri.* Macro- and microconidia (**u**), simple conidiophore (**v**) and chlamydospores in chain (**w**) of *Ilyonectria* sp. Bars = 10 µm.

Table 1. Mean dimensions of aseptate and septate conidia of nine representative *Dactylonectria* and *Ilyonectria* isolates obtained in this study.

Species	Isolate	Microconidia				Macroconidia					
		Aseptate		One-septate		One-septate		Two-septate		Three-septate	
		Length	Width	Length	Width	Length	Width	Length	Width	Length	Width
Dactylonectria macrodidyma	URU-VD-80	10.32 ± 1.08	3.38 ± 0.34	14.11 ± 1.43	3.89 ± 0.27	22.08 ± 1.99	4.29 ± 0.28	24.17 ± 2.34	4.35 ± 0.40	-	-
D. macrodidyma	URU-VD-231	10.37 ± 1.38	3.42 ± 0.37	13.62 ± 1.89	3.71 ± 0.32	23.53 ± 2.69	5.05 ± 0.69	28.77 ± 1.76	5.98 ± 0.74	31.48 ± 0.82	5.11 ± 0.74
D. novozelandica	URU-VD-64	10.64 ± 0.61	3.29 ± 0.22	14.61 ± 2.22	3.56 ± 0.39	27.52 ±1.65	4.74 ± 0.37	31.17 ± 2.94	5.41 ± 0.77	33.25 ± 2.01	5.56 ± 0.43
D. novozelandica	URU-VD-71	10.95 ± 1.18	3.01 ±0.47	14.89 ±2.03	3.66 ± 0.33	27.07 ±1.67	4.62 ± 0.42	29.02 ± 1.66	5.07 ± 0.43	31.45 ± 2.50	5.19 ± 0.48
D. torresensis	URU-VD-79	11.30 ± 1.37	3.84 ± 0.55	15.01 ± 2.14	4.26 ± 0.57	26.76 ± 3.00	5.92 ± 0.47	29.56 ± 2.10	5.79 ± 0.38	30.04 ± 0.04	5.87 ± 0.55
D. torresensis	URU-VD-234	12.00 ± 1.87	4.05 ± 0.49	14.65 ± 2.04	4.65 ± 0.30	29.35 ± 4.04	6.23 ± 0.58	32.42 ± 2.45	7.03 ± 0.81	34.47 ± 4.12	7.18 ± 0.70
D. palmicola	URU-VD-54	12.79 ± 3.13	5.30 ± 1.46	-	-	37.22 ± 2.14	8.30 ± 0.82	36.44 ± 2.09	8.15 ± 0.60	37.37 ± 2.27	8.30 ± 0.70
Ilyonectria liriodendri	URU-VD-242	9.39 ± 1.60	3.75 ± 0.43	13.02 ± 2.53	3.66 ± 0.48	22.70 ± 1.92	4.42 ± 0.75	27.01 ± 2.35	4.59 ± 0.35	29.13 ± 3.04	4.95 ± 0.50
Ilyonectria sp.	URU-VD-84	10.79 ± 1.65	4.07 ± 0.40	17.41 ± 2.35	4.59 ± 0.45	24.88 ± 2.24	5.03 ± 0.45	27.59 ± 1.88	5.60 ± 0.81	29.11	4.84

3.4 Pathogenicity tests

All the evaluated isolates were pathogenic on 'Gravesac' rootstock cuttings. At 3 months after inoculation, significant reductions ($P = 0.0193$) of mean root biomass were recorded from the inoculation treatments compared with the control treatment (Table 2). The inoculated plants had sunken necrotic lesions on roots and more brownish roots than the non-inoculated plants. Mean root dry weights ranged from 1.14 g to 1.76 g in inoculated plants and was 2.03 g for the non-inoculated controls. According to root dry weight reduction, both *D. macrodidyma* isolates, URU-VD-80 and URU-VD-231, were the most virulent, causing, respectively, 44% and 42% reductions compared with the non-inoculated control. The isolates of *I. liriodendri* (URU-VD-242), *D. torresensis* (URU-VD-234) and *D. novozelandica* (URU-VD-71) were the least virulent (causing, respectively, 20%, 18% and 13% reductions in root dry weight), but the mean root weights from these isolates were not significantly different ($P > 0.05$) from the control treatment. The other evaluated isolates showed intermediate behaviour. In addition, all the inoculated fungi were re-isolated from inoculated plants, with re-isolation rates ranging from 22% to 100%, whereas no pathogens were re-isolated from the non-inoculated controls (Table 2).

Table 2. Mean root dry weights and proportions of inoculated fungus re-isolations for selected *Dactylonectria* and *Ilyonectria* isolates inoculated on rooted grapevine cuttings of 'Gravesac' rootstock.

Fungal species	Isolate	Dry root weights (g)[a]	Re-isolation (%)
Dactylonectria macrodidyma	URU-VD-80	1.14 a	80
D. macrodidyma	URU-VD-231	1.17 a	100
D. torresensis	URU-VD-79	1.21 ab	86
Ilyonectria sp.	URU-VD-84	1.32 ab	22
D. palmicola	URU-VD-54	1.37 ab	57
D. novozelandica	URU-VD-64	1.47 ab	100
I. liriodendri	URU-VD-242	1.62 abc	83
D. torresensis	URU-VD-234	1.66 abc	25
D. novozelandica	URU-VD-71	1.76 bc	83
Non-inoculated control		2.03 c	0

[a] Data are the mean of six replicates for each isolate. Means with same letter are not significantly different ($P = 0.05$) according to Duncan test.

4. DISCUSSION

Based on phylogenetic analyses, morphological studies and pathogenicity tests, the present study has identified five species of *Dactylonectria* and *Ilyonectria* causing black foot in locally produced nursery grapevines in Uruguay. The species identified were *D. macrodidyma* (31 isolates), *D. novozelandica* (14 isolates), *D. torresensis* (ten isolates), *I. liriodendri* (nine isolates) and *D. palmicola* (three isolates), while four *Ilyonectria* isolates could not be identified to species level.

All isolates were recovered from nursery grapevine plants showing typical black foot symptoms (wood necrosis at the trunk bases, dark brown streaks developing from the bases of plants, and sunken necrotic lesions on roots), as previously described by Halleen *et al*. (2006a) and Agustí-Brisach and Armengol (2013). Incidence of black foot based on proportions of pathogen isolations, was approx. 60% in 2017 and 2019, but substantially less (15%) in 2018. This difference was probably because isolations in 2018 were predominantly from the basal parts of the rootstocks. Probst *et al*. (2019) demonstrated that both *D. macrodidyma* and *I. liriodendri* can infect grapevines through wounded roots and callused basal ends. Results obtained in the present study indicate that under Uruguayan nursery production conditions, wounded roots are the main pathway of infection for these pathogens, rather than the basal callus tissues of the plants.

The multilocus phylogenetic approach allowed identification of black foot pathogens at species level, and morphological characterization supported these results. Colony morphology and characteristics (shape and size) of macro- and microconidia, as well as production of chlamydospores by some isolates, were consistent with those expected for the identified species (Halleen *et al*., 2004; 2006b; Cabral *et al*., 2012a; Gordillo and Decock, 2017).

Dactylonectria macrodidyma was the prevalent species found causing black foot in the nursery plants analysed. This species was first described associated with grapevine in South Africa as *C. macrodidyma* by Halleen *et al*. (2004), and subsequently named as *D. macrodidyma* by Lombard *et al*. (2014). This species has been associated with black foot disease in several other countries, including New Zealand (Halleen *et al*., 2004; Probst *et al*., 2019), Chile (Auger *et al*., 2007), Spain (Alaniz *et al*., 2007), Switzerland (Hofstetter *et al*., 2009), Canada (Petit *et al*., 2011; Úrbez-Torres *et al*., 2014), Portugal (Cabral *et al*., 2012a; Reis *et al*., 2013), Turkey (Özben *et al*., 2012; Akgül *et al*., 2022),

Brazil (dos Santos *et al*., 2014), Algeria (Aigoun-Mouhous *et al*., 2019), China (Ye *et al*., 2021) and Argentina (Longone *et al*., 2022). In a previous study in Uruguay, Abreo *et al.* (2010) found *D. macrodidyma* as the prevalent species causing black foot on symptomatic plants collected from commercial vineyards.

The second most common pathogen found was *D. novozelandica*, which was first described in grapevine as *I. novozelandica* by Cabral *et al*. (2012a), and then re-named *D. novozelandica* by Lombard *et al.* (2014). This species has been associated with black foot in New Zealand (Cabral *et al*., 2012a), Peru (Alvarez *et al*., 2012), South Africa (Cabral *et al*., 2012a), United States (Cabral *et al*., 2012a), Portugal (Reis *et al*., 2013), Spain (Agustí-Brisach *et al*., 2013), Algeria (Aigoun-Mouhous *et al*., 2019) and Turkey (Akgül *et al*., 2022). In Uruguay, *D. novozelandica* has been found causing crown and root necrosis on strawberry (Vigliecca *et al*., 2022).

Dactylonectria torresensis was first described by Cabral *et al*. (2012a) as *I. torresensis* in grapevine in Portugal and was then reclassified as *D. torresensis* by Lombard *et al*. (2014). This species has been reported as the prevalent cause of black foot in Portugal (Reis *et al*., 2013), Italy (Carlucci *et al*., 2017), Spain (Berlanas *et al*., 2017), Algeria (Aigoun-Mouhous *et al*., 2019) and Turkey (Akgül *et al*., 2022). In addition, the fungus has been associated with black foot in Australia, New Zealand, South Africa, United States (Cabral *et al*., 2012a), Canada (Úrbez-Torres *et al*., 2014), and China (Ye *et al*., 2021).

Dactylonectria palmicola was the fourth *Dactylonectria* species found associated with black foot in this study. This species was described by Gordillo and Decock (2017) in *Euterpe precatoria* in the Amazon rainforest of Ecuador. The present study is the first record of *D. palmicola* causing black foot on grapevine. The isolates URU-VD-52 and URU-VD-54 identified as *D. palmicola* in the present study, were previously misidentified as *D. pauciseptata* when phylogenetic analysis was performed using only the HIS3 gene region (Carbone *et al*., 2022). Although the HIS3 region has been demonstrated to be the most robust locus for identification of black foot pathogens (Cabral *et al*., 2012a), the present results suggest that multilocus sequence analysis, including HIS3, TUB2 and TEF, is essential to ensure correct identification of closely related fungi causing black foot.

Within *Ilyonectria*, *I. liriodendri* was the prevalent species found in the present study. This pathogen was first described in grapevine by Halleen *et al*. (2006b) as *C. liriodendri*, and subsequently classified as *I. liriodendri* by Chaverri *et al*. (2011). This species has been reported on grapevine in South Africa (Halleen *et al*., 2006b), Australia (Whitelaw-Weckert *et al*., 2007), Spain (Alaniz *et al*., 2007), Switzerland (Casieri *et al*., 2009), Iran (Mohammadi *et al*., 2009), Brazil (Russi *et al*., 2010), United States (Petit *et al*., 2011), Canada (Petit *et al*., 2011; Úrbez-Torres *et al*., 2014), Portugal (Reis *et al*., 2013), New Zealand (Pathrose *et al*., 2014), Italy (Carlucci *et al*., 2017), Argentina (Longone *et al*., 2022) and Turkey (Akgül *et al*., 2022). In Uruguay, *I. liriodendri* was first reported affecting symptomatic plants in commercial vineyards by Abreo *et al*. (2010).

Isolates classified as *Ilyonectria* sp. in the present study were grouped with the unidentified South African *Ilyonectria* strain STEU 8918, but with a low support value (0.75) in the BI analysis, and absence of this clade in the ML analysis. For this South African isolate, which was obtained by van der Merwe (2019) from the crown of a nectarine nursery tree, only the HIS3 gene region is available on the GenBank database. This probably explains the low support of the clade in the BI phylogenetic tree and absence of this clade in the ML tree. The pathogenicity tests conducted in the present study confirmed pathogenicity of this species to grapevine, which emphasizes the importance of prescriptive description of this new species.

Results obtained here have shown that all inoculated *Dactylonectria* and *Ilyonectria* isolates infected rooted 'Gravesac' rootstocks, but virulence varied among species and between isolates within species, which is in accordance with previous studies (Probst *et al*., 2019; Aigoun-Mouhous *et al*., 2019; Berlanas *et al*., 2020; Akgül *et al*., 2022). After 3 months from inoculation, the maximum reduction in root dry weight was 44%, and no plant death was recorded. A longer post inoculation period may have resulted in greater reductions of root biomass, because development of black foot symptoms is usually slow (Whitelaw-Weckert, *et al*. 2007), and may have allowed all isolates to significantly reduce root dry weights compared to the control treatment. Whitelaw-Weckert *et al*. (2007) were unable to detect consistent black foot symptoms after 18 months from inoculation with *C. liriodendri* of 1-year-old rooted *V. vinifera* plants, although they confirmed pathogenicity by re-isolation of this fungus, as occurred in the present study.

Dactylonectria macrodidyma was the most aggressive species in the present study. Both isolates of this fungus caused the lowest root dry weights. This result agrees with those of Ye *et al*. (2021) in China, where *D. macrodidyma* was the most aggressive pathogen compared with *D. torresensis*, *D. alcacerensis*, *Cylindrocladiella lageniformis* and *Neonectria* sp. In contrast, in research conducted in Algeria by Aigoun-Mouhous *et al*. (2019), an isolate of *D. torresensis* was the most virulent, followed by isolates of *D. novozelandica* and *D. macrodidyma*. Pathogenicity tests recently conducted in Turkey on '1103P' rootstock cuttings showed that *D. novozelandica* was the most virulent species compared with *Cylindrodendrum alicantinum*, *Cylindrocladiella peruviana*, *D. macrodidyma*, *D. torresensis*, *I. liriodendri* and *I. robusta* (Akgül *et al*., 2022). This is in accordance with the study by Berlanas *et al*. (2020) in Spain, where a strain of *D. novozelandica* was found to be the most virulent compared with several black foot fungi, including *D. macrodidyma*, *D. torresensis* and *I. liriodendri*, inoculated on *V. vinifera* 'Tempranillo'. In contrast, Probst *et al*. (2019) testing different inoculation methods and propagule types in New Zealand, observed that *I. liriodendri* was generally more pathogenic than *D. macrodidyma.*

In conclusion, the present study has shown that about 39% of analysed ready-to-plant nursery vines were infected by black foot pathogens. This high proportion is likely to compromise the longevity of new vineyards. This result emphasizes the need to implement integrated management strategies to reduce black foot incidence in Uruguayan grapevine nurseries. Physical practices such as hot-water treatments have shown promising results for controlling black foot in several countries, but with unacceptable levels of disease control (Gramaje and Armengol, 2011). Nevertheless, this technology should be evaluated in each grapevine region. Use of antagonist microorganisms is currently a major objective of the research to prevent grapevine trunk diseases, but the results remain unconvincing (Martínez-Diz *et al.*, 2021). Other practices, such as biofumigation with *Brassica* spp., have been shown to reduce soilborne pathogen inoculum levels and help prevent infection by black foot pathogens in young plants (Berlanas *et al.*, 2018). Appropriate and environmentally-friendly chemical controls can also be considered, while local regulations allow the use of promising chemical active ingredients. Taking this into account, future studies should focus on evaluating different practices to avoid or reduce fungal infections by black foot pathogens in nursery grapevines under local conditions.

5. REFERENCES

Abreo E., Martinez S., Bettucci L., Lupo S., 2010. Morphological and molecular characterization of *Campylocarpon* and *Cylindrocarpon* spp. Associated with black foot disease of grapevines in Uruguay. *Australasian Plant Pathology* 39: 446–452. https://doi.org/10.1071/AP10021

Agustí-Brisach C., Armengol J., 2013. Black-foot disease of grapevine: an update on taxonomy, epidemiology and management strategies. *Phytopathologia Mediterranea* 52: 245–261. https://doi.org/10.14601/Phytopathol_Mediterr-12662

Agustí-Brisach C., Gramaje D., León M., García-Jiménez J., Armengol J., 2011. Evaluation of vineyard weeds as potential hosts of blackfoot and Petri disease pathogens. *Plant Disease* 95: 803-810. https://doi.org/10.1094/PDIS-12-10-0888

Agustí-Brisach C., Gramaje D., García-Jiménez J., Armengol J., 2013. Detection of black-foot disease pathogens in the grapevine nursery propagation process in Spain. *European Journal of Plant Pathology* 137: 103–112. https://doi.org/10.1007/s10658-013-0221-8

Aigoun-Mouhous W., Elena G., Cabral A., León M., Sabaou N., … Berraf-Tebbal A., 2019. Characterization and pathogenicity of *Cylindrocarpon*-like asexual morphs associated with black foot disease in Algerian grapevine nurseries, with the description of *Pleiocarpon algeriense* sp. Nov.. *European Journal of Plant Pathology* 154: 887–901. https://doi.org/10.1007/s10658-019-01708-z

Akgül D.S., Yıldız M., Güngör Savaş N., Bülbül İ., Özarslandan M., … Armengol J., 2022. Occurrence and diversity of black-foot pathogens on asymptomatic nursery-produced grapevines in Turkiye. *European Journal of Plant Pathology* 164: 21–32. https://doi.org/10.1007/s10658-022-02535-5

Alaniz S., León M., Vicent A., García-Jiménez J., Abad-Campos P., Armengol J., 2007. Characterization of *Cylindrocarpon* species associated with black foot disease of grapevine in Spain. *Plant Disease* 91: 1187–1193. https://doi.org/10.1094/PDIS-91-9-1187

Alvarez L.A., Tamayo D., Castilla C., Munive J., Agustí-Brisach C., … Armengol J., 2012. Occurrence of grapevine trunk pathogens in nurseries and vineyards in the northern

and southern coast of Peru. *8th International Workshop on Grapevine Trunk Diseases*, Valencia, 18-21, June 2012.

Auger J., Esterio M., Pérez I., 2007. First report of black foot disease of grapevine caused by *Cylindrocarpon macrodidymum* in Chile. *Plant Disease* 91(4): 470. https://doi.org/10.1094/PDIS-91-4-0470A

Berlanas C., López-Manzanares B., Gramaje D., 2017. Estimation of viable propagules of black-foot disease pathogens in grapevine cultivated soils and their relation to production systems and soil properties. *Plant Soil* 417: 467–479. https://doi.org/10.1007/s11104-017-3272-3

Berlanas C., Andrés-Sodupe M., López-Manzanares B., Maldonado-González M.M., Gramaje D., 2018. Effect of white mustard cover crop residue, soil chemical fumigation and *Trichoderma* spp. root treatment on black-foot disease control in grapevine. *Pest management science* 74: 2864–2873. https://doi.org/10.1002/ps.5078

Berlanas C., Ojeda S., López-Manzanares B., Andrés-Sodupe M., Bujanda R., … Gramaje D., 2020. Occurrence and diversity of black-foot disease fungi in symptomless grapevine nursery stock in Spain. *Plant Disease* 104: 94–104. https://doi.org/10.1094/PDIS-03-19-0484-RE

Cabral A., Rego C., Nascimento T., Oliveira H., Johannes Z., … Crous P.W., 2012a. Multi-gene analysis and morphology reveal novel *Ilyonectria* species associated with black foot disease of grapevines. *Fungal Biology* 116: 62–80. https://doi.org/10.1016/j.funbio.2011.09.010

Cabral A., Groenewald J.Z., Rego C., Oliveira H., Crous P.W., 2012b. Cylindrocarpon root rot: multi-gene analysis reveals novel species within the *Ilyonectria radicicola* species complex. *Mycological Progress* 11: 655–688. https://doi.org/10.1007/s11557-011-0777-7

Cardoso M., Diniz I., Cabral A., Rego C., Oliveira H., 2013. Unveiling inoculum sources of black foot pathogens in a commercial grapevine nursery. *Phytopathologia Mediterranea* 52: 298–312. https://doi.org/10.14601/Phytopathol_Mediterr-11593

Carbone M.J., Gelabert M., Moreira V., Mondino P., Alaniz S., 2022. Grapevine nursery propagation material as source of fungal trunk disease pathogens in Uruguay. *Frontiers in Fungal Biology* 3: 958466. https://doi.org/10.3389/ffunb.2022.958466

Carlucci A., Lops F., Mostert L., Halleen F., Raimondo M., 2017. Occurrence fungi causing black foot on young grapevines and nursery rootstock plants in Italy. *Phytopathologia Mediterranea* 56: 10–39. https://doi.org/10.14601/Phytopathol_Mediterr-18769

Casieri L., Hofstetter V., Viret O., Gindro K., 2009. Fungal communities living in the wood of different cultivars of young *Vitis vinifera* plants. *Phytopathologia Mediterranea* 48: 73-83. https://doi.org/10.14601/Phytopathol_Mediterr-2876

Chaverri P., Salgado C., Hirooka Y., Rossman A.Y., Samuels G.J., 2011. Delimitation of *Neonectria* and *Cylindrocarpon* (*Nectriceae*, *Hypocreales*, *Ascomycota*) and related genera *Cylindrocarpon*-like anamorphs. *Studies in Mycology* 68: 57–78. https://doi.org/10.3114/sim.2011.68.03

Crous P.W., Groenewald J.Z., Risède J.M., Simoneau P., Hywel-Jones N.L., 2004. *Calonectria* species and their *Cylindrocladium* anamorphs: species with clavate vesicles. *Studies in Mycology* 55(1): 213-226. https://doi.org/10.3114/sim.55.1.213

Darriba D., Taboada G. L., Doallo R., Posada D., 2012. jModelTest 2: more models, new heuristics and parallel computing. *Nature Methods* 9: 772. https://doi.org/10.1038/nmeth.2109

Delgado L., Mondino P., Alaniz S., 2016. Botryosphariaceae species associated with stem canker, die-back and fruit rot on apple in Uruguay. *European Journal of Plant Pathology* 146: 637–655. https://doi.org/10.1007/s10658-016-0949-z

dos Santos R.F., Blume E., Muniz M.F.B., Heckler L.I., Finger G., ..., Garrido L.R., 2014. First report of *Ilyonectria macrodidyma* associated with black foot disease of grapevine in Brazil. *Plant Disease* 98(1): 156-156. https://doi.org/10.1094/PDIS-04-13-0424-PDN

Fourie P.H., Halleen F., 2001. Diagnosis of fungal diseases and their involvement in dieback disease of young vines. *Wynboer* 149: 19–23.

Glass N.L., Donaldson G., 1995. Development of primer sets designed for use with PCR to amplify conserved genes from filamentous ascomycetes. *Applied and Environmental Microbiology* 61: 1323-1330. https://doi.org/10.1128/aem.61.4.1323-1330.1995

Gordillo A., Decock C., 2017. *Cylindrocarpon*-like (Ascomycota, Hypocreales) species from the Amazonian rain forests in Ecuador: additions to *Campylocarpon* and

Dactylonectria. Cryptogamie, Mycologie 38(4): 409-434. https://doi.org/10.7872/crym/v38.iss4.2017.409

Gramaje D., Armengol J., 2011. Fungal trunk pathogens in the grapevine propagation process: potential inoculum sources, detection, identification, and management strategies. *Plant Disease* 95: 1040–1055. https://doi.org/10.1094/PDIS-01-11-0025

Gubler, W.D., Baumgartner K., Browne G.T. Eskalen A., Latham S.R., … Bayramian L.A., 2004. Root diseases of grapevines in California and their control. *Australasian Plant Pathology* 33: 157–165. https://doi.org/10.1071/AP04019

Halleen F., Crous P.W., Petrini O., 2003. Fungi associated with healthy grapevine cuttings in nurseries, with special reference to pathogens involved in the decline of young vines. *Australasian Plant Pathology* 32: 47–52. https://doi.org/10.1071/AP02062

Halleen F., Schoroers H., Groenewald J., Crous P. 2004. Novels species of *Cylindrocarpon* (*Neonectria*) and *Campylocarpon* gen. nov. associated with black-foot disease of grapevines (*Vitis* spp.). *Studies in Mycology* 50: 431–455.

Halleen F., Fourie P.H., Crous P.W., 2006a. A review of black foot disease of grapevine. *Phytopathologia Mediterranea* 45: 55–67. https://doi.org/10.1400/52261

Halleen F., Schroers H.J., Groenewald J.Z., Rego C., Oliveira H., Crous P.W., 2006b. *Neonectria liriodendri* sp. nov., the main causal agent of black foot disease of grapevines. *Studies in Mycology* 55(1): 227-234. https://doi.org/10.3114/sim.55.1.227

Hofstetter V., Casieri L., Viret O., Gindro K., 2009. Esca de la vigne et communauté fongique. *Revue Suisse de Viticulture, Arboriculture, Horticulture* 41: 247–253.

Lombard L., Van der Merwe N.A., Groenewald J.Z., Crous P.W., 2014. Lineages in *Nectriaceae*: Re-evaluating the generic status of *Ilyonectria* and allied genera. *Phytopathologia Mediterranea* 53: 515–532. https://doi.org/10.14601/Phytopathol_Mediterr-14976

Longone V., Escoriaza G., Paolinelli M., Gramaje D., 2022. First report of *Dactylonectria alcacerensis*, *Dactylonectria macrodidyma*, and *Ilyonectria liriodendri* associated with black foot disease of grapevine in Argentina. *Plant Disease* 106: 1996. https://doi.org/10.1094/PDIS-10-21-2346-PDN

Martínez-Diz M.P., Díaz-Losada E., Andrés-Sodupe M., Bujanda R., Maldonado-González M.M., … Gramaje D., 2021. Field evaluation of biocontrol agents against black-foot and Petri diseases of grapevine. *Pest Management Science* 77(2): 697–708. https://doi.org/10.1002/ps.6064

Mohammadi H., Alaniz S., Banihashemi Z., Armengol J., 2009. Characterization of *Cylindrocarpon liriodendri* associated with black foot disease of grapevine in Iran. *Journal of Phytopathology* 157: 642-645. https://doi.org/10.1111/j.1439-0434.2009.01555.x

Mohammadi H., Banihashemi Z., Gramaje D., Armengol J., 2013. Fungal pathogens associated with grapevine trunk diseases in Iran. *Journal of Agricultural Science and Technology* 15: 137-150.

O'Donnell K., Cigelnik E., 1997. Two divergent intragenomic rDNA ITS2 types within a monophyletic lineage of the fungus *Fusarium* are nonorthologous. *Molecular Phylogenetics and Evolution* 7: 103–116. https://doi.org/10.1006/mpev.1996.0376

Özben S., Demirci F., Değirmenci K., Uzunok S., 2012. First report of *Cylindrocarpon macrodidymum* associated with black foot diseases of grapevine in Turkey. *Plant Disease* 96: 762. https://doi.org/10.1094/PDIS-05-11-0393-PDN

Pathrose B., Jones E.E., Jaspers M.V., Ridgway H.J., 2014. High genotypic and virulence diversity in *Ilyonectria liriodendri* isolates associated with black foot disease in New Zealand vineyards. *Plant Pathology* 63: 613-624. https://doi.org/10.1111/ppa.12140

Pečenka J., Eichmeier A., Peňázová E., Baránek M., León M., Armengol J., 2018. First report of *Dactylonectria torresensis* causing black-foot disease on grapevines in the Czech Republic. *Plant Disease* 102: 2038 https://doi.org/10.1094/PDIS-03-18-0411-PDN

Petit E., Gubler W.D., 2005. Characterization of *Cylindrocarpon* species, the cause of black foot disease of grapevine in California. *Plant Disease* 89(10): 1051-1059. https://doi.org/10.1094/PD-89-1051

Petit E., Barriault E., Baumgartner K., Wilcox W., Rolshausen P., 2011. *Cylindrocarpon* species associated with black-foot of grapevine in Northeastern United States and Southeastern Canada. *American Journal of Enology and Viticulture*. 62: 177-183. https://doi.org/10.5344/ajev.2011.10112

Pintos C., Redondo V., Costas D., Aguín O., Mansilla P., 2018. Fungi associated with grapevine trunk diseases in nursery-produced *Vitis vinifera* plants. *Phytopathologia Mediterranea* 57: 407–424. https://doi.org/10.14601/Phytopathol_Mediterr-22964

Probst C.M., Ridgway H.J., Jaspers M.V., Jones E.E., 2019. Pathogenicity of *Ilyonectria liriodendri* and *Dactylonectria macrodidyma* propagules in grapevines. *European Journal of Plant Pathology* 154: 405–421. https://doi.org/10.1007/s10658-018-01664-0

Rayner R.W., 1970. A Mycological Colour Chart. British Mycological Society and CAB International Mycological Institute, Kew, Surrey, UK.

Rego C., Oliveira H., Carvalho A., Phillips A.J.L., 2000. Involvement of *Phaeoacremonium* spp. and *Cylindrocarpon destructans* with grapevine decline in Portugal. *Phytopathologia Mediterranea* 39: 76–79. https://doi.org/10.1400/57814

Reis P., Cabral A., Nascimento T., Oliveira H., Rego, C., 2013. Diversity of *Ilyonectria* species in a young vineyard affected by black foot disease. *Phytopathologia Mediterranea* 52(2): 335–346 https://doi.org/10.14601/Phytopathol_Mediterr-12719

Russi A., Nalin R., Dequigiovanni G., Gava R., Quecini V., ... Ritschel P., 2010. Study of the genetic variability of Brazilian populations of *Cylindrocarpon* spp., causal agent of grapevine black foot. Abstracts of oral and poster presentations given at the 7th International Workshop on Grapevine Trunk Diseases, Santa Cruz, Chile, 17–21 January 2010. *Phytopathologia Mediterranea* 49: 103-133. https://doi.org/10.14601/Phytopathol_Mediterr-8452

Úrbez-Torres J.R., Haag P., Bowen P., O'Gorman D.T., 2014. Grapevine trunk diseases in British Columbia: incidence and characterization of the fungal pathogens associated with black foot disease of grapevine. *Plant Disease* 98(4): 456-468. https://doi.org/10.1094/PDIS-05-13-0524-RE

van der Merwe R., 2019. Occurrence of Canker And Wood Rot Pathogens on Stone Fruit Propagation Material and Nursery Stone Fruit Trees. Master Thesis, University of Stellenbosch, Stellenbosh, South Africa, 142pp.

Viglieca M., González P., Machín A., Vicente E., Silvera E., 2022. First report of root and crown rot caused by *Dactylonectria novozelandica* on strawberry in Uruguay. *Agrociencia Uruguay* 26(2): e962. https://doi.org/10.31285/AGRO.26.962

Whitelaw-Weckert M.A., Nair N.G., Lamont R., Alonso M., Priest M.J., Huang R., 2007. Root infection of *Vitis vinifera* by *Cylindrocarpon liriodendri* in Australia. *Australasian Plant Pathology* 36: 403–406. https://doi.org/10.1071/AP07041

Ye Q., Zhang W., Jia J., Li X., Zhou Y., Han C., Wu X., Yan J., 2021. Fungal pathogens associated with black foot of grapevine in China. *Phytopathologia Mediterranea* 60(2): 303-319. https://doi.org/10.36253/phyto-12353

6. SUPPLEMENTARY MATERIAL

Supplementary Table 1. Accession numbers of DNA sequences obtained from GenBank and used for the phylogenetic analyses in this study.

Genus	Species	Strain number	Host	Country	GenBank accession No.		
					TUB2	HIS3	TEF
Campylocarpon	***C. fasciculare***	**CBS 112613**	*Vitis vinifera*	South Africa	AY677221	JF735502	JF735691
	C. pseudofasciculare	**CBS 112679**	*Vitis vinifera*	South Africa	AY677214	JF735503	JF735692
Dactylonectria	***D. alcacerensis***	**CBS 129087**	*Vitis vinifera*	Portugal	AM419111	JF735630	JF735819
	D. alcacerensis	Cyl-01	*Vitis vinifera*	Spain	-	MG745823	-
	D. alcacerensis	Cy133	*Vitis vinifera*	Spain	JF735459	JF735628	JF735817
	D. amazonica	**MUCL55430**	*Piper* sp.	Ecuador	MF683643	MF683685	MF683664
	D. amazonica	MUCL55433	*Piper* sp.	Ecuador	MF683644	MF683686	MF683665
	D. anthuriicola	**CBS 564.95**	*Anthurium* sp.	Netherlands	JF735430	JF735579	JF735768
	D. ecuadoriensis	**MUCL55424**	*Piper* sp.	Ecuador	MF683641	MF683683	MF683662
	D. ecuadoriensis	MUCL55425	*Piper* sp.	Ecuador	MF683642	MF683684	MF683663
	D. estremocencsis	**CBS 129085**	*Vitis vinifera*	Portugal	JF735448	JF735617	JF735806
	D. estremocencsis	Cy135	*Vitis vinifera*	Portugal	AM419105	JF735615	JF735804
	D. hispanica	**CBS 142827**	*Pinus halepensis*	Spain	KY676876	KY676864	KY676870
	D. hispanica	Cy228	*Ficus* sp.	Portugal	JF735429	JF735578	JF735767
	D. hordeicola	**CBS 162.89**	*Hordeum vulgare*	Netherlands	AM419084	JF735610	JF735799
	D. macrodidyma	**CBS 112615**	*Vitis vinifera*	South Africa	AY677233	JF735647	JF735836
	D. macrodidyma	STE-U 9098	*Olea europaea* subsp. *Europaea*	South Africa	-	MT309058	-
	D. macrodidyma	Cy15UFSM	*Vitis vinifera*	Brazil	-	KF633159	-
	D. macrodidyma	Cy175	*Vitis vinifera*	Portugal	JF735473	JF735652	JF735841
	D. macrodidyma	CBS 112594	*Vitis vinifera*	South Africa	AY677231	JF735643	JF735832
	D. macrodidyma	CBS 112605	*Vitis vinifera*	South Africa	AY677230	JF735646	JF735835
	D. novozelandica	**CBS 113552**	*Vitis* sp.	New Zealand	AY677237	JF735633	JF735822

	D. novozelandica	CBS 112608	*Vitis vinifera*	South Africa	AY677235	JF735632	JF735821
	D. novozelandica	CBS 112593	*Vitis vinifera*	South Africa	AY677236	JF735631	JF735820
	D. novozelandica	Cy115			JF735460	JF735634	JF735823
	D. palmicola	**MUCL55426**	*Euterpe precatoria*	Ecuador	MF683645	MF683687	MF683666
	D. pauciseptata	**CBS 120171**	*Vitis* sp.	Slovenia	EF607066	JF735587	JF735776
	D. pauciseptata	BV-1354	*Vitis vinifera*	Spain	MK602798	MK579256	MK602813
	D. pinicola	**CBS 173.37**	*Pinus laricio*	United Kingdom	JF735447	JF735614	JF735803
	D. pinicola	Cy200	*Vitis vinifera*	Portugal	JF735445	JF735612	JF735801
	D. riojana	**BV-1396**	*Vitis* sp.	Spain	MK602811	MK602831	MK602826
	D. riojana	BV-1397	*Vitis* sp.	Spain	MK602812	MK602832	MK602827
	D. torresensis	**CBS 129086**	*Vitis vinifera*	Portugal	JF735492	JF735681	JF735870
	D. torresensis	CBS 112598	*Vitis vinifera*	South Africa	JF735479	JF735662	JF735851
	D. torresensis	CBS 188.49	*Abies nordmanniana*	Netherlandas	AM419087	JF735658	JF735847
	D. valentina	**CBS 14826**	*Ilex aquifolium*	Spain	KY676875	KY676863	KY676869
	D. valentina	STE-U 9105	*Olea europaea* subsp. *europaea*	South Africa	-	MT309072	-
	D. vitis	**CBS 129082**	*Vitis vinifera*	Portugal	JF735431	JF735580	JF735769
Ilyonectria	***I. capensis***	**CBS 132815**	*Protea* sp.	South Africa	JX231103	JX231135	JX231119
	I. capensis	CBS 132816	*Protea* sp.	South Africa	JX231112	JX231144	JX231128
	I. coprosmae	CBS 119606	*Metrosideros* sp.	Canada	JF735373	JF735505	JF735694
	I. crassa	**CBS 139.30**	*Lilium* sp.	Netherlandas	JF735393	JF735534	JF735723
	I. crassa	CBS 158.31	*Narcissus* sp.	Netherlandas	JF735394	JF735535	JF735724
	I. crassa	CBS 129083	*Panax quinquefolium*	Canada	JF735395	JF735536	JF735725
	I. cyclaminicola	**CBS 302.93**	*Cyclamen* sp.	The Netherlands	JF735432	JF735581	JF735770
	I. europaea	**CBS 129078**	*Vitis vinifera*	Portugal	JF735421	JF735567	JF735756
	I. europaea	CBS 102892	Stem	Germany	JF735422	JF735569	JF735758
	I. gamsii	**CBS 940.97**	Soil	The Netherlands	AM419089	JF735577	JF735766
	I. ilicicola	**CBS 142828**	*Ilex* sp.	Spain	KY676878	KY676866	KY676872
	I. ilicicola	Cy-FO-226	*Ilex* sp.	Spain	KY676879	KY676867	KY676873

I. leucospermi	**CBS 132809**	Leucospermum sp.	South Africa	JX231113	JX231145	JX231129
I. leucospermi	CBS 132810	*Protea* sp.	South Africa	JX231114	JX231146	JX231130
I. liliigena	**CBS 189.49**	*Lilium regale*	Netherlands	JF735425	JF735573	JF735762
I. liiligena	CBS 732.74	*Lilium* sp.	Netherlands	JF735426	JF735574	JF735763
I. liriodendri	**CBS 110.81**	*Liriodedron tulipifera*	USA	DQ178170	JF735507	JF735696
I. liriodendri	CBS 112596	*Vitis vinifera*	South Africa	AY677239	JF735511	JF735700
I. lusitanica	**CBS 129080**	*Vitis vinifera*	Portugal	JF735423	JF735570	JF735759
I. mors-panacis	**CBS 306.35**	*Pa. quinquefolium*	Canada	JF735414	JF735557	JF735746
I. mors-panacis	CBS 124662	*Pa. ginseng*	Japan	JF735416	JF735559	JF735748
I. palmarum	**CBS 135754**	*Howea forsteriana*	Italy	HF922608	HF922620	HF922614
I. palmarum	CBS 135753	*Howea forsteriana*	Italy	HF922609	HF922621	HF922615
I. panacis	**CBS 129079**	*Panax quinquefolium*	Canada	JF735424	JF735572	JF735761
I. protearum	**CBS 132811**	*Protea* sp.	South Africa	JX231109	JX231141	JX231125
I. protearum	CBS 132812	*Protea* sp.	South Africa	JX231117	JX231149	JX231133
I. pseudodestructans	**CBS 129081**	*Vitis vinifera*	Portugal	AM419091	JF735563	JF735752
I. pseudodestructans	CBS 117824	*Quercus* sp.	Austria	JF735419	JF735562	JF735751
I. radicicola	**CBS 264.65**	*Cyclamen persicum*	Sweden	AY677256	JF735506	JF735695
I. robusta	**CBS 308.35**	*Panax quinquefolium*	Canada	JF735377	JF735518	JF735707
I. robusta	CBS 773.83	*Anodonta* sp.	The Netherlands	AY677254	JF735519	JF735708
I. rufa	**CBS 153.37**	*Dune sand*	France	AY677251	JF735540	JF735729
I. rufa	CBS 640.77	*Abies alba*	France	JF735399	JF735542	JF735731
I. venezuelensis	**CBS 102032**	Bark	Venezuela	AY677255	JF735571	JF735760
I. vredehoekensis	**CBS 132807**	*Protea* sp.	South Africa	JX231107	JX231139	JX231123
I. vredehoekensis	CBS 132814	*Protea* sp.	South Africa	JX231110	JX231142	JX231126
***Ilyonectria* sp.**	**STEU 8918**	*Prunus persica* sp.	South Africa	-	MK765799	-

Supplementary Table 2. Uruguayan *Dactylonectria* and *Ilyonectria* isolates obtained from nursery grapevines plants with typical black foot symptoms.

Fungal species	Isolate name	Cultivar/rootstock	Year of collection	GenBank accession No.		
				HIS3	TUB2	TEF
Dactylonectria macrodydima	URU-VD-214	Tannat/101-14	2017	OQ990143	OQ990266	OQ990195
	URU-VD-215	Tannat/101-14	2017	OQ990144	OQ990267	OQ990196
	URU-VD-216	Tannat/101-14	2017	OQ990145	OQ990268	OQ990197
	URU-VD-218	Tannat/101-14	2017	OQ990146	OQ990269	OQ990198
	URU-VD-219	Tannat/101-14	2017	OQ990147	OQ990270	OQ990199
	URU-VD-220	Tannat/101-14	2017	OQ990148	OQ990271	OQ990200
	URU-VD-221	Tannat/101-14	2017	OQ990149	OQ990272	OQ990201
	URU-VD-222	Tannat/101-14	2017	OQ990150	OQ990273	OQ990202
	URU-VD-224	Tannat/101-14	2017	OQ990151	OQ990274	OQ990203
	URU-VD-225	Prosecco/SO4	2017	OQ990152	OQ990275	OQ990204
	URU-VD-226	Prosecco/SO4	2017	OQ990153	OQ990276	OQ990205
	URU-VD-227	Prosecco/SO4	2017	OQ990154	OQ990277	OQ990206
	URU-VD-228	Prosecco/SO4	2017	OQ990155	OQ990278	OQ990207
	URU-VD-229	Prosecco/SO4	2017	OQ990156	OQ990279	OQ990208
	URU-VD-230	M. de Hamburgo/Gravesac	2017	OQ990157	OQ990280	OQ990209
	URU-VD-231	Tannat/101-14	2017	OQ990158	OQ990281	OQ990210
	URU-VD-235	Prosecco/SO4	2017	OQ990159	OQ990282	OQ990211
	URU-VD-236	Prosecco/SO4	2017	OQ990160	OQ990283	OQ990212
	URU-VD-47	Merlot/101-14	2018	ON573132	OQ990254	OQ990183
	URU-VD-49	Merlot/101-14	2018	ON573133	OQ990255	OQ990184
	URU-VD-51	Merlot/101-14	2018	ON573134	OQ990256	OQ990185
	URU-VD-66	Tannat/1103P	2019	ON573135	OQ990257	OQ990186

	URU-VD-67	Tannat/1103P	2019	ON573150	OQ990258	OQ990187
	URU-VD-73	Albariño/101-14	2019	ON573136	OQ990259	OQ990188
	URU-VD-75	Albariño/Gravesac	2019	ON573137	OQ990260	OQ990189
	URU-VD-77	Albariño/Gravesac	2019	ON573138	OQ990261	OQ990190
	URU-VD-78	Albariño/Gravesac	2019	ON573139	OQ990262	OQ990191
	URU-VD-80 [a]	Tannat/1103P	2019	ON573140	OQ990263	OQ990192
	URU-VD-81	Tannat/1103P	2019	ON573141	OQ990264	OQ990193
	URU-VD-82	Tannat/1103P	2019	ON573142	OQ990265	OQ990194
	URU-VD-248	Albariño/Gravesac	2019	OQ990161	OQ990284	OQ990213
Dactylonectria novozelandica	URU-VD-58	Albariño/101-14	2019	ON573143	OQ990285	OQ990214
	URU-VD-60	Albariño/101-14	2019	ON573144	OQ990286	OQ990215
	URU-VD-61	Albariño/101-14	2019	ON573145	OQ990287	OQ990216
	URU-VD-62	Albariño/101-14	2019	ON573146	OQ990288	OQ990217
	URU-VD-63	Albariño/101-14	2019	ON573147	OQ990289	OQ990218
	URU-VD-64 [a]	Albariño/Gravesac	2019	ON573148	OQ990290	OQ990219
	URU-VD-65	Albariño/Gravesac	2019	ON573149	OQ990291	OQ990220
	URU-VD-68	Tannat/1103P	2019	ON573151	OQ990292	OQ990221
	URU-VD-69	Tannat/1103P	2019	ON573152	OQ990293	OQ990222
	URU-VD-70	Albariño/101-14	2019	ON573153	OQ990294	OQ990223
	URU-VD-71 [a]	Albariño/101-14	2019	ON573154	OQ990295	OQ990224
	URU-VD-72	Albariño/101-14	2019	ON573155	OQ990296	OQ990225
	URU-VD-74	Albariño/101-14	2019	ON573156	OQ990297	OQ990226
	URU-VD-76	Albariño/Gravesac	2019	ON573157	OQ990298	OQ990227
Dactylonectria torresensis	URU-VD-232	Cabernet Franc/3309	2017	OQ990139	OQ990250	OQ990179
	URU-VD-233	Cabernet Franc/3309	2017	OQ990140	OQ990251	OQ990180
	URU-VD-234 [a]	Cabernet Franc/3309	2017	OQ990141	OQ990252	OQ990181
	URU-VD-237	Tannat/101-14	2017	OQ990142	OQ990253	OQ990182
	URU-VD-48	Merlot/101-14	2018	ON573161	OQ990244	OQ990173

	URU-VD-50	Merlot/101-14	2018	ON573162	OQ990245	OQ990174
	URU-VD-53	Tannat/Gravesac	2018	ON573163	OQ990246	OQ990175
	URU-VD-55	Chardonnay/SO4	2018	ON573164	OQ990247	OQ990176
	URU-VD-56	Lácrima/1103P	2018	ON573165	OQ990248	OQ990177
	URU-VD-79 [a]	Albariño/Gravesac	2019	ON573166	OQ990249	OQ990178
Dactylonectria palmicola	URU-VD-247	Tannat/101-14	2017	OQ990138	OQ990243	OQ990172
	URU-VD-52	Tannat/Gravesac	2018	ON573158	OQ990241	OQ990170
	URU-VD-54 [a]	Chardonnay/SO4	2018	ON573159	OQ990242	OQ990171
Ilyonectria liriodendri	URU-VD-85	Cabernet Franc/3309	2017	ON573168	OQ990303	OQ990232
	URU-VD-86	Prosecco/SO4	2017	ON573169	OQ990304	OQ990233
	URU-VD-87	Tannat/101-14	2017	ON573170	OQ990305	OQ990234
	URU-VD-88	Prosecco/SO4	2017	ON573171	OQ990306	OQ990235
	URU-VD-241	Prosecco/SO4	2017	OQ990165	OQ990307	OQ990236
	URU-VD-242 [a]	Tannat/Gravesac	2018	OQ990166	OQ990308	OQ990237
	URU-VD-244	Albariño/Gravesac	2019	OQ990167	OQ990309	OQ990238
	URU-VD-245	Albariño/Gravesac	2019	OQ990168	OQ990310	OQ990239
	URU-VD-246	Tannat/1103P	2019	OQ990169	OQ990311	OQ990240
Ilyonectria sp.	URU-VD-84 [a]	Tannat/101-14	2017	ON573173	OQ990299	OQ990228
	URU-VD-238	Tannat/101-14	2017	OQ990162	OQ990300	OQ990229
	URU-VD-239	Tannat/101-14	2017	OQ990163	OQ990301	OQ990230
	URU-VD-240	Tannat/Gravesac	2018	OQ990164	OQ990302	OQ990231

[a] Isolates selected for morphological characterization and pathogenicity test.

ARTÍCULO 3

Drought influences fungal community dynamics in the grapevine rhizosphere and root microbiome

MARÍA JULIA CARBONE[1], SANDRA ALANIZ[1], PEDRO MONDINO[1], MATÍAS GELABERT[1], ALES EICHMEIER[2], DOROTA TEKIELSKA[2], REBECA BUJANDA[3], DAVID GRAMAJE[3]

[1]Departamento de Protección Vegetal, Facultad de Agronomía, Universidad de la República

[2]Faculty of Horticulture, Mendeleum – Institute of Genetics, Mendel University in Brno

[3]Instituto de Ciencias de la Vid y del Vino, Consejo Superior de Investigaciones Científicas – Universidad de la Rioja – Gobierno de La Rioja

Publicado en: *Journal of Fungi* (2021) 7:686 https://doi.org/10.3390/jof7090686

Drought influences fungal community dynamics in the grapevine rhizosphere and root microbiome

ABSTRACT

Plant roots support complex microbial communities that can influence nutrition, plant growth, and health. In grapevine, little is known about the impact of abiotic stresses on the belowground microbiome. In this study, we examined the drought-induced shifts in fungal composition in the root endosphere, the rhizosphere and bulk soil by internal transcribed spacer (ITS) high-throughput amplicon sequencing (HTAS). We imposed three irrigation regimes (100%, 50%, and 25% of the field capacity) to one-year old grapevine rootstock plants cv. SO_4 when plants had developed 2–3 roots. Root endosphere, rhizosphere, and bulk soil samples were collected 6- and 12-months post-plantation. Drought significantly modified the overall fungal composition of all three compartments, with the root endosphere compartment showing the greatest divergence from well-watered control (100%). The overall response of the fungal microbiota associated with black-foot disease (*Dactylonectria* and "*Cylindrocarpon*" genera) and the potential biocontrol agent *Trichoderma* to drought stress was consistent across compartments, namely that their relative abundances were significantly higher at 50–100% than at 25% irrigation regime. We identified a significant enrichment in several fungal genera such as the arbuscular mycorrhizal fungus *Funneliformis* during drought at 25% watering regime within the roots. Our results reveal that drought stress, in addition to its well-characterized effects on plant physiology, also results in the restructuring of grapevine root microbial communities, and suggest the possibility that members of the altered grapevine microbiota might contribute to plant survival under extreme environmental conditions.

Keywords: black-foot disease, drought, high-throughput next generation sequencing, *Vitis vinifera* L., water stress

1. INTRODUCTION

Drought is one of the major environmental stresses in agriculture, resulting in significant economic losses worldwide [1]. Climate projections indicate that frequency and severity of drought events are likely to increase in some regions, which will require major adaptations in order to maintain agricultural production [1,2].

Mechanisms of water stress responses in plants involve adaptations at the morphological, physiological, and molecular levels [3]. Among those, drought avoidance (e.g., increased root growth, leaf rolling, and stomatal closure) and drought tolerance (e.g., osmotic adjustment, antioxidant defense system, and increased ABA production) are considered the two major general mechanisms to water stress resistance in plants [3,4].

Plants are closely related with microorganisms that inhabit in the soil-rhizosphere-root endosphere continuum [5,6]. These microorganisms can provide benefits to plants, contributing with nutrient mobilization and transport, protection against pathogens or pests, and stress alleviation [6–8].

Changes in environmental factors that affect plants are also expected to influence plant-associated microbiomes, and vice versa [9]. Drought affects the structure of microbial soil community [10,11] as a result of the selection in favor of taxa tolerant to low moisture content and shifts in diffusion rates and soil chemistry [12]. Edaphic communities are the predominant source of microorganisms for the root-associated compartments, therefore changes in the microbial soil community caused by drought have consequences on the composition of root-associated microbiome [5]. Additionally, plant responses to drought stress, such as modifications in the root morphology [13] and shifts in root exudation profile [14,15], also directly affect the activity and structure of root-associated microbial communities [5,12].

Many studies have noticed the influence of drought on root-associated bacterial communities. Bouasria et al. [16] observed that drought had a significant effect on rhizosphere bacterial community diversity in different species of grass. Barnard et al. [10] studied the responses of soil bacterial and fungal communities to desiccation and rewetting in grasslands and concluded that only bacterial communities were significantly affected by dry-down. An enrichment of bacterial taxa *Actinobacteria* in the root endosphere and rhizosphere of drought-treated plants, as well as in the soil, has been observed across multiple host species [5,17–21].

In contrast, the effect of drought on soil and root-associated fungal communities remains largely unexplored [10,12,16,17,22]. Barnard et al. [10] observed that soil fungal communities in grasslands were largely unaffected by dry-down, suggesting a high degree of resistance to changes in soil water availability. Similar results were found by Naylor et al. [17], who observed that drought had no significant effect on soil, rhizosphere, and root endosphere fungal community composition in various grass lineages. However, recent research demonstrated that drought significantly altered the rhizosphere and root endosphere fungal community diversity on rice crop plant [5].

Grapevine (*Vitis vinifera* L.) is a traditionally non-irrigated crop [23]. Nevertheless, agronomic practices such as rootstock use, tillage or no-tillage, controlled cover crop, and irrigation are largely used to balance vine vegetative and reproductive growth [23,24]. In the context of predicted increased drought events, management strategies including use of drought-resistant cultivars [25] and soil conservation measures [24] are being increasingly employed.

The belowground grapevine microbiome is affected in composition and diversity by soil-plant compartment [26,27]. Diversity of bacterial [26] and fungal [27] communities is higher in the rhizosphere and the bulk soil compared with the root endosphere compartment. Plant-associated properties such as rootstock genotype [28,29] and phenological stage [30] play a significant role in shaping grapevine microbiome. Environmental factors related with soil physicochemical properties and moisture content [26,31–33], as well as management practices such as tillage and irrigation [24], has been identified as factors that significantly influence in the grapevine rhizosphere microbiome diversity.

Potential black-foot disease (BFD) pathogens have been found determining the dissimilarities in the fungal microbiome between soil-grapevine compartments [27]. BFD of grapevine is an important disease in nurseries and young vineyards in most grapevine growing regions worldwide [34,35]. Symptoms include necrotic lesions on root tissue and black discoloration and necrosis of wood tissue in the base of the rootstock, which lead to the death of young vines [34]. Causal agents of BFD are soilborne pathogens belonging to genera *Campylocarpon*, *Cylindrocladiella*, *Dactylonectria*, *Ilyonectria*, *Neonectria*, *Pleiocarpon*, and *Thelonectria* [36,37]. BFD incidence is favored by poor drained conditions, high moisture content, and heavy texture of soil [34].

Grapevine physiological and molecular responses to water stress has been extensively studied [23]; however, little is known about the effect of drought on fungal microbiome structure and composition in the bulk soil, rhizosphere, and root endosphere in grapevine. Understanding the effect of extreme environments on fungal community composition will provide information about how the network of grapevine-microbiome interactions is reshaped under challenging scenarios. Moreover, identification of root-associated fungal taxa that develop under drought conditions could lead to the detection of beneficial fungal symbionts that are able to mediate plant stress tolerance through diverse mechanisms.

In this study, we conducted a greenhouse-based experiment to explore the impact of drought on the root-associated fungal communities of cultivated grapevine. The compositional shifts in the bulk soil, rhizosphere, and root endosphere communities in the most prevalent grapevine rootstock genotype and predominant soil type of the main grapevine growing area in Uruguay were examined. In addition, the effect of drought on the metabolic function of the fungal communities in the three plant compartments was analyzed. We were particularly interested in evaluating the impact of extreme environments on BFD fungal abundance. This approach has allowed us to determine the conservation and extent of the drought-mediated shifts accomplished by the beneficial and pathogenic fungal microbiota.

2. MATERIALS AND METHODS

2.1 Experimental design and treatments

In November 2018, seventy-two Selection Oppenheim 4 (SO4; *Vitis berlandieri X Vitis riparia*) rootstock cuttings, previously callused, were planted in 11 L pots (one plant per pot) containing natural soil (Table S1). The soil was collected from a commercial grapevine nursery (34°34′48″ S, 56°17′50″ W) located in Canelones, the major grape-growing region in Uruguay [38]. During the experiment, the potted plants were maintained in a greenhouse located in the Faculty of Agronomy (Montevideo, Uruguay). Rootstock SO4 is the most widely used rootstock in Uruguay, accounting for 63% of the grapevine growing area [39].

One month after sprouting, potted SO4 plants were randomly divided into three treatments, simulating three types of irrigation regimes. The treatments were (1) irrigation at 25% of field capacity (severe water deficit: SWD), (2) irrigation at 50% of field

capacity (moderate water deficit: MWD), and (3) irrigation at 100% of field capacity (absence of water deficit: AWD). Soil water content at field capacity was previously calculated according to Silva et al. [40]. An automated drip irrigation system was adjusted for each irrigation treatment, by measuring the dielectric constant of soil. The irrigation treatments were maintained over 18 months. The experimental design consisted of four randomized blocks per irrigation treatment, each containing 6 plants (24 plants per irrigation treatment).

During the growing season, predawn leaf water potential was measured every 20 days approximately with a pressure chamber [41]. After the leaf fall, 18 months from the beginning of the experiment (July 2020), plants were pruned, and the pruning weight was registered. The data were subjected to analysis of variance and mean values were separated according to Tukey's honestly significant difference at *p*-value = 0.05, with Statistix 10 software (Analytical Software, Tallahasese, FL, USA).

2.2 Sample collection

Bulk soil, rhizosphere (soil surrounding roots), and root samples were collected at six months (June 2019) and twelve months (December 2019) after the irrigation treatments were established. Twenty-four replicates were collected from each plant compartment and irrigation treatment.

Bulk soil samples were collected with a sterile shovel close to the edge of the pot at depths of 15–20 cm. Roots and rhizosphere were collected with a sterile spade close to the stem at depths where the root system was denser [27]. Samples were kept in sterile bags and stored on dry ice at the time of sampling. Immediately, samples were transported to the laboratory for further processing. Roots with rhizosphere particles attached were separated according to Berlanas et al. [29]. After that, roots were rinsed and cleaned with distilled water and surface disinfected with sodium hypochlorite (1%) for 30 s. Finally, roots were washed three times with sterile distilled water and the root cortex was removed with sterile scalpel. All samples were stored at −80 °C until DNA extraction. A total of 432 samples were collected.

2.3 DNA extraction, amplification and sequencing

Genomic rhizosphere and bulk soil DNA were extracted from 0.5 g sample using the DNeasy PowerSoil Kit (Qiagen, Hilden, Germany), following the kit protocol. The

root endosphere DNA was extracted from 0.05 g sample using the DNeasy Plant Pro Kit (Qiagen, Hilden, Germany). Roots were first ground into powder in liquid nitrogen and then the kit protocol was followed. DNA yields were quantified using the Invitrogen Qubit 4 Fluorometer with Qubit dsDNA HS (High Sensitivity) Kit (Thermo Fisher Scientific, Waltham, MA, USA) and the extracts were adjusted to 10–15 ng/µL. After DNA quantification, samples were pooled in groups of two, resulting in a total of twelve replicates per plant-compartment, irrigation treatment, and sampling time for every batch of 24 plants.

For fungal library preparation, the complete fungal ITS2 region was amplified using the primers ITS86F [42] and ITS4 [43]. Primers were modified to include the Illumina sequencing primers. PCR were carried out in a final volume of 25 µL, containing 2.5 µL of template DNA, 0.5 µM of the primers, 12.5 µL of Supreme NZYTaq 2x Green Master Mix (NZYTech), and ultrapure water up to 25 µL. PCR amplifications consisted of an initial denaturation step at 95 °C for 5 min, followed by 35 cycles of 95 °C for 30 s, 49 °C for 30 s, 72 °C for 30 s, and a final extension step at 72 °C for 10 min. A secondary PCR was conducted to index the amplicons with identical conditions, but for only 5 cycles and with 60 °C as the annealing temperature. Libraries were purified using the Mag-Bind RXNPure Plus magnetic beads (Omega Biotek, Norcross, GE, USA), following the instructions provided by the manufacturer. The purified libraries were pooled in equimolar amounts according to the quantification data provided by the Qubit dsDNA HS Assay (Thermo Fisher Scientific, Waltham, MA, USA). Samples were sequenced in the MiSeq platform (Illumina, San Diego, CA, USA) at the AllGenetics and Biology SL (Galicia, Spain) (www.allgenetics.eu, accessed on 15/05/2020, using a paired-end 2× 300 bp (PE 300) sequencing and the MiSeq Reagent Kit v3 (Illumina, San Diego, USA). Negative controls during library preparation and DNA extraction, and a positive control containing DNA of a grapevine rhizosphere sample [29] were included.

2.4 Data analysis

Sequence quality was visualized using FastQC-0.10.1 [44]. The further data processing was completed using SEED v2.0 [45]. Raw forward and reverse sequences for each sample were assembled into paired-end reads using the fastq-join 1.1.2 tool from the eatools suite [46]. Sequences were then quality filtered, Q = 30; trimmed on the length > 250 bases; and ambiguous bases were removed. Sequences were grouped by barcode motives and then labelled by sample names. Fungal ITS were extracted using ITSx 1.0.11

[47]. Then, the sequences were clustered into operational taxonomic units (OTUs) and chimeric sequences were removed with Usearch-UPARSE 8.1.1861 [48] with a threshold of 97% pairwise identity against UNITE fungal dynamic database [49]. The representative consensus sequences were extracted from the clusters using MAFFT 7.222 [50]. Finally, the identification of OTUs was performed by blastn, tblastx, and makeblastdb 2.5.0+ (https://blast.ncbi.nlm.nih.gov/Blast.cgi, accessed on 28/09/2020). The dataset was normalized applying Total Sum Scaling standard approach and samples were rarefied to 15,736 fungal sequences (the minimum library size).

2.5 Fungal diversity and statistical analysis

Alpha diversity was calculated using Shannon and Chao1 indices in Phyloseq package, as implemented in MicrobiomeAnalyst [51,52]. Beta diversity was estimated using a principal coordinates analysis (PCoA) based on Bray–Curtis metrics [53] with MicrobiomeAnalyst. PERMANOVA analysis was carried out to evaluate which OTUs significantly differed in abundance among experimental factors. Good's coverage values and rarefaction curves were calculated using MicrobiomeAnalyst.

The Linear Discriminant Analysis Effect Size (LEfSe) algorithm was used to identify taxa (genus level or higher) that differed in relative abundance between water stress regime and time of sampling among each compartment [54]. MicrobiomeAnalyst LEfSe implementation was used; the threshold for the logarithmic Linear Discriminant Analysis (LDA) score was set at 2.0 and the FDR-adjusted *p*-value cutoff at 0.1. The fungal OTUs shared among compartments, water stress regimes and time of sampling were obtained by a Venn diagram analysis using the software available at http://bioinformatics.psb.ugent.be, accessed on 15/10/2020. Correlation network analysis was performed by MicrobiomeAnalyst based on the SparCC algorithm [55]. The permutation was settled at 100 with a *p*-value threshold of 0.01 and a correlation threshold of 0.5 at the genus taxonomical level.

2.6 Functional prediction of fungal communities

The function of fungal communities in the three irrigation conditions in the soil-plant compartments was investigated using FUNGuild v1.0 [56]. According to three trophic modes (pathotrophs, saprotrophs, and symbiotrophs), eleven guilds were classified: plant pathogens, animal pathogens, fungal parasites, lichen parasites, undefined saprotrophs, soil saprotrophs, wood saprotrophs, dung saprotrophs, plant

saprotrophs, endophytes, and arbuscular mycorrhizal. OTUs that did not match taxa in the database were classified as “unassigned”. Guilds considered “probable” and “highly probable” according to the fungal database were selected for further analysis. Relative abundance of OTUs according to guilds were calculated to the three irrigation conditions at the three soil-plant compartments analyzed. The effect of water stress conditions on the relative abundance of OTUs according to the trophic modes was assessed performing ANOVA, with Statistix 10 software (Analytical Software). Data were transformed to $\sqrt{x}$ prior to analysis. Transformed data means were compared using Tukey’s honestly significant difference at *p*-value = 0.05.

3. RESULTS

3.1 Water potential and pruning weight

Predawn water potential and the pruning weight data differed among irrigation treatments ($p < 0.05$). In the 2018–2019 growing season, the predawn water potential ranged from −0.70 to −0.60 MPa in the SWD regime, from −0.45 to −0.36 MPa in the MWD regime, and from −0.12 to −0.09 MPa in the AWD regime. In the 2019–2020 growing season, the predawn water potential ranged from −0.78 to −0.58 MPa, from −0.51 to −0.28 MPa, and from −0.14 to −0.07 in the SWD, MWD, and AWD regimes, respectively (Figure S1). The pruning weight in the SWD regime was significantly lower (1.72 g/plant) compared to the MWD (31.25 g/plant) and the AWD (54.83 g/plant) regimes (Figure S2).

3.2 High-throughput amplicon sequencing

A total of 4,963,651 fungal ITS sequences were generated from 207 samples after paired-end alignments, quality filtering, and deletion of singletons, chimeric, chloroplast, and mitochondrial sequences. Nine samples were removed from the analysis due to the low number of sequences reads. Sequences were assigned to 339 fungal OTUs (Table S2). Good’s coverage values in all samples ranged from 99.9 to 100% (Table S3). Chao1 diversity estimator ranged from 15.0 to 87.5, while Shannon diversity estimator ranged from 1.7 to 3.2 (Table S3). Sequencing data are deposited under BioProject acc. no. PRJNA707008, where the SRA experiments are available by acc. nos. SRX10263838–SRX10366007.

3.3 Fungal communities differed among soil-plant compartments

The alpha diversity of fungal communities differed significantly among soil-plant compartments (Table 1). Chao1 and Shannon's estimators indicated that fungal diversity in rhizosphere and bulk soil was significantly higher than in root (Figure 1a,b). Principal coordinates analysis (PCoA) of Bray–Curtis data demonstrated that soil-plant compartment was a source of beta diversity (R^2 = 0.15, p < 0.001) (Figure S3). The relative abundance of fungal phylum, family, and genus detected in bulk soil, rhizosphere, and root is shown in Figure S4. Considering data from all soil-plant compartments, the most abundant phyla were Ascomycota, followed by Basidiomycota, and Mucoromycota (Figure S4a).

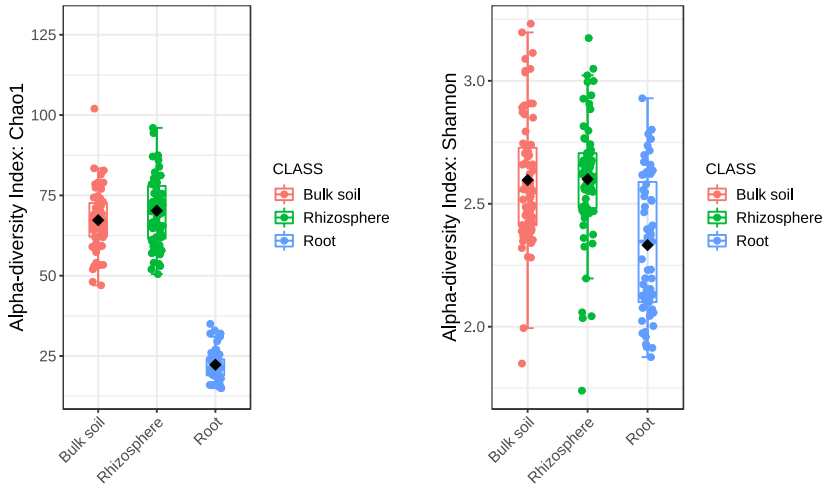

(**a**) (**b**)

Figure 1. Boxplot illustrating the differences in (**a**) Chao1 and (**b**) Shannon diversity measures of the fungal communities in the soil-plant compartments.

In the root, the most abundant families were Nectriaceae (18.5%), Ceratobasidiaceae (12.2%), and Mortierellaceae (7.8%) (Figure S4b). In the rhizosphere, most abundant families were Mortierellaceae (18.7%), followed by Nectriaceae (16,4%), and Ceratobasidiaceae (9.9%), whereas in bulk soil, the most abundant families were Mortierellaceae (25.2%), followed by Nectriaceae (13.8%), and an unidentified family (8.2%) (Figure S4b).

Table 1. Experimental factors predicting alpha diversity of bulk soil-, rhizosphere- and root-associated fungal communities.

Dataset	Factor	Indexes	
		Shannon	**Chao1**
Whole	Plant-soil compartments	$F = 23.93$ $\mathbf{p = 4.62 \times 10^{-10}}$	$F = 693.64$ $\mathbf{p = 1.01 \times 10^{-91}}$
Bulk soil	Sampling time	$F = 4.93$ $\mathbf{p = 7.69 \times 10^{-6}}$	$F = -1.43$ $p = 0.158$
	Irrigation regime	$F = 4.63$ $\mathbf{p = 0.0130}$	$F = 8.58$ $\mathbf{p = 0.0005}$
	Sampling time × irrigation regime	$F = 9.69$ $\mathbf{p = 5.69 \times 10^{-7}}$	$F = 7.26$ $\mathbf{p = 1.8 \times 10^{-5}}$
Rhizosphere	Sampling time	$F = 0.96$ $p = 0.3396$	$F = 0.22$ $p = 0.8267$
	Irrigation regime	$F = 12.73$ $\mathbf{p = 2.22 \times 10^{-5}}$	$F = 10.15$ $\mathbf{p = 0.0002}$
	Sampling time × irrigation regime	$F = 8.19$ $\mathbf{p = 5.72 \times 10^{-6}}$	$F = 10.19$ $\mathbf{p = 3.96 \times 10^{-7}}$
Root	Sampling time	$F = -4.16$ $\mathbf{p = 0.0001}$	$F = -0.63$ $p = 0.5336$
	Irrigation regime	$F = 45.58$ $\mathbf{p = 4.25 \times 10^{-13}}$	$F = 22.85$ $\mathbf{p = 3.06 \times 10^{-8}}$
	Sampling time × irrigation regime	$F = 49.73$ $\mathbf{p = 2.01 \times 10^{-20}}$	$F = 8.93$ $\mathbf{p = 1.99 \times 10^{-6}}$
Bulk soil/ Sampling time 1	Irrigation regime	$F = 5.81$ $\mathbf{p = 0.0069}$	$F = 3.36$ $\mathbf{p = 0.0470}$
Bulk soil/ Sampling time 2	Irrigation regime	$F = 4.37$ $\mathbf{p = 0.0208}$	$F = 11.98$ $\mathbf{p = 0.0001}$
Root/Sampling time 1	Irrigation regime	$F = 114.15$ $\mathbf{p = 5.04 \times 10^{-15}}$	$F = 20.39$ $\mathbf{p = 2.23 \times 10^{-6}}$
Root/Sampling time 2	Irrigation regime	$F = 116.18$ $\mathbf{p = 3.96 \times 10^{-15}}$	$F = 26.81$ $\mathbf{p = 1.74 \times 10^{-7}}$

ANOVA, analysis of variance. Bold values indicate statistically significant results. *p*-value < 0.05. Sampling time 1: 6 months after the establishment of the irrigation regimes. Sampling time 2: 12 months after the establishment of the irrigation regimes.

3.4 Sampling time influence on fungal diversity

Fungal microbiome diversity significantly differed between sampling times in the root and bulk soil (Table 1). In root samples, Shannon diversity increased towards the 12-month sampling, whereas the opposite was found in bulk soil samples (Figure S5). The Bray–Curtis metric of beta diversity also was affected by sampling time in root (R^2 = 0.22, $p < 0.001$) and bulk soil (R^2 = 0.24, $p < 0.001$), which reinforced the differences

observed in the community composition over time (Figure S6a,c). In the rhizosphere, sampling time did not predict alpha diversity (Table 1), but affected the Bray–Curtis metrics of beta diversity ($R^2 = 0.30$, $p < 0.001$) (Figure S6b).

Regarding fungal OTUs, the proportion of OTUs shared among both sampling times was 33.2% in the root compartment (Figure S7a), 74.5% in the rhizosphere (Figure S7b), and 68.6% in bulk soil (Figure S7c).

The LEfSe detected that 26 genera determined the dissimilarities among sampling times in root (Figure S8a). In the rhizosphere, the relative abundance of 56 genera was affected by sampling time, whereas 45 genera determined the dissimilarities between sampling times in bulk soil (Figure S8b,c).

3.5 Water deficit affects fungal diversity in soil-plant compartments

Our results demonstrated that fungal microbiome varied significantly among irrigation regimes. This pattern was consistent to community-level measure of alpha diversity in root, rhizosphere, and bulk soil in both sampling times (Table 1). The relative abundance of fungal phyla, family, and genus detected across the soil-plant compartments in the different conditions of water stress is shown in Figure S9.

Regarding root samples, the richness and diversity of OTUs in the AWD regime (Sampling time 1 = Chao1: 28.40 ± 1.42, Shannon: 2.78 ± 0.04; Sampling time 2 = Chao1: 19.64 ± 0.56, Shannon: 2.61 ± 0.02) was significantly higher than in the SWD regime (Sampling time 1 = Chao1: 17.88 ± 0.74, Shannon: 2.06 ± 0.03; Sampling time 2 = Chao1: 15.27 ± 0.45, Shannon: 2.13 ± 0.03) in both sampling times (Figure 2). At 6-month sampling, the alpha diversity indexes of fungal communities were similar between SWD and MWD (Chao1: 21.75 ± 1.26; Shannon: 2.11 ± 0.04) regimes (Figure 2a,b). However, at the 12-month sampling time, alpha diversity measure in MWD regime (Chao1: 21.17 ± 0.71; Shannon: 2.41 ± 0.02) increased with respect to SWD treatment (Figure 2c,d). PCoA of Bray–Curtis data demonstrated that irrigation regime was a source of beta diversity at the 6-month ($R^2 = 0.86$, $p < 0.001$) (Figure 3a) and at 12-month sampling times ($R^2 = 0.39$, $p < 0.001$) (Figure 3b).

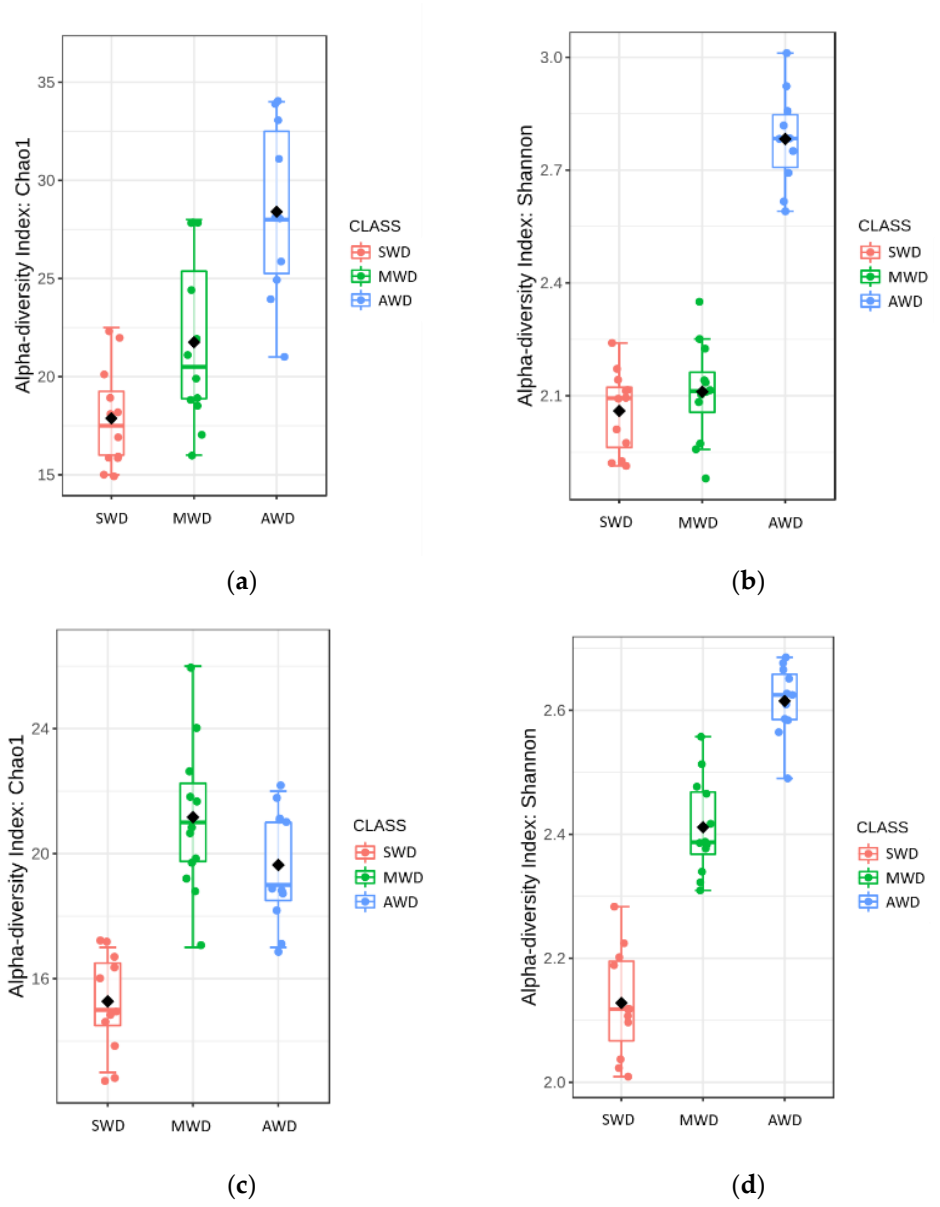

Figure 2. Boxplot illustrating the differences in (**a**) Chao1 and (**b**) Shannon diversity measures at the 6-month sampling time and (**c**) Chao1 and (**d**) Shannon diversity measures at the 12-month sampling time of the fungal communities in the root, at different irrigation regimes: severe water deficit (SWD), moderate water deficit (MWD), and absence of water deficit (AWD).

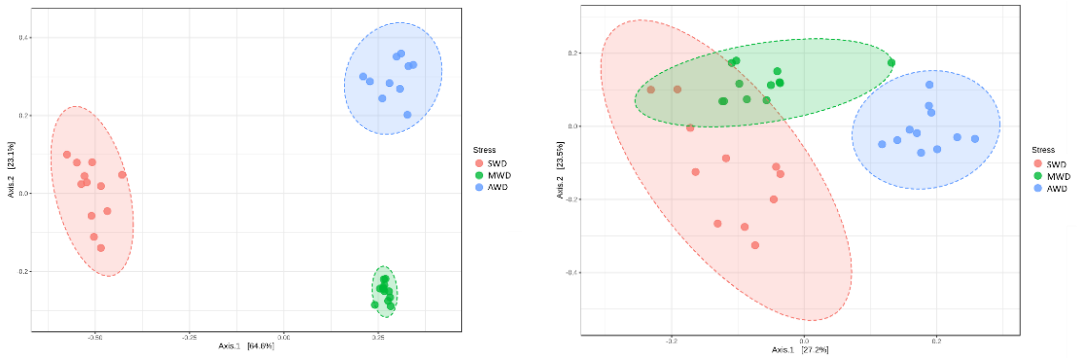

(**a**) (**b**)

Figure 3. Principal Coordinate Analysis (PCoA) based on Bray–Curtis dissimilarity metrics, showing the distance in the fungal communities among irrigation regimes (SWD: severe water deficit, MWD: moderate water deficit, and AWD: absence of water deficit) at (**a**) 6-month sampling and (**b**) 12-month sampling times in the root.

Rhizosphere samples at both sampling times were analzyed together, due to the lack of significant differences in the alpha diversity measures between sampling times (Table 1). Chao1 richness and Shannon diversity measures were affected by the irrigation regime, although there was not a clear pattern (Figure 4). Chao1 estimator measures were higher in SWD regime (84.04 ± 2.19) than in MWD (71.48 ± 2.37) and AWD (73.12 ± 1.78) regimes, whereas Shannon diversity estimator predicted the highest values in the AWD regime (2.81 ± 0.05) (Figure 4a,b). Bray–Curtis metric of beta diversity was affected by the irrigation regime (R^2 = 0.12, p < 0.001) (Figure 5).

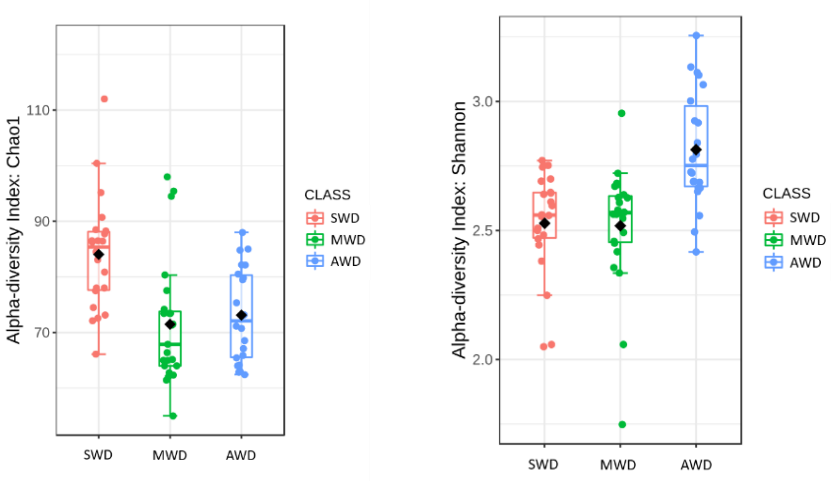

(**a**) (**b**)

Figure 4. Boxplot illustrating the differences in (**a**) Chao1 and (**b**) Shannon diversity measures at both sampling times of the fungal communities in the rhizosphere at different

irrigation regimes: severe water deficit (SWD), moderate water deficit (MWD), and absence of water deficit (AWD).

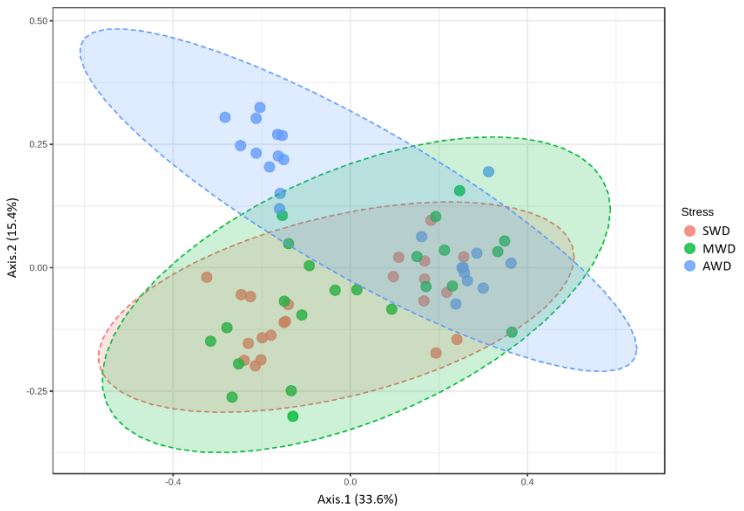

Figure 5. Principal Coordinate Analysis (PCoA) based on Bray–Curtis dissimilarity metrics, showing the distance in the fungal communities among irrigation regimes (SWD: severe water deficit, MWD: moderate water deficit, and AWD: absence of water deficit), at both sampling times of the fungal communities in the rhizosphere.

In the bulk soil at 6-month sampling, richness and diversity of OTUs in the MWD regime (Chao1: 75.87 ± 2.98; Shannon: 2.84 ± 0.10) was higher than in the SWD regime (Chao1: 67.06 ± 2.07; Shannon: 2.55 ± 0.03), but similar with the AWD regime (Chao1: 72.10 ± 2.07; Shannon: 2.86 ± 0.08) (Figure 6a,b). At 12-month sampling time, Chao1 diversity estimator indicated that the diversity in the AWD (74.89 ± 1.45) and MWD (70.17 ± 1.48) regimes was higher than in the SWD regime (62.32 ± 2.41), whereas Shannon estimator did not detect differences between SWD (2.41 ± 0.06) and MWD (2.42 ± 0.03) regimes, which were lower than the AWD (2.57 ± 0.03) (Figure 6c,d). Irrigation regimes also affected the Bray–Curtis metric of beta diversity at both 6-month (R^2 = 0.52, p < 0.001) (Figure 7a) and 12-month sampling times (R^2 = 0.25, p < 0.001) (Figure 7b).

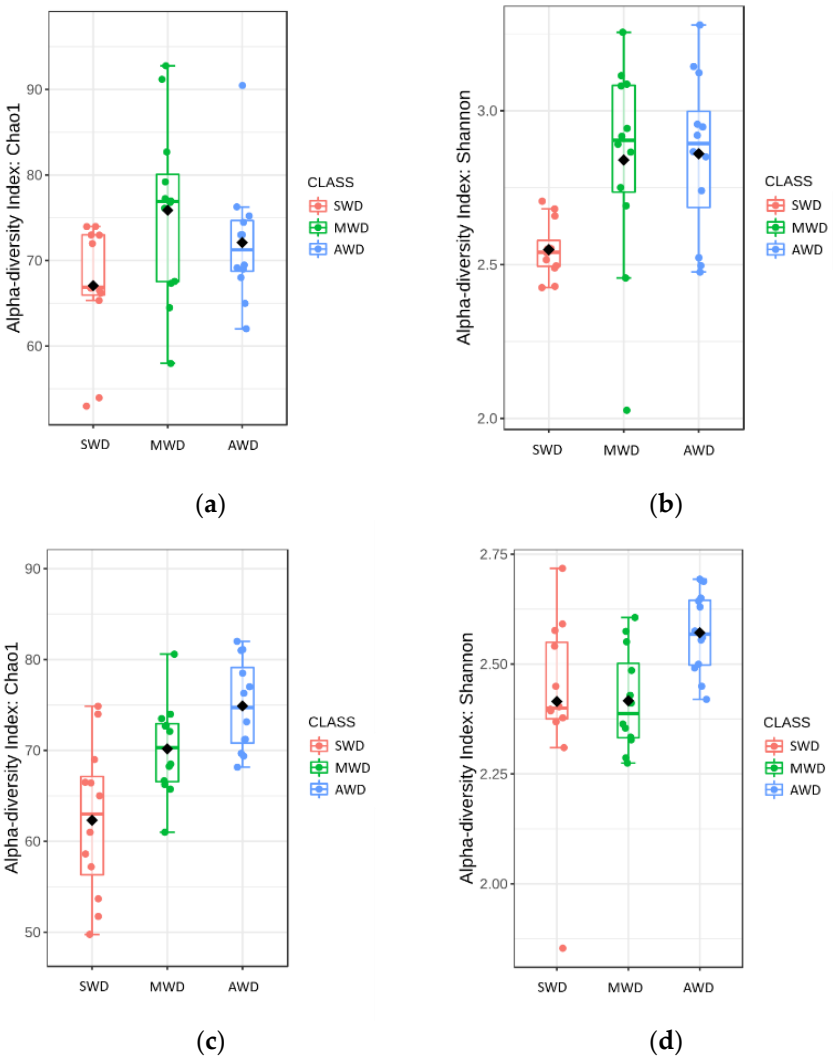

Figure 6. Boxplot illustrating the differences in (**a**) Chao1 and (**b**) Shannon diversity measures at 6-month sampling time and (**c**) Chao1 and (**d**) Shannon diversity measures at 12-month sampling time of the fungal communities in the bulk soil, at different irrigation regimes: severe water deficit (SWD), moderate water deficit (MWD), and absence of water deficit (AWD).

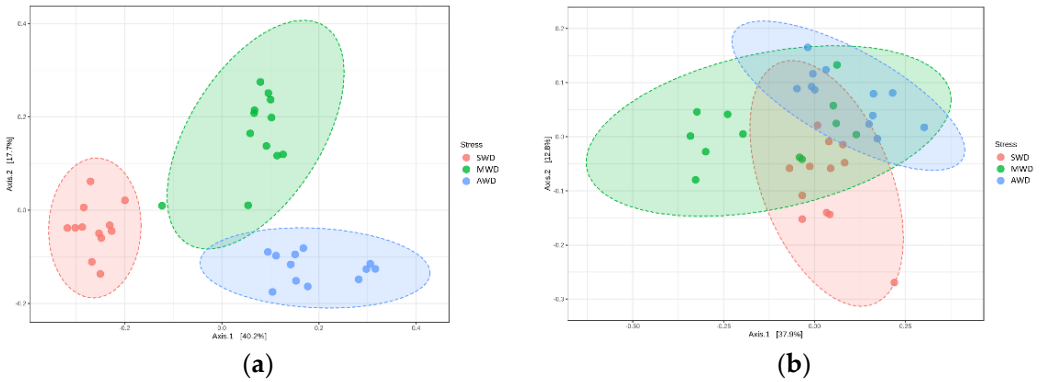

Figure 7. Principal Coordinate Analysis (PCoA) based on Bray–Curtis dissimilarity metrics, showing the distance in the fungal communities among irrigation regimes (SWD: severe water deficit, MWD: moderate water deficit, and AWD: absence of water deficit) at (**a**) 6-month and (**b**) 12-month sampling times in the bulk soil.

Regarding the LEfSe analysis, 50 genera determined the dissimilarities in the fungal community among irrigation regimes in the root at 6-months sampling time, whereas 20 genera discriminated among irrigation regimes at 12-month sampling time (Figure S10a). Relative abundances of the black-foot fungi "*Cylindrocarpon*" and *Dactylonectria* significantly increased at AWD and MWD regimes, respectively, at both sampling times. *Thelonectria* spp. were more abundant at MWD at both sampling times. The fungal genus *Trichoderma*, a potential biocontrol agent of black-foot pathogens, was found with highest abundance at AWD treatment at 6-months sampling and at MWD treatment at 12-months sampling, and with the lowest abundance at SWD treatment at both sampling times. The genus *Funneliformis*, which is an arbuscular mycorrhizal fungus (AMF), showed significantly higher abundance at SWD than the other treatments at 6-month sampling time.

In the rhizosphere, the relative abundance of 51 genera determined the differences among irrigation regimes (considering both sampling time) (Figure S10b). Relative abundances of "*Cylindrocarpon*" and *Dactylonectria* significantly increased at AWD and MWD treatments, respectively. The fungal genus *Funneliformis* showed significantly higher abundance at SWD treatment than the other treatments.

In the bulk soil, the LEfSe detected 48 genera and 22 genera which determined the dissimilarities in the fungal community among irrigation regimes at 6-month and 12-month sampling times, respectively (Figure S10c). Relative abundance of "*Cylindrocarpon*" and *Trichoderma* were significantly higher at MWD treatment than the other treatments at 6-month sampling time. *Thelonectria* relative abundance was higher at AWD at 6-months sampling time and at MWD at 12-month sampling time. *Funneliformis* showed significantly higher abundance at SWD treatment than the other treatments, at 6-month sampling time, although its abundance was higher at AWD treatment than the other treatments at 12-month sampling time.

3.6 Irrigation regime-specific and shared fungal assemblages

The three soil-plant compartments showed specific fungal OTUs for each irrigation regimes and a cluster of shared OTUs. In the root, 22.3% of fungal OTUs were shared among irrigation regimes, while specific fungal OTUs associated with each irrigation regime ranged from 10.4% to 23.3% (Figure 8a). In the rhizosphere, specific fungal OTUs associated with irrigation regimes ranged from 2.5% to 9% whereas shared OTUs among irrigation regimes represented the 66.8% of the rhizosphere fungal communities (Figure 8b). In bulk soil, 55.6% of fungal OTUs were shared among irrigation regimes and specific OTUs associated with each irrigation regime ranged from 4.1% to 8.9% (Figure 8c). The OTUs that were unique in each of the irrigation regime within each soil-plant compartment are shown in Table S4.

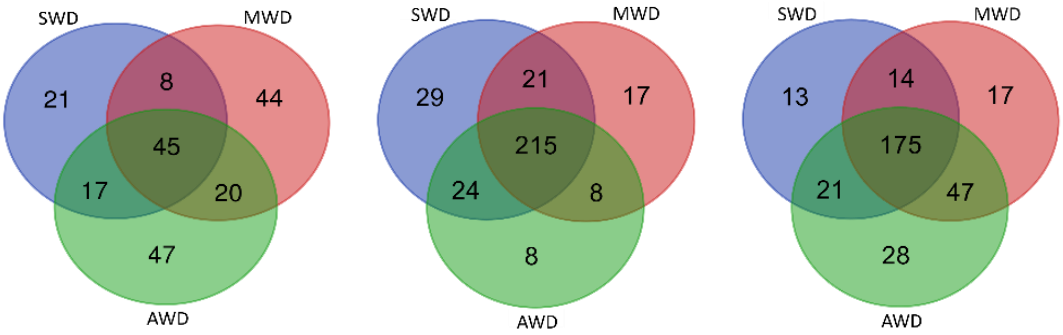

Figure 8. Venn diagram illustrating the overlap of the number of OTUs identified in the fungal microbiota among irrigation regimes (SWD: severe water deficit, MWD: moderate water deficit and AWD: absence of water deficit) in the (**a**) root, (**b**) rhizosphere, and (**c**) bulk soil.

3.7 High level of connectivity among black-foot fungi in the root

A higher quantity of significant edges and connections was observed with rhizosphere (n = 116) compared to the root (n = 112) and the bulk soil (n = 102) (Figure 9; Table S5). In the root (Figure 9a), the black-foot fungal genera “Cylindrocarpon”, Dactylonectria, and Thelonectria correlated positively among them. The biocontrol agent Trichoderma correlated positively with Dactylonectria, while the AMF Funneliformis correlated negatively with Thelonectria. No correlations were established among black-foot fungi and/or biocontrol agents in both the rhizosphere (Figure 9b) or in the bulk soil (Figure 9c).

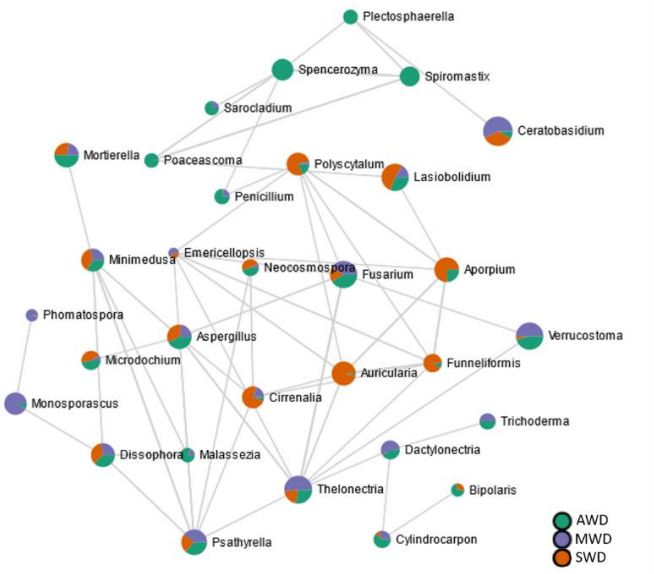
Plectosphaerella
Spencerozyma
Spiromastix
Saroclad
Ceratobasidium
Mortierella
Poaceascoma
Polyscytalum
Lasiobolidium
Penicillium
Minimedusa
Emericellopsis
Neocosmospora
Fusarium
Aporpium
Phomatospora
Aspergillus
Verrucostoma
Microdochium
Auricularia
Funneliformis
Cirrenalia
Monosporascus
Trichoderma
Dissophora
Malassezia
Dactylonectria
Thelonectria
Bipolaris
Psathyrella
Cylindrocarpon
AWD
MWD
SWD

(**a**)

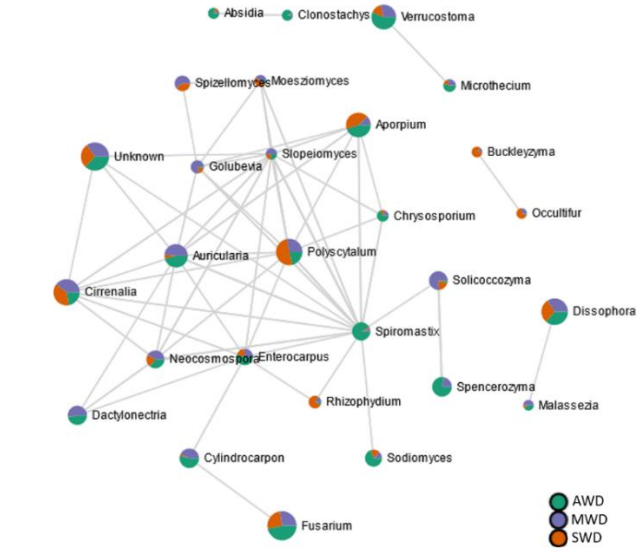
Absidia
Clonostachys
Verrucostoma
Spizellomyces
Moesziomyces
Microthecium
Aporpium
Unknown
Golubevia
Slopeiomyces
Buckleyzyma
Chrysosporium
Occultifur
Auricularia
Polyscytalum
Solicoccozyma
Cirrenalia
Dissophora
Spiromastix
Neocosmospora
Enterocarpus
Spencerozyma
Rhizophydium
Malassezia
Dactylonectria
Cylindrocarpon
Sodiomyces
Fusarium
AWD
MWD
SWD

(**b**)

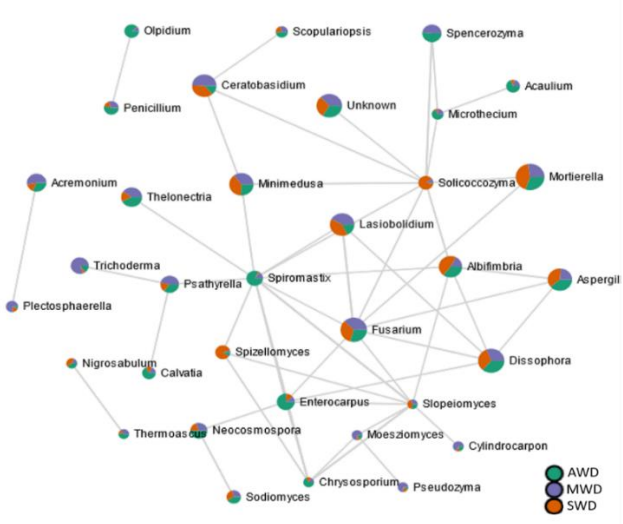
Olpidium
Scopulariopsis
Spencerozyma
Ceratobasidium
Acaulium
Penicillium
Unknown
Microthecium
Acremonium
Minimedusa
Solicoccozyma
Mortierella
Thelonectria
Lasiobolidium
Trichoderma
Albifimbria
Psathyrella
Spiromastix
Aspergil
Plectosphaerella
Fusarium
Spizellomyces
Dissophora
Nigrosabulum
Calvatia
Enterocarpus
Slopeiomyces
Thermoascus
Neocosmospora
Moesziomyces
Cylindrocarpon
Chrysosporium
Pseudozyma
Sodiomyces
AWD
MWD
SWD

(**c**)

Figure 9. SparCC correlation analysis at genus level among irrigation regimes (SWD: severe water deficit, MWD: moderate water deficit, and AWD: absence of water deficit) in the (**a**) root, (**b**) rhizosphere, and (**c**) bulk soil.

3.8 Water deficit affects fungal functionality in the root

Overall, the relative abundance of fungal OTUs identified as trophic modes with pathotrophs, saprotrophs, and symbiotrophs ranged from 90.6% to 96.2% in the root, 92.2% to 95.6% in the rhizosphere, and 92.2% to 94.8% in the bulk soil, while the remaining OTUs were unassigned (Figure 10). There were signficant differences in the relative proportion of fungal functions within each irrigation regimes in each soil-plant compartment (p-value < 0.05) (Table S6).

In the root, the trophic mode was dominated by saprothrophs, followed by pathotrophs and symbiotrophs, altough there were no significant differences between pathotrophs and symbiotrophs in the SWD treatment (p-value < 0.05). Pathotrophs were found at SWD treatment (26.3%) in a lower proportion compared with MWD (34.5%) (Figure 10a). In rhizosphere and bulk soil samples, the trophic mode was dominated by saprotrophs, followed by pathotrophs and symbiotrophs at all watering regimes, without significant differences between pathotrophs and symbiotrophs (p-value < 0.05) (Figure 10b,c).

Plant pathogens were the dominant taxa in the pathotroph group in the root and rhizosphere (Table S7). In the saprotroph group, undefined saptrotrophs were the dominant taxa in the three compartments at all irrigation regimes (Table S7). In the symbiotrophs group, endophytes were the most abundant taxa in the bulk soil and rhizosphere, whereas no differences were found between endophytes and arbuscular mycorrhiza at SWD and MWD regimes in the root (Table S7).

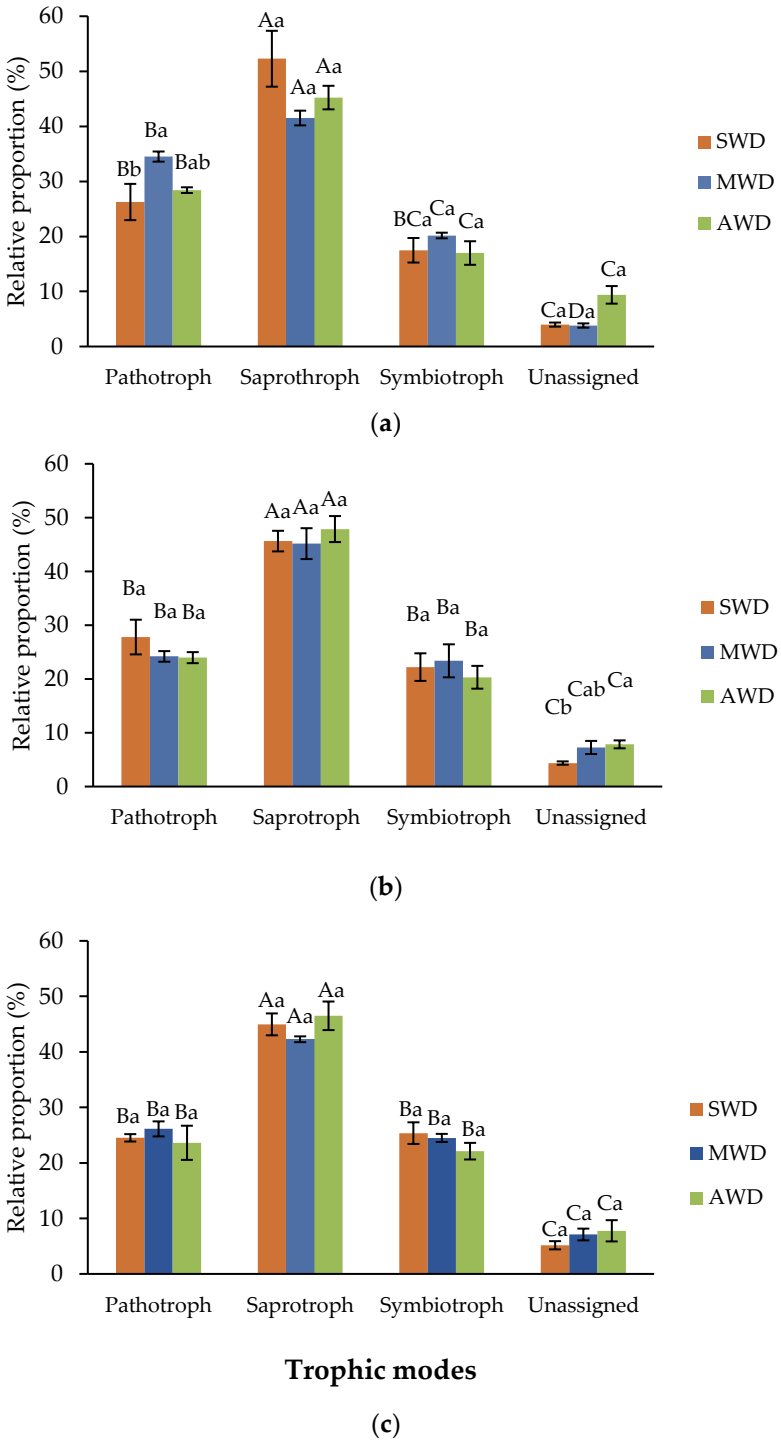

Figure 10. Variations in fungal function inferred by FUNGuild in in the (**a**) root, (**b**) rhizozphere and (**c**) bulk soil, at different irrigation regimes: severe water deficit (SWD), moderte water deficit (MWD), and absence of water deficit (AWD). Tukey's test at *p*-value < 0.05 level. Means followed by the same letter do not differ significantly. Capital letters are for comparison of means among functional groups within each irrigation

regime. Small letters are for comparison of means among irrigation regimes within each functional group.

4. DISCUSSION

This study focused on exploring the influence of different scenarios of soil water availability on the root endosphere, rhizosphere, and bulk soil fungal microbiome of grapevine, by ITS HTAS approach. We were particularly interested in understanding the impact of drought-stress on the root-associated fungal communities, with special attention to BFD fungal abundance.

The fungal community composition was influenced by the soil-plant compartment. Our study detected that fungal diversity decreased in the root compartment with respect to the the rhizosphere and bulk soil compartments, and this is in accordance with previous research aiming to decipher the bacterial and fungal microbiome of grapevine [26–28,30,57,58].

The major fungal phyla detected in our work were largely composed of Ascomycota and Basidiomycota, which accounted between 62 to 89% of the relative abundance in the soil-plant compartments, across the three watering scenarios. This taxonomic pattern is consistent with results obtained in previous studies that explored the belowground grapevine fungal microbiome, supporting the idea that the selective forces defining fungal root microbiome structure at a high taxonomic rank are constant under various environmental conditions [27,29,30,57–62].

The fungal phylum Mucoromycota was mostly found in the rhizosphere and bulk soil compared with the root endosphere, and was largely represented by the family Mortierellaceae, particularly by the genus *Mortierella*. Our results showed that *Mortierella* was one of the most abundant genera found in the rhizosphere and bulk soil, accounting for 9 to 17% and 14 to 20% of the relative abundance of all genera, respectively. Similar results were found in previous grapevine studies, in which Mortierellaceae was the most abundant family in the bulk soil and rhizosphere, and *Mortierella* was the most dominant genus in the root-zone soil and showed lower abundances in the plant-compartments (root, leaf, flower, and grape) [27,30,63]. The genus *Mortierella* is a phosphate solubilizing fungus which plays an important role in the phosphorus cycling in the rhizosphere [64]. Interestingly, the co-inoculation of

Mortierella with an AMF showed a positive effect on enhancing plant growth and phosphorus uptake of avocado crop [65].

Our results indicated that the fungal microbiome diversity in root and bulk soil varied according to the sampling time, although this effect was not consistent in the rhizosphere. We detected an increase in fungal diversity towards the twelve-month sampling in root, whereas the opposite was observed in bulk soil. The 6-month sampling (June) coincides with the time after leaf senescence (late fall in southern hemisphere), whereas at the 12-month sampling (December), grapevines were in active vegetative development. Liu and Howell [30] observed that the grapevine associated microbiota is affected by the plant developmental stage throughout the growing season from flowering to harvest, in above- (grape and leaf) and belowground compartments, and suggested that veraison is the most distinct stage. In addition, they found that the fungal diversity fluctuation was similar in rhizosphere and root samples [30], reinforcing the idea that root microbiomes are partially derived from the rhizosphere and, in turn, that root and exudation and morphology profile can influence the composition of the rhizosphere microbiome [57,66]. On the other hand, in a previous research conducted in Spain, Berlanas et al. [29] observed a non-clear pattern of fluctuation of fungal diversity in the rhizosphere of vines grown in two vineyards of different geographical location, age, climate, and soil management practices. Year of sampling has also been pointed out as a major factor that can influence the diversity and composition of the microbiota in grapevine [29,63]. This phenomenon can be attributed to distinct root responses to different environmental factors, such as precipitation or temperature [29,67]. Further research is therefore needed to better understand shifts in fungal community composition throughout the annual growth cycle and how the year of sampling may influence the community succession.

The irrigation regimes strongly influenced fungal diversity and composition of the belowground compartments of grapevine. Overall, the major differences in fungal diversity were observed between the treatments of SWD and the full-watered condition (AWD). A decrease in the relative abundances of pathotrophs were predicted in roots at SWD. Although several previous studies have shown that drought influences the bacterial composition across many plant species [5,10,12,16–21], the overall impact of drought on the fungal grapevine microbiome had not yet been unravelled. Our results showed that diversity of OTUs significantly decreased towards the treatment of SWD in the three soil-

plant compartments. A strong correlation between the water status (relative soil moisture and evaporation) and the grapevine fungal microbiome composition has been shown by Liu and Howell [30]. In contrast, Swift et al. [58] did not find a large impact of irrigation on patterns of grapevine microbial diversity, although a differential abundance of fungal and bacterial taxa varied as a consequence of the irrigation treatments. However, the amount of seasonal precipitation received during their experiment could have been enough to obscure some of the signal from the severe water stress [58]. Drought triggers a series of responses in plants, ranging from shifts in the root morphology to metabolic perturbations, which alter the root exudate profile and may also affect the belowground associated microbiome [5,12,30]. Under drought conditions, the plant root system is able to attract and favour the establishment of microorganisms, which may improve the ecosystem services required to support plant growth and development [68,69]. Interestingly, in SO_4 rootstock, inoculation with plant growth promoting (PGP) bacteria contributed to enhance grapevine adaptation to drought through a water stress-induced promotion capacity, rather than a per se trait of the PGP bacteria tested [69].

Several genera contributed to the dissimilarities observed among the irrigation regimes in the three soil plant compartments, according to the Linear Discriminant Analysis Effect Size. For instance, a significant enrichment of the AMF genus *Funneliformis* was observed in root (at six-month sampling) and in rhizosphere samples at the condition of SWD. The genus *Funneliformis*, previously classified in the former genus *Glomus* sensu lato, is a fungus from the Glomeraceae family, the taxon that largely dominates the AMF communities detected in cultivated grapevine, and also in wild grapevine [62,70–72]. We also detected in our study the presence of the AMF *Rhizophagus* (Glomerales), *Acaulospora* (Diversisporales), and *Diversispora* (Diversisporales), previously reported in vineyards [73], but in very low abundances. The AMF-grapevine symbiosis provides several ecosystemic services for grapevine production, which may be of benefit in terms of adaptation to new challenges of pest management and climate change, such as increasing droughts [73]. AMF are an important groups of soil microorganisms which provide an increased interface between roots and soil, therefore improving grapevine growth and nutrition by enhancing soil nutrients uptake, as well as increasing tolerance to biotic and abiotic stresses, such as water stress [73]. Indeed, Donkó et al. [74] reported that the degree of grapevine mycorrhizal colonization was higher in drier soil areas in Hungary. Our results may suggest that

grapevine mycorrhization is expected to naturally increase as a consequence of drought. Nevertheless, aspects concerning soil characteristics [70,75], vineyard agricultural practices, such as tillage, high fertilizers inputs [76], and pesticide application [77,78], as well as characteristics relating to the host, such as the rootstock genotype [79] and to a lesser extent the plant phenological stage [80], can greatly impact on AMF diversity and grapevine mycorrhization. Management practices that conserve the biodiversity of AMF in vineyards may be essential to profit from the ecosystem services concerning increased drought tolerance in the grapevine that AMF provides.

Cylindrocarpon-like asexual morphs associated with BFD, namely "*Cylindrocarpon*", *Dactylonectria*, and *Thelonectria* showed significantly higher abundances at treatments of MWD and AWD of water deficit rather than at the treatment of SWD. Correlation network analysis also highlighted the high level of connectivity among black-foot fungi in the root under the same irrigation conditions. A wide diversity of *Cylindrocarpon*-like asexual morphs has been reported to co-exist on the same tissue [81], but their interactions have never been studied. Research on effects of co-infections on symptom expression among black-foot fungi and other grapevine trunk disease pathogens has been published. Grapevines infected with *Botryosphaeriaecea* spp. [82] or Petri disease pathogens [83] and black-foot fungi had increased disease incidence and severity than with single pathogen infections. In vitro assays showed that "*Cylindrocarpon*" spp. isolates showed reduced mycelial growth as water potential decreased in the culture medium [84]. It is widely recognized that BFD incidence is favored by poor drainage conditions and high moisture content of soil [34]. Our results suggest that extreme conditions of water deficit may be unfavorably for black-foot pathogens survival. Further long-term assays are necessary to evaluate if the lower presence of black-foot pathogens detected at the condition of SWD compared with the full-irrigated regime also implies a reduction in BFD severity and incidence in grapevine.

Another interesting hypothesis which might partially explain the lowest presence of black-foot pathogens observed in the root and rhizosphere at the SWD condition, could be the enrichment of AMF detected in this irrigation regime. The presence of AMF has been negatively correlated with pathotrophic fungi in wild grapevine [62]. Furthermore, some AMF are cataloged as biocontrol agents [85]. For instance, inoculation with *Rhizophagus irregularis* (syn. *Glomus intradices*), from Glomeraceae, reduced the disease severity and incidence of root lesions caused by black-foot pathogens on *Vitis*

rupestris [86]. By contrast, the application of commercial AMF as a pre-planting strategy against black-foot fungi did not result in the suppression of disease incidence, but instead increased the abundance of the pathogens [87].

Several studies on biological control of BFD have evaluated the application of *Trichoderma* spp. in young vineyards and grapevine nurseries [88–93], but with inconsistent results. Overall, we detected the presence of the genus *Trichoderma* in a similar pattern of distribution that black-foot pathogens, with higher abundances at treatments of MWD and AWD, rather than at the treatment of SWD. Our results suggest that, in regions where drought events are expected to increase [1,2], the use of *Trichoderma*-based biological products against BFD, and other grapevine trunk disease fungi, will require further analysis to evaluate the success of *Trichoderma* spp. as biological control fungi in challenging environment conditions.

5. CONCLCUSIONS

Our study demonstrated that water deficit influences fungal community dynamics of the belowground grapevine microbiome, with OTUs diversity significantly decreasing towards the treatment of SWD in the root endosphere, rhizosphere, and bulk soil. Black-foot fungi belonging to the genera "*Cylindrocarpon*", *Dactylonectria*, and *Thelonectria* were severely affected by drought, and presented a high level of connectivity among them in the root under the same irrigation conditions. Other fungal genera, such as the AMF *Funneliformis* were enriched under extreme conditions (SWD), which would make these microorganisms viable, strong, and vital options for water stress mitigation in grapevine. Further studies focusing on examining the impact of SWD condition on belowground microbiomes of different grapevine rootstocks and rootstock/scion combinations, and in diverse soil types, will be indispensable to improve our understanding of how prolonged and more frequent drought events would affect the root-associated fungal microbiome on grapevine, and the consequences of altering the microbial terroir, including the abundance of potential soil-borne pathogens of grapevine.

6. REFERENCES

1. Lesk, C.; Rowhani, P.; Ramankutty, N. Influence of extreme weather disasters on global crop production. *Nature* 2016, *529*, 84–87. https://doi.org/10.1038/nature16467

2. Santillán, D.; Iglesias, A.; La Jeunesse, I.; Garrote, L.; Sotes, V. Vineyards in transition: A global assessment of the adaptation needs of grape producing regions under climate change. *Sci. Total Environ.* 2019, *657*, 839–852. https://doi.org/10.1016/j.scitotenv.2018.12.079

3. Fang, Y.; Xiong, L. General mechanisms of drought response and their application in drought resistance improvement in plants. *Cell Mol. Life Sci*. 2015, *72*, 673–689. https://doi.org/10.1007/s00018-014-1767-0

4. Yue, B.; Xue, W.; Xiong, L.; Yu, X.; Luo, L.; Cui, K.; Jin, D.; Xing, Y.; Zhang, Q. Genetic basis of drought resistance at reproductive stage in rice: Separation of drought tolerance from drought avoidance. *Genetics* 2006, *172*, 1213–1228. https://doi.org/10.1534/genetics.105.045062

5. Santos-Medellín, C.; Edwards, J.; Liechty, Z.; Nguyen, B.; Sundaresan, V. Drought stress results in a compartment-specific restructuring of the rice root-associated microbiomes. *Mbio* 2017, *8*, e00764-17. https://doi.org/10.1128/mBio.00764-17

6. Trivedi, P.; Leach, J.E.; Tringe, S.G.; Sa, T.; Singh, B.K. Plant-microbiome interactions: From community assembly to plant health. *Nat. Rev. Microbiol*. 2020, *18*, 607–621. https://doi.org/10.1038/s41579-020-0412-1

7. Yang, J.; Kloepper, J.W.; Ryu, C.M. Rhizosphere bacteria help plants tolerate abiotic stress. *Trends Plant. Sci.* 2009, *14*, 1–4. https://doi.org/10.1016/j.tplants.2008.10.004

8. Lugtenberg, B.; Kamilova, F. Plant-growth-promoting rhizobacteria. *Annu. Rev. Microbiol*. 2009, *63*, 451–556. https://doi.org/10.1146/annurev.micro.62.081307.162918

9. Wardle, D.A.; Bardgett, R.D.; Klironomos, J.N.; Setälä, H.; van der Putten, W.H.; Wall, D.H. Ecological linkages between aboveground and belowground biota. *Science* 2004, *304*, 1629–1633. https://doi.org/10.1126/science.1094875

10. Barnard, R.L.; Osborne, C.A.; Firestone, M.K. Responses of soil bacterial and fungal communities to extreme desiccation and rewetting. *ISME J.* 2013, *7*, 2229–2241. https://doi.org/10.1038/ismej.2013.104

11. Bouskill, N.J.; Lim, H.C.; Borglin, S.; Salve, R.; Wood, T.E.; Silver, W.L.; Brodie, E.L. Pre-exposure to drought increases the resistance of tropical forest soil

bacterial communities to extended drought. *ISME J.* 2013, *7*, 384–394. https://doi.org/10.1038/ismej.2012.113

12. Naylor, D.; Coleman-Derr, D. Drought stress and root-associated bacterial communities. *Front. Plant. Sci.* 2018, *8*, 2223. https://doi.org/10.3389/fpls.2017.02223

13. Smith, S.; De Smet, I. Root system architecture: Insights from *Arabidopsis* and cereal crops. *Phil. Trans. R. Soc. B* 2012, *367*, 1441–1452. https://doi.org/10.1098/rstb.2011.0234

14. Henry, A.; Doucette, W.; Norton, J.; Bugbee, B. Changes in crested wheatgrass root exudation caused by flood, drought, and nutrient stress. *J. Environ. Qual*. 2007, *36*, 904–912. https://doi.org/10.2134/jeq2006.0425sc

15. Song, F.; Han, X.; Zhu, X.; Herbert, S.J. Response to water stress of soil enzymes and root exudates from drought and non-drought tolerant corn hybrids at different growth stages. *Can. J. Soil Sci.* 2012, *92*, 501–507. https://doi.org/10.4141/cjss2010-057

16. Bouasria, A.; Mustafa, T.; De Bello, F.; Zinger, L.; Lemperiere, G.; Geremia, R.A.; Choler, P. Changes in root-associated microbial communities are determined by species-specific plant growth responses to stress and disturbance. *Eur. J. Soil Biol*. 2012, *52*, 59–66. https://doi.org/10.1016/j.ejsobi.2012.06.003

17. Naylor, D.; DeGraaf, S.; Purdom, E.; Coleman-Derr, D. Drought and host selection influence bacterial community dynamics in the grass root microbiome. *ISME J.* 2017, *11*, 2691–2704. https://doi.org/10.1038/ismej.2017.118

18. Edwards, J.A.; Santos-Medellín, C.M.; Liechty, Z.S.; Nguyen, B.; Lurie, E.; Eason, S.; Phillips, G.; Sundaresan, V. Compositional shifts in root-associated bacterial and archaeal microbiota track the plant life cycle in field-grown rice. *PLoS Biol*. 2018, *16*, e2003862. https://doi.org/10.1371/journal.pbio.2003862

19. Fitzpatrick, C.R.; Copeland, J.; Wang, P.W.; Guttman, D.S.; Kotanen, P.M.; Johnson, M.T.J. Assembly and ecological function of the root microbiome across angiosperm plant species. *Proc. Natl. Acad. Sci. USA* 2018, *115*, E1157–E1165. https://doi.org/10.1073/pnas.1717617115

20. Xu, L.; Naylor, D.; Dong, Z.; Simmons, T.; Pierroz, G.; Hixson, K.K.; Kim, Y.-M.; Zink, E.M.; Engbrecht, K.M.; Wang, Y.; et al. Drought delays development of the

sorghum root microbiome and enriches for monoderm bacteria. *Proc. Natl. Acad. Sci. USA* 2018, *115*, E4284–E4293. https://doi.org/10.1073/pnas.1717308115

21. Simmons, T.; Styer, A.B.; Pierroz, G.; Gonçalves, A.P.; Pasricha, R.; Hazra, A.B.; Bubner, P.; Coleman-Derr, D. Drought drives spatial variation in the millet root microbiome. *Front. Plant. Sci.* 2020, *11*, 599. https://doi.org/10.3389/fpls.2020.00599

22. Fuchslueger, L.; Bahn, M.; Hasibeder, R.; Kienzl, S.; Fritz, K.; Schmitt, M.; Watzka, M.; Richter, A. Drought history affects grassland plant and microbial carbon turnover during and after a subsequent drought event. *J. Ecol.* 2016, *104*, 1453–1465. https://doi.org/10.1111/1365-2745.12593

23. Lovisolo, C.; Perrone, I.; Carra, A.; Ferrandino, A.; Flexas, J.; Medrano, H.; Schubert, A. Drought-induced changes in development and function of grapevine (*Vitis* spp.) organs and in their hydraulic and non-hydraulic interactions at the whole-plant level: A physiological and molecular update. *Funct. Plant. Biol*. 2010, *37*, 98–116. https://doi.org/10.1071/FP09191

24. Vink, S.N.; Chrysargyris, A.; Tzortzakis, N.; Falcão Salles, J. Bacterial community dynamics varies with soil management and irrigation practices in grapevines (*Vitis vinifera* L.). *Appl. Soil Ecol*. 2021, *158*, 103807. https://doi.org/10.1016/j.apsoil.2020.103807

25. Fraga, H.; Malheiro, A.C.; Moutinho-Pereira, J.; Santos, J.A. An overview of climate change impacts on European viticulture. *Food Energy Secur*. 2012, *1*, 94–110. https://doi.org/10.1002/fes3.14

26. Zarraonaindia, I.; Owens, S.M.; Weisenhorn, P.; West, K.; Hampton-Marcell, J.; Lax, S.; Bokulich, N.A.; Mills, D.A.; Martin, G.; Taghavi, S.; et al. The soil microbiome influences grapevine-associated microbiota. *Mbio* 2015, *6*, e02527-14. https://doi.org/10.1128/mBio.02527-14

27. Martínez-Diz, M.P.; Andrés-Sodupe, M.; Bujanda, R.; Díaz-Losada, E.; Eichmeier, A.; Gramaje, D. Soil-plant compartments affect fungal microbiome diversity and composition in grapevine. *Fungal Ecol*. 2019, *41*, 234–244. https://doi.org/10.1016/j.funeco.2019.07.003

28. Marasco, R.; Rolli, E.; Fusi, M.; Michoud, G.; Daffonchio, D. Grapevine rootstocks shape underground bacterial microbiome and networking but not potential functionality. *Microbiome* 2018, *6*, 3. https://doi.org/10.1186/s40168-017-0391-2

29. Berlanas, C.; Berbegal, M.; Elena, G.; Laidani, M.; Cibriain, J.F.; Sagües, A.; Gramaje, D. The fungal and bacterial rhizosphere microbiome associated with grapevine rootstock genotypes in mature and young vineyards. *Front. Microbiol.* 2019, *10*, 1142. https://doi.org/10.3389/fmicb.2019.01142

30. Liu, D.; Howell, K. Community succession of the grapevine fungal microbiome in the annual growth cycle. *Environ. Microbiol*. 2021, *23*, 1842–1857. https://doi.org/10.1111/1462-2920.15172

31. Fernández-Calviño, D.; Martín, A.; Arias-Estévez, M.; Baath, E.; Díaz-Raviña, M. Microbial community structure of vineyard soils with different pH and copper content. *Appl. Soil Ecol*. 2010, *46*, 276–282. https://doi.org/10.1016/j.apsoil.2010.08.001

32. Burns, K.N.; Kluepfel, D.A.; Strauss, S.L.; Bokulich, N.A.; Cantu, D.; Steenwerth, K.L. Vineyard soil bacterial diversity and composition revealed by 16S rRNA genes: Differentiation by geographic features. *Soil Biol. Biochem.* 2015, *91*, 232–247. https://doi.org/10.1016/j.soilbio.2015.09.002

33. Holland, T.C.; Bowen, P.A.; Bogdanoff, C.P.; Lowery, T.D.; Shaposhnikova, O.; Smith, S.; Hart, M.M. Evaluating the diversity of soil microbial communities in vineyards relative to adjacent native ecosystems. *Appl. Soil Ecol*. 2016, *100*, 91–103. https://doi.org/10.1016/j.apsoil.2015.12.001

34. Halleen, F.; Fourie, P.H.; Crous, W. A review of black foot disease of grapevine. *Phytopathol. Mediterr*. 2006, *45*, S55–S67.

35. Gramaje, D.; Armengol, J. Fungal trunk pathogens in the grapevine propagation process: Potential inoculum sources, detection, identification, and management strategies. *Plant. Dis*. 2011, *95*, 1040–1055. https://doi.org/10.1094/PDIS-01-11-0025

36. Gramaje, D.; Úrbez-Torres, J.R.; Sosnowski, M.R. Managing grapevine trunk diseases with respect to etiology and epidemiology: Current strategies and future prospects. *Plant. Dis.* 2018, *102*, 12–39. https://doi.org/10.1094/PDIS-04-17-0512-FE

37. Aigoun-Mouhous, W.; Elena, G.; Cabral, A.; León, M.; Sabaou, N.; Armengol, J.; Chaouia, C.; Mahamedi, A.E.; Berraf-Tebbal, A. Characterization and pathogenicity of *Cylindrocarpon*-like asexual morphs associated with black foot disease in Algerian grapevine nurseries, with the description of *Pleiocarpon algeriense* sp. nov. *Eur. J. Plant. Pathol*. 2019, *154*, 887–901. https://doi.org/10.1007/s10658-019-01708-z

38. Silva, A.; Docampo, R.; Camejo, C.; Barboza, C. *Inventario de Los Suelos Bajo Viña Del Uruguay. Principales Características Edafológicas de Los Viñedos Uruguayos*; INIA: Montevideo, Uruguay, 2018; pp. 59–71.

39. Bertola, B.; Crovetto, A.; Secco, Y.; Bertola, L. *Estadísticas de Viñedos 2020 Datos Nacionales*; INAVI: Canelones, Uruguay, 2020; p. 59.

40. Silva, A.; Ponce de León, J.; García, F.; Durán, A. *Aspectos Metodológicos en la Determinación de la Capacidad de Retener Agua de Los Suelos Del Uruguay*; Facultad de Agronomía: Montevideo, Uruguay, 1988; pp. 14–15.

41. Scholander, P.F.; Bradstreet, E.D.; Hemmingsen, E.A.; Hammel, H.T. Sap pressure in vascular plants: Negative hydrostatic pressure can be measured in plants. *Science* 1965, *148*, 339–346. https://doi.org/10.1126/science.148.3668.339

42. Turenne, C.Y.; Sanche, S.E.; Hoban, D.J.; Karlowsky, J.A.; Kabani, A.M. Rapid identification of fungi by using the ITS2 genetic region and an automated fluorescent capillary electrophoresis system. *J. Clin. Microbiol*. 1999, *37*, 1846–1851. https://doi.org/10.1128/JCM.37.6.1846-1851.1999

43. White, T.J.; Bruns, T.; Lee, S.H.; Taylor, J.W. Amplification and direct sequencing of fungal ribosomal RNA genes for phylogenetics. In *PCR Protocols: A Guide to Methods and Applications;* Innis, M.A., Gelfand, D.H., Sninsky, J.J., White, T.J., Eds.; Academic Press: San Diego, CA, USA, 1990; pp. 315–322. https://doi.org/10.1016/B978-0-12-372180-8.50042-1

44. Andrews, S. FastQC: A Quality Control Tool for High Throughput Sequence Data. 2010. Available online: http://www.bioinformatics.babraham.ac.uk/projects/fastqc (accessed on 28/9/2020).

45. Vetrovsky, T.; Baldrian, P.; Morais, D. SEED 2: A user-friendly platform for amplicon high-throughput sequencing data analyses. *Bioinformatics* 2018, *34*, 2292–2294. https://doi.org/10.1093/bioinformatics/bty071

46. Aronesty, E. Ea-utils: Command-line tools for processing biological sequencing data. *Expr. Anal. Durham.* 2011. Available online: http://code.google.com/p/ea-utils (accessed on 10/10/2020).

47. Bengtsson-Palme, J.; Ryberg, M.; Hartmann, M.; Branco, S.; Wang, Z.; Godhe, A.; De Wit, P.; Sanchez-García, M.; Ebersberger, I.; de Sousa, F.; et al. Improved software detection and extraction of ITS1 and ITS2 from ribosomal ITS sequences of fungi and other eukaryotes for use in environmental sequencing. *Methods Ecol. Evol*. 2013, *4*, 914–919. https://doi.org/10.1111/2041-210X.12073

48. Edgar, R.C. UPARSE: Highly accurate OTU sequences from microbial amplicon reads. *Nat. Methods* 2013, *10*, 996–998. https://doi.org/10.1038/nmeth.2604

49. Abarenkov, K.; Henrik Nilsson, R.; Larsson, K.H.; Alexander, I.J.; Eberhardt, U.; Erland, S.; Kõljalg, U. The UNITE database for molecular identification of fungi–recent updates and future perspectives. *New Phytologist.* 2010, *186*, 281–285. https://doi.org/10.1111/j.1469-8137.2009.03160.x

50. Katoh, K.; Asimenos, G.; Toh, H. Multiple Alignment of DNA Sequences with MAFFT. In *Bioinformatics for DNA Sequence Analysis. Methods in Molecular Biology*; Posada, D., Ed.; Humana Press: Totowa, NJ, USA, 2009; Volume 537, pp. 39–64. https://doi.org/10.1007/978-1-59745-251-9_3

51. Dhariwal, A.; Chong, J.; Habib, S.; King, I.L.; Agellon, L.B.; Xia, J. MicrobiomeAnalyst: A web-based tool for comprehensive statistical, visual and meta-analysis of microbiome data. *Nucleic Acids Res.* 2017, *45*, W180–W188. https://doi.org/10.1093/nar/gkx295

52. Chong, J.; Liu, P.; Zhou, G.; Xia, J. Using MicrobiomeAnalyst for comprehensive statistical, functional, and meta-analysis of microbiome data. *Nat. Protoc*. 2020, *15*, 799–821. https://doi.org/10.1038/s41596-019-0264-1

53. Vázquez-Baeza, Y.; Pirrung, M.; Gonzalez, A.; Knight, R.; EMPeror: A tool for visualizing high-throughput microbial community data. *GigaScience* 2013, *2*, 16. https://doi.org/10.1186/2047-217X-2-16

54. Segata, N.; Izard, J.; Waldron, L.; Gevers, D.; Miropolsky, L.; Garrett, W.S.; Huttenhower, C. Metagenomic biomarker discovery and explanation. *Genome Biol*. 2011, *12*, R60. https://doi.org/10.1186/gb-2011-12-6-r60

55. Friedman, J.; Alm, E.J. Inferring correlation networks from genomic survey data. *PLoS Comput. Biol*. 2012, *8*, e1002687. https://doi.org/10.1371/journal.pcbi.1002687

56. Nguyen, N.H.; Song, Z.; Bates, S.T.; Branco, S.; Tedersoo, L.; Menke, J.; Schilling, J.S.; Kennedy, P.G. FUNGuild: An open annotation tool for parsing fungal community datasets by ecological guild. *Fungal Ecol*. 2016, *20*, 241–248. https://doi.org/10.1016/j.funeco.2015.06.006

57. Deyett, E.; Rolshausen, P.E. Endophytic microbial assemblage in grapevine. *FEMS Microbiol*. *Ecol*. 2020, *96*, 5. https://doi.org/10.1093/femsec/fiaa053

58. Swift, J.F.; Hall, M.E.; Harris, Z.N.; Kwasniewski, M.T.; Miller, A.J. Grapevine microbiota reflect diversity among compartments and complex interactions within and among root and shoot systems. *Microorganisms* 2021, *9*, 92. https://doi.org/10.3390/microorganisms9010092

59. Castañeda, L.E.; Barbosa, O. Metagenomic analysis exploring taxonomic and functional diversity of soil microbial communities in Chilean vineyards and surrounding native forests. *PeerJ* 2017, *5*, e3098. https://doi.org/10.7717/peerj.3098

60. Longa, C.; Nicola, L.; Antonielli, L.; Mescalchin, E.; Zanzotti, R.; Turco, E.; Pertot, I. Soil microbiota respond to green manure in organic vineyards. *J. Appl. Microbiol*. 2017, *123*, 1547–1560. https://doi.org/10.1111/jam.13606

61. Manici, L.M.; Saccà, M.L.; Caputo, F.; Zanzotto, A.; Gardiman, M.; Fila. G. Long-term grapevine cultivation and agro-environment affect rhizosphere microbiome rather than plant age. *Appl. Soil Ecol.* 2017, *119*, 214–225. https://doi.org/10.1016/j.apsoil.2017.06.027

62. Radić, T.; Likar, M.; Hančević, K.; Regvar, M.; Čarija, M.; Zdunić, G. Root-associated community composition and co-occurrence patterns of fungi in wild grapevine. *Fungal Ecol*. 2021, *50*, 101034. https://doi.org/10.1016/j.funeco.2020.101034

63. Cureau, N.; Threlfall, R.; Savin, M.; Marasini, D.; Lavefve, L.; Carbonero, F. Year, location, and variety impact on grape-, soil-, and leaf-associated fungal microbiota of arkansas-grown table grapes. *Microb. Ecol*. 2021, *82*, 73–86. https://doi.org/10.1007/s00248-021-01698-8

64. Osorio, N.W.; Habte, M. Synergistic influence of an arbuscular mycorrhizal fungus and a P solubilizing fungus on growth and P uptake of *Leucaena leucocephala* in an oxisol. *Arid Land Res. Manag*. 2001, *15*, 263–274. https://doi.org/10.1080/15324980152119810

65. Tamayo-Velez, A.; Osorio, N.W. Co-inoculation with an arbuscular mycorrhizal fungus and a phosphate-solubilizing fungus promotes the plant growth and phosphate uptake of avocado plantlets in a nursery. *Botany* 2017, *95*, 539–545. https://doi.org/10.1139/cjb-2016-0224

66. Berg, G.; Smalla, K. Plant species and soil type cooperatively shape the structure and function of microbial communities in the rhizosphere. *FEMS Microbiol. Ecol*. 2009, *68*, 1–13. https://doi.org/10.1111/j.1574-6941.2009.00654.x

67. Wagner, M.R.; Lundberg, D.S.; del Rio, T.G.; Tringe, S.G.; Dangl, J.L.; Mitchell-Olds, T. Host genotype and age shape the leaf and root microbiomes of a wild perennial plant. *Nat. Commun.* 2016, *7*, 12151. https://doi.org/10.1038/ncomms12151

68. Marasco, R.; Rolli, E.; Ettoumi, B.; Vigani, G.; Mapelli, F.; Borin, S.; Abou-Hadid, A.F.; El-Behairy, U.A.; Sorlini, C.; Cherif, A.; et al. A drought resistance-promoting microbiome is selected by root system under desert farming. *PLoS ONE* 2012, *7*, e48479. https://doi.org/10.1371/journal.pone.0048479

69. Rolli, E.; Marasco, R.; Vigani, G.; Ettoumi, B.; Mapelli, F.; Deangelis, M.L.; Gandolfi, C.; Casati, E.; Previtali, F.; Gerbino, R.; et al. Improved plant resistance to drought is promoted by the root-associated microbiome as a water stress-dependent trait. *Environ. Microbiol*. 2015, *17*, 316–331. https://doi.org/10.1111/1462-2920.12439

70. Schreiner, R.P.; Mihara, K.L. The diversity of arbuscular mycorrhizal fungi amplified from grapevine roots (*Vitis vinifera* L.) in Oregon vineyards is seasonally stable and influenced by soil and vine age. *Mycologia* 2009, *101*, 599–611. https://doi.org/10.3852/08-169

71. Likar, M.; Hančević, K.; Radić, T.; Regvar, M. Distribution and diversity of arbuscular mycorrhizal fungi in grapevines from production vineyards along the eastern Adriatic coast. *Mycorrhiza* 2013, *23*, 209–219. https://doi.org/10.1007/s00572-012-0463-x

72. Massa, N.; Bona, E.; Novello, G.; Todeschini, L.; Boatti, F.; Mignone, E.; Gamalero, G.; Lingua, G.; Berta, G.; Cesaro, P. AMF communities associated to *Vitis vinifera* in an Italian vineyard subjected to integrated pest management at two different phenological stages. *Sci. Rep*. 2020, *10*, 9197. https://doi.org/10.1038/s41598-020-66067-w

73. Trouvelot, S.; Bonneau, L.; Redecker, D.; van Tuinen, D.; Adrian, M.; Wipf, D. Arbuscular mycorrhiza symbiosis in viticulture: A review. *Agron. Sustain. Dev*. 2015, *35*, 1449–1467. https://doi.org/10.1007/s13593-015-0329-7

74. Donkó, Á.; Zanathy, G.; Èros-Honti, Z.; Villangó, S.; Bisztray, G.D. Changes of mycorrhizal colonization along moist gradient in a vineyard of Eger (Hungary). *Acta Univ. Sapientiae Agric. Environ.* 2014, *6*, 13–23. https://doi.org/10.2478/ausae-2014-0008

75. Balestrini, R.; Magurno, F.; Walker, C.; Lumini, E.; Bianciotto, V. Cohorts of arbuscular mycorrhizal fungi (AMF) in *Vitis vinifera*, a typical Mediterranean fruit crop. *Environ. Microbiol. Rep*. 2010, *2*, 594–604. https://doi.org/10.1111/j.1758-2229.2010.00160.x

76. Verbruggen, E.; Kiers, E.T. Evolutionary ecology of mycorrhizal functional diversity in agricultural systems. *Evol. Appl*. 2010, *3*, 547–560. https://doi.org/10.1111/j.1752-4571.2010.00145.x

77. Likar, M.; Stres, B.; Rusjan, D.; Potisek, M.; Regvar, M. Ecological and conventional viticulture gives rise to distinct fungal and bacterial microbial communities in vineyard soils. *Appl. Soil Ecol*. 2017, *113*, 86–95. https://doi.org/10.1016/j.apsoil.2017.02.007

78. Zaller, J.G.; Cantelmo, C.; Santos, G.D.; Muther, S.; Gruber, E.; Pallua, P.; Mandl, K.; Friedrich, B.; Hofstetter, I.; Schmuckenschlager, B.; et al. Herbicides in vineyards reduce grapevine root mycorrhization and alter soil microorganisms and the nutrient composition in grapevine roots, leaves, xylem sap and grape juice. *Environ. Sci. Pollut. Res*. 2018, *25*, 23215–23226. https://doi.org/10.1007/s11356-018-2422-3

79. Moukarzel, R.; Ridgway, H.; Guerin-Laguette, A.; Jones, E. Grapevine rootstocks drive the community structure of arbuscular mycorrhizal fungi in New Zealand vineyards. *J. Appl. Microbiol.* 2021, in press. https://doi.org/10.1111/jam.15160

80. Schreiner, R.P. Spatial and temporal variation of roots, arbuscular mycorrhizal fungi, and plant and soil nutrients in a mature Pinot Noir (*Vitis vinifera* L.) vineyard in Oregon, USA. *Plant. Soil* 2005, *276*, 219–234. https://doi.org/10.1007/s11104-005-4895-0

81. Berlanas, C.; Ojeda, S.; López-Manzanares, B.; Andrés-Sodupe, M.; Bujanda, R.; Martínez-Diz, M.P.; Díaz-Losada, E.; Gramaje, D. Occurrence and diversity of black-foot disease fungi in symptomless grapevine nursery stock in Spain. *Plant. Dis*. 2020, *104*, 94–104. https://doi.org/10.1094/PDIS-03-19-0484-RE

82. Whitelaw-Weckert, M.; Rahman, L.; Appleby, L.M.; Hall, A.; Clark, A.C.; Waite, H.; Hardie, W.J. Co-infection by Botryosphaeriaceae and *Ilyonectria* spp. fungi during propagation causes decline of young grafted grapevines. *Plant. Pathol*. 2013, *62*, 1226–1237. https://doi.org/10.1111/ppa.12059

83. Probst, C.; Jones, E.E.; Ridgway, H.J.; Jaspers, M.V. Cylindrocarpon black foot in nurseries-two factors that can increase infection. *Aust. Plant. Pathol*. 2012, *41*, 157–163. https://doi.org/10.1007/s13313-011-0103-5

84. Agustí-Brisach, C.; Armengol, J. Effects of temperature, pH and water potential on mycelial growth, sporulation and chlamydospore production in culture of *Cylindrocarpon* spp. associated with black foot of grapevines. *Phytopathol. Mediterr*. 2012, *51*, 37–50. https://doi.org/10.14601/Phytopathol_Mediterr-9499

85. Tahat, M.M.; Kamaruzaman, S.; Othman, R. Mycorrhizal fungi as a biocontrol agent. *Plant. Pathol. J.* 2010, *9*, 198–207. https://doi.org/10.3923/ppj.2010.198.207

86. Petit, E.; Gubler, W.D. Influence of *Glomus intraradices* on black foot disease caused by *Cylindrocarpon macrodidymum* on *Vitis rupestris* under controlled conditions. *Plant. Dis*. 2006, *90*. 1481–1484. https://doi.org/10.1094/PD-90-1481

87. Holland, T.; Bowen, P.; Kokkoris, V.; Úrbez-Torres, J.R.; Hart, M. Does inoculation with arbuscular mycorrhizal fungi reduce trunk disease in grapevine rootstocks? *Horticulturae* 2019, *5*, 61. https://doi.org/10.3390/horticulturae5030061

88. Fourie, P.H.; Halleen, F.; van der Vyver, J.; Schreuder, W. Effect of *Trichoderma* treatments on the occurrence of decline pathogens in the roots and rootstocks of nursery grapevines. *Phytopathol. Mediterr*. 2001, *40*, S473–S478.

89. Fourie, P.H.; Halleen, F. Chemical and biological protection of grapevine propagation material from trunk disease pathogens. *Eur. J. Plant. Pathol*. 2006, *116*, 255–265. https://doi.org/10.1007/s10658-006-9057-9

90. Santos, R.; Heckler, L.; Lazarotto, M.; Garrido, L.; Rego, C.; Blume, E. *Trichoderma* spp. and *Bacillus subtilis* for control of *Dactylonectria macrodidyma* in grapevine. *Phytopathol. Mediterr*. 2016, *55*, 293–300. https://doi.org/10.14601/Phytopathol_Mediterr-18048

91. Berlanas, C.; Andrés-Sodupe, M.; López-Manzanares, B.; Maldonado-González, M.M.; Gramaje, D. Effect of white mustard cover crop residue, soil chemical fumigation and *Trichoderma* spp. root treatment on black-foot disease control in grapevine. *Pest. Manag. Sci*. 2018, *74*, 2864–2873. https://doi.org/10.1002/ps.5078

92. Berbegal, M.; Ramón-Albalat, A.; León, M.; Armengol, J. Evaluation of long-term protection from nursery to vineyard provided by *Trichoderma atroviride* SC1 against fungal grapevine trunk pathogens. *Pest. Manag. Sci*. 2020, *76*, 967–977. https://doi.org/10.1002/ps.5605

93. Martínez-Diz, M.P.; Díaz-Losada, E.; Andrés-Sodupe, M.; Bujanda, R.; Maldonado-González, M.M.; Ojeda, S.; Yacoub, A.; Rey, P.; Gramaje, D. Field evaluation of biocontrol agents against black-foot and Petri diseases of grapevine. *Pest. Manag. Sci*. 2021, *77*, 697–708. https://doi.org/10.1002/ps.6064

7. SUPPLEMENTARY MATERIAL

Table S1. Physicochemical properties of the grapevine nursery soil examined in this study.

	Grapevine nursery soil
Coordinates	34°34'48" S, 56°17´50" W
Location	Canelones
Altitude (m)	33
Physicochemical properties	
pH H_2O	6.0
K meq/100g	1.33
Mg meq/100g	3.3
Ca meq/100g	11.5
Na meq/100g	1.25
P Bray mg/Kg	137.0
N-NO3 mg/kg	52.0
SOM%	4.8
Clay%	28.9
Sand%	12.3
Silt%	58.8
Water content at field capacity %*	34.78

***** % soil moisture by weight

Table S2. Number of reads, total OTUs and alpha diversity indices.

Index	Bulk soil					
	Sampling Time 1			Sampling Time 2		
	SWD[a]	MWD[b]	AWD[c]	SWD	MWD	AWD
Reads	23102.7 ± 416.8[d]	22924.8 ± 363.9	22429.8 ± 399.4	22859.1 ± 838.1	23285.8 ± 1057.6	28348.4 ± 722.4
OTUs	153	205	212	187	200	215
Chao1	67.06 ± 2.07	75.87 ± 2.98	72.1 ± 2.07	62.32 ± 2.41	70.17 ± 1.48	74.89 ± 1.45
Shannon	2.55 ± 0.03	2.84 ± 0.10	2.86 ± 0.08	2.41 ± 0.06	2.42 ± 0.03	2.57 ± 0.03
Index	Rhizosphere					
	Sampling Time 1			Sampling Time 2		
	SWD	MWD	AWD	SWD[e]	MWD[f]	AWD[g]
Reads	23863.8 ± 737.9	24057 ± 1222.0	23169.3 ± 531.0	24016.8 ± 2410.3	22719.8 ± 948.5	23993.4 ± 1055.0
OTUs	245	195	217	229	219	192
Chao1	87.37 ± 3.15	64.78 ± 1.28	77.14 ± 2.11	80.04 ± 2.63	78.79 ± 3.69	68.31 ± 2.25
Shannon	2.59 ± 0.04	2.44 ± 0.08	2.91 ± 0.08	2.45 ± 0.07	2.61 ± 0.05	2.70 ± 0.02
Index	Root					
	Sampling Time 1			Sampling Time 2		
	SWD	MWD	AWD[h]	SWD[i]	MWD	AWD[j]
Reads	23059.3 ± 391.9	22204.4 ± 309.6	22251.8 ± 371.7	22077.7 ± 629.8	26496.8 ± 685.3	30785.9 ± 845.2
OTUs	47	85	96	63	65	65
Chao1	17.88 ± 0.74	21.75 ± 1.26	28.40 ± 1.42	15.27 ± 0.45	21.17 ± 0.71	19.64 ± 0.56
Shannon	2.06 ± 0.03	2.11 ± 0.04	2.78 ± 0.04	2.13 ± 0.03	2.41 ± 0.02	2.61 ± 0.02

[a] Severe Water Deficit
[b] Moderate Water Deficit
[c] Absence of Water Deficit
[d] Values are the mean of 12 replicates
[e] Samples SU206 and SU223 were removed from the analysis due to the low number of sequences reads
[f] Sample SU245 was removed from the analysis due to the low number of sequences reads
[g] Samples SU289 and SU290 were removed from the analysis due to the low number of sequences reads
[h] Samples SU168 and SU174 were removed from the analysis due to the low number of sequences reads
[i] Sample SU214 was removed from the analysis due to the low number of sequences reads
[j] Sample SU283 was removed from the analysis due to the low number of sequences reads

Table S3. Estimates of number of reads, sample coverage and diversity indices at the genus level for fungal profiles

Sample ID	Number of reads	Good's coverage (%)	Chao1 richness	Shannon diversity
SU3	24878	99.97	66.8±1.4	2.5
SU4	23362	99.99	53.0±0.0	2.4
SU5	20782	99.97	72.0±5.5	2.5
SU6	21329	99.99	74.0±2.3	2.6
SU7	22289	99.97	73.0±0.2	2.7
SU8	24341	99.98	66.5±2.6	2.4
SU11	23552	100.00	16.0±0.5	2.0
SU14	22100	99.99	15.0±0.0	1.9
SU16	22775	99.99	18.0±0.5	2.1
SU17	23200	99.99	15.0±0.0	1.9
SU18	21102	99.97	16.0±0.2	2.0
SU19	21094	99.98	17.0±0.2	1.9
SU23	22107	99.99	78.0±1.8	2.8
SU24	20820	99.96	86.3±5.5	2.5
SU25	22674	99.95	86.5±2.9	2.6
SU26	28490	99.96	95.2±7.4	2.2
SU27	21681	99.98	87.8±4.2	2.6
SU28	22186	99.98	80.9±1.4	2.6
SU33	24624	99.99	65.3±0.9	2.5
SU34	21563	99.99	54.0±0.0	2.7
SU35	23383	99.96	66.2±0.5	2.5
SU36	24500	99.99	73.0±0.2	2.5
SU37	24156	99.97	74.0±0.0	2.7
SU38	22025	99.97	67.0±1.8	2.6
SU43	24552	99.99	16.0±0.0	2.1
SU44	21713	99.99	18.0±0.5	2.1
SU45	23795	99.99	22.0±0.2	2.1
SU46	24193	100.00	22.5±2.6	2.2
SU47	25385	99.99	20.0±0.5	2.2
SU48	23250	99.99	19.0±0.5	2.1
SU53	23306	99.98	78.0±0.0	2.6
SU54	22080	99.96	112.0±10.0	2.7
SU55	24762	99.97	88.3±0.7	2.6
SU56	28583	99.96	100.4±5.5	2.7
SU57	24267	99.95	72.1±5.0	2.5
SU58	25410	99.94	83.1±4.0	2.5
SU63	24236	99.97	67.3±0.9	2.9
SU64	23698	99.99	79.2±1.8	3.1
SU65	21659	99.99	77.0±0.0	3.1

SU66	22208	99.98	92.8±4.2	2.9
SU67	20778	99.94	76.1±2.5	2.8
SU68	23147	99.99	67.6±1.2	2.9
SU73	22580	99.97	28.0±1.8	2.1
SU74	21579	99.99	24.5±2.6	2.3
SU75	22201	99.99	18.5±1.3	1.9
SU76	21264	99.98	16.0±0.0	2.0
SU77	20731	99.99	19.0±0.5	2.1
SU78	22232	100.00	17.0±0.2	2.1
SU83	24288	99.99	62.3±0.9	2.6
SU84	22429	99.97	67.9±2.3	2.7
SU85	21801	99.99	55.0±0.1	2.5
SU86	23695	99.97	62.0±3.2	2.6
SU87	30673	99.96	66.4±0.8	2.4
SU88	22445	99.99	64.0±2.9	2.6
SU98	25128	99.96	82.7±2.0	3.3
SU99	22284	100.00	77.3±0.7	3.1
SU100	22103	99.97	91.2±0.6	2.9
SU101	22773	99.97	76.8±2.8	2.7
SU102	24454	99.99	64.5±2.6	2.5
SU103	22629	99.98	58.0±0.0	2.0
SU107	21738	99.99	28.0±1.8	2.1
SU108	22219	99.99	28.0±4.6	2.4
SU109	20824	99.98	21.0±1.8	2.0
SU110	23451	99.99	22.0±0.2	2.2
SU111	23515	99.99	20.0±0.5	2.1
SU112	24119	99.99	19.0±0.0	2.1
SU118	21202	100.00	62.8±1.4	2.3
SU119	21186	99.99	65.0±4.2	2.6
SU120	20658	99.99	64.0±0.2	2.5
SU121	22743	99.99	65.1±0.5	2.5
SU122	34634	99.98	71.3±4.1	1.7
SU123	22930	99.96	71.5±2.9	2.1
SU126	21900	99.99	73.0±13.2	2.5
SU130	21708	99.98	62.0±0.0	2.9
SU131	22637	99.99	65.0±3.4	2.7
SU132	22867	99.99	73.0±0.1	2.9
SU133	22318	99.94	76.3±1.7	2.9
SU134	23056	99.99	75.2±1.8	2.9
SU135	21977	99.97	69.5±4.1	2.5
SU136	23981	100.00	25.0±0.0	2.6
SU138	21227	100.00	26.0±0.0	2.8
SU139	22792	99.99	28.0±2.3	2.7
SU140	21706	100.00	28.0±0.0	2.8
SU141	21726	100.00	24.0±0.0	2.8

SU142	24609	100.00	21.0±0.0	2.8
SU147	24581	99.96	70.8±2.0	2.4
SU148	23010	99.97	82.1±4.7	2.7
SU150	27500	99.94	73.2±2.3	3.1
SU151	24965	99.94	84.8±5.8	2.5
SU152	21854	99.99	71.1±0.5	3.0
SU153	22850	99.97	85.0±10.8	3.1
SU157	23062	99.99	69.0±0.0	3.3
SU158	26107	99.99	68.0±0.0	3.0
SU159	20574	99.98	74.5±3.2	2.5
SU160	21810	99.99	69.2±0.6	3.1
SU161	21142	99.97	90.5±2.2	3.1
SU166	21744	100.00	31.0±0.5	2.9
SU169	21585	100.00	34.0±0.0	2.9
SU172	21154	100.00	34.0±2.3	2.6
SU175	21994	99.99	33.0±0.0	3.0
SU177	22028	99.94	79.8±2.8	2.9
SU179	20904	99.97	88.0±2.6	3.1
SU180	23800	99.99	63.0±0.5	2.9
SU182	22331	99.97	79.5±6.4	2.8
SU183	23680	99.97	75.3±0.9	3.1
SU184	20529	100.00	73.0±0.2	3.3
SU186	21970	99.98	49.8±1.4	2.5
SU187	22833	99.94	66.5±1.9	2.4
SU188	22289	99.97	57.2±4.3	2.4
SU189	23412	99.96	69.0±8.0	2.4
SU190	21706	99.96	51.8±1.4	2.4
SU192	31736	99.96	53.7±2.0	1.9
SU193	20213	100.00	13.0±0.0	2.0
SU194	20565	99.99	16.0±0.0	2.2
SU195	20195	100.00	17.0±0.0	2.0
SU196	23293	99.99	15.0±2.3	2.2
SU198	21022	100.00	14.0±0.0	2.0
SU199	20002	99.99	13.0±0.0	2.1
SU200	25087	99.92	90.7±3.8	2.8
SU201	25492	99.95	66.1±2.3	2.6
SU202	15736	99.94	84.5±4.1	2.6
SU203	23892	99.94	77.5±4.5	2.7
SU204	15869	99.97	74.5±1.9	2.4
SU207	22915	99.95	74.0±2.6	2.7
SU208	21617	99.94	74.9±2.3	2.6
SU209	22387	99.96	65.0±1.6	2.3
SU210	20762	99.96	61.0±1.8	2.6
SU211	21779	99.94	58.6±2.8	2.4
SU212	20903	99.95	66.4±1.9	2.4

SU215	25791	99.99	17.0±0.0	2.1
SU216	25747	99.99	16.0±0.0	2.1
SU217	22074	100.00	15.0±0.0	2.1
SU218	22251	99.98	15.0±0.2	2.2
SU219	21702	99.98	17.0±0.0	2.3
SU222	42442	99.90	73.1±3.4	2.1
SU224	20636	99.96	72.6±2.5	2.0
SU225	21343	99.96	86.5±4.1	2.5
SU226	28382	99.96	86.4±5.5	2.6
SU227	21289	99.94	88.5±4.5	2.4
SU229	26180	99.96	68.5±2.2	2.5
SU230	25129	99.99	61.0±0.2	2.6
SU231	33461	99.90	74.0±13.2	2.4
SU232	21980	99.97	72.7±2.2	2.6
SU233	22855	99.94	66.7±2.2	2.4
SU234	20907	99.96	80.6±5.3	2.6
SU236	26697	99.99	21.0±0.2	2.5
SU237	23264	99.98	22.0±0.5	2.4
SU238	28513	99.99	22.0±0.0	2.3
SU239	26429	99.99	24.0±0.0	2.5
SU240	21113	99.99	26.0±0.5	2.6
SU241	26670	99.99	23.0±0.5	2.4
SU243	22142	99.95	74.2±7.4	2.5
SU244	21991	99.94	77.5±2.6	2.7
SU246	24709	99.96	73.4±5.5	2.6
SU247	24709	99.94	73.4±5.5	2.6
SU248	22029	99.95	65.0±6.6	2.6
SU250	22955	99.97	72.8±1.3	2.3
SU251	20544	99.95	66.3±5.4	2.3
SU252	20209	99.95	73.5±1.3	2.4
SU253	22302	99.94	72.1±0.4	2.3
SU254	21452	99.97	68.3±0.7	2.4
SU255	21455	99.98	65.8±1.4	2.3
SU257	27601	99.99	17.0±0.2	2.4
SU258	28745	99.98	20.0±2.3	2.3
SU259	28713	99.99	21.0±0.5	2.3
SU260	28908	99.98	19.0±0.0	2.5
SU261	25658	99.99	20.0±0.0	2.4
SU262	25650	99.99	19.0±0.0	2.4
SU264	27765	99.97	94.5±10.6	3.0
SU265	17036	99.94	80.3±2.6	2.7
SU266	21352	99.97	73.4±7.3	2.4
SU267	18387	99.97	95.4±12.6	2.6
SU268	23950	99.93	98.0±11.0	2.7
SU269	25848	99.94	61.4±5.5	2.6

SU271	31009	99.96	78.5±3.7	2.7
SU272	27626	99.92	73.1±4.7	2.7
SU273	30232	99.91	71.2±1.5	2.6
SU274	29494	99,94	81.0±8.9	2.5
SU275	29105	99.96	82.0±8.0	2.5
SU276	25957	99.95	77.0±8.5	2.4
SU278	30265	99.99	19.0±0.5	2.6
SU279	28055	100.00	17.0±0.0	2.6
SU280	32832	100.00	19.0±0.5	2.7
SU281	29860	100.00	17.0±0.0	2.5
SU282	33962	100.00	18.0±0.0	2.7
SU285	25278	99.96	80.5±6.4	2.8
SU286	15806	99.94	62.9±2.3	2.7
SU287	25581	99.96	65.4±5.5	2.7
SU288	28364	99.92	67.1±5.0	2.7
SU292	33713	99.96	71.2±4.3	2.4
SU293	26410	99.96	69.4±0.8	2.7
SU294	27041	99.94	69.7±2.2	2.6
SU295	26558	99.94	76.3±0.7	2.6
SU296	24790	99.94	68.2±0.5	2.6
SU298	28246	99.92	81.1±7.2	2.6
SU299	30218	100.00	19.0±0.0	2.6
SU300	27367	99.99	21.0±0.0	2.6
SU301	29303	99.99	22.0±0.5	2.6
SU302	27560	100.00	21.0±0.0	2.7
SU303	33656	100.00	22.0±0.0	2.7
SU304	35567	100.00	21.0±0.0	2.6
SU307	26928	99.96	68.5±6.6	2.6
SU308	23409	99.94	64.1±4.6	2.7
SU309	24066	99.97	82.2±7.4	2.8
SU310	23826	99.94	62.4±1.9	2.7
SU311	23429	99.96	65.9±2.3	2.7
SU312	23247	99.96	64.0±3.4	2.7

Table S4. Fungal OTUs that were unique in each irrigation regime in the soil-plant compartments.

Bulk soil			Rhizosphere			Root		
SWD[a]	MWD[b]	AWD[c]	SWD	MWD	AWD	SWD	MWD	AWD
Alfaria	*Achaetomium*	*Acrophialophora*	*Bacillicladium*	*Achroiostachys*	*Allomyces*	*Achroiostachys*	*Absidia*	*Campylocarpon*
Allomyces	*Achroiostachys*	*Alnicola*	*Bolbitius*	*Alfaria*	*Coniolariella*	*Allomyces*	*Acaulospora*	*Conocybe*
Arxiella	*Bolbitius*	*Bacillicladium*	*Burgoa*	*Auxarthronopsis*	*Echinusitheca*	*Ascotricha*	*Achaetomium*	*Cystobasidium*
Auxarthronopsis	*Echinusitheca*	*Candida*	*Chordomyces*	*Flavodon*	*Geminibasidium*	*Bolbitius*	*Alfaria*	*Gymnoascus*
Holtermanniella	*Fellomyces*	*Colletotrichum*	*Cladorrhinum*	*Fumagopsis*	*Hydnangium*	*Bullera*	*Alnicola*	*Heteroradulum*
Hydnangium	*Kurtzmaniella*	*Coprinus*	*Cyberlindnera*	*Fusicolla*	*Parawiesneriomyces*	*Byssochlamys*	*Anthracocystis*	*Holtermanniella*
Myriococcum	*Laetisaria*	*Coralloidiomyces*	*Diversispora*	*Hormodochis*	*Pezicula*	*Calvatia*	*Arachnotheca*	*Hyaloseta*
Paecilomyces	*Lectera*	*Diatrypella*	*Entyloma*	*Lobulomyces*	*Sistotrema*	*Chlorophyllum*	*Arizonaphlyctis*	*Ijuhya*
Pezicula	*Mucidula*	*Drechmeria*	*Harposporium*	*Marasmius*		*Gymnascella*	*Arthrocladium*	*Laetisaria*
Phaeoannellomyces	*Phialocephala*	*Elsinoe*	*Holtermanniella*	*Melanoleuca*		*Hapsidospora*	*Atractiella*	*Leucoagaricus*
Phaeophlebiopsis	*Pseudophialophora*	*Hyphodontia*	*Kurtzmaniella*	*Mucidula*		*Hyalorbilia*	*Auxarthronopsis*	*Lindtneria*
Pluteus	*Remispora*	*Kalmanozyma*	*Laccaria*	*Phaeoannellomyces*		*Kraurogymnocarpa*	*Buckleyzyma*	*Lipomyces*
Tulasnella	*Rhizophagus*	*Laccaria*	*Mycena*	*Phialocephala*		*Lentithecium*	*Classicula*	*Lobulomyces*
	Sistotrema	*Lentithecium*	*Myriococcum*	*Pleiocarpon*		*Metapochonia*	*Climacocystis*	*Marasmius*
	Sporothrix	*Marasmius*	*Phylliscum*	*Remispora*		*Minimelanolocus*	*Coprinellus*	*Matsushimaea*
	Sterigmatomyces	*Megasporoporia*	*Pluteus*	*Saccharomyces*		*Neoidriella*	*Coralloidiomyces*	*Megasporoporia*
	Trametes	*Mycena*	*Pseudophialophora*	*Thyronectria*		*Olpidium*	*Currahmyces*	*Meira*
		Mycoleptodiscus	*Pseudothielavia*			*Phaeoacremonium*	*Cyberlindnera*	*Microascus*
		Neopaxillus	*Ramariopsis*			*Phylliscum*	*Debaryomyces*	*Microthecium*
		Parawiesneriomyces	*Rhinocladiella*			*Spizellomyces*	*Dimorphiseta*	*Mucor*
		Pleohelicoon	*Rosasphaeria*			*Synfenestella*	*Eichleriella*	*Papiliotrema*
		Polytolypa	*Sporidiobolus*				*Elsinoe*	*Phaeophlebiopsis*
		Ramariopsis	*Stagonospora*				*Epichloe*	*Pluteus*
		Saccharomyces	*Subulicystidium*				*Erythrobasidium*	*Pochonia*
		Sporisorium	*Synfenestella*				*Farysia*	*Polycephalomyces*
		Taphrina	*Trichosporonaceae*				*Geastrum*	*Porpoloma*
		Tilletiopsis	*Tulasnella*				*Gilbertella*	*Pseudallescheria*
		Wojnowiciella	*Tygervalleyomyces*				*Golubevia*	*Pseudohyphozyma*
			Vaginatispora				*Harposporium*	*Pseudozyma*

Lindtneria	*Psilocybe*
Meyerozyma	*Rasamsonia*
Microstroma	*Resupinatus*
Naganishia	*Rhizophagus*
Neostrelitziana	*Sampaiozyma*
Paecilomyces	*Scedosporium*
Peniophora	*Sistotremastrum*
Phialocephala	*Spiromastix*
Remispora	*Sporobolomyces*
Sporothrix	*Sterigmatomyces*
Tetracoccosporium	*Striatibotrys*
Tulasnella	*Talaromyces*
Tulostoma	*Trematosphaeria*
Udeniozyma	*Trichomerium*
Vaginatispora	*Trichosporonaceae*
	Veronaea
	Wallemia
	Wojnowiciella

[a] Severe Water Deficit
[b] Moderate Water Deficit
[c] Absence of Water Deficit

Table S5. SparCC correlation analysis at genus level in the bulk soil, rhizosphere and root.

Bulk soil				Rhizosphere				Root			
Taxon1	Taxon2	Correlation	*p*-value	Taxon1	Taxon2	Correlation	*p*-value	Taxon1	Taxon2	Correlation	*p*-value
Acaulium	*Microthecium*	0.5704	0.0099	*Absidia*	*Clonostachys*	0.5493	0.0099	*Aporpium*	*Auricularia*	0.8039	0.0099
Acremonium	*Plectosphaerella*	0.5569	0.0099	*Aporpium*	*Auricularia*	0.6864	0.0099	*Aporpium*	*Emericellopsis*	0.5153	0.0099
Albifimbria	*Aspergillus*	0.6357	0.0099	*Aporpium*	*Chrysosporium*	-0.5182	0.0099	*Aporpium*	*Funneliformis*	0.7903	0.0099
Albifimbria	*Dissophora*	0.5247	0.0099	*Aporpium*	*Golubevia*	-0.5347	0.0099	*Aporpium*	*Lasiobolidium*	0.5147	0.0099
Albifimbria	*Slopeiomyces*	0.5078	0.0099	*Aporpium*	*Polyscytalum*	0.5732	0.0099	*Aporpium*	*Polyscytalum*	0.695	0.0099
Albifimbria	*Solicoccozyma*	0.6486	0.0099	*Aporpium*	*Slopeiomyces*	0.5956	0.0099	*Aspergillus*	*Cirrenalia*	-0.5248	0.0099
Albifimbria	*Spiromastix*	-0.5157	0.0099	*Aporpium*	*Spiromastix*	-0.7376	0.0099	*Aspergillus*	*Emericellopsis*	-0.5029	0.0099
Aspergillus	*Albifimbria*	0.6357	0.0099	*Auricularia*	*Aporpium*	0.6864	0.0099	*Aspergillus*	*Fusarium*	0.6541	0.0099
Aspergillus	*Dissophora*	0.531	0.0099	*Auricularia*	*Cirrenalia*	0.549	0.0099	*Aspergillus*	*Malassezia*	-0.5123	0.0099
Aspergillus	*Fusarium*	0.5694	0.0099	*Auricularia*	*Dactylonectria*	0.5232	0.0099	*Aspergillus*	*Microdochium*	-0.5006	0.0099
Calvatia	*Psathyrella*	0.5562	0.0099	*Auricularia*	*Enterocarpus*	0.55	0.0099	*Aspergillus*	*Minimedusa*	0.6593	0.0099
Ceratobasidium	*Minimedusa*	0.5631	0.0099	*Auricularia*	*Golubevia*	-0.5924	0.0099	*Aspergillus*	*Psathyrella*	0.6552	0.0099
Ceratobasidium	*Scopulariopsis*	0.5053	0.0099	*Auricularia*	*Neocosmospora*	0.5914	0.0099	*Aspergillus*	*Thelonectria*	0.7568	0.0099
Ceratobasidium	*Solicoccozyma*	0.5834	0.0099	*Auricularia*	*Polyscytalum*	0.6131	0.0099	*Auricularia*	*Aporpium*	0.8039	0.0099
Chrysosporium	*Enterocarpus*	-0.5663	0.0099	*Auricularia*	*Slopeiomyces*	0.6751	0.0099	*Auricularia*	*Cirrenalia*	0.5246	0.0099
Chrysosporium	*Moesziomyces*	0.5425	0.0099	*Auricularia*	*Spiromastix*	-0.7853	0.0099	*Auricularia*	*Emericellopsis*	0.6216	0.0099
Chrysosporium	*Slopeiomyces*	-0.7904	0.0099	*Auricularia*	*Unknown*	0.557	0.0099	*Auricularia*	*Funneliformis*	0.8496	0.0099
Chrysosporium	*Spiromastix*	0.7599	0.0099	*Buckleyzyma*	*Occultifur*	0.5155	0.0099	*Auricularia*	*Polyscytalum*	0.5524	0.0099
Chrysosporium	*Spizellomyces*	0.6206	0.0099	*Chrysosporium*	*Aporpium*	-0.5182	0.0099	*Auricularia*	*Thelonectria*	-0.6497	0.0099
Cylindrocarpon	*Slopeiomyces*	-0.5264	0.0099	*Chrysosporium*	*Polyscytalum*	-0.5673	0.0099	*Bipolaris*	*Cylindrocarpon*	-0.5001	0.0099
Dissophora	*Albifimbria*	0.5247	0.0099	*Chrysosporium*	*Slopeiomyces*	-0.5718	0.0099	*Ceratobasidium*	*Plectosphaerella*	-0.5808	0.0099
Dissophora	*Aspergillus*	0.531	0.0099	*Chrysosporium*	*Spiromastix*	0.6547	0.0099	*Cirrenalia*	*Aspergillus*	-0.5248	0.0099
Dissophora	*Enterocarpus*	0.5749	0.0099	*Cirrenalia*	*Auricularia*	0.549	0.0099	*Cirrenalia*	*Auricularia*	0.5246	0.0099
Dissophora	*Fusarium*	0.6267	0.0099	*Cirrenalia*	*Enterocarpus*	0.6174	0.0099	*Cirrenalia*	*Funneliformis*	0.5339	0.0099
Dissophora	*Lasiobolidium*	0.5665	0.0099	*Cirrenalia*	*Neocosmospora*	0.6008	0.0099	*Cirrenalia*	*Neocosmospora*	-0.6248	0.0099
Enterocarpus	*Chrysosporium*	-0.5663	0.0099	*Cirrenalia*	*Polyscytalum*	0.5706	0.0099	*Cirrenalia*	*Psathyrella*	-0.5547	0.0099
Enterocarpus	*Dissophora*	0.5749	0.0099	*Cirrenalia*	*Slopeiomyces*	0.648	0.0099	*Cylindrocarpon*	*Bipolaris*	-0.5001	0.0099
Enterocarpus	*Fusarium*	0.5324	0.0099	*Cirrenalia*	*Spiromastix*	-0.6191	0.0099	*Cylindrocarpon*	*Dactylonectria*	0.529	0.0099
Enterocarpus	*Neocosmospora*	0.6053	0.0099	*Cirrenalia*	*Unknown*	0.5029	0.0099	*Dactylonectria*	*Cylindrocarpon*	0.529	0.0099

Enterocarpus	*Slopeiomyces*	0.6792	0.0099	*Clonostachys*	*Absidia*	0.5493	0.0099	*Dactylonectria*	*Thelonectria*	0.5102	0.0099
Enterocarpus	*Spiromastix*	-0.6172	0.0099	*Cylindrocarpon*	*Enterocarpus*	0.5825	0.0099	*Dactylonectria*	*Trichoderma*	0.511	0.0099
Fusarium	*Aspergillus*	0.5694	0.0099	*Cylindrocarpon*	*Fusarium*	0.5216	0.0099	*Dissophora*	*Malassezia*	-0.6225	0.0099
Fusarium	*Dissophora*	0.6267	0.0099	*Dactylonectria*	*Auricularia*	0.5232	0.0099	*Dissophora*	*Minimedusa*	0.6389	0.0099
Fusarium	*Enterocarpus*	0.5324	0.0099	*Dactylonectria*	*Enterocarpus*	0.5245	0.0099	*Dissophora*	*Monosporascus*	-0.5595	0.0099
Fusarium	*Lasiobolidium*	0.7815	0.0099	*Dactylonectria*	*Neocosmospora*	0.6283	0.0099	*Dissophora*	*Psathyrella*	0.6333	0.0099
Fusarium	*Mortierella*	0.5663	0.0099	*Dissophora*	*Malassezia*	0.5006	0.0099	*Emericellopsis*	*Aporpium*	0.5153	0.0099
Fusarium	*Slopeiomyces*	0.5507	0.0099	*Enterocarpus*	*Auricularia*	0.55	0.0099	*Emericellopsis*	*Aspergillus*	-0.5029	0.0099
Fusarium	*Solicoccozyma*	0.5769	0.0099	*Enterocarpus*	*Cirrenalia*	0.6174	0.0099	*Emericellopsis*	*Auricularia*	0.6216	0.0099
Fusarium	*Spiromastix*	-0.5423	0.0099	*Enterocarpus*	*Cylindrocarpon*	0.5825	0.0099	*Emericellopsis*	*Funneliformis*	0.6342	0.0099
Lasiobolidium	*Dissophora*	0.5665	0.0099	*Enterocarpus*	*Dactylonectria*	0.5245	0.0099	*Emericellopsis*	*Fusarium*	-0.5976	0.0099
Lasiobolidium	*Fusarium*	0.7815	0.0099	*Enterocarpus*	*Neocosmospora*	0.6078	0.0099	*Emericellopsis*	*Polyscytalum*	0.5661	0.0099
Lasiobolidium	*Spiromastix*	-0.5251	0.0099	*Enterocarpus*	*Polyscytalum*	0.5502	0.0099	*Emericellopsis*	*Thelonectria*	-0.5674	0.0099
Microthecium	*Acaulium*	0.5704	0.0099	*Enterocarpus*	*Rhizophydium*	-0.5521	0.0099	*Funneliformis*	*Aporpium*	0.7903	0.0099
Microthecium	*Solicoccozyma*	-0.5104	0.0099	*Enterocarpus*	*Slopeiomyces*	0.6156	0.0099	*Funneliformis*	*Auricularia*	0.8496	0.0099
Microthecium	*Spencerozyma*	0.5266	0.0099	*Enterocarpus*	*Spiromastix*	-0.5635	0.0099	*Funneliformis*	*Cirrenalia*	0.5339	0.0099
Minimedusa	*Ceratobasidium*	0.5631	0.0099	*Fusarium*	*Cylindrocarpon*	0.5216	0.0099	*Funneliformis*	*Emericellopsis*	0.6342	0.0099
Minimedusa	*Solicoccozyma*	0.6639	0.0099	*Golubevia*	*Aporpium*	-0.5347	0.0099	*Funneliformis*	*Polyscytalum*	0.5772	0.0099
Minimedusa	*Spiromastix*	-0.5969	0.0099	*Golubevia*	*Auricularia*	-0.5924	0.0099	*Funneliformis*	*Thelonectria*	-0.539	0.0099
Moesziomyces	*Chrysosporium*	0.5425	0.0099	*Golubevia*	*Moesziomyces*	0.5495	0.0099	*Fusarium*	*Aspergillus*	0.6541	0.0099
Moesziomyces	*Pseudozyma*	0.5644	0.0099	*Golubevia*	*Polyscytalum*	-0.5758	0.0099	*Fusarium*	*Emericellopsis*	-0.5976	0.0099
Moesziomyces	*Slopeiomyces*	-0.5899	0.0099	*Golubevia*	*Slopeiomyces*	-0.5766	0.0099	*Fusarium*	*Polyscytalum*	-0.533	0.0099
Mortierella	*Fusarium*	0.5663	0.0099	*Golubevia*	*Spiromastix*	0.6808	0.0099	*Fusarium*	*Thelonectria*	0.912	0.0099
Mortierella	*Solicoccozyma*	0.5315	0.0099	*Golubevia*	*Spizellomyces*	0.5278	0.0099	*Fusarium*	*Verrucostoma*	0.5282	0.0099
Neocosmospora	*Enterocarpus*	0.6053	0.0099	*Malassezia*	*Dissophora*	0.5006	0.0099	*Lasiobolidium*	*Aporpium*	0.5147	0.0099
Neocosmospora	*Sodiomyces*	0.6406	0.0099	*Microthecium*	*Verrucostoma*	0.569	0.0099	*Lasiobolidium*	*Poaceascoma*	-0.5526	0.0099
Nigrosabulum	*Thermoascus*	0.6	0.0099	*Moesziomyces*	*Golubevia*	0.5495	0.0099	*Malassezia*	*Aspergillus*	-0.5123	0.0099
Olpidium	*Penicillium*	0.5207	0.0099	*Moesziomyces*	*Polyscytalum*	-0.5165	0.0099	*Malassezia*	*Dissophora*	-0.6225	0.0099
Penicillium	*Olpidium*	0.5207	0.0099	*Moesziomyces*	*Slopeiomyces*	-0.5564	0.0099	*Malassezia*	*Minimedusa*	-0.6099	0.0099
Plectosphaerella	*Acremonium*	0.5569	0.0099	*Moesziomyces*	*Spiromastix*	0.6601	0.0099	*Malassezia*	*Psathyrella*	-0.5497	0.0099
Psathyrella	*Calvatia*	0.5562	0.0099	*Moesziomyces*	*Spizellomyces*	0.5191	0.0099	*Microdochium*	*Aspergillus*	-0.5006	0.0099
Psathyrella	*Spiromastix*	0.5421	0.0099	*Neocosmospora*	*Auricularia*	0.5914	0.0099	*Minimedusa*	*Aspergillus*	0.6593	0.0099
Psathyrella	*Trichoderma*	0.5924	0.0099	*Neocosmospora*	*Cirrenalia*	0.6008	0.0099	*Minimedusa*	*Dissophora*	0.6389	0.0099

Pseudozyma	*Moesziomyces*	0.5644	0.0099	*Neocosmospora*	*Dactylonectria*	0.6283	0.0099	*Minimedusa*	*Malassezia*	-0.6099	0.0099
Scopulariopsis	*Ceratobasidium*	0.5053	0.0099	*Neocosmospora*	*Enterocarpus*	0.6078	0.0099	*Minimedusa*	*Mortierella*	0.5438	0.0099
Slopeiomyces	*Albifimbria*	0.5078	0.0099	*Neocosmospora*	*Polyscytalum*	0.6054	0.0099	*Minimedusa*	*Psathyrella*	0.7953	0.0099
Slopeiomyces	*Chrysosporium*	-0.7904	0.0099	*Neocosmospora*	*Slopeiomyces*	0.7164	0.0099	*Monosporascus*	*Dissophora*	-0.5595	0.0099
Slopeiomyces	*Cylindrocarpon*	-0.5264	0.0099	*Neocosmospora*	*Spiromastix*	-0.7184	0.0099	*Monosporascus*	*Phomatospora*	0.5714	0.0099
Slopeiomyces	*Enterocarpus*	0.6792	0.0099	*Occultifur*	*Buckleyzyma*	0.5155	0.0099	*Mortierella*	*Minimedusa*	0.5438	0.0099
Slopeiomyces	*Fusarium*	0.5507	0.0099	*Polyscytalum*	*Aporpium*	0.5732	0.0099	*Neocosmospora*	*Cirrenalia*	-0.6248	0.0099
Slopeiomyces	*Moesziomyces*	-0.5899	0.0099	*Polyscytalum*	*Auricularia*	0.6131	0.0099	*Neocosmospora*	*Psathyrella*	0.6049	0.0099
Slopeiomyces	*Spiromastix*	-0.8402	0.0099	*Polyscytalum*	*Chrysosporium*	-0.5673	0.0099	*Penicillium*	*Polyscytalum*	-0.5458	0.0099
Slopeiomyces	*Spizellomyces*	-0.6129	0.0099	*Polyscytalum*	*Cirrenalia*	0.5706	0.0099	*Penicillium*	*Spencerozyma*	0.5152	0.0099
Sodiomyces	*Neocosmospora*	0.6406	0.0099	*Polyscytalum*	*Enterocarpus*	0.5502	0.0099	*Phomatospora*	*Monosporascus*	0.5714	0.0099
Solicoccozyma	*Albifimbria*	0.6486	0.0099	*Polyscytalum*	*Golubevia*	-0.5758	0.0099	*Plectosphaerella*	*Ceratobasidium*	-0.5808	0.0099
Solicoccozyma	*Ceratobasidium*	0.5834	0.0099	*Polyscytalum*	*Moesziomyces*	-0.5165	0.0099	*Plectosphaerella*	*Spencerozyma*	0.5703	0.0099
Solicoccozyma	*Fusarium*	0.5769	0.0099	*Polyscytalum*	*Neocosmospora*	0.6054	0.0099	*Plectosphaerella*	*Spiromastix*	0.6269	0.0099
Solicoccozyma	*Microthecium*	-0.5104	0.0099	*Polyscytalum*	*Slopeiomyces*	0.8008	0.0099	*Poaceascoma*	*Lasiobolidium*	-0.5526	0.0099
Solicoccozyma	*Minimedusa*	0.6639	0.0099	*Polyscytalum*	*Spiromastix*	-0.834	0.0099	*Poaceascoma*	*Spencerozyma*	0.7259	0.0099
Solicoccozyma	*Mortierella*	0.5315	0.0099	*Rhizophydium*	*Enterocarpus*	-0.5521	0.0099	*Poaceascoma*	*Spiromastix*	0.7905	0.0099
Solicoccozyma	*Spencerozyma*	-0.7287	0.0099	*Rhizophydium*	*Spiromastix*	0.5392	0.0099	*Polyscytalum*	*Aporpium*	0.695	0.0099
Solicoccozyma	*Spiromastix*	-0.5835	0.0099	*Slopeiomyces*	*Aporpium*	0.5956	0.0099	*Polyscytalum*	*Auricularia*	0.5524	0.0099
Solicoccozyma	*Unknown*	0.5399	0.0099	*Slopeiomyces*	*Auricularia*	0.6751	0.0099	*Polyscytalum*	*Emericellopsis*	0.5661	0.0099
Spencerozyma	*Microthecium*	0.5266	0.0099	*Slopeiomyces*	*Chrysosporium*	-0.5718	0.0099	*Polyscytalum*	*Funneliformis*	0.5772	0.0099
Spencerozyma	*Solicoccozyma*	-0.7287	0.0099	*Slopeiomyces*	*Cirrenalia*	0.648	0.0099	*Polyscytalum*	*Fusarium*	-0.533	0.0099
Spiromastix	*Albifimbria*	-0.5157	0.0099	*Slopeiomyces*	*Enterocarpus*	0.6156	0.0099	*Polyscytalum*	*Penicillium*	-0.5458	0.0099
Spiromastix	*Chrysosporium*	0.7599	0.0099	*Slopeiomyces*	*Golubevia*	-0.5766	0.0099	*Psathyrella*	*Aspergillus*	0.6552	0.0099
Spiromastix	*Enterocarpus*	-0.6172	0.0099	*Slopeiomyces*	*Moesziomyces*	-0.5564	0.0099	*Psathyrella*	*Cirrenalia*	-0.5547	0.0099
Spiromastix	*Fusarium*	-0.5423	0.0099	*Slopeiomyces*	*Neocosmospora*	0.7164	0.0099	*Psathyrella*	*Dissophora*	0.6333	0.0099
Spiromastix	*Lasiobolidium*	-0.5251	0.0099	*Slopeiomyces*	*Polyscytalum*	0.8008	0.0099	*Psathyrella*	*Malassezia*	-0.5497	0.0099
Spiromastix	*Minimedusa*	-0.5969	0.0099	*Slopeiomyces*	*Spiromastix*	-0.8649	0.0099	*Psathyrella*	*Minimedusa*	0.7953	0.0099
Spiromastix	*Psathyrella*	0.5421	0.0099	*Slopeiomyces*	*Unknown*	0.5563	0.0099	*Psathyrella*	*Neocosmospora*	0.6049	0.0099
Spiromastix	*Slopeiomyces*	-0.8402	0.0099	*Sodiomyces*	*Spiromastix*	-0.5354	0.0099	*Psathyrella*	*Thelonectria*	0.5504	0.0099
Spiromastix	*Solicoccozyma*	-0.5835	0.0099	*Solicoccozyma*	*Spencerozyma*	-0.8005	0.0099	*Sarocladium*	*Spencerozyma*	0.5688	0.0099
Spiromastix	*Spizellomyces*	0.5924	0.0099	*Solicoccozyma*	*Spiromastix*	-0.5319	0.0099	*Spencerozyma*	*Penicillium*	0.5152	0.0099
Spiromastix	*Thelonectria*	0.588	0.0099	*Spencerozyma*	*Solicoccozyma*	-0.8005	0.0099	*Spencerozyma*	*Plectosphaerella*	0.5703	0.0099

Spizellomyces	*Chrysosporium*	0.6206	0.0099	*Spiromastix*	*Aporpium*	-0.7376	0.0099	*Spencerozyma*	*Poaceascoma*	0.7259	0.0099
Spizellomyces	*Slopeiomyces*	-0.6129	0.0099	*Spiromastix*	*Auricularia*	-0.7853	0.0099	*Spencerozyma*	*Sarocladium*	0.5688	0.0099
Spizellomyces	*Spiromastix*	0.5924	0.0099	*Spiromastix*	*Chrysosporium*	0.6547	0.0099	*Spencerozyma*	*Spiromastix*	0.8837	0.0099
Thelonectria	*Spiromastix*	0.588	0.0099	*Spiromastix*	*Cirrenalia*	-0.6191	0.0099	*Spiromastix*	*Plectosphaerella*	0.6269	0.0099
Thermoascus	*Nigrosabulum*	0.6	0.0099	*Spiromastix*	*Enterocarpus*	-0.5635	0.0099	*Spiromastix*	*Poaceascoma*	0.7905	0.0099
Trichoderma	*Psathyrella*	0.5924	0.0099	*Spiromastix*	*Golubevia*	0.6808	0.0099	*Spiromastix*	*Spencerozyma*	0.8837	0.0099
Unknown	*Solicoccozyma*	0.5399	0.0099	*Spiromastix*	*Moesziomyces*	0.6601	0.0099	*Thelonectria*	*Aspergillus*	0.7568	0.0099
				Spiromastix	*Neocosmospora*	-0.7184	0.0099	*Thelonectria*	*Auricularia*	-0.6497	0.0099
				Spiromastix	*Polyscytalum*	-0.834	0.0099	*Thelonectria*	*Dactylonectria*	0.5102	0.0099
				Spiromastix	*Rhizophydium*	0.5392	0.0099	*Thelonectria*	*Emericellopsis*	-0.5674	0.0099
				Spiromastix	*Slopeiomyces*	-0.8649	0.0099	*Thelonectria*	*Funneliformis*	-0.539	0.0099
				Spiromastix	*Sodiomyces*	-0.5354	0.0099	*Thelonectria*	*Fusarium*	0.912	0.0099
				Spiromastix	*Solicoccozyma*	-0.5319	0.0099	*Thelonectria*	*Psathyrella*	0.5504	0.0099
				Spiromastix	*Unknown*	-0.5216	0.0099	*Thelonectria*	*Verrucostoma*	0.6075	0.0099
				Spizellomyces	*Golubevia*	0.5278	0.0099	*Trichoderma*	*Dactylonectria*	0.511	0.0099
				Spizellomyces	*Moesziomyces*	0.5191	0.0099	*Verrucostoma*	*Fusarium*	0.5282	0.0099
				Unknown	*Auricularia*	0.557	0.0099	*Verrucostoma*	*Thelonectria*	0.6075	0.0099
				Unknown	*Cirrenalia*	0.5029	0.0099				
				Unknown	*Slopeiomyces*	0.5563	0.0099				
				Unknown	*Spiromastix*	-0.5216	0.0099				
				Verrucostoma	*Microthecium*	0.569	0.0099				

Table S6. Relative proportion (%) of fungal function from soil-plant compartments at each irrigation regime inferred by FunGuild.

	Bulk soil			Rhizosphere			Root		
	SWD[a]	MWD[b]	AWD[c]	SWD	MWD	AWD	SWD	MWD	AWD
Pathotroph	24.52±0.67 Ba	26.13±1.35 Ba	23.62±3.08 Ba	27.79±3.22 Ba	24.20±0.98 Ba	23.97±1.03 Ba	26.25±3.29 Bb	34.50±0.92 Ba	28.41±0.52 Bab
Saprotroph	44.96±1.97 Aa	42.27±0.52 Aa	46.50±2.57 Aa	45.63±1.91 Aa	45.16±2.87 Aa	47.87±2.42Aa	52.28±5.07 Aa	41.51±1.34 Aa	45.22±2.14 Aa
Symbiotroph	25.37±1.94 Ba	24.50±0.73 Ba	22.11±1.49 Ba	22.21±2.57 Ba	23.38±3.07 Ba	20.32±2.12 Ba	17.48±2.23 BCa	20.17±0.51 Ca	16.98±2.14 Ca
Unassigned	5.16±0.74 Ca	7.10±1.06 Ca	7.77±1.91 Ca	4.37±0.31 Cb	7.26±1.22 Cab	7.85±0.74 Ca	3.98±0.37 Ca	3.81±0.39 Da	9.38±1.60 Ca

[a] Severe Water Deficit
[b] Moderate Water Deficit
[c] Absence of Water Deficit
Tukey's test at $P < 0.05$ level. Means followed by the same letter do not differ significantly ($P< 0.05$). Capital letters are for comparison of means among functional groups within each irrigation regime. Small letters are for comparison of means among irrigation regimes within each functional group.

Table S7. Compositions and relative abundance (%) of fungal functional groups (guild) inferred by FunGuild.

		Bulk soil			Rhizosphere			Root		
		SWD[a]	**MDW[b]**	**AWD[c]**	**SWD**	**MWD**	**AWD**	**SWD**	**MWD**	**AWD**
Pathotroph	Plant Pathogen	8.02 Aa	10.21 Aa	7.57 Aa	15.79 Aa	15.28 Aa	12.77 Aa	17.49 Aab	20.27 Aa	11.94 Ab
	Animal Pathogen	6.81 Aa	6.37 ABa	7.49 Aa	4.44 Ba	4.21 Ba	5.72 Ba	3.80 Ba	5.71 Ba	7.90 Ba
	Fungal Parasite	3.34 Ba	3.59 Ba	3.49 Aa	2.32 Ba	0.82 Ca	1.07 Ca	1.58 Ba	3.99 Ba	3.32 Da
	Lichen Parasite	6.35 Aa	5.95 ABa	5.07 Aa	5.25 Ba	3.89 Ba	4.42 Ba	3.39 Ba	4.54 Ba	5.24 Ca
Saprotroph	Soil Saprotroph	13.56 Ba	10.32 Ba	12.15 Ba	11.21 Ba	8.70 Ba	9.80 Ba	4.23 Ba	6.10 Ba	8.50 Ba
	Wood Saprotroph	7.41 Ca	8.82 Ba	8.50 Ba	7.42 BCa	5.34 BCb	10.16 Bab	10.93 ABa	8.63 Ba	10.22 Ba
	Dung Saprotroph	2.28 Da	2.90 Da	1.43 Da	3.27 Ca	4.60 BCa	3.63 Ca	6.15 Ba	1.56 Cb	3.14 Cab
	Plant Saprotroph	2.37 Db	2.62 Ca	3.77 Ca	3.29 Ca	1.86 Ca	2.64 Ca	3.01 Ba	6.44 Ba	5.04 Ca
	Undefined Saprotroph	19.34 Aa	17.60 Aa	20.65 Aa	20.44 Aa	24.66 Aa	21.64 Aa	27.97 Aa	18.77 Aa	18.33 Aa
Symbiotroph	Endophyte	21.24 Aa	19.44 Aa	20.68 Aa	16.31 Aa	14.82 Aa	16.17 Aa	7.74 Aa	9.79 Aa	15.25 Aa
	Arbuscular Mycorrhizal	4.12 Ba	5.05 Ba	1.43 Ba	5.89 Ba	8.56 Ba	4.15 Ba	9.74 Aa	10.38 Aa	1.74 Ab
Unassigned		5.16 a	7.10 a	7.77 a	4.37 b	7.26 ab	7.85 a	3.99 a	3.82 a	9.38 a

[a] Severe Water Deficit
[b] Moderate Water Deficit
[c] Absence of Water Deficit
Tukey's test at $P < 0.05$ level. Means followed by the same letter do not differ significantly ($P< 0.05$). Capital letters are for comparisons of means of functional groups within each trophic mode, irrigation regime and soil-plant compartment. Small letters are for comparison of means of each functional group among irrigation regimes within each soil-plant compartment.

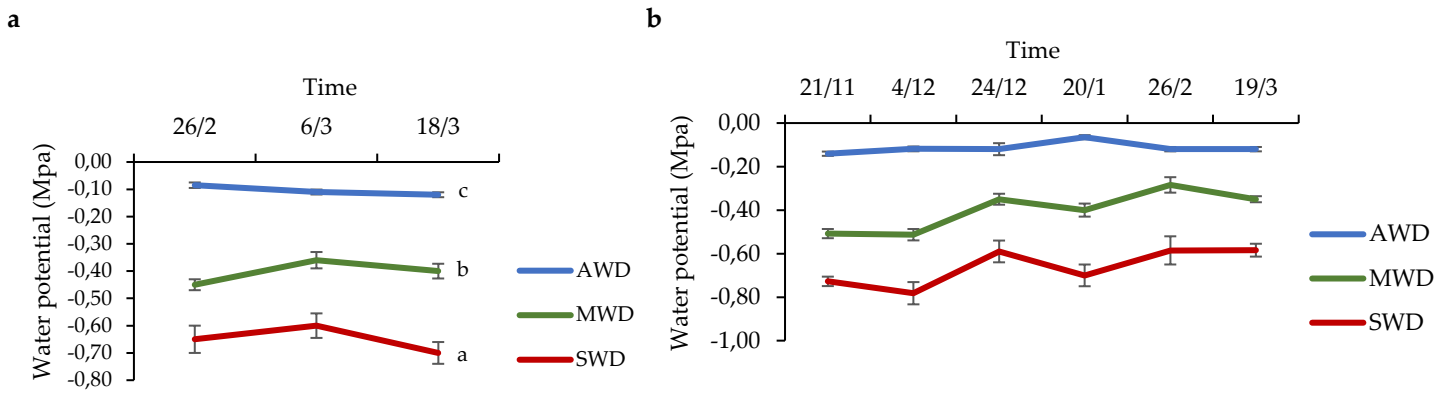

Figure S1. Predawn leaf water potential at the irrigation regimes. Absence of water deficit (AWD), moderate water deficit (MWD) and severe water deficit (SWD). (a) Growing season 2018-2019 and (b) 2019-2020. Tukey´s test at *p*-value < 0.05 level. Means followed by the same letter do not differ significantly.

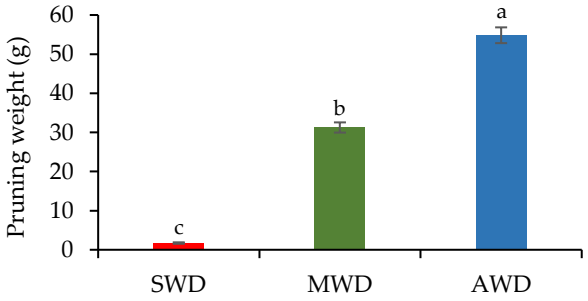

Figure S2. Pruning weight at the irrigation regimes. Absence of water deficit (AWD), moderate water deficit (MWD) and severe water deficit (SWD). Pruning made in winter 2020. Tukey´s test at p-value < 0.05 level. Means followed by the same letter do not differ significantly.

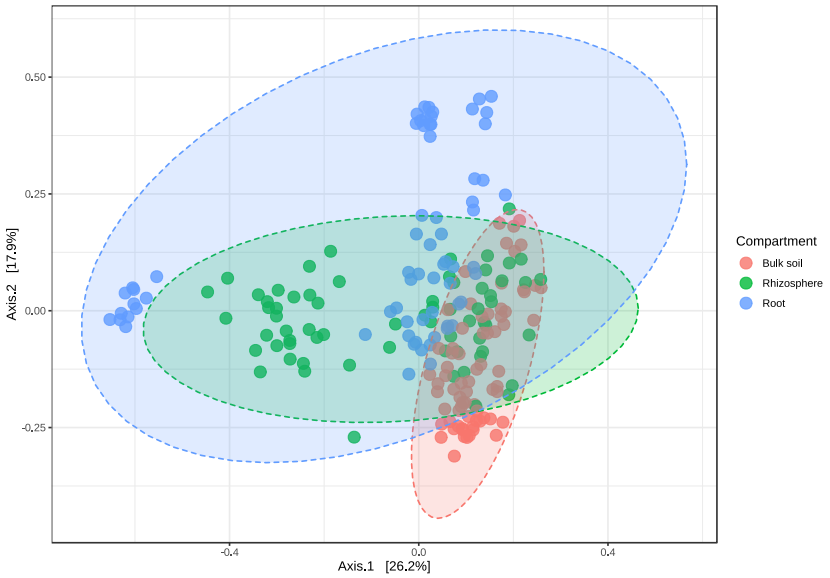

Figure S3. Principal Coordinate Analysis (PCoA) based on Bray Curtis dissimilarity metrics, showing the distance in the fungal communities among soil-plant compartments.

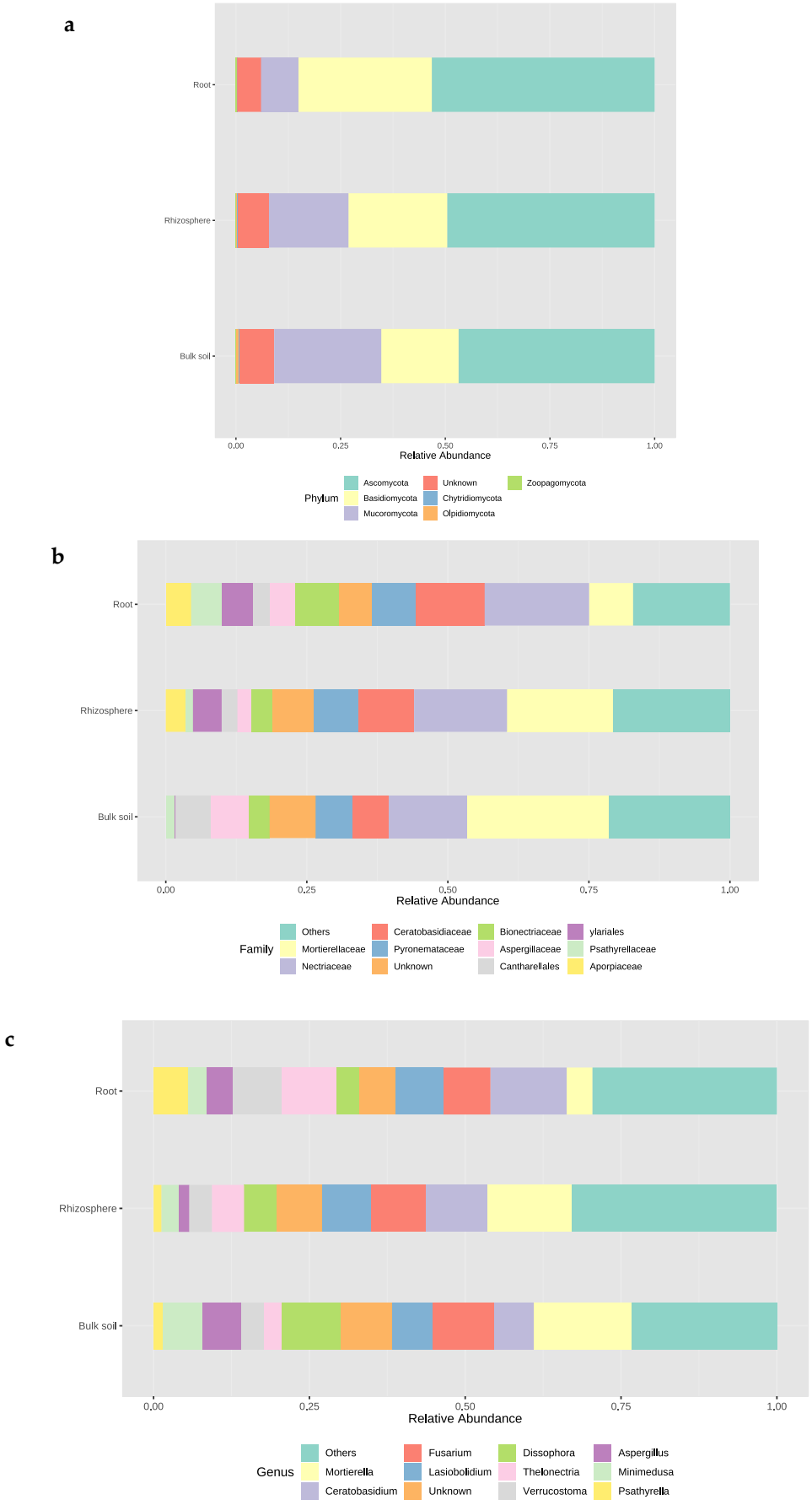

Figure S4. Relative abundance of the most abundant (a) phyla, (b) families and (c) genera in bulk-soil, rhizosphere and root samples

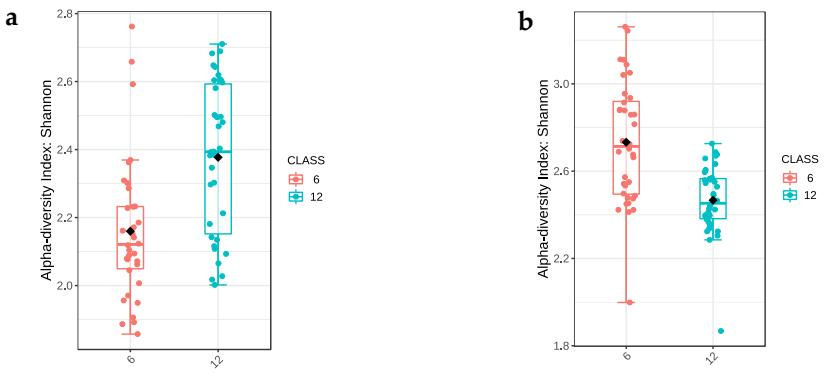

Figure S5. Boxplot illustrating the differences in Shannon diversity measure of the fungal communities in (a) root and (b) bulk soil between 6- and 12-month sampling time.

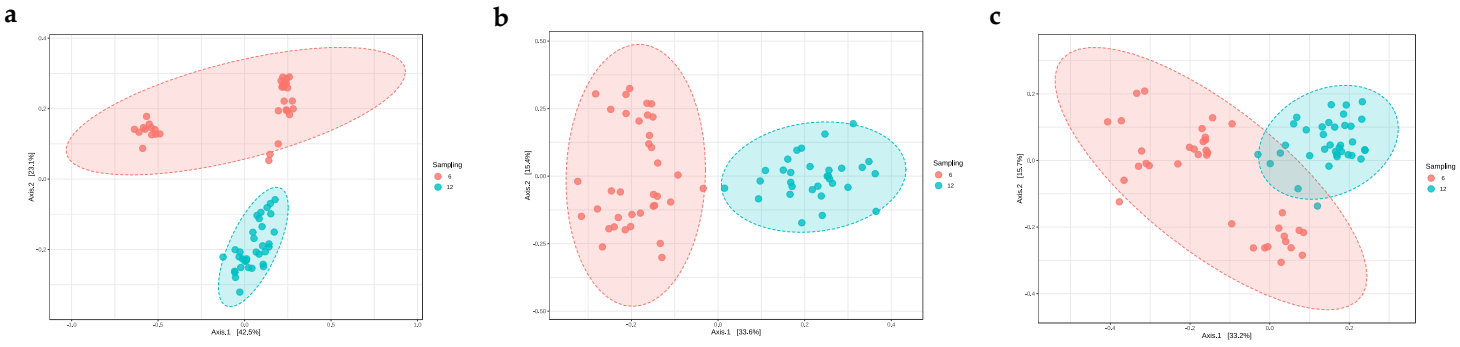

Figure S6. Principal Coordinate Analysis (PCoA) based on Bray Curtis dissimilarity metrics, showing the distance in the fungal communities in (a) root, (b) rhizosphere and (c) bulk soil between 6- and 12-month sampling time.

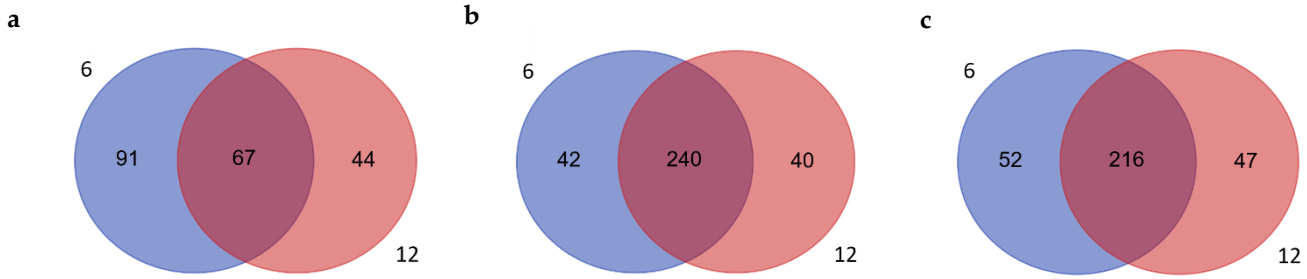

Figure S7. Venn diagram illustrating the overlap of the OTUs identified in the fungal microbiota between 6- and 12-month sampling time in the (a) root, (b) rhizosphere and (c) bulk-soil.

a

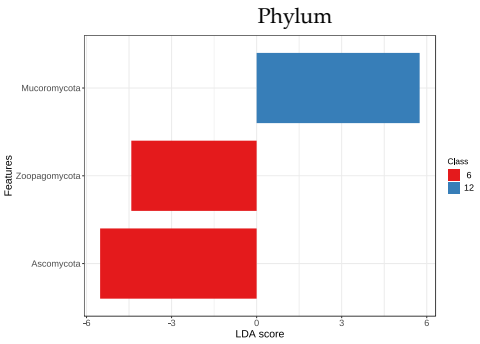
Phylum
Mucoromycota
Zoopagomycota
Ascomycota
Features
Class
6
12
-6
-3
0
3
6
LDA score

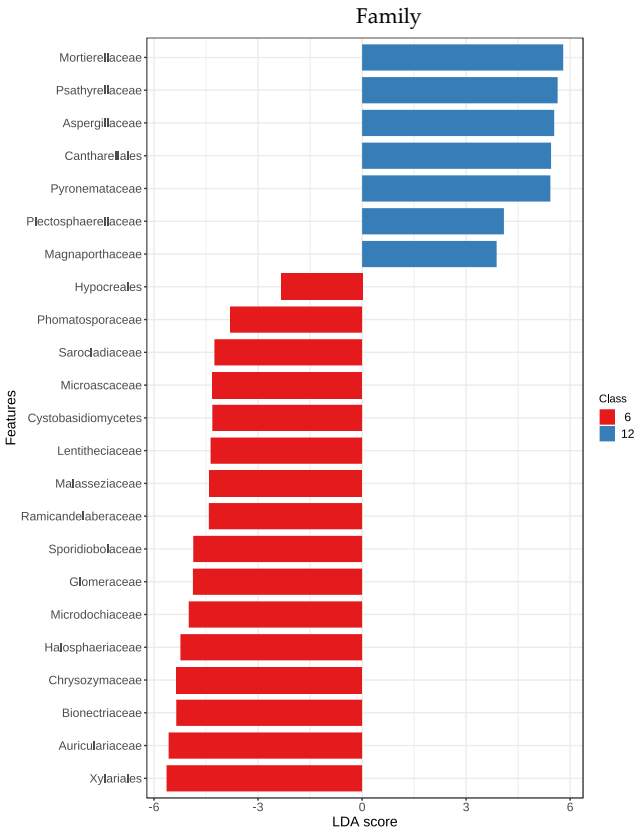
Family
Mortierellaceae
Psathyrellaceae
Aspergillaceae
Cantharellales
Pyronemataceae
Plectosphaerellaceae
Magnaporthaceae
Hypocreales
Phomatosporaceae
Sarocladiaceae
Microascaceae
Cystobasidiomycetes
Lentitheciaceae
Malasseziaceae
Ramicandelaberaceae
Sporidiobolaceae
Glomeraceae
Microdochiaceae
Halosphaeriaceae
Chrysozymaceae
Bionectriaceae
Auriculariaceae
Xylariales
Features
Class
6
12
-6
-3
0
3
6
LDA score

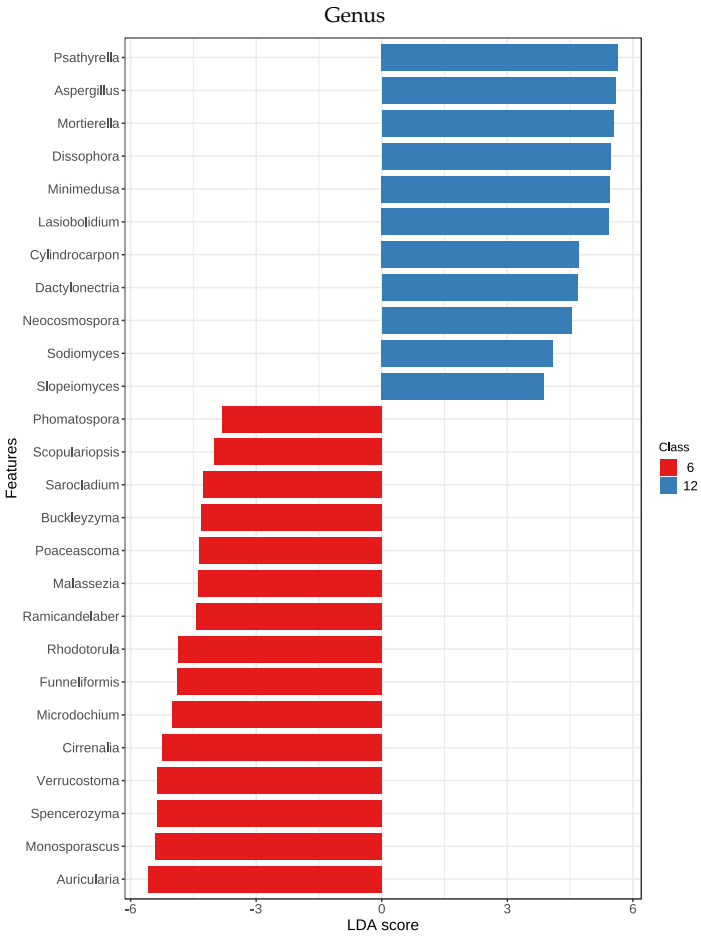
Genus
Psathyrella
Aspergillus
Mortierella
Dissophora
Minimedusa
Lasiobolidium
Cylindrocarpon
Dactylonectria
Neocosmospora
Sodiomyces
Slopeiomyces
Phomatospora
Scopulariopsis
Sarocladium
Buckleyzyma
Poaceascoma
Malassezia
Ramicandelaber
Rhodotorula
Funneliformis
Microdochium
Cirrenalia
Verrucostoma
Spencerozyma
Monosporascus
Auricularia
Features
Class
6
12
-6
-3
0
3
6
LDA score

b

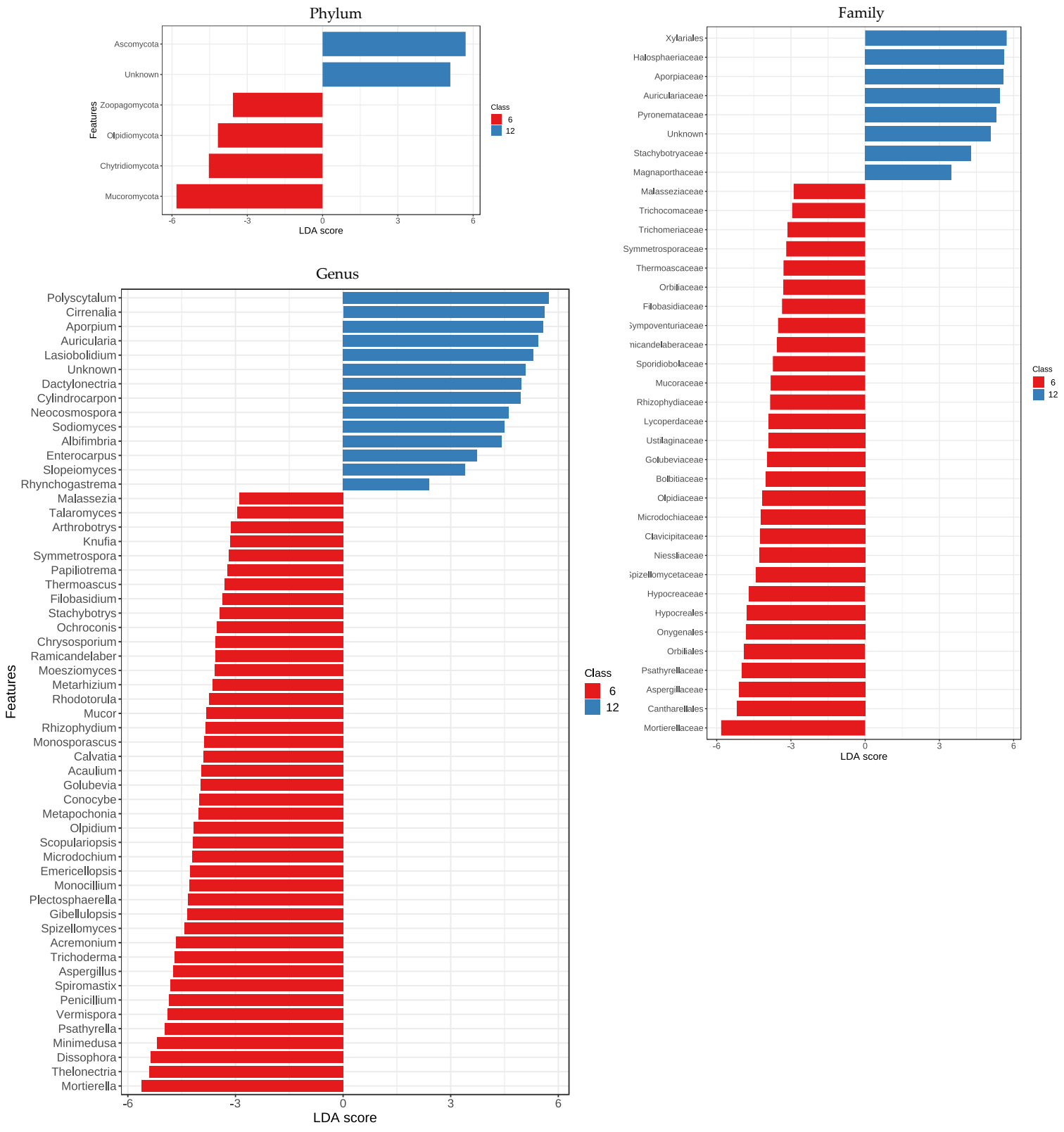
Phylum
Ascomycota
Unknown
Zoopagomycota
Olpidiomycota
Chytridiomycota
Mucoromycota
Features
-6
-3
0
3
6
LDA score
Class
6
12
Family
Xylariales
Halosphaeriaceae
Aporpiaceae
Auriculariaceae
Pyronemataceae
Unknown
Stachybotryaceae
Magnaporthaceae
Malasseziaceae
Trichocomaceae
Trichomeriaceae
Symmetrosporaceae
Thermoascaceae
Orbiliaceae
Filobasidiaceae
Mucoraceae
Rhizophydiaceae
Lycoperdaceae
Ustilaginaceae
Golubeviaceae
Bolbitiaceae
Olpidiaceae
Microdochiaceae
Clavicipitaceae
Niessliaceae
Hypocreaceae
Hypocreales
Onygenales
Orbiliales
Psathyrellaceae
Aspergillaceae
Cantharellales
Mortierellaceae
-6
-3
0
3
6
LDA score
Class
6
12
Genus
Polyscytalum
Cirrenalia
Aporpium
Auricularia
Lasiobolidium
Unknown
Dactylonectria
Cylindrocarpon
Neocosmospora
Sodiomyces
Albifimbria
Enterocarpus
Slopeiomyces
Rhynchogastrema
Malassezia
Talaromyces
Arthrobotrys
Knufia
Symmetrospora
Papiliotrema
Thermoascus
Filobasidium
Stachybotrys
Ochroconis
Chrysosporium
Ramicandelaber
Moesziomyces
Metarhizium
Rhodotorula
Mucor
Rhizophydium
Monosporascus
Calvatia
Acaulium
Golubevia
Conocybe
Metapochonia
Olpidium
Scopulariopsis
Microdochium
Emericellopsis
Monocillium
Plectosphaerella
Gibellulopsis
Spizellomyces
Acremonium
Trichoderma
Aspergillus
Spiromastix
Penicillium
Vermispora
Psathyrella
Minimedusa
Dissophora
Thelonectria
Mortierella
Features
-6
-3
0
3
6
LDA score
Class
6
12

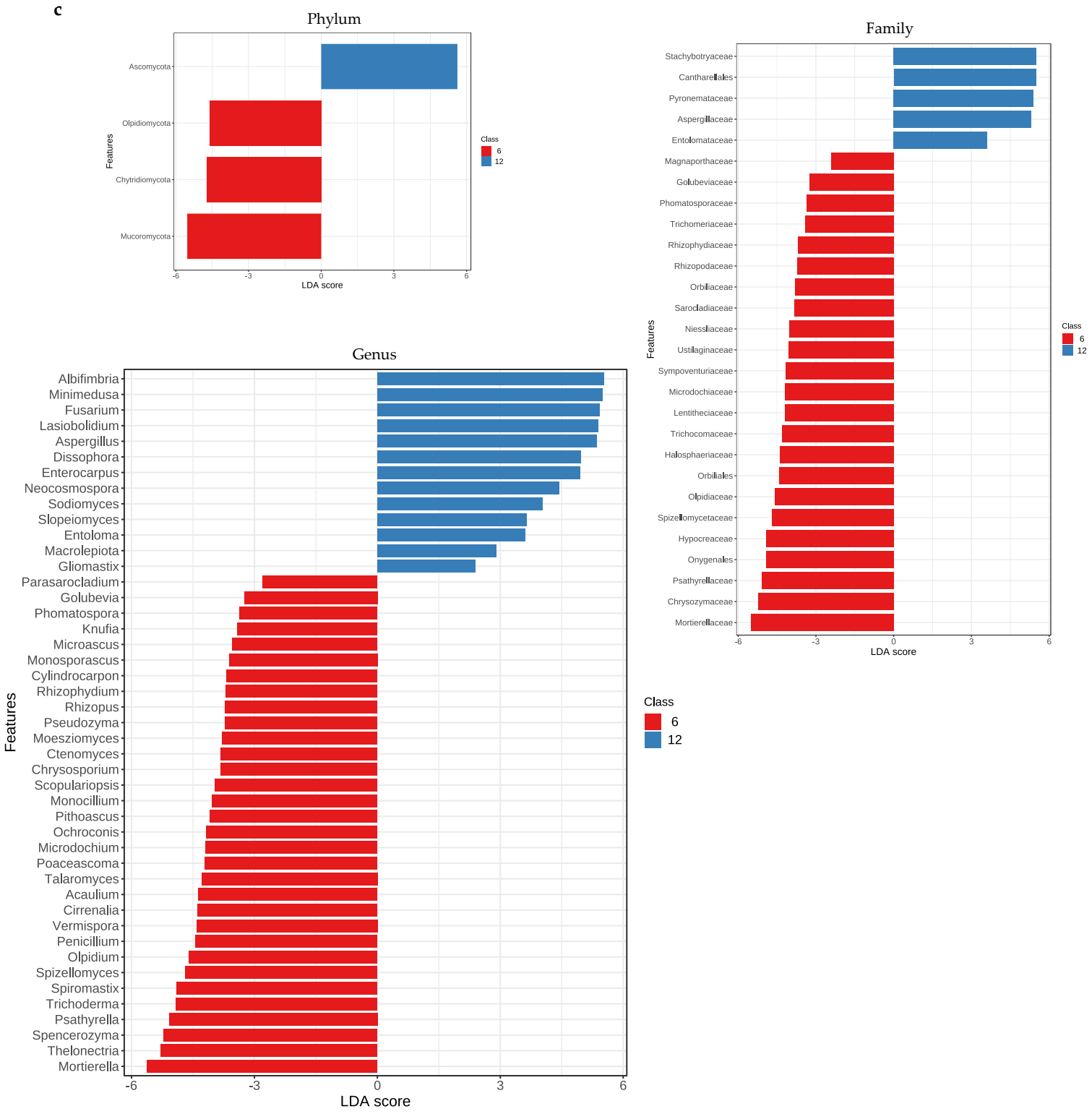

Figure S8. Bar graph of LEfSe showing the most differentially taxa between 6- and 12- month sampling time in (a) root, (b) rhizosphere and (c) bulk-soil. Only taxa meeting an LDA significant threshold >2 are shown.

a

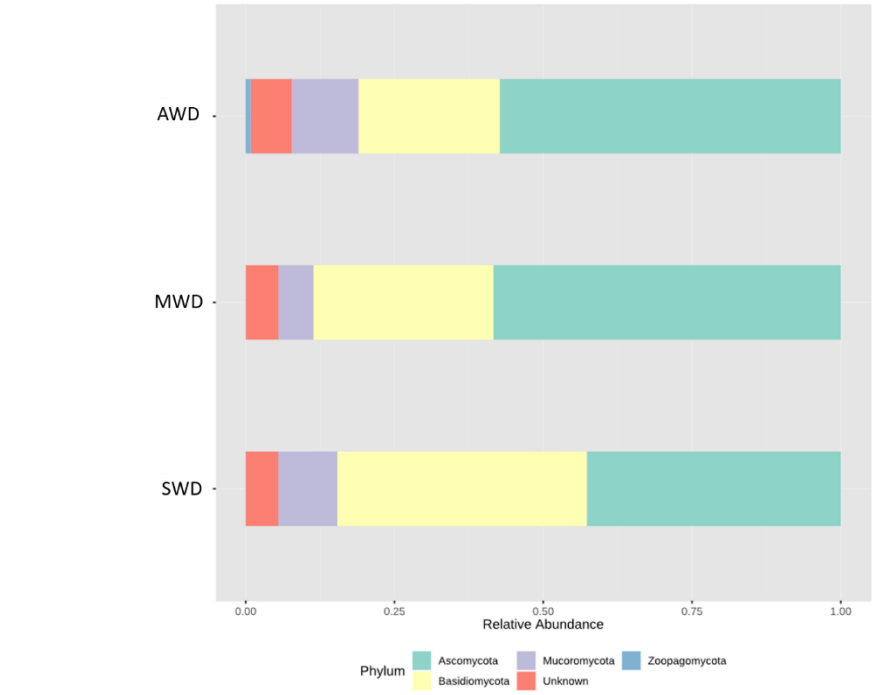
AWD
MWD
SWD
0.00
0.25
0.50
0.75
1.00
Relative Abundance
Phylum
Ascomycota
Basidiomycota
Mucoromycota
Unknown
Zoopagomycota

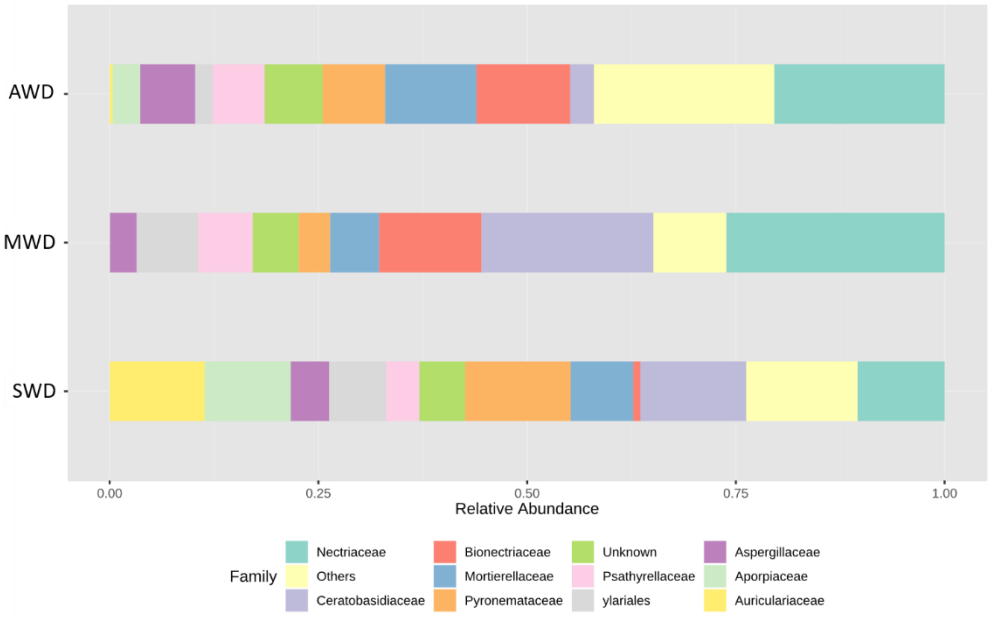
AWD
MWD
SWD
0.00
0.25
0.50
0.75
1.00
Relative Abundance
Family
Nectriaceae
Others
Ceratobasidiaceae
Bionectriaceae
Mortierellaceae
Pyronemataceae
Unknown
Psathyrellaceae
ylariales
Aspergillaceae
Aporpiaceae
Auriculariaceae

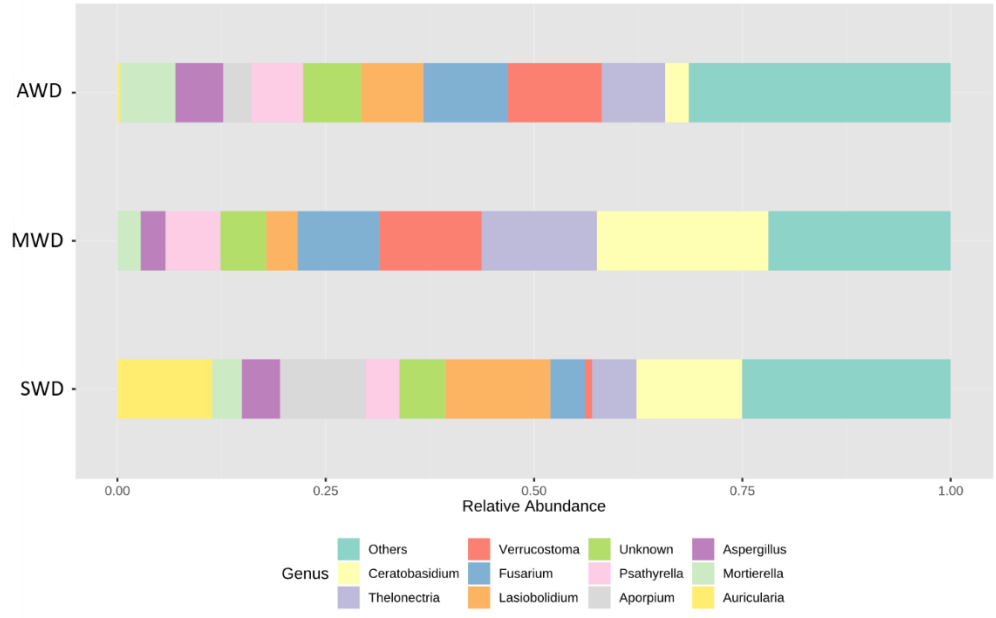
AWD
MWD
SWD
0.00
0.25
0.50
0.75
1.00
Relative Abundance
Genus
Others
Ceratobasidium
Thelonectria
Verrucostoma
Fusarium
Lasiobolidium
Unknown
Psathyrella
Aporpium
Aspergillus
Mortierella
Auricularia

b

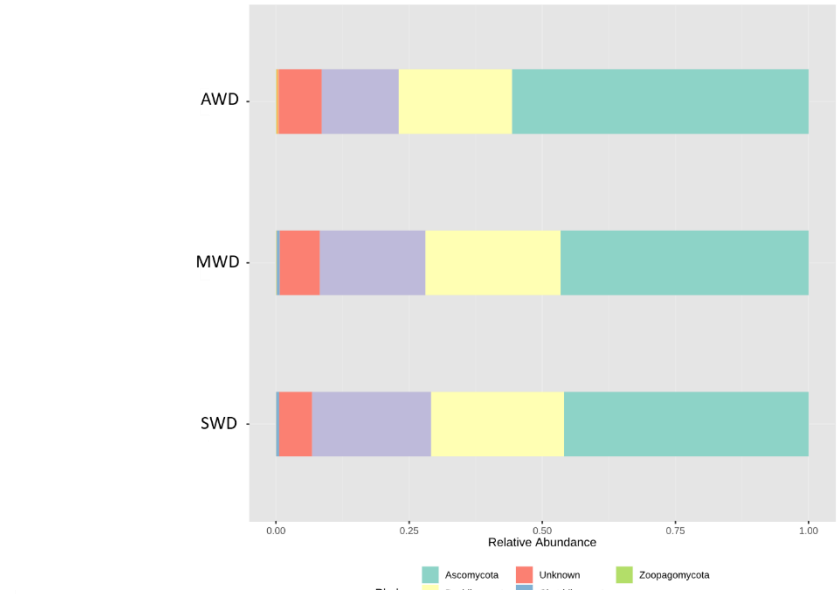
AWD
MWD
SWD
0.00
0.25
0.50
0.75
1.00
Relative Abundance
Ascomycota
Unknown
Zoopagomycota

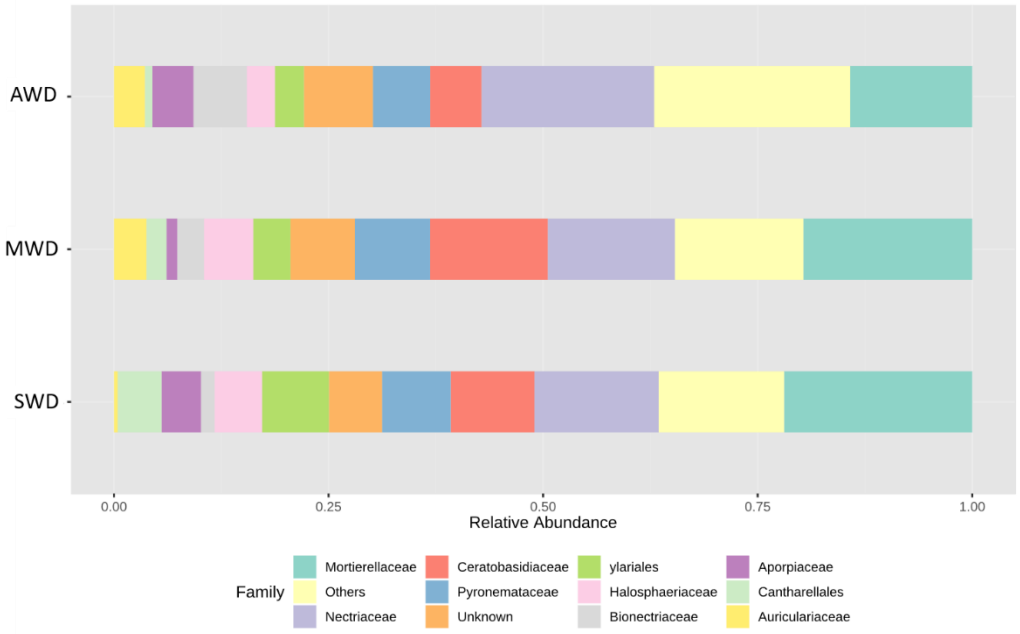
AWD
MWD
SWD
0.00
0.25
0.50
0.75
1.00
Relative Abundance
Family
Mortierellaceae
Others
Nectriaceae
Ceratobasidiaceae
Pyronemataceae
Unknown
ylariales
Halosphaeriaceae
Bionectriaceae
Aporpiaceae
Cantharellales
Auriculariaceae

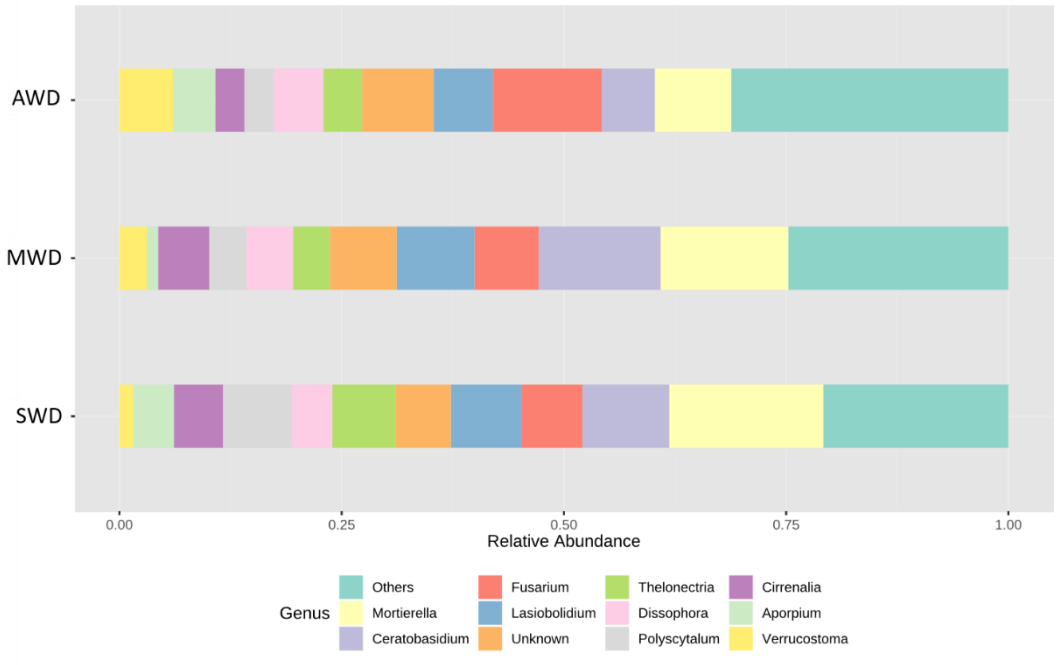
AWD
MWD
SWD
0.00
0.25
0.50
0.75
1.00
Relative Abundance
Genus
Others
Mortierella
Ceratobasidium
Fusarium
Lasiobolidium
Unknown
Thelonectria
Dissophora
Polyscytalum
Cirrenalia
Aporpium
Verrucostoma

c

Figure S9. Relative abundance of the most abundant taxa in (a) root, (b) rhizosphere and (c) bulk-soil in each watering regime.

a

Root: Phylum at 6-month sampling

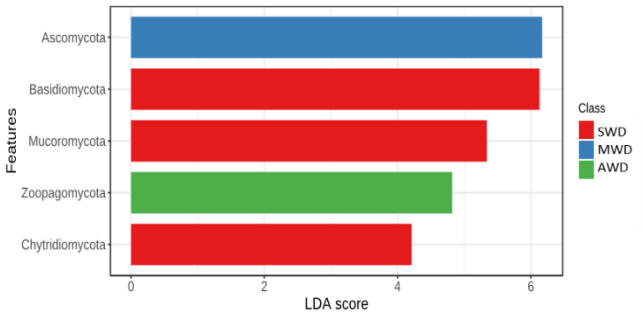

Root: Phylum at 12-month sampling

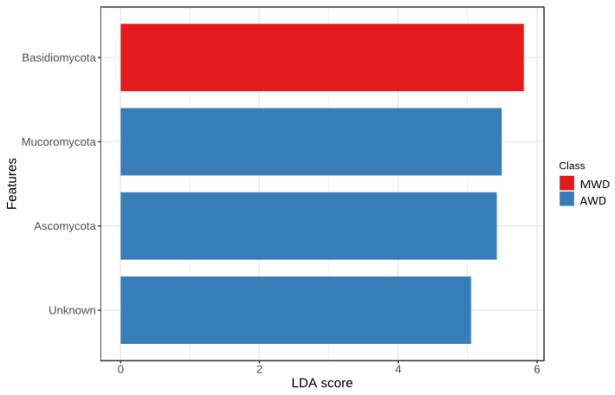

Root: Family at 6-month sampling

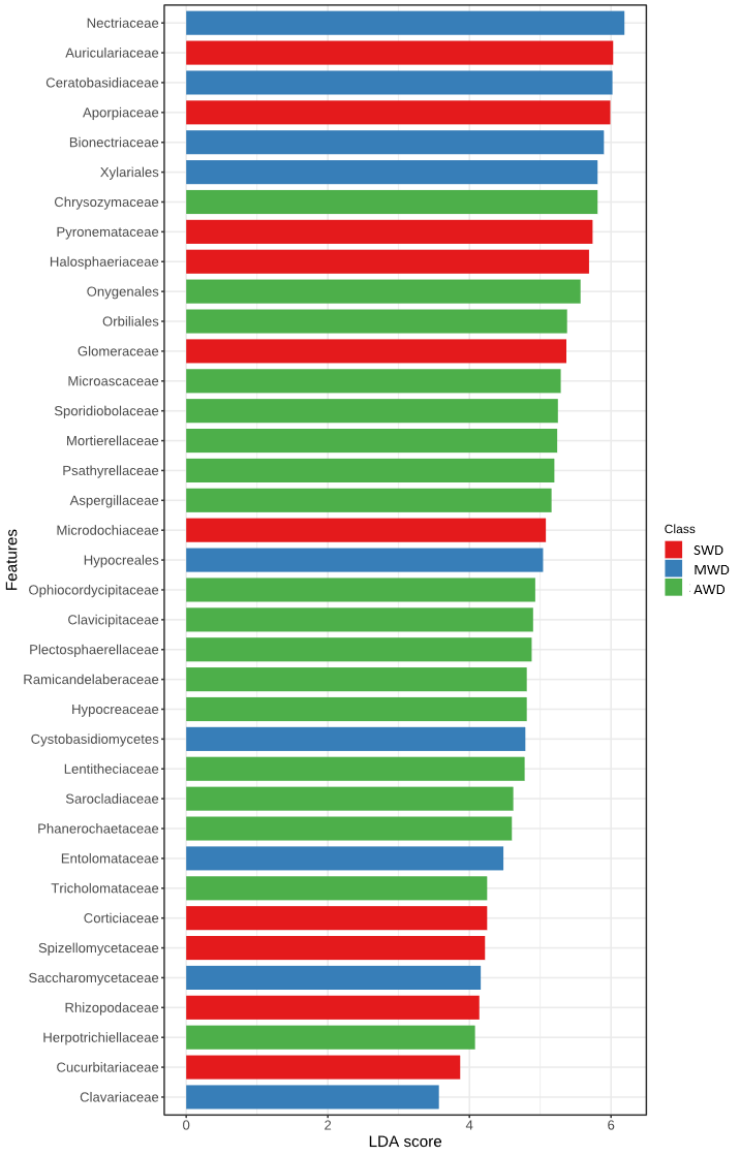

Root: Family at 12-month sampling

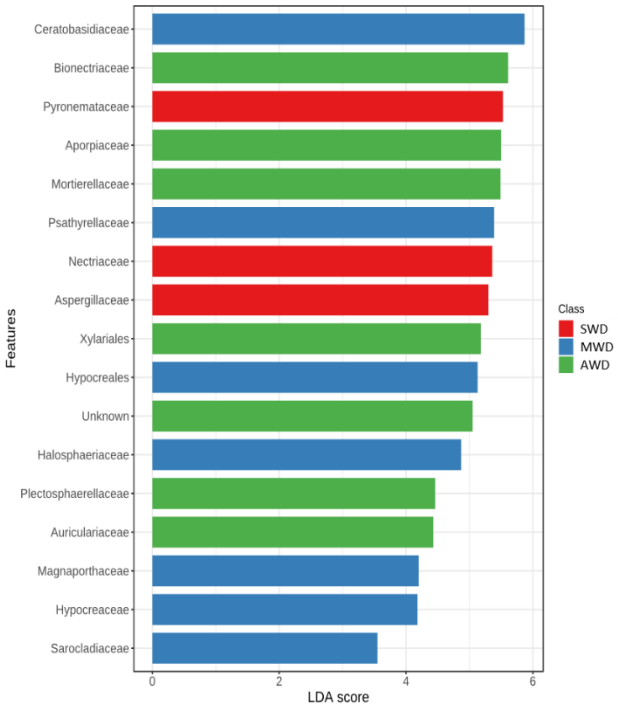

Root: Genus at 6-month sampling

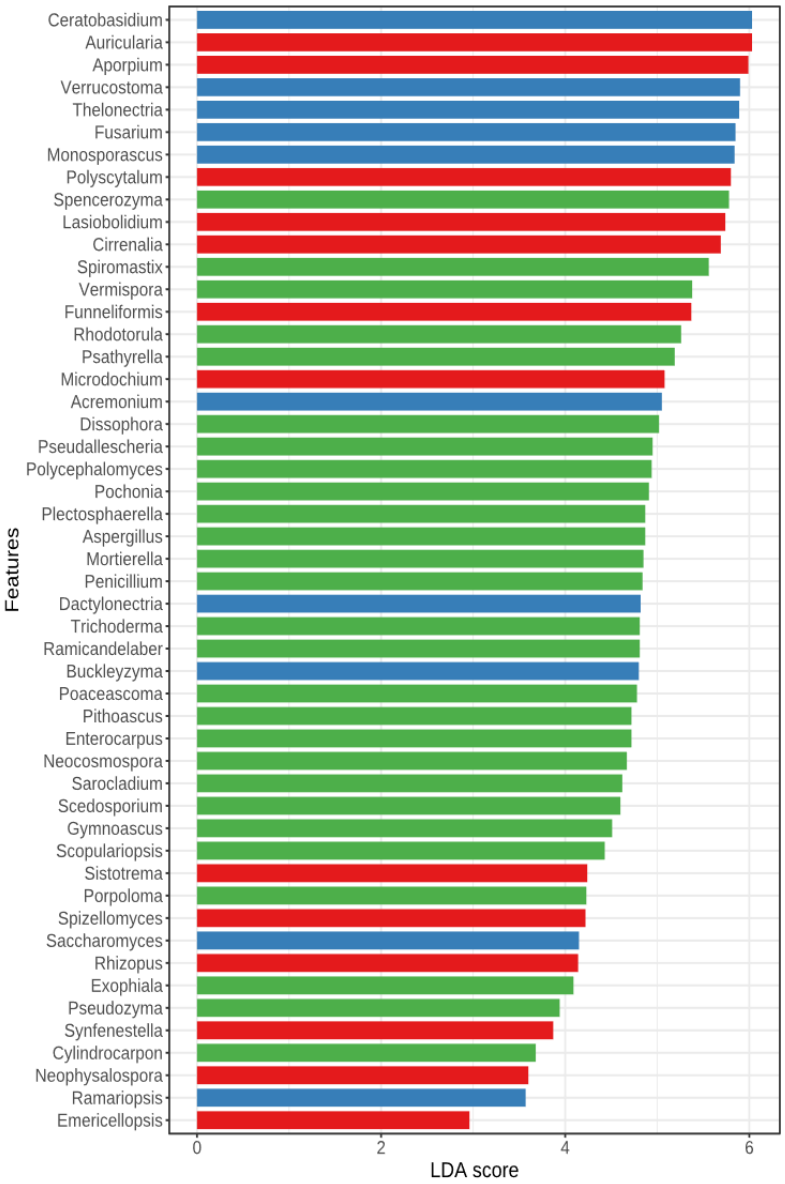

Root: Genus at 12-month sampling

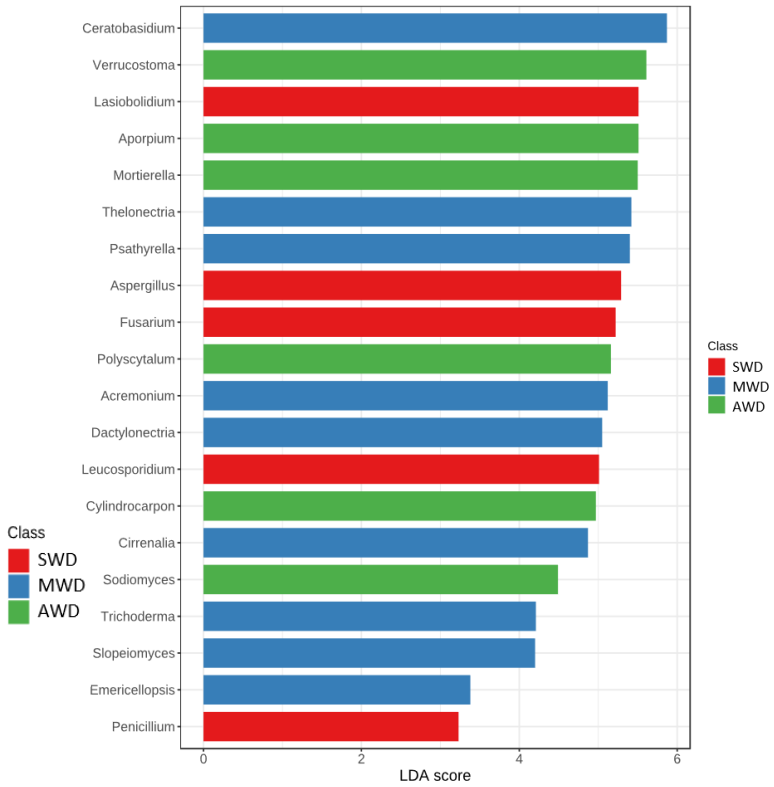

b

Rhizosphere: Phylum

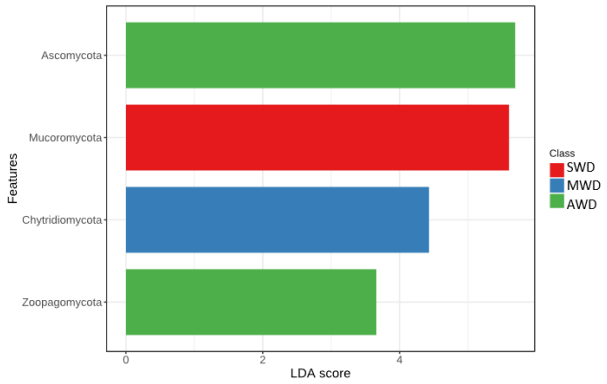

Rhizosphere: Family

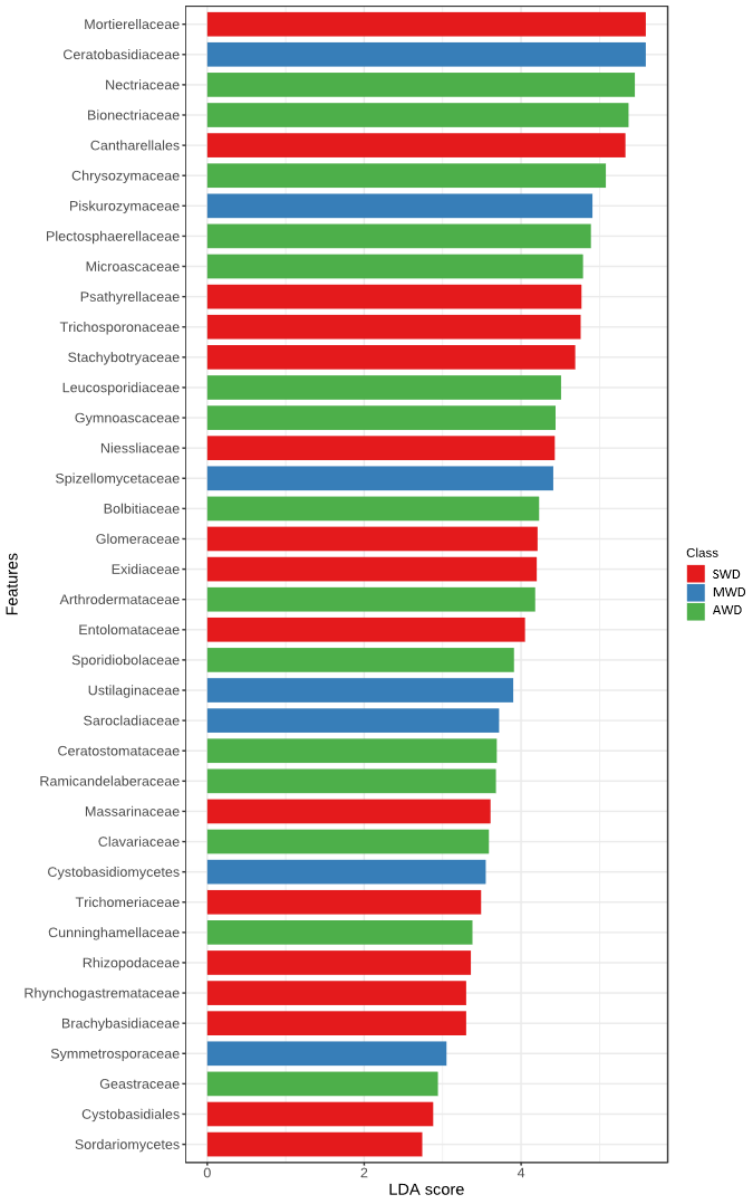

Rhizosphere: Genus

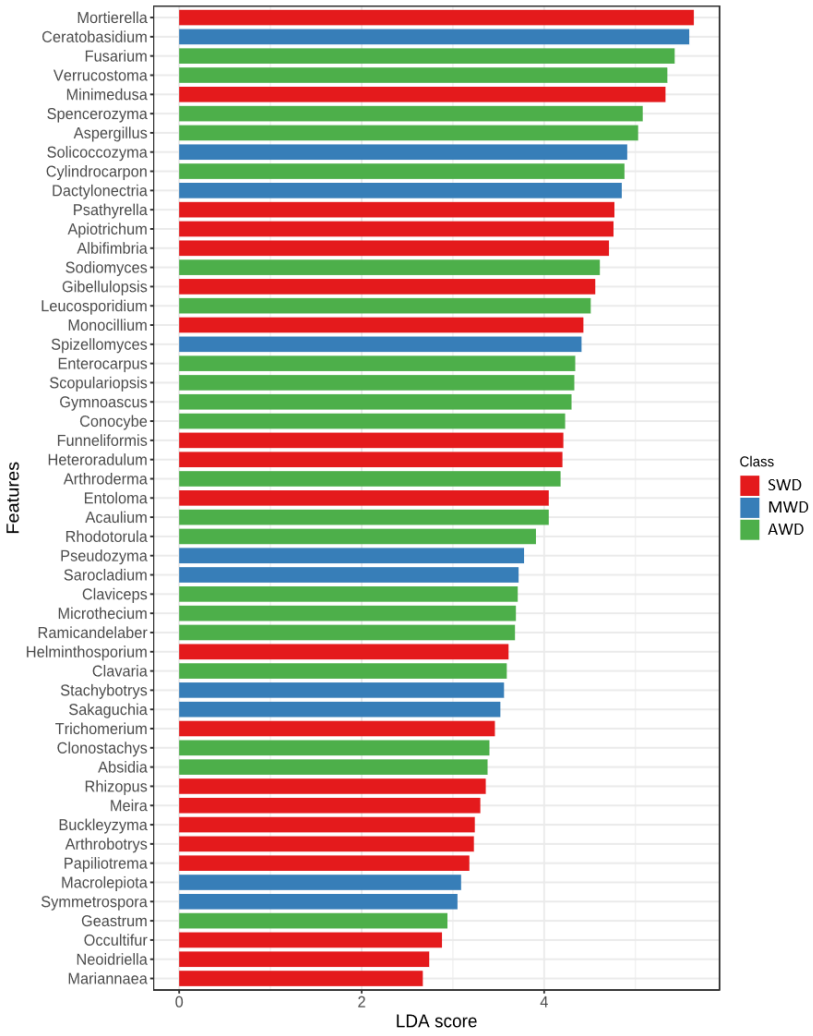

c

Bulk-soil: Phyla at 6-month sampling

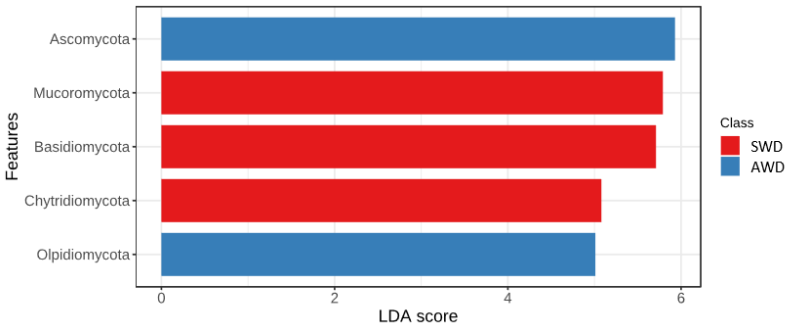

Bulk-soil: Phyla at 12-month sampling

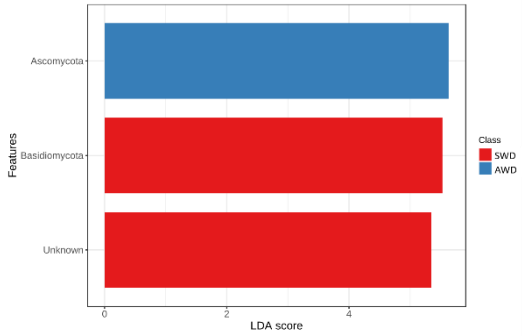

Bulk-soil: Family at 6-month sampling

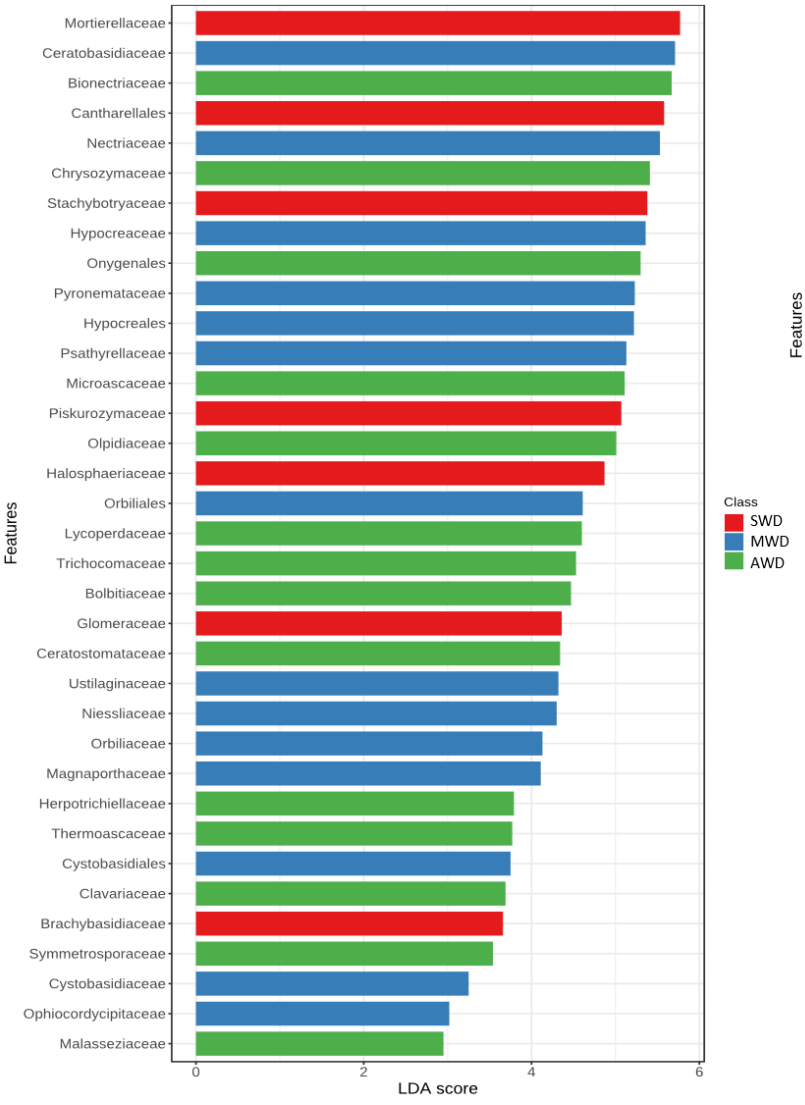

Bulk-soil: Family at 12-month sampling

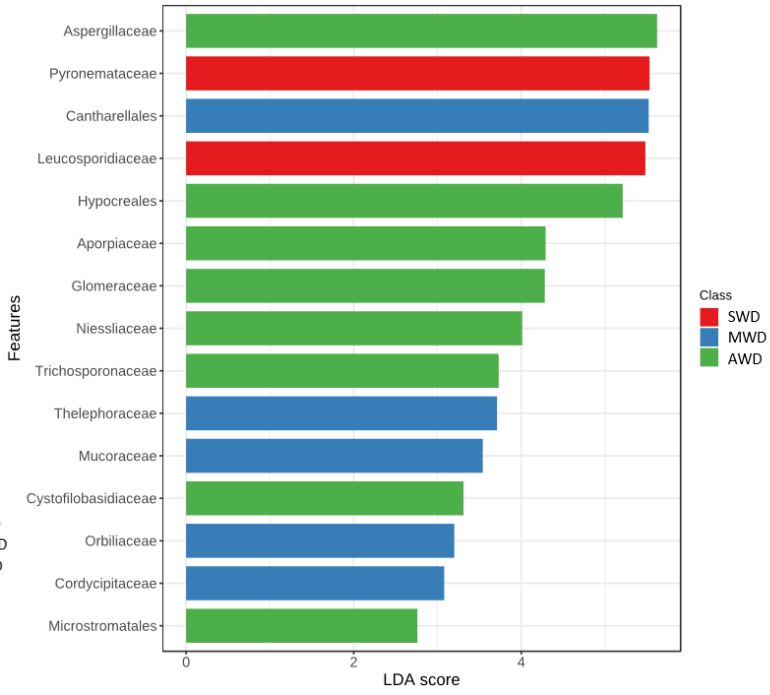

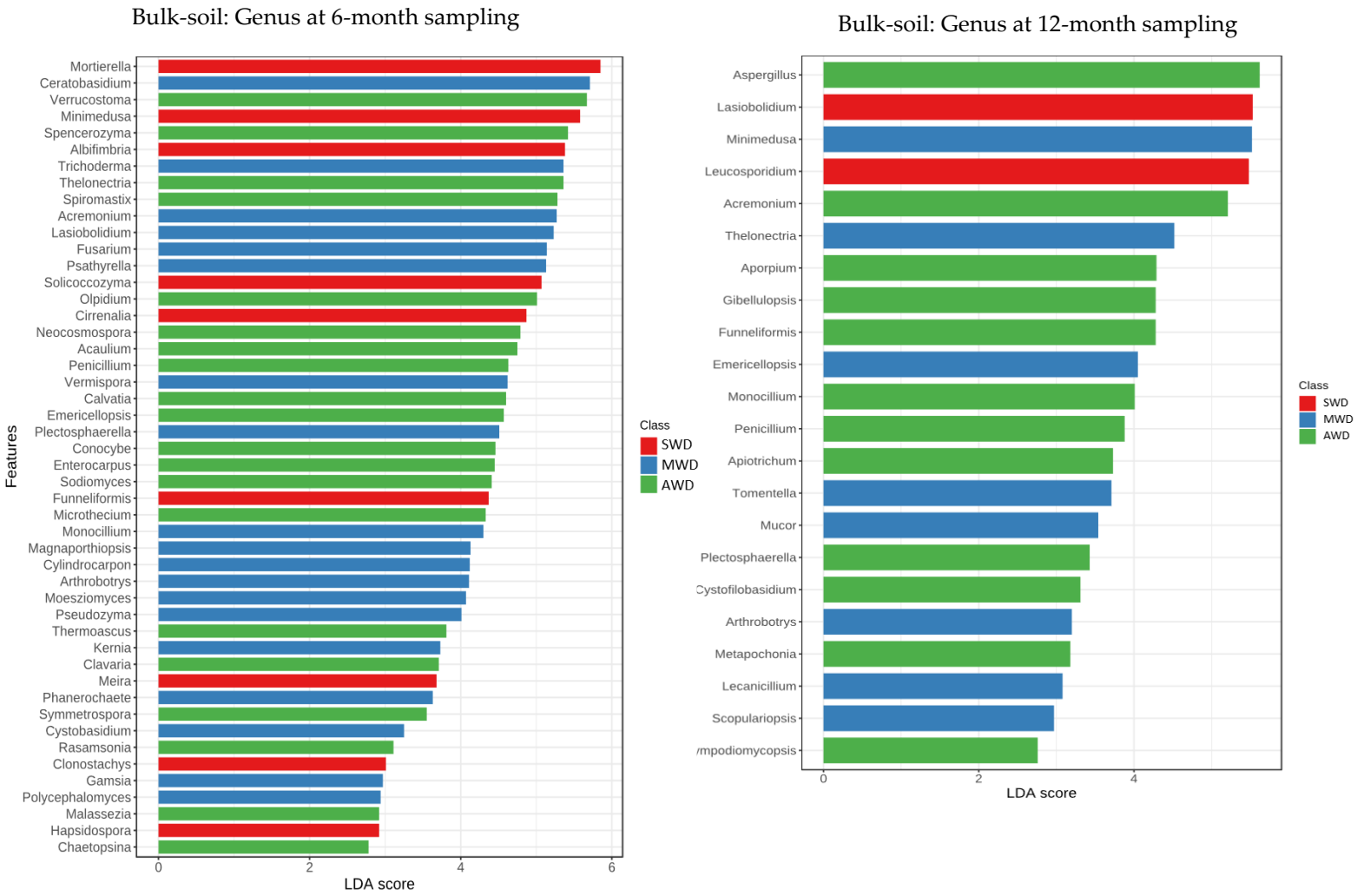

Figure S10. Bar graph of LEfSe showing the most differentially abundant taxa among the irrigation regimes in each sampling time in (a) root, (b) rhizosphere and (c) bulk-soil. Only taxa meeting an LDA significant threshold >2 are shown.

ARTÍCULO 4

Four *Diaporthe* species associated with grapevine wood in nursery plants and commercial vineyards in Uruguay

MARÍA JULIA CARBONE, ROSSANA REYNA, VICTORIA MOREIRA, PEDRO MONDINO, SANDRA ALANIZ

Departamento de Protección Vegetal, Facultad de Agronomía, Universidad de la República

A enviar a *Plant Pathology*

Four *Diaporthe* species associated with grapevine wood in nursery plants and commercial vineyards in Uruguay

ABSTRACT

Diaporthe species cause Diaporthe dieback disease in many grape-growing countries causing general vine decline, shoot dieback and dead spur with perennial cankers and internal trunk necrosis. These pathogens are also the causal agents of Phomopsis cane and leaf spot, a common foliar disease affecting grapevine around the world. In this study, we specifically investigated the presence of *Diaporthe* spp. colonizing the internal wood of grapevine. A collection of 59 *Diaporthe* isolates were obtained from symptomatic and asymptomatic wood samples of commercial grapevines (nine cultivars) and nursery vines (eleven materials including scion and rootstocks cuttings, and grafted plants) and were characterized based on DNA phylogenetic analysis, phenotypical characteristics, and pathogenicity test. *Diaporthe ampelina* was the most frequent species identified (86.4%), followed by *D. foeniculina* (8.5%), *D. eres* (3.4%) and *D. terebinthifolii* (1.7%). *Diaporthe ampelina* was the only species found causing symptoms of Diaporthe dieback in field vines and was also isolated from samples with internal necrosis in association with external Phomopsis cane and leaf spot symptoms, whereas the other species were isolated solely from nursery material. The pathogenicity of all species was confirmed, with *D. ampelina* being the most virulent. Further studies are needed to understand the epidemiology of Diaporthe dieback to design a management programme to prevent the disease development.

Keywords: *Diaporthe ampelina*, *Diaporthe eres*, *Diaporthe foeniculina*, *Diaporthe terebinthifolii*, Diaporthe dieback, *Vitis vinifera*

1. INTRODUCTION

Viticulture is an important and traditional activity in Uruguay. Currently, grapevines are the second most important fruit crop in the country in terms of cultivated area. The wine sector comprises 5848 ha with an annual production of approximately 100,000 ton, mostly destined for wine production (IANVI, 2022). Several fungal diseases affect the aerial part of the grapevine due to the humid climate of the country (Alaniz et al., 2016). In addition, since the early 2000s, grapevine trunk diseases (GTDs) have become one of the most serious problems for local winegrowers.

GTDs are a complex of diseases caused by a high diversity of pathogenic fungi that colonize wood of perennial organs and are widespread in almost all grape-growing regions of the world (Mondello et al., 2018). Internally, infected vines show wood necrosis, wood discolorations and dark vascular streaks. Externally, GTDs cause a variety of symptoms which may vary according to the disease, including reduced vigour, delayed or absent sprouting, chlorotic foliage with necrotic margin, leaves showing multiple discolorations, wilting, dead arm or eventually death of plant (Mondello et al., 2018). The consequences are loss of productivity, reduced longevity of vineyards and increment in management costs, generating significant economic losses (Gramaje and Armengol, 2011).

In Uruguay, several research has shown the occurrence of Botryosphaeria dieback, Esca, Petri disease and Black foot disease (GTDs) affecting commercial vineyards (Abreo et al., 2010, 2011, 2013). In addition, a recent study revealed that Botryosphaeria dieback, Petri disease and Black foot were present in local nursery vines (Carbone et al., 2022). Moreover, that study showed that nursery vines were also infected by *Diaporthe* spp., the causal agent of Diaporthe dieback (DD) (Carbone et al., 2022).

Diaporthe dieback was proposed by Úrbez-Torres et al. (2013) to be included in the GTDs complex after providing strong evidence about the role of *D. ampelina* (syn. *Phomopsis viticola*) as a canker-causing organism in California. Symptoms are characterized by a general vine decline, shoot dieback and dead spurs with perennial cankers and vascular discoloration, like those caused by species of Botryosphaeriaceae and *Eutypa lata*, causal agents of the GTDs Botryosphaeria dieback and Eutypa dieback, respectively (Baumgartner et al., 2013; Úrbez-Torres et al., 2013).

Previously, *D. ampelina* had been found associated with grapevine cankers in Texas (Úrbez-Torres et al., 2009), Arkansas and Missouri (Úrbez-Torres et al., 2012), and with other *Diaporthe* species in Croatia (Kaliterna et al., 2012) and in the eastern region of North America (Baumgartner et al., 2013). Several *Diaporthe* species were then also associated with that symptoms in Chile (Larach et al., 2021), China (Dissanayake et al., 2015; Manawasinghe et al., 2019), Europe (Guarnaccia et al., 2018; Makris et al., 2022), North America (Lawrence et al., 2015), South Africa (Lesuthu et al., 2019) and Turkey (Akgül and Nawaz Awan, 2022), being *D. ampelina* and *D. eres* the most commonly species found (Úrbez-Torres et al., 2009; Kaliterna et al., 2012; Úrbez-Torres et al., 2013; Lawrence et al., 2015; Guarnaccia et al., 2018; Dissanayake et al., 2015; Manawasinghe et al., 2019).

The genus status of *Diaporthe* has been deeply revised in recent years (Udayanga et al. 2014; Hilário et al., 2021) and due to the abolition of dual nomenclature for fungi, *Diaporthe* has been retained over *Phomopsis* following the recommendation of Rossman et al., (2015), as it was introduced first and represents most species. *Diaporthe* species are well-known as endophytes in asymptomatic plants, saprobes on decaying tissues and plant pathogens of a wide range of hosts worldwide (Gao et al., 2017; Guarnaccia et al., 2018). In Uruguay, *Diaporthe* species have been found associated with wood disease symptoms in deciduous fruits (Sessa et al., 2017) and causing stem canker in sunflower (Moschini et al., 2019) and soybean (Mena et al., 2020). In grapevine, *Diaporthe ampelina* was found in field vines with symptoms of canker, although its role as a canker causing organism was discarded by Abreo (2011). In addition, this species is known to cause Phomopsis cane and leaf spot disease, which is widespread in the wine-growing region of the country (Alaniz et al., 2016).

Phomopsis cane and leaf spot of grape is a common disease in many grape-growing regions around the world caused by *D. ampelina* (Nita et al., 2006), which can affect all green parts of the vine during spring. Symptoms consist of black to brown lesions on the basal internodes of shoots, often accompanied by elongated cracks in the epidermal layers. After lignification, affected canes remain bleached. The lower leaves of the shoots show small dark brown spots with a yellowish halo, whereas in the cluster, causes necrosis of rachis and fruit rot, often leading to cluster drop (Nita et al., 2006). Although both diseases are cause by the same pathogen, the relationship between

Phomopsis cane and leaf spot and DD is not yet well understood (Baumgartner et al., 2013).

Owing to *Diaporthe* species were found colonizing the internal wood of symptomatic (internal vascular necrosis) and asymptomatic grapevine nursery plants (Carbone et al., 2022), these materials may be considered as a source of inoculum of these pathogens for new commercial plantings. Based on this finding, the objectives of this study were: (i) to evaluate the presence of *Diaporthe* spp. colonizing internal wood in field vines; (ii) to characterize a collection of *Diaporthe* isolates collected from symptomatic (internal vascular necrosis, cankers) and asymptomatic wood samples from commercial grapevines and nursery materials, based on DNA phylogenetic analysis, phenotypical characteristics, and pathogenicity test.

2. MATERIALS AND METHODS

2.1 Sampling and fungal isolation

Vineyards were extensively surveyed for DD symptoms in 2021 including 17 sites located in the south of Uruguay (Canelones, Montevideo, Maldonado, and San José departments), the main region of grapevine production. Wood samples from cordons or trunks showing perennial cankers in declining vines and canes from vines showing bleached canes with longitudinal lesions, the typical symptoms of Phomopsis cane and leaf spot, were collected from Cabernet Sauvignon, Gewürztraminer, Marselan, Merlot, Moscatel, Perlón, Sauvignon Blanc, Tannat and Ugni Blanc cultivars. Samples were surface sterilized by soaking each portion in 95% ethanol for 1 s followed by flaming. The bark was removed, and cross and longitudinal cuts were made to reveal internal necrosis and/or symptoms of vascular browning. Seven pieces of wood, approx. 5 mm long x 1 mm wide, were taken from the margin between necrotic and apparently healthy tissues, using a sterile scalpel, and plated onto potato dextrose agar (PDA) (Oxoid Ltd.) supplemented with 0.4 g L−1 of streptomycin sulphate (PDAS) (Sigma-Aldrich). From samples with external Phomopsis cane and leaf spot disease symptoms but without internally associated necrosis, pieces of wood apparently healthy were taken at random after removing the bark and processed as indicated above.

Isolation plates were incubated at 25°C in darkness until fungal colonies were observed. Fungal colonies with Diaporthe spp. characteristics (colony white and cottony, with an irregular margin and concentric rings) were subculture and purified by

transferring hyphal tips to fresh PDA plates (Baumgartner et al., 2013). Plates were incubated at 20°C under near ultraviolet (UV) light in 12 h light-dark cycles for 4 weeks to stimulate sporulation of Diaporthe spp. (spherical, black pycnidia scattered throughout the colony with exudation of cream-colored droplets of alfa and/or beta conidia) (Baumgartner et al., 2013; Guarnaccia et al., 2018; Úrbez-Torres et al., 2013). Isolates with confirmed Diaporthe spp. characteristics were stored on sterile colonized filter papers at -20°C and deposited in the fungal culture collection of the Department of Plant Protection, Faculty of Agronomy, University of the Republic, Uruguay. In addition, 28 isolates obtained from symptomatic (internal vascular necrosis) and asymptomatic propagation material (including scion and rootstocks cuttings, and grafted plants) from a local nursery in 2018 and 2019 (Carbone et al., 2022) were included in this study (Table 1).

2.2 Molecular identification

The commercial Quick-DNATM Fungal/Bacterial Miniprep Kit (ZymoResearch) was used to extract total genomic DNA from 10-day-old pure cultures grown on PDA at 25°C in the dark. Identification of Diaporthe spp. was conducted by sequencing partial regions of the translation elongation factor 1-α (TEF) and beta-tubulin (TUB2) genes, and the internal transcribed spacer region and 5.8S rRNA (ITS) (Lesuthu et al., 2019; Santos et al., 2017). The primers used were EF1-728F/EF1-986R for TEF (Carbone and Kohn, 1999), T1/Bt2b for TUB2 (Glass and Donaldson, 1995; O´Donnell and Cigelnik, 1997) and ITS1/ITS4 for ITS (White et al., 1990).

Polymerase chain reaction (PCR) amplifications were performed on a MultiGene™ Mini (Labnet International Inc.). Each PCR reaction contained 1× PCR buffer, 2.5 mM MgCl2, 0.4 mM of each dNTP, 0.4 μM of each primer, 0.5 U of DNA polymerase (Bioron), and 1 μL of template DNA. The PCR reaction was adjusted to a final volume of 20 μL with MQ water. The PCR conditions consist of an initial step at 94°C for 3 min followed by 34 cycles, annealing at 55°C for TEF and 57°C for TUB2 and ITS for 30 s, and elongation at 72°C for 45 s. A final extension was performed at 72°C for 10 min. PCR products were visualized in 1.5% agarose gels stained with GelRedTM, through a transilluminator under UV light. A GeneRuler 100-bp DNA ladder plus (Thermo) was used as a molecular weight marker. PCR products were purified and sequenced by Macrogen Inc., Seoul, Korea.

Preliminary identification was conducted by comparing the sequences with those deposited in the GenBank using the BLAST search tool (https://blast.ncbi.nlm.nih.gov/Blast.cgi). Then, a multilocus phylogenetic analysis was performed on the three combined gene regions. Firstly, sequences of each gene region were aligned using the ClustalW program, available within MEGA 11.0.11 (https://www.megasoftware.net/) and were manually edited when necessary. Related sequences and sequences of the phylogenetically closest species obtained from GenBank, including ex-type isolates, were incorporated into the alignments (Table 2). Multilocus alignment was carried out using Sequence Matrix v.1.8 (http://www.ggvaidya.com/taxondna/). Multilocus phylogenetic analysis was constructed using Bayesian inference (BI) and Maximum likelihood (ML) methods. BI and ML analyses were inferred with MrBayes v3.2.7a and RAxML v8.2.12 programs, respectively, implemented in CIPRES Science Gateway v3.3 (http://www.phylo.org/). For BI analysis, best-fit models of nucleotide substitution were selected for each gene according to the Akaike information criterion (AIC), using the jModelTest2 v2.1.6 tool implemented in CIPRES Science Gateway v3.3. Four Markov chain Monte Carlo (MCMC) chains were run simultaneously, starting from a random tree to 10 million generations. Trees were sampled every 1000 generations, and the first 2500 were discarded as the burn-in phase of each analysis. Posterior probabilities were determined from a majority-rule consensus tree generated from the remaining 7500 trees. For the ML analysis, the Generalized Time Reversible (GTR) model, with gamma correction (G) nucleotide substitution, and 1000 bootstrap iterations, was indicated. The other parameters were used as default settings. Sequences obtained in this study were submitted to the GenBank database (Table 1).

Table 1. Collection details and GenBank accession numbers of *Diaporthe* isolates characterized in this study.

Sample origin	Fungal specie	Isolate	Cultivar, rootstock or cultivar/rootstock	Geographical origin Department/Area	External symptom	Internal symptom	GenBank accesion number		
							TEF	TUB2	ITS
Commercial vineyard	*Diaporthe ampelina*	URU-VD-183	Marselan	Canelones/Las Brujas	Phomopsis disease [5]	Vascular necrosis	OR702900	OR702959	OR643959
		URU-VD-184	Cabernet Sauvignon	Canelones/Las Brujas	Phomopsis disease	Vascular necrosis	OR702901	OR702960	OR643960
		URU-VD-185	Cabernet Sauvignon	Canelones/Las Brujas	Phomopsis disease	Vascular necrosis	OR702902	OR702961	OR643961
		URU-VD-186	Cabernet Sauvignon	Canelones/Las Brujas	Phomopsis disease	Vascular necrosis	OR702903	OR702962	OR643962
		URU-VD-187	Cabernet Sauvignon	Canelones/Las Brujas	Phomopsis disease	Vascular necrosis	OR702904	OR702963	OR643963
		URU-VD-188	Marselan	Canelones/Las Brujas	Phomopsis disease	Vascular necrosis	OR702905	OR702964	OR643964
		URU-VD-189	Marselan	Canelones/Las Brujas	Phomopsis disease	Asymptomatic	OR702906	OR702965	OR643965
		URU-VD-190	Marselan	Canelones/Las Brujas	Phomopsis disease	Vascular necrosis	OR702907	OR702966	OR643966
		URU-VD-191	Ugni Blanc	Canelones/Las Violetas	Phomopsis disease	Asymptomatic	OR702908	OR702967	OR643967
		URU-VD-192	Ugni Blanc	Canelones/Las Violetas	Phomopsis disease	Asymptomatic	OR702909	OR702968	OR643968
		URU-VD-193	Marselan	Canelones/Las Brujas	Phomopsis disease	Vascular necrosis	OR702910	OR702969	OR643969
		URU-VD-194	Cabernet Sauvignon	Canelones/Las Brujas	Phomopsis disease	Asymptomatic	OR702911	OR702970	OR643970
		URU-VD-195	Perlón	Canelones/Las Piedras	Phomopsis disease	Asymptomatic	OR702912	OR702971	OR643971
		URU-VD-196	Merlot	Canelones/Las Piedras	Phomopsis disease	Asymptomatic	OR702913	OR702972	OR643972
		URU-VD-197	Cabernet Sauvignon	Canelones/Las Piedras	Phomopsis disease	Asymptomatic	OR702914	OR702973	OR643973
		URU-VD-198	Gewürztraminer	Canelones/Las Piedras	Phomopsis disease	Asymptomatic	OR702915	OR702974	OR643974
		URU-VD-199	Cabernet Sauvignon	Canelones/Las Piedras	Phomopsis disease	Vascular necrosis	OR702916	OR702975	OR643975
		URU-VD-200	Moscatel	San José/Kiyú	Phomopsis disease	Vascular necrosis	OR702917	OR702976	OR643976
		URU-VD-201	Moscatel	San José/Kiyú	Phomopsis disease	Asymptomatic	OR702918	OR702977	OR643977
		URU-VD-202	Moscatel	San José/Kiyú	Phomopsis disease	Vascular necrosis	OR702919	OR702978	OR643978
		URU-VD-203	Moscatel	San José/Kiyú	Phomopsis disease	Asymptomatic	OR702920	OR702979	OR643979
		URU-VD-204	Cabernet Sauvignon	San José/Kiyú	Phomopsis disease	Asymptomatic	OR702921	OR702980	OR643980
		URU-VD-205	Cabernet Sauvignon	San José/Kiyú	Phomopsis disease	Vascular necrosis	OR702922	OR702981	OR643981
		URU-VD-206	Cabernet Sauvignon	San José/Kiyú	Phomopsis disease	Asymptomatic	OR702923	OR702982	OR643982
		URU-VD-207	Cabernet Sauvignon	San José/Kiyú	Phomopsis disease	Vascular necrosis	OR702924	OR702983	OR643983
		URU-VD-208	Cabernet Sauvignon	San José/Kiyú	Phomopsis disease	Vascular necrosis	OR702925	OR702984	OR643984
		URU-VD-209	Cabernet Sauvignon	San José/Kiyú	Phomopsis disease	Vascular necrosis	OR702926	OR702985	OR643985
		URU-VD-210	Cabernet Sauvignon	San José/Kiyú	Phomopsis disease	Vascular necrosis	OR702927	OR702986	OR643986

		URU-VD-211	Moscatel	San José/Kiyú	Phomopsis disease	Asymptomatic	OR702928	OR702987	OR643987
		URU-VD-212	Tannat	Canelones/Juanicó	Cordon perennial canker	Sectorial wood necrosis	OR702929	OR702988	OR643988
		URU-VD-213	Sauvignon Blanc	Maldonado/Garzón	Cordon perennial canker	Sectorial wood necrosis	OR702930	OR702989	OR643989
Nursery material		**URU-VD-155**	3309C [1]	Canelones/Las Violetas	Asymptomatic	Vascular necrosis	ON573112	OR702939	OR643939
		URU-VD-156	Tannat [1]	Canelones/Las Violetas	Asymptomatic	Asymptomatic	ON573113	OR702940	OR643940
		URU-VD-157	Marselan [2]	Canelones/Las Violetas	Asymptomatic	Asymptomatic	ON573114	OR702941	OR643941
		URU-VD-158	Marselan [2]	Canelones/Las Violetas	Asymptomatic	Asymptomatic	ON573115	OR702942	OR643942
		URU-VD-159	Marselan [2]	Canelones/Las Violetas	Asymptomatic	Vascular necrosis	ON573116	OR702943	OR643943
		URU-VD-162	Moscatel de Hamburgo/SO4 [3]	Canelones/Las Violetas	Asymptomatic	Asymptomatic	ON573117	OR702944	OR643944
		URU-VD-163	Tannat/Gravesac [4]	Canelones/Las Violetas	Asymptomatic	Vascular necrosis	ON573118	OR702945	OR643945
		URU-VD-164	Moscatel de Hamburgo/SO4 [3]	Canelones/Las Violetas	Asymptomatic	Asymptomatic	ON573119	OR702946	OR643946
		URU-VD-165	Cabernet Franc/3309C [4]	Canelones/Las Violetas	Asymptomatic	Vascular necrosis	ON573120	OR702947	OR643947
		URU-VD-166	Merlot/101-14 [4]	Canelones/Las Violetas	Asymptomatic	Vascular necrosis	ON573121	OR702948	OR643948
		URU-VD-167	Merlot/101-14 [4]	Canelones/Las Violetas	Asymptomatic	Vascular necrosis	ON573122	OR702949	OR643949
		URU-VD-168	Tannat/Gravesac [4]	Canelones/Las Violetas	Asymptomatic	Vascular necrosis	ON573123	OR702950	OR643950
		URU-VD-169	Tannat/Gravesac [4]	Canelones/Las Violetas	Asymptomatic	Vascular necrosis	ON573124	OR702951	OR643951
		URU-VD-170	Tannat/Gravesac [4]	Canelones/Las Violetas	Asymptomatic	Vascular necrosis	ON573125	OR702952	OR643952
		URU-VD-173	Tannat [1]	Canelones/Las Violetas	Asymptomatic	Asymptomatic	ON573126	OR702953	OR643953
		URU-VD-174	Marselan [1]	Canelones/Las Violetas	Asymptomatic	Asymptomatic	ON573127	OR702954	OR643954
		URU-VD-175	Marselan [1]	Canelones/Las Violetas	Asymptomatic	Vascular necrosis	ON573128	OR702955	OR643955
		URU-VD-179	Albariño/101-14 [4]	Canelones/Las Violetas	Asymptomatic	Vascular necrosis	ON573130	OR702956	OR643955
		URU-VD-180	Tannat/Gravesac [3]	Canelones/Las Violetas	Asymptomatic	Vascular necrosis	ON573131	OR702957	OR643957
		URU-VD-182	Marselan [2]	Canelones/Las Violetas	Asymptomatic	Asymptomatic	OR702899	OR702958	OR643958
	Diaporthe eres	**URU-VD-171**	Chardonnay/SO4 [4]	Canelones/Las Violetas	Asymptomatic	Vascular necrosis	ON573108	OR702936	OR643936
		URU-VD-172	Chardonnay/SO4 [4]	Canelones/Las Violetas	Asymptomatic	Vascular necrosis	ON573109	OR702937	OR643937
	Diaporthe foeniculina	**URU-VD-160**	Albariño [2]	Canelones/Las Violetas	Asymptomatic	Asymptomatic	ON573106	OR702931	OR643931
		URU-VD-161	Albariño [2]	Canelones/Las Violetas	Asymptomatic	Vascular necrosis	ON573107	OR702932	OR643932
		URU-VD-177	Tannat [1]	Canelones/Las Violetas	Asymptomatic	Vascular necrosis	ON573110	OR702933	OR643933

	URU-VD-178	Albariño/101-14 [4]	Canelones/Las Violetas	Asymptomatic	Vascular necrosis	ON573111	OR702934	OR643934
	URU-VD-181	101-14 [2]	Canelones/Las Violetas	Asymptomatic	Asymptomatic	OR702898	OR702935	OR643935
Diaporthe terebinthifolii	**URU-VD-176**	Marselan [1]	Canelones/Las Violetas	Asymptomatic	Asymptomatic	ON573129	OR702938	OR643938

[1] Rootstocks and scions cuttings from mother plants

[2] Rootstocks and scion cuttings after cold storage and hydratation step of the nursery process

[3] Grafted plants after callusing step in the nursery process

[4] Nursery vines ready to plant

[5] Phomopsis disease: bleached canes with black to brown lesions on the basal internodes accompanied by elongated cracks in the epidermal layers (Phompsis cane and leaf spot disease symptoms)

Isolates selected for phenotypical characterization and pathogenicity tests are indicatye in bold

Table 2. GenBank accesion numbers of DNA sequences of the strains used for the phylogenetic analysis in this study.

Species	**Strain number**	**Host**	**GenBank accesion No.**		
			TEF	**TUB2**	**ITS**
Diaporthe ambigua	**CBS 114015**	*Pyrus communis*	KC343736	KC343978	KC343010
	CBS 117167	*Aspalathus linearis*	KC343737	KC343979	KC343011
Diaporthe ampelina	**CBS 114016**	*Vitis vinifera*	GQ250351	JX275452	AF230751
	CBS 111888	*Vitis vinifera*	KC343742	KC343984	KC343016
	CPC 29674	*Vitis vinifera*	MG281514	MG281166	MG280993
Diaporthe amygdali	**CBS 126679**	*Prunus dulcis*	KC343748	KC343990	KC343022
	CBS 111811	*Vitis vinifera*	KC343745	KC343987	KC343019
Diaporthe anacardii	**CBS 720.97**	*Anacardium occidentale*	KC343750	KC343992	KC343024
Diaporthe baccae	**CBS 136972**	*Vaccinium corymbosum*	KJ160597	MF418509	KJ160565
	CPC 29659	*V. vinifera*	MG281527	MG281179	MG281006
Diaporthe bohemiae	**CBS 143347**	*Vitis* spp.	MG281536	MG281188	MG281015
	CBS 143348	*Vitis* spp.	MG281537	MG281189	MG281016
Diaporthe chamaeropis	CBS 454.81	*Chamaerops humilis*	KC343774	KC344016	KC343048
	CBS 753.70	*Spartium junceum*	KC343775	KC344017	KC343049
Diaporthe eres	**CBS 138594**	*Ulmus laevis*	KJ210550	KJ420799	KJ210529
	CBS 138597	*Vitis vinifera*	KJ210542	KJ420783	KJ210518

(syn. *D. celastrina*)	CBS 139.27	*Celastrus* sp.	KC343773	KC344015	KC343047
(syn. *D. celeris*)	CBS 143349	*Vitis vinifera*	MG281538	MG281190	MG281017
	CPC 28267	*Vitis vinifera*	MG281540	MG281192	MG281019
(syn. *D. helicis*)	CBS 138596	*Hedera helix*	KJ210559	KJ420828	KJ210538
(syn. *D. pulla*)	CBS 338.89	*Hedera helix*	KC343878	KC344120	KC343152
Diaporthe fibrosa	CBS 109751	*Rhamnus cathartica*	KC343825	KC344067	KC343099
Diaporthe foeniculina	**CBS 111553**	*Foeniculum vulgare*	KC343827	KC344069	KC343101
	CBS 187.27	*Camellia sinensis*	KC343833	KC344075	KC343107
	CBS 123209	*Foeniculum vulgare*	KC343831	KC344073	KC343105
Diaporthe helianthi	**CBS 592.81**	*Helianthus annuus*	KC343841	KC344083	KC343115
Diaporthe hispaniae	**CBS 143351**	*Vitis vinifera*	MG281644	MG281296	MG281123
	CBS 143352	*Vitis vinifera*	MG281645	MG281297	MG281124
Diaporthe hungariae	**CBS 143353**	*Vitis vinifera*	MG281647	MG281299	MG281126
	CBS 143354	*Vitis vinifera*	MG281648	MG281300	MG281127
Diaporthe phaseolorum	CBS 113425	*Olearia* cf. *rani*	KC343900	KC344142	KC343174
	CBS 127465	*Actinidia chinensis*	KC343903	KC344145	KC343177
Diaporthe rudis	**CBS 109292**	*Laburnum anagyroides*	KC843090	KC843177	KC843331
	CBS 113201	*Vitis vinifera*	KC343960	KC344202	KC343234
Diaporthe schini	**CBS 133181**	*Schinus terebinthifolius*	KC343917	KC344159	KC343191
Diaporthe sojae	**CBS 139282**	*Glycine max*	KJ590762	KJ610875	KJ590719
	CBS 116019	*Caperonia palustris*	KC343901	KC344143	KC343175
Diaporthe terebinthifolii	**CBS 133180**	*Schinus terebinthifolius*	KC343942	KC344184	KC343216
Diaporthella corylina	CBS 121124	*Corylus* sp.	KC343730	KC343972	KC343004

Note: Ex-type strains are indicated in bold.

2.3 Phenotypical characterization

A subset of 16 isolates representing the four species identified by molecular analyses were selected for phenotypical characterization, *D. ampelina* (n=9), *D. foeniculina* (n=4), *D. eres* (n=2) y *D. terebinthifolii* (n=1). Cultures were grown on PDA and incubated at 20°C under near UV light in 12 h light-dark cycles for 4 to 8 weeks to induce sporulation (Guarnaccia et al., 2018). The length and width of 30 alfa and 30 beta conidia per isolate (when present) were randomly measured at 400× magnification, using a digital camera (Microscope eye-piece camera, AM-4023X, Taiwan) incorporated into the microscope (Olympus CX23). Shape of conidia and colony colour were also recorded (Rayner, 1970).

The effect of temperature on the mycelial growth was determined on PDA. Mycelial plugs of 5 mm in diameter were taken from actively growing margins of 7-day-old colonies growing on PDA at 25°C and transferred to the centre of fresh PDA plates. Plates were incubated at 5, 10, 15, 20, 25, 30, and 35°C in darkness. For each isolate and temperature combination, three replicates were performed. After 7 days of incubation under a completely randomized design, colonies diameter was measured along two perpendicular axes, averaged and radial growth in millimetres per day was calculated.

2.4 Pathogenicity tests

The pathogenicity of 16 isolates of the four *Diaporthe* species identified (the same as those used for phenotypical characterization) was evaluated on detached green shoots and lignified canes in two separate assays. The plant material was collected from a commercial vineyard of Cabernet Sauvignon, one of the most susceptible cultivars to *Diaporthe* pathogens (Úrbez-Torres et al., 2013),

The first pathogenicity test was carried out by inoculating conidial suspensions on green shoots. For that, healthy green shoots, 50 cm long, were collected and the leaves, tendrils and branches were immediately removed. The cuttings were placed in a 200 ml glass flask with moistened sand. An internode area in the centre of the cutting was surface sterilized with 70% ethanol by wiping with cotton swabs (Kaliterna et al., 2012) and a 5 mm bevelled cut was made in the centre of the sterilized area with a sterilized scalpel. Immediately a 20 µl drop of the corresponding conidial suspension was pipetted into the wound.

Conidial suspensions of each isolate were prepared by pipetting 2 ml of sterile distilled water onto the surface of 4-weeks-old colonies grown at 20°C under near UV light in 12 h light-dark cycles, with visible mature pycnidia. The concentration of alfa and/or beta conidia was determined with a hemacytometer and adjusted to 10^6 conidia/ml (Baumgartner et al., 2013; Lawrence et al., 2015). Eight cuttings per isolate were inoculated, and eight cuttings inoculated with 20 µl of sterile distilled water were used as controls. Immediately after inoculation, the cuttings were covered with moist plastic bags as humid chambers for 1 week. In addition, the glass flasks with sand were watered periodically. After 4 weeks at 25°C of incubation, the bark of each green shoot was removed, and the length of the necrotic lesion (discoloured wood radiating above and below the inoculation site) was measured upwards and downwards from the point of inoculation. Small pieces of wood from the edge of each lesion were taken and plated onto PDAS to recover the inoculated fungus and complete Koch´s postulate. Fungal identity was verified by morphological characteristics.

The second pathogenicity trial was conducted on dormant lignified canes by inoculating mycelial plugs (Úrbez-Torres et al., 2009; Kaliterna et al., 2012). Healthy lignified canes, 50 cm long, were collected, placed upright in a 200 ml glass flask with moistened sand, and surface sterilized as indicated above. A wound 4 mm in diameter and 2 mm deep was made in the centre of the sterilized area of each cane with a sterile scalpel and the bark was removed, exposing the cambium. Four-millimetre mycelial plugs from the growing margin of 7-day-old cultures on PDA were placed onto the wound and immediately covered with cotton wool soaked in sterile water and fixed with parafilm to prevent them from drying out. Eight canes were inoculated per isolate, and eight canes inoculated with non-colonized sterile agar plugs were used as controls. The glass flasks with canes were kept at 25°C and periodically watered, as indicated above. After 12 weeks, the bark was removed, and the length of the necrotic lesion was measured upwards and downwards from the point of inoculation. Koch´s postulates were completed as indicated above.

As the pathogenicity tests datasets did not meet with ANOVA assumptions verified by the Shapiro-Wilk and Levene´s test, the data were analyzed by a nonparametric Kruskal-Wallis test at the 5% significance level, using InfoStat/E version 2020 (http://www.infostat.com.ar).

3. RESULTS

3.1 Field symptoms and fungal isolations

Grapevines showing decline symptoms and perennial cankers were found in all vineyards sampled. Cross-sections of affected trunks showed wedge-shaped wood necrosis together with other grapevine trunk diseases symptoms like brown to black vascular streaking and white to yellow softwood rot (Figure 1 a and b). Symptoms of Phomopsis cane and leaf spot disease were also found in the sampled vineyards (Figure 1 c and d). When the bark of bleached canes with external longitudinal lesions was removed, internal vascular necrosis associated with the external symptoms was observed in some samples (Figure 1 e).

Figure 1. Symptoms associated with *Diaporthe* spp. observed in vineyards from the main grape-growing regions of Uruguay. Cross-section of trunks showing perennial cankers with internal sectorial necroses (a and b), together with other grapevine trunk diseases symptoms like white to yellow softwood rot (a) and black vascular spots (b); bleached canes with necrotic lesions on the basal internodes accompanied by elongated cracks in the epidermal layers, typical symptoms of Phomopsis cane and leaf spot (c and d); internal necrotic lesions observed after removing the bark of canes with Phomopsis cane and leaf spot symptoms (e).

From vines with perennial cankers, only two *Diaporthe* strains were isolated (Table 1). A predominance of strains belonging to the Botryosphaeriaceae was isolated from these samples, followed by Esca disease pathogens (others GTDs pathogens, data not shown). Regarding samples with Phomopsis cane and leaf spot symptoms, a total of 29 *Diaporthe* isolates were obtained. Of these, 16 strains were isolated from internal vascular necroses associated with the external longitudinal lesions, while the remaining 13 strains were isolated from asymptomatic internal tissue. The collection was completed with the 28 isolates obtained from symptomatic (internal vascular necrosis, n = 17) and asymptomatic nursery materials (n = 11) (Carbone et al., 2022), giving a total of 59 *Diaporthe* isolates (Table 1).

3.2 Phylogenetic analysis

Phylogenies of the individual datasets of TEF, TUB2 and ITS gene regions did not show significant conflicts in tree topology, thus they were combined in a multilocus phylogenetic analysis. The combined dataset contained 98 taxa (59 from this study) and 1734 characters including gaps (TEF = 354; TUB2 = 831; ITS = 549), of which 547 were parsimony informative. The AIC best-fit evolutionary models of nucleotide substitution used for the BI analysis were GTR with gamma distributed with invariant site rates for TEF and ITS, and GTR with gamma distributed for TUB2. The tree topologies inferred from BI and ML consensus tree were consistent with each other, so only the BI tree with posterior probability and bootstrap support values is presented.

Fifty-one of the Uruguayan *Diaporthe* isolates were grouped in a well-supported clade (1/95, posterior probability and maximum likelihood bootstrap support values, respectively) with *D. ampelina* strains, including the ex-type of this species. The remaining eight isolates were grouped in others three well-supported clades with *D. foeniculina* (five isolates, node support values 1/79) *D. eres* (two isolates, node support values 0.97/) and *D. terebinthifolii* strains (one isolate, node support values 1/97), including the ex-type of each species (Figure 2). *Diaporthe ampelina* isolates were obtained from both commercial vineyards (31 isolates) and nursey material (20 isolates), while *D. foeniculina*, *D. eres* and *D. terebinthifolii* strains were exclusively from nursery material (Table 1).

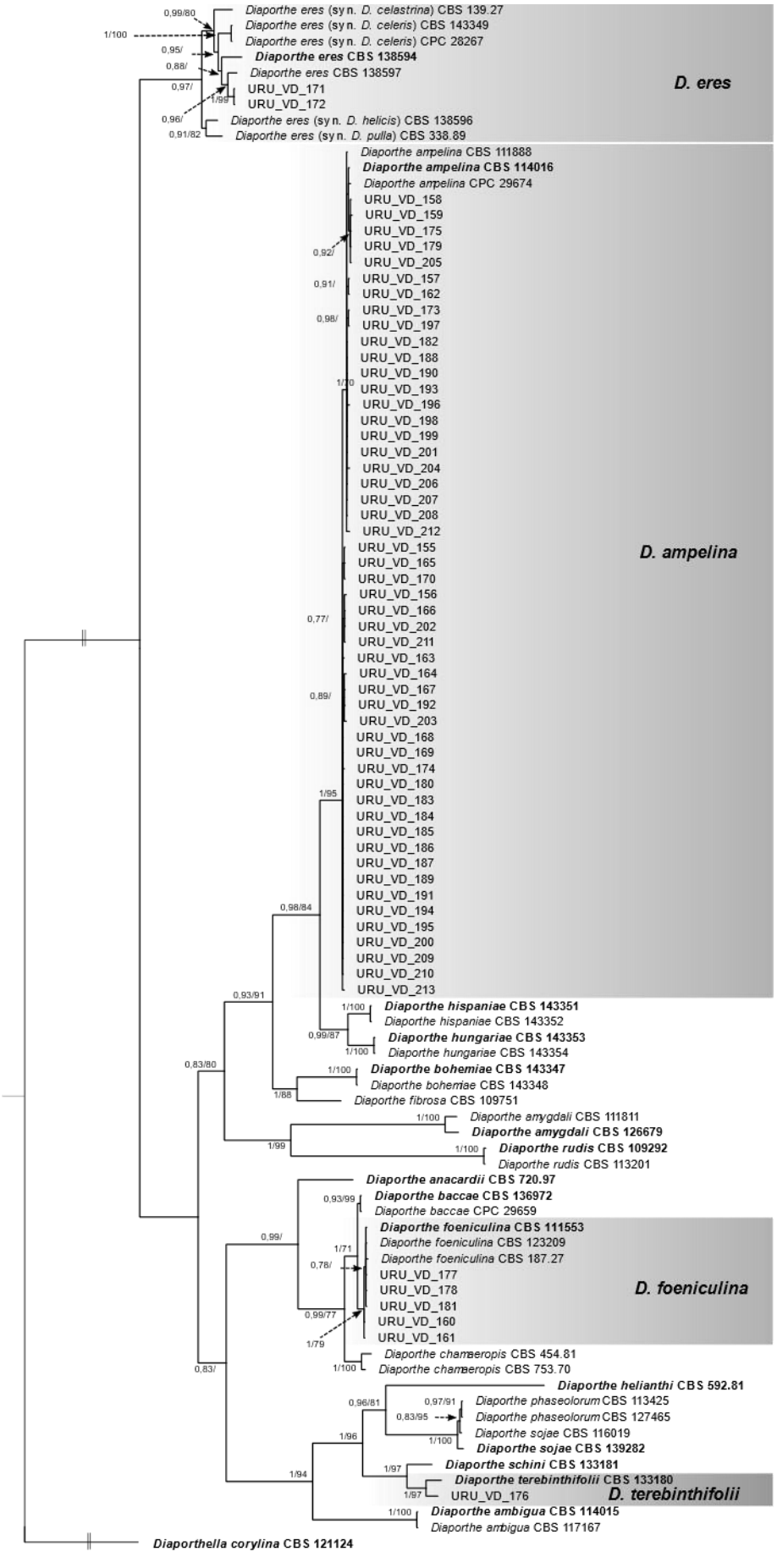
Diaporthe eres (syn. D. celastrina) CBS 139.27
Diaporthe eres (syn. D. celeris) CBS 143349
Diaporthe eres (syn. D. celeris) CPC 28267
Diaporthe eres CBS 138594
Diaporthe eres CBS 138597
URU_VD_171
URU_VD_172
Diaporthe eres (syn. D. helicis) CBS 138596
Diaporthe eres (syn. D. pulla) CBS 338.89
D. eres
Diaporthe ampelina CBS 111888
Diaporthe ampelina CBS 114016
Diaporthe ampelina CPC 29674
URU_VD_158
URU_VD_159
URU_VD_175
URU_VD_179
URU_VD_205
URU_VD_157
URU_VD_162
URU_VD_173
URU_VD_197
URU_VD_182
URU_VD_188
URU_VD_190
URU_VD_193
URU_VD_196
URU_VD_198
URU_VD_199
URU_VD_201
URU_VD_204
URU_VD_206
URU_VD_207
URU_VD_208
URU_VD_212
URU_VD_155
URU_VD_165
URU_VD_170
URU_VD_156
URU_VD_166
URU_VD_202
URU_VD_211
URU_VD_163
URU_VD_164
URU_VD_167
URU_VD_192
URU_VD_203
URU_VD_168
URU_VD_169
URU_VD_174
URU_VD_180
URU_VD_183
URU_VD_184
URU_VD_185
URU_VD_186
URU_VD_187
URU_VD_189
URU_VD_191
URU_VD_194
URU_VD_195
URU_VD_200
URU_VD_209
URU_VD_210
URU_VD_213
D. ampelina
Diaporthe hispaniae CBS 143351
Diaporthe hispaniae CBS 143352
Diaporthe hungariae CBS 143353
Diaporthe hungariae CBS 143354
Diaporthe bohemiae CBS 143347
Diaporthe bohemiae CBS 143348
Diaporthe fibrosa CBS 109751
Diaporthe amygdali CBS 111811
Diaporthe amygdali CBS 126679
Diaporthe rudis CBS 109292
Diaporthe rudis CBS 113201
Diaporthe anacardii CBS 720.97
Diaporthe baccae CBS 136972
Diaporthe baccae CPC 29659
Diaporthe foeniculina CBS 111553
Diaporthe foeniculina CBS 123209
Diaporthe foeniculina CBS 187.27
URU_VD_177
URU_VD_178
URU_VD_181
URU_VD_160
URU_VD_161
D. foeniculina
Diaporthe chamaeropis CBS 454.81
Diaporthe chamaeropis CBS 753.70
Diaporthe helianthi CBS 592.81
Diaporthe phaseolorum CBS 113425
Diaporthe phaseolorum CBS 127465
Diaporthe sojae CBS 116019
Diaporthe sojae CBS 139282
Diaporthe schini CBS 133181
Diaporthe terebinthifolii CBS 133180
URU_VD_176
D. terebinthifolii
Diaporthe ambigua CBS 114015
Diaporthe ambigua CBS 117167
Diaporthella corylina CBS 121124
0.08

Figure 2. Bayesian inference phylogenetic tree built using the concatenated sequences of the TEF, TUB2 and ITS genomic regions of 59 *Diaporthe* strains isolated from Uruguayan vineyards and nursery material and sequences retrieved from the GenBank (ex-type indicated in bold). *Diaporthe corylina* CBS 121124 was used as outgroup. Posterior probability and maximum likelihood bootstrap support values higher than 0.70 and 70 are shown at the nodes before and after the bar, respectively. The scripts indicate that the nodes do not exist in the maximum likelihood tree. Double hash marks indicate branch lengths shortened at least 2-fold to facilitate visualization. Scale bar represents the estimated number of substitutions per site.

3.3 Phenotypical characterization

Diaporthe ampelina isolates showed slightly raised white mycelium, becoming light brown in the following days and with prominent growth rings. Pycnidia were observed after 1 month under near UV light and were brown to black and globose. All colonies produced hyaline, ellipsoidal and unicellular *alpha conidia*, and some isolates (URU-VD-155, URU-VD-156, URU-VD-191 and URU-VD-213) also produced hyaline, filiform, and slightly curved *beta conidia*. *Diaporthe foeniculina* colonies showed white sparse mycelium, with greenish yellow pigmentation in reverse. Pycnidia were formed after 1 month under near UV light and were black, globose to subglobose, and produced abundant hyaline, aseptate and slightly curved *beta conidia*, while no *alfa conidia* were observed after 2 months under near UV light in any of the strains. *Diaporthe eres* cultures presented white and fluffy mycelium and produced abundant black pycnidia after 1 month under near UV light. *Alfa conidia* were rarely observed and were aseptate, hyaline, ovate to ellipsoidal, whereas *beta conidia* were abundant with hyaline, fusiform to hooked with base sub-truncate aspect. *Diaporthe terebinthifolii* colony was characterized by a fast-growing aerial mycelium cottony, greyish white and with the reverse buff to brown. Pycnidia were visible after 2 months under near UV light and were globose to conical, brown to black, and produced hyaline, curved or hamate *beta conidia*, while no *alfa conidia* were observed (Figure 3). The size of *alpha* and *beta conidia* is summarised in Table 3.

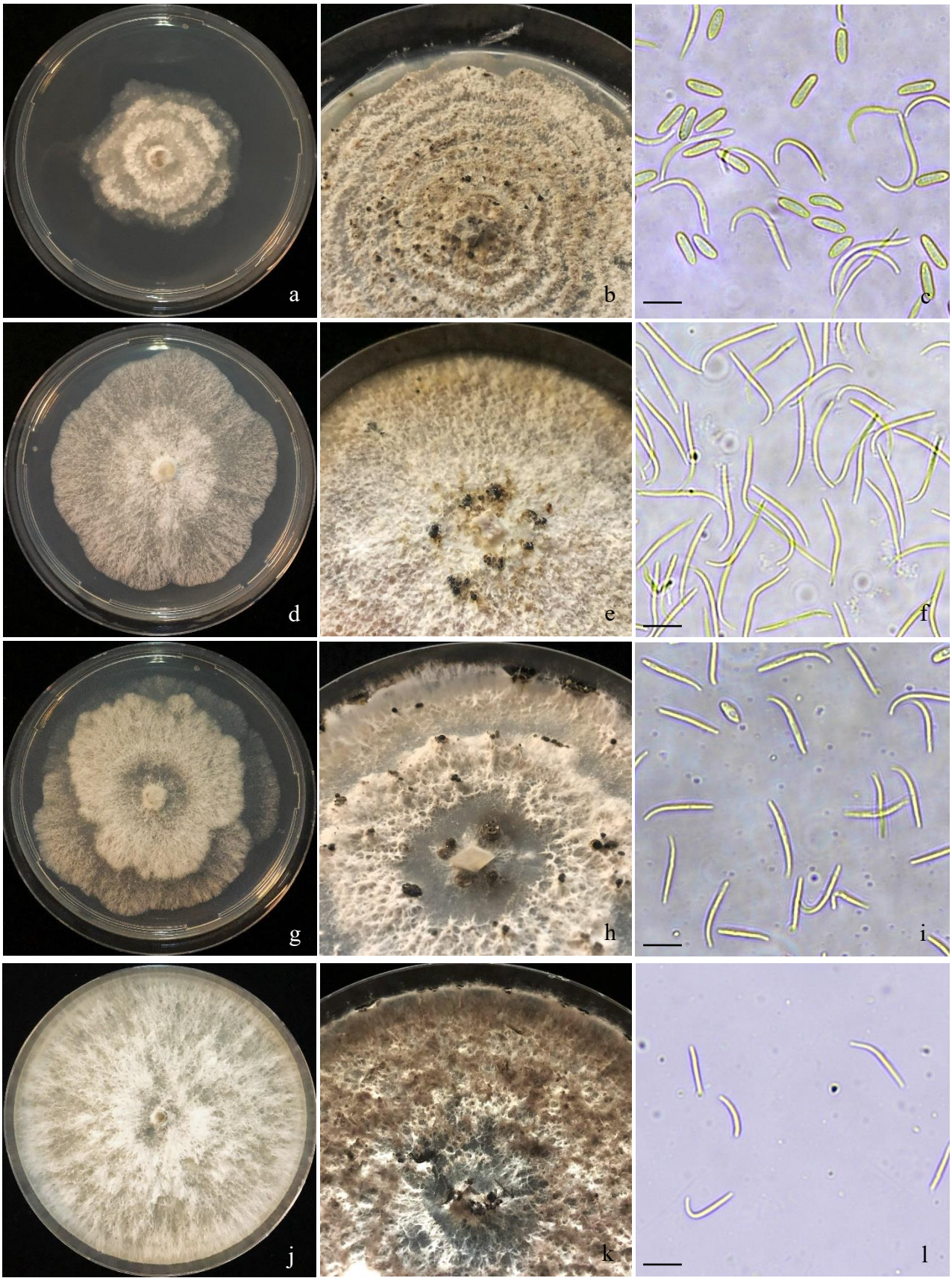

Figure 3. Morphological characteristics of *Diaporthe* species isolated from grapevine in Uruguay. Five-days-old colonies on Potato Dextrose Agar (PDA) at 25°C (left), 1-month-

old colonies under near UV light in 12 h light-dark cycles (medium) and *alfa* and *beta* conidia (right) of *D. ampelina* URU-VD-212 (a-c), *D. foeniculina* URU-VD-177 (d-f) (only *beta* conidia), *D. eres* URU-VD-171 (g-i) and *D. terebinthifolii* URU-VD-176 (j-l) (only *beta* conidia). Bars = 10 µm.

Table 3. Size of *alfa* and *beta* conidia of the four *Diaporthe* species of grapevine characterized in this study.

Species	*Alpha conidia* (µm)		*Beta conidia* (µm)	
	Length	Width	Length	Width
D. ampelina[a] (n=9)	8.72 ± 1.32	3,24 ± 0.18	26.57 ± 2.54	1.51 ± 0.06
D. foeniculina (n=4)	-	-	24.89 ± 1.42	1.18 ± 0.06
D. eres (n=2)	6.65 ± 0.31	2,67 ± 0.01	19.55 ± 0.97	1.57 ± 0.14
D. terebinthifolii (n=1)	-	-	19.29 ± 1.97	1.44 ± 0.21

[a] All *D. ampelina* isolates analyzed produced alfa conidia but only four produced beta conidia (isolates URU-VD-155, URU-VD-156, URU-VD-191 and URU-VD-213)

All isolates tested were able to grow between 5°C and 35ºC. The optimum mycelial growth temperature was around 25°C for *D. ampelina* (6.7 mm/day), *D. foeniculina* (10.2 mm/day) and *D. eres* (12.7 mm/day) isolates, while for *D. terebinthifolii* was closer to 30°C and with a growth rate substantially higher than the other three species (19 mm/day). At 5ºC the growth rate was extremely slow with an average 0.1 mm/day for *D. ampelina* and *D. foeniculina* isolates, 0.2 mm/day for *D. terebinthifolii* and 0.4 mm/day for *D. eres*. Similar behaviour was observed at 35°C, the growth rate averaged 0.2 mm/day for *D. ampelina*, 0.3 mm/day for *D. foeniculina*, and 0.5 mm/day for *D. eres* while *D. terebinthifolli* grew slightly faster, 2 mm/day (Figure 4).

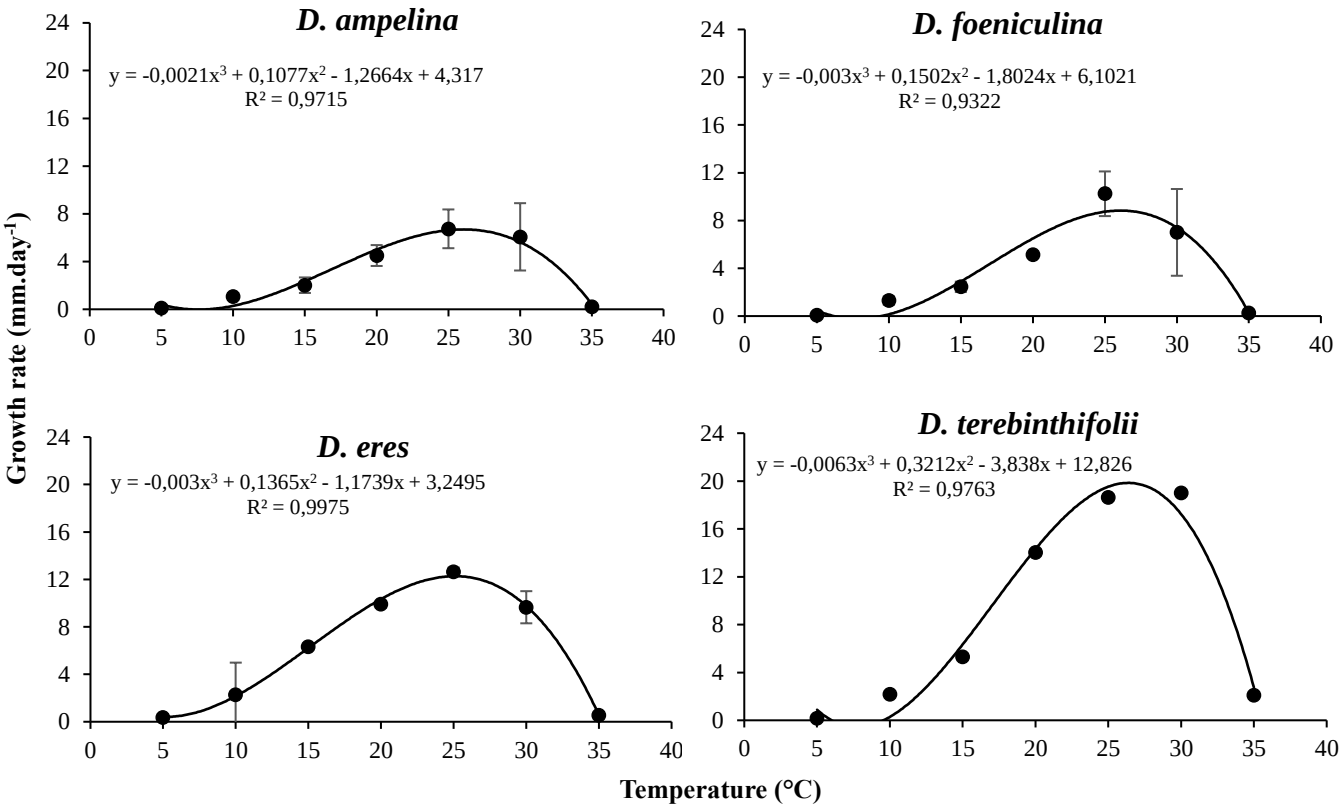

Figure 4. Effect of temperature on colony daily growth rate (mm) of *Diaporthe* species growing on Potato Dextrose Agar (PDA) at 5, 10, 15, 20, 25, 30 and 35°C during seven days. The data represent the average of a group of representative isolates of each species (*D. ampelin*a n = 9, *D. foeniculina* n = 4, *D.eres* n = 2, and *D. terebinthifolii* n = 1). Data for each species were fitted to a non-linear regression curve. Vertical bars are the standard error of the means.

3.4 Pathogenicity tests

The statistical analysis indicated a significant effect of *Diaporthe* spp. isolates on lesion length of inoculated green shoots ($P < 0.0001$). Four weeks after inoculation, *Diaporthe ampelina* isolates caused necrotic lesions from 9.6 to 26.7 mm, with a mean of 15mm, and were statistically longer compared to the control whose lesion size matched the size of the wound made. Within *D. ampelina* isolates, URU-VD-156 and URU-VD-212 showed the longest lesions. The isolate of *D. terebinthifolii* caused, on average, necrotic lesions of 7 mm in length, and was statistically longer compared to the control treatment. *Diaporthe foeniculina* isolates caused necrotic lesions averaging 5 mm in

length but were not statistically different from the control treatment. In the case of the *D. eres* isolates, no necrotic lesions developed beyond the wound scar, although the lesion was darker than those present in the control shoots. All inoculated *Diaporthe* isolates were successfully recovered from the inner tissue of green shoots with re-isolation rates ranging from 63 to 100% (Figure 5 and Figure 6).

As for the pathogenicity test on lignified canes, a significant effect of *Diaporthe* spp. isolates on lesion length was also observed ($P < 0.0001$). The lesions length caused by *D. ampelina* isolates ranged from 6 mm to 32 mm, with a mean of 13 mm, and except for the isolate URU-VD-155, were statistically longer than those of the control treatment whose lesion size matched the size of the wound made. *Diaporthe eres* isolates caused an average lesion length of 8 mm and were statistically longer than the control treatment. *Diaporthe foeniculina* caused an average lesion length of 7 mm but only two isolates (URU-VD-177 and URU-VD-178) caused a lesion significantly longer than the control treatment. The lesion length caused by the isolate of *D. terebinthifolii* was 6 mm and was not statistically different from the control. Re-isolation rates ranged from 14 to 83%, with all inoculated *Diaporthe* isolates successfully recovered from the inner tissue of lignified canes (Figure 5 and Figure 6).

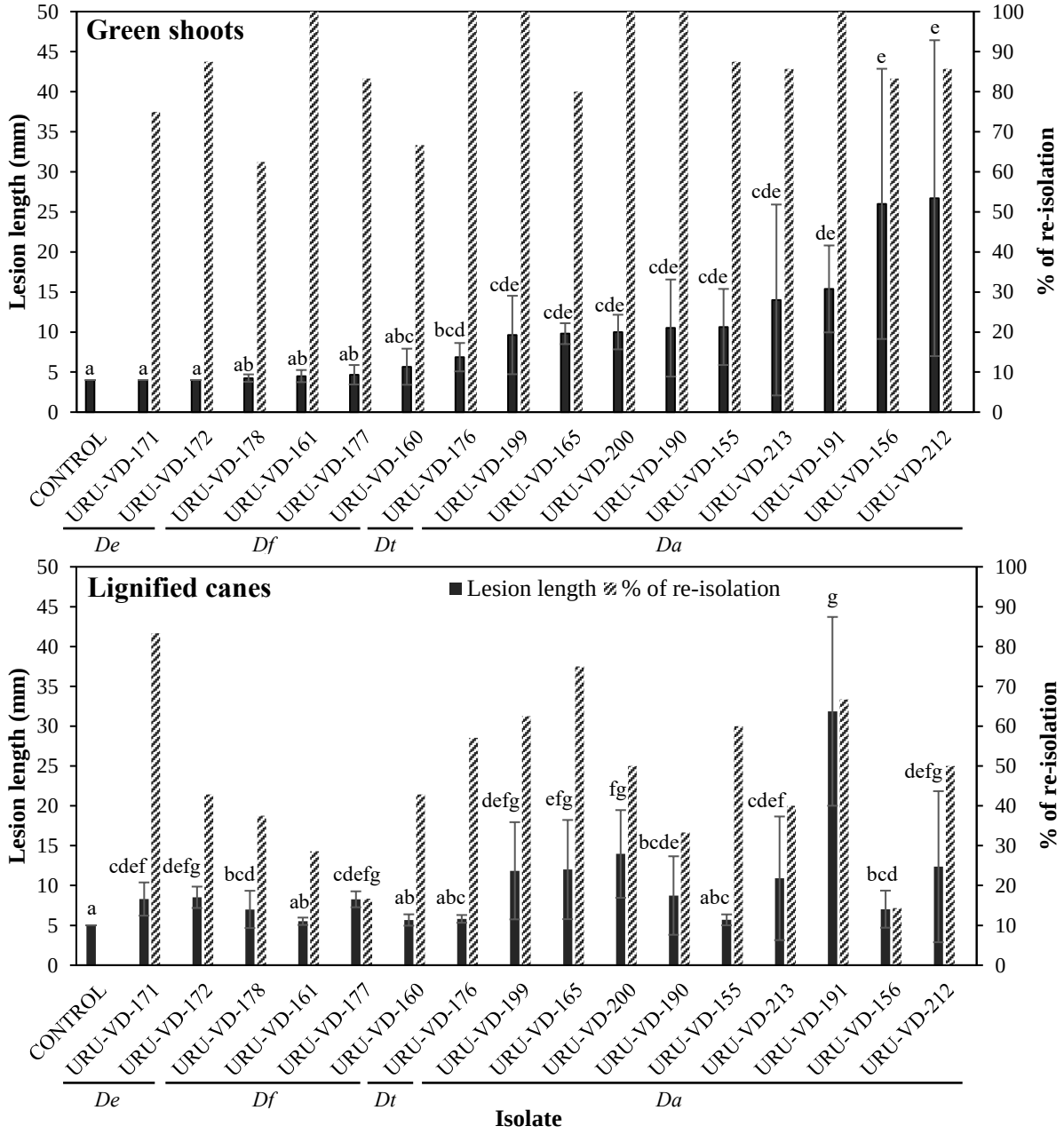

Figure 5. Results of pathogenicity tests showing the mean length of necrotic lesions caused by *Diaporthe* spp. isolates (*Da = D. ampelina*, *De = D. eres*, *Df = D. feoniculina*, *Dt = D. terebinthifolii*) and percentage of re-isolation on detached green shoots and lignified canes of Cabernet Sauvignon cultivar. Mean values of lesion length followed by different letters indicate significant differences according to Kruskal-Wallis test ($p \leq 0.05$). Vertical bars on lesion length represent the standard error of the means.

Figure 6. Necrotic lesions caused by *Diaporthe* spp. inoculated on detached green shoots and lignified canes of Cabernet Sauvignon cultivar. Green shoots after 4 weeks of inoculation by conidial suspensions: non-inoculated control (a), *D. ampelina* URU-VD-156 (b), *D. foeniculina* URU-VD-161 (c), *D. eres* URU-VD-171 (d), and *D. terebinthifolii* URU-VD-176 (e). Lignified canes after 12 weeks of inoculation by mycelial plugs: non-inoculated control (f), *D. ampelina* URU-VD-199 (g), *D. foeniculina* URU-VD-177 (h), *D. eres* URU-VD-171 (i), and *D. terebinthifolii* URU-VD-176 (j).

4. DISCUSSION

To our knowledge, the present study represents the first attempts to survey the presence of DD in commercial vineyards and to identify and characterize *Diaporthe* species associated with grapevine trunk diseases in Uruguay. *Diaporthe ampelina* (51 isolates), *D. foeniculina* (five isolates), *D. eres* (two isolates) and *D. terebinthifolii* (one isolate) were found infecting symptomatic and asymptomatic adult vines and grapevine nursery material.

Symptoms of general decline and perennial cankers were observed in all commercial vineyards sampled, and *Diaporthe* fungi were recovered from symptomatic

grapevine confirming the presence of DD in Uruguayan field vines. However, the most frequent fungi associated with perennial cankers were pathogens of Botryosphaeria dieback and Esca disease (data not shown), which is consistent with previous reports by Abreo et al., (2011; 2013). This finding suggests that the importance of *Diaporthe* as a canker-causing organism in Uruguayan vineyards remains low.

On the other hand, *Diaporthe* was also isolated from the internal tissue of canes showing the typical symptoms of Phomopsis cane and leaf spot disease (bleached canes with brown lesions on the basal internodes accompanied by elongated cracks in the epidermal layers). After removing the bark, internal necrosis was observed in the woody tissue below the external lesions on the cane in some samples, which indicates that the fungus was able to colonize the wood after infecting and causing Phomopsis cane an leaf spot disease symptom on the shoots. Furthermore, the fact that the fungus was also isolated from samples with external Phomopsis cane and leaf disease symptoms but without internal symptoms of necrosis, suggest that the fungus was able to colonize even though symptoms had not yet developed. A frequent co-occurrence of Phomopsis cane a leaf spot symptoms and wood cankers was previously suggested. It has been argued that wood canker may be the result of systemic spread of infections initiated in green tissues (Baumgartner et al., 2013). Regardless of this, it was also confirmed that *Diaporthe* species can cause wood cankers through infection on pruning wounds (Baumgartner et al., 2013).

Identification of *Diaporthe* species has historically been based on morphology and host association, however, it is well known that within the genus multiple species can be found on a single host, and a single species can be associated with different hosts (Udayanga et al., 2014). Currently, the separation of species in the *Diaporthe* genus is based on multilocus phylogenetic analysis (Santos et al., 2017). The loci used in this work, TEF, TUB2 and ITS, were selected in accordance with previous studies because of their usefulness for accurate species identification (Lesuthu et al., 2019; Santos et al., 2017). Furthermore, the morphological characteristics assessed were consistent and in agreement with those expected for the species identified, supporting the phylogenetic results (Gomes et al., 2013; Hilario et al., 2021; Mostert et al., 2001; Udayanga et al., 2014).

As reported in California (Úrbez-Torres et al., 2013), Croatia (Kaliterna et al., 2012) and Texas (Úrbez-Torres et al., 2009), *D. ampelina* is the most prevalent species

within *Diaporthe* genus affecting grapevine wood in Uruguay. Moreover, this species was the only one found in adult vines showing general decline and perennial cankers, and from internal necrosis in canes showing external Phomopsis cane and leaf spot symptoms. Also, this species was the most aggressive in the pathogenicity tests in agreement with several previous studies worldwide (Baumgartner et al., 2013; Kaliterna et al., 2012; Lawrence et al., 2015; Lesuthu et al., 2019; Úrbez-Torres et al., 2013). It is noteworthy that a high variability among the virulence of *D. ampelina* isolates was registered in the pathogenicity tests, suggesting a high intraspecific variability, as it was previous reported for *Diaporthe* spp. (Lawrence et al.; 2015; Lesuthu et al., 2019).

Diaporthe foeniculina (syn. *D. neotheicola*) was isolated from symptomatic (internal vascular necrosis) and asymptomatic nursery material. This species was originally described from *Foeniculum vulgare* in Portugal and has since been found in association with multiple hosts (Gomes et al., 2013; Udayanga et al., 2014), including grapevine in California (Lawrence et al., 2015; Úrbez-Torres et al., 2013), Croatia (Kaliterna et al., 2012) and South Africa (Lesuthu et al., 2019). In the pathogenicity tests, lesion length caused by this species were not statistically different from the control, except for two isolates inoculated on lignified canes. However, the pathogen was recovered from inoculated green shoots in a high percentage (78% on average) and, to a lesser extent, from inoculated lignified canes (31% on average), indicating that it was able to infect and colonize. These results suggests that *D. foeniculina* is a weak pathogen on grapevine as was indicated by Kaliterna et al. (2012), Lawrence et al. (2015) and Úrbez-Torres et al. (2013). These authors also suggested that this species could even act as endophyte after colonizing grapevine wood. Interestingly, *D. foeniculina* was previously found associated with reddish sunken cankers on apple tree branches in Uruguay, although its pathogenicity was not evaluated (Sessa et al., 2017).

Regarding *D. eres*, this species was isolated exclusively from nursery material showing internal vascular necrosis. *Diaporthe eres* was first reported as pathogen on grapevine in Croatia (Kaliterna et al., 2012) and, since then, has been found in North America (Baumgartner et al., 2013; Úrbez-Torres et al., 2013), Europe (Guarnaccia et al., 2018), South Africa (Lesuthu et al., 2019) and China (Dissanayake et al., 2015; Manawasinghe et al., 2019). Particularly in China was found as the most prominent and widespread pathogen of grapevine within this genus. In Uruguay, *D. eres* was previously isolated from apple branches showing reddish sunken cankers with a higher prevalence

than *D. foeniculina* (Sessa et al., 2017). Our pathogenicity tests results were inconsistent, as on green shoots the lesions caused by this pathogen were darker but not longer than those observed in the control treatment, while on lignified canes they were statistically longer (8 mm, while the control showed 5 mm). However, the pathogen was successfully recovered from both inoculated material (81% and 63% on average, from green shoots and lignified canes, respectively), indicating that *D. eres* is a weak or moderate pathogen on grapevine, as proposed in previous works (Baumgartner et al., 2013; Kaliterna et al., 2012).

In this work, only one specimen of *D. terebinthifolii* was obtained. This single strain was isolated from asymptomatic nursery material. However, the results of pathogenicity tests indicated that it is a pathogen of grapevine, although with markedly lower virulence than *D. ampelina*. *Diaporthe terebinthifolii* was described by Gomes et al. (2013) as an endophytic of leaves of *Schinus terebinthifolius* in Paraná, Brazil, and to our knowledge, it has been associated with grapevine only in Uruguay (Carbone et al., 2022). In Uruguay, this species has also been isolated from wood samples of pear branches associated with apical dead shoots, but its pathogenicity was not evaluated (Sessa et al., 2017). Although this species does not seem to be of major importance as a vine pathogen, it was the one that best adapted to temperatures above 30ºC, so it is advisable to monitor whether its incidence increases in the coming years in a scenario of global warming.

In summary, the presence of *Diaporthe* species colonizing the internal wood of field vines was confirmed. Despite the lower incidence as a canker-causing organism than other well-known GTDs pathogens observed in the present study, the high prevalence of *Diaporthe ampelina* is of concern due we demonstrated that is the most aggressive species affecting grapevine wood within this genus. According to our findings, after infecting green shoots and causing Phomopsis cane and leaf spot disease symptoms, *Diaporthe ampelina* can colonize internal wood causing necrosis. Nevertheless, further studies are needed to establish the main way of infection of *Diaporthe* as a canker-causing organism, to better understand the epidemiology of DD. Also, future studies should focus on assessing the susceptibility of different cultivars, as well as evaluating the efficacy of fungicides against *Diaporthe* species, contributing to the design of an integrated management programme to prevent the disease from progressing throughout the grape growing area.

5. REFERENCES

Abreo, E., Martínez, S., Bettucci, L. & Lupo, S. (2010) Morphological and molecular characterization of *Campylocarpon* and *Cylindrocarpon* spp. associated with black foot disease of grapevines in Uruguay. *Australasian Plant Pathology,* 39, 446-452.

Abreo, E. (2011) Comunidad fúngica asociada a las enfermedades del tronco de la vid en Uruguay: composición, diagnóstico molecular y patogenicidad. PhD thesis, Montevideo, PEDECIBA Ciencias Biológicas, Universidad de la República.

Abreo, E., Martínez, S., Bettucci, L. & Lupo, S. (2011) *Phaeomoniella chlamydospora* and *Phaeoacremonium* spp. in grapevines from Uruguay. *Phytopathologia Mediterranea*, 50, 77-85.

Abreo, E., Martínez, S., Bettucci, L. & Lupo, S. (2013) Characterization of *Botryosphaeriaceae* species associated with grapevines in Uruguay. *Australasian Plant Pathology,* 42, 241-249.

Alaniz, S., Gepp, V., Mondino, P., Leoni, C., Núñez, S., Mujica, V., et al. (2016) Guía de identificación y monitoreo de enfermedades y plagas en frutales de hoja caduca y vid bajo manejo integrado. Asociación de Fruticultores de Producción Integrada.

Akgül, D.S. & Nawaz Awan, Q. (2021) Characterization of *Diaporthe ampelina* isolates and their sensitivity to hot-water treatment and fungicides in vitro. *KSU Journal of Agriculture and Nature*, 25, 6, 1378-1389.

Baumgartner, K., Fujiyoshi, P.T., Travadon, R., Castelbury, L.A., Wilcox, W.F. & Rolshausen, P.E. (2013) Characterization of species of *Diaporthe* from wood cankers of grape in eastern North American vineyards. *Plant Disease*, 97, 912-920.

Carbone, I. & Kohn, L. M. (1999) A method for designing primer sets for speciation studies in filamentous ascomycetes. *Mycologia* 91, 553-6.

Carbone, M.J., Gelabert, M., Moreira. V., Mondino, P. & Alaniz, S. (2022) Grapevine nursery propagation material as source of fungal trunk disease pathogens in Uruguay. *Frontiers in Fungal Biology*, 3, 958466.

Dissanayake, A.J., Liu, M., Zhang, W., Chen, Z., Udayanga, D., Chukeatirote. et al. (2015) Morphological and molecular characterisation of *Diaporthe* species associated with grapevine trunk disease in China. *Fungal Biology*, 119, 5, 283-294.

Gao, Y., Liu, F., Duan, W., Crous, P.W. & Cai, L. (2017) *Diaporthe* is paraphyletic. *IMA Fungus* 8, 153–187.

Glass N.L. & Donaldson G. (1995) Development of primer sets designed for use with PCR to amplify conserved genes from filamentous ascomycetes. *Applied and Environmental Microbiology* 61: 1323-1330.

Gomes, R.R., Glienke, C., Videira, S.I.R., Lombard, L., Groenewald, J.Z., & Crous, P.W. (2013) *Diaporthe*: a genus of endophytic, saprobic and plant pathogenic fungi. *Persoonia*, 31, 1-41.

Gramaje, D. & Armengol, J. (2011) Fungal trunk pathogens in the grapevine propagation process: potential inoculum sources, detection, identification, and management strategies. *Plant Disease* 95, 1040-1055.

Guarnaccia, V., Groenewald, J.Z., Woodhall, J., Armengol, J., Cinelli, T., Eichmeier, A. et al. (2018) *Diaphorte* diversity and pathogenicity revealed from a broad survey of grapevine diseases in Europe. *Persoonia* 40, 135-153.

Hilário, S., Gonçalves, M.F.M. & Alves, A. (2021) Using genealogical concordance and coalescent-based species delimitation to assess species boundaries in the *Diaporthe eres* complex. *Journal of Fungi*, 7, 507, 1-25.

INAVI (2022). Estadísticas de viñedos 2022, datos nacionales. Instituto Nacional de Vitivinicultura (INAVI), Departamento Registro de Viñedos. Available at: https://www.inavi.com.uy/uploads/vinedo/e114169ff8dd5bd2a83547b5a8c60636eb4aebcc.pdf [Accessed 1 September 2023].

Kaliterna, J., Miliĉević, T. & Cvjetković, B. (2012) Grapevine trunk diseases associated with fungi from the *Diaporthaceae* family in Croatian vineyards. *Archives of Industrial Hygiene and Toxicology*, 63, 471-479.

Larach, A., Riquelme, N., Salinas, A., Rolshausen, P.E., Seeger, M. & Besoian, X. (2021) First Report of *Diaporthe ambigua* associated with dead arm disease on grapevine in Chile. *Plant Disease*, 106, 7, 1988.

Lawrence, D.P., Travadon, R. & Baumgartner, K. (2015) Diversity of *Diaporthe* species associated with wood cankers of fruit and nut crops in northern California. *Mycologia*, 107, 5, 926-940.

Lesuthu, P., Mostert, L., Spies, C.F.J., Moyo, P., Regnier, T. & Halleen, F. (2019). *Diaporthe nebulae* sp. nov. and first report of *D. cynaroidis*, *D. novem*, and *D. serafiniae* on grapevines in South Africa. *Plant Disease*, 103, 5, 808-817.

Makris, G., Solonos, S., Christodoulou, M., & Kanetis, L.I. (2022) First report of *Diaporthe foeniculina* associated with grapevine trunk diseases on *Vitis vinifera* in Cyprus. Plant Disease, 106, 4, 1294.

Manawasinghe, I.S., Dissanayake, A.J., Li, X., Liu, M., Wanasinghe, D.N., Xu, J. et al. (2019) High genetic diversity and species complexity of *Diaporthe* associated with grapevine dieback in China. *Frontiers in Microbiology,* 10, 1936, 1-28.

Mena, E., Stewart, S., Montesano, M. & Ponce de León, I. (2020) Soybean stem canker caused by *Diaporthe caulivora*; pathogen diversity, colonization process, and plant defense activation. *Frontiers in Plant Science*, 10, 1733, 1-21.

Mondello, V., Songy, A., Battiston, E., Pinto, C., Coppin, C., Trotel-Aziz, P., et al. (2018) Grapevine Trunk Diseases: a review of fifteen years of trials for their control with chemicals and biocontrol agents. *Plant Disease*, 102, 1189-1217.

Moschini, R.C., Rodríguez, M.J., Martínez, M.I. & Stewart, S. (2019) Weather-based predictive models for *Diaporthe helianthi* ascospore release in Uruguay. *Australasian Plant Pathology*, 48, 519-527.

Mostert, L., Crous, P.W., Kang, J., & Phillips, A.J.L. (2001). Species of *Phomopsis* and a *Libertella* sp. occurring on grapevines with specific reference to South Africa: morphological, cultural, molecular and pathological characterization. *Mycologia*, 93, 1, 146-167.

Nita, M., Ellis, M.A., Wilson, L.L. & Madden, L.V. (2006) Evaluation of a disease warning system for Phomopsis Cane and Leaf Spot of Grape: a field study. *Plant Disease,* 90, 9, 1239-1246.

O'Donnell, K. & Cigelnik, E. (1997) Two divergent intragenomic rDNA ITS2 types within a monophyletic lineage of the fungus Fusarium are nonorthologous. *Molecular Phylogenetics and Evolution*, 7, 103-116.

Rayner R.W. (1970) A Mycological Colour Chart. British Mycological Society and CAB International Mycological Institute, Kew, Surrey, UK.

Rossman, A.Y., Adams, G.C., Cannon, P.F., Castlebury, L.A., Crous, P.W., Gryzenhout, M., et al. (2015) Recommendations of generic names in Diaporthales competing for protection or use. *Ima Fungus*, 6, 1, 145-154.

Santos, L., Alves, A., & Alves, R. (2017) Evaluating multi-locus phylogenies for species boundaries determination in the genus *Diaporthe*. *PeerJ*, 5:e3120.

Sessa, L., Abreo, E., Betucci, L. & Lupo, S. (2017). Diversity and virulence of *Diaporthe* species associated with wood disease symptoms in deciduous fruit trees in Uruguay. Phytopathologia mediterranea, 56, 3, 431-444.

Udayanga, D., Castlebury, L.A., Rossman, A.Y. & Hyde, K.D. (2014) Species limits in *Diaporthe*: molecular re-assessment of *D. citri*, *D. cytosporella*, *D. foeniculina* and *D. rudis.* Persoonia, 32, 83-101.

Úrbez-Torres, J. R., Peduto, F., Smith, R. & Gubler, W. (2013) Phomopsis dieback: A grapevine trunk disease caused by *Phomopsis viticola* in California. *Plant Disease,* 97, 1571-1579.

Úrbez-Torres, J.R., Adams, P., Kamas, J. & Gubler, W.D. (2009) Identification, incidence and pathogenicity of fungal species associated with grapevine dieback in Texas. *American Journal of Enology and Viticulture*, 60, 4, 497-507.

Úrbez-Torres, J.R., Peduto, F., Striegler, R.K., Urrea-Romero, K.E., Rupe, J.C., Cartwright, R.D., et al. (2012) Characterization of fungal pathogens associated with grapevine trunk diseases in Arkansas and Missouri. *Fungal Diversity,* 52, 169-189.

White, T. J., Bruns, T. D., Lee, S. & Taylor, J. W. (1990) Amplification and direct sequencing of fungal ribosomal RNA genes for phylogenetics. In: PCR *Protocols: A guide to Methods and Applications* (M.A. Innes, D.H. Gelfand, J.J. Sninsky and T.J. White, ed.), Academic Press Inc., New York, NY, USA, 315-322.

DISCUSIÓN GENERAL

La complejidad y gravedad de las EM como limitante sanitaria del cultivo de la vid en el mundo se debe a múltiples razones. En primer lugar, constituyen un conjunto de enfermedades causadas por diversos hongos patógenos que suelen presentarse en simultáneo en una misma planta de cualquier edad. En segundo lugar, y salvo algunas excepciones, los síntomas que causan en el follaje se confunden, lo que dificulta su diagnóstico en el campo, sumado al hecho de que la manifestación de dichos síntomas ocurre cuando el daño interno en la madera ya está avanzado. En tercer lugar, las alternativas de control son mayoritariamente preventivas, una vez que los patógenos infectan y colonizan los tejidos leñosos, solo resta eliminar las partes afectadas o la planta entera. Esto se debe a que las medidas de manejo que pueden emplearse para curar las infecciones son prácticamente inexistentes. La única medida curativa es la termoterapia que puede utilizarse en materiales de propagación, aunque su eficacia ha sido cuestionada (Gramaje y Armengol, 2011). Por último, debido al sistema de propagación del cultivo, las plantas de vivero suelen ser una importante vía de diseminación de estas enfermedades, lo que implica que los nuevos viñedos establecidos ven comprometida su productividad y longevidad desde el comienzo (Mondello et al., 2018).

El presente trabajo constituye el primer abordaje exhaustivo de la problemática de EM en el proceso de propagación de plantas de vid en Uruguay. Durante el 2018 y 2019 se analizaron en total 2400 materiales provenientes de diferentes etapas del proceso de propagación, abarcando cinco variedades de portainjerto y ocho cultivares, procedentes del principal vivero vitícola del país. En este trabajo se constató que la mayoría de las plantas de vivero prontas para ser comercializadas tenían en su interior al menos uno de los síntomas típicos de EM (necrosis vascular, necrosis sectorial y/o necrosis en la base de la planta). La identificación de los hongos aislados, realizada en base a características morfológicas y al análisis filogenético de una única región génica (la más adecuada para cada grupo de patógenos según la bibliografía), permitió constatar la presencia de más de 20 especies de patógenos asociados a la Enfermedad de Petri (n = 4), Pie Negro (n = 7), Decaimiento por Botryosphaeria (n = 7) y Decaimiento por Diaporthe (n = 4) afectando las plantas de vivero producidas en el país. En base a la incidencia de los patógenos aislados, el 84,7% y 83,3% de las plantas analizadas en 2018 y 2019, respectivamente, estaban afectadas por al menos una EM. Estos resultados confirman que, al igual que en otras regiones vitícolas del mundo, el material de propagación local tiene un rol

preponderante como vía de diseminación de estos patógenos (Halleen et al., 2003; Aroca et al., 2006; Rego et al., 2009; Spagnolo et al., 2011; Carlucci et al., 2017; Pintos et al., 2018).

Por otra parte, se observó que la incidencia de las EM fue incrementándose en los materiales a medida que se avanzaba en el proceso de producción de plantas, lo cual sugiere que estos patógenos pueden infectar en diferentes momentos durante este proceso. Se constató que los materiales madre utilizados en la propagación, tanto de portainjertos como de variedades, presentaban en promedio una incidencia de síntomas de EM del 10%, y que, en base a los patógenos aislados, estaban afectados por Enfermedad de Petri, Decaimiento por Botryosphaeria y Decaimiento por Diaporthe. Tras la fase de hidratación de los materiales y salvo algunas excepciones, no se observó un incremento en la incidencia de síntomas, mientras que tras la fase de injertación y encallado de las plantas, se registró un aumento considerable tanto de síntomas (55% de incidencia de síntomas en promedio) como de patógenos aislados (73 patógenos aislados en 175 materiales procesados). No obstante, el mayor incremento tanto de síntomas como de patógenos aislados, se registró al analizar las plantas de vivero terminadas, es decir luego de la fase de enraizamiento en el suelo del vivero (casi 100% de incidencia de síntomas en promedio y 330 patógenos aislados en 158 materiales procesados). Si bien al final del proceso es esperable que lo que se observe sea el resultado de la acumulación de infecciones que pudieron darse en las etapas previas, el fuerte incremento registrado sugiere que la fase de enraizamiento en el suelo del vivero es una etapa clave en la que ocurren infecciones.

Luego de la fase de enraizamiento se registró un marcado incremento en la incidencia de la Enfermedad de Petri y se encontró por primera vez Pie Negro. Este resultado se explica porque los patógenos causantes de la Enfermedad de Petri, al igual que los patógenos causantes de Pie Negro, pueden sobrevivir en el suelo e infectar a través de heridas en la base de la planta (Mostert et al., 2006). Giménez-Jaime y colaboradores (2006) analizaron plantas de vivero en España y concluyeron que durante la fase de enraizamiento en el suelo pueden ocurrir importantes infecciones por los patógenos causantes de la Enfermedad de Petri. A esta conclusión llegaron al encontrar la presencia de la enfermedad en plantas luego de haber pasado la fase de enraizamiento y no en las etapas previas. Por el contrario, Fourie y Halleen (2004) en Sudáfrica compararon la sanidad de plantas enraizadas en suelo de vivero con la de plantas enraizadas en sustrato estéril y demostraron que el aumento de la incidencia de esta enfermedad en plantas luego

de la fase de enraizamiento se explica mayormente por el desarrollo de infecciones ocurridas en etapas previas que por infecciones ocurridas durante la fase de enraizamiento. Nuestros resultados sugieren que en las condiciones locales ocurren infecciones de Enfermedad de Petri durante todo el proceso de vivero, destacándose la fase de enraizamiento como la etapa más crítica para ello.

Con respecto al Pie Negro, la incidencia de esta enfermedad en plantas prontas fue de 15% a 60%, dependiendo del año de evaluación. La no detección de esta enfermedad en etapas previas a la fase de enraizamiento coincide con lo encontrado por investigadores en otras regiones como Portugal (Rego et al., 2001), Sudáfrica (Fourie y Halleen, 2002; Halleen et al., 2003) y España (Agustí-Brisach et al., 2013a). Los resultados obtenidos indican que los patógenos de Pie Negro infectan a las plantas durante el enraizamiento y que, por lo tanto, el suelo del vivero constituye la principal fuente de inóculo para estos patógenos (Rego et al., 2001; Halleen et al., 2006; Agustí-Brisach et al., 2013b, 2014; Berlanas et al., 2017).

La identificación realizada de los patógenos en base a observaciones de caracteres morfológicos (forma y color de las colonias y tipo de conidios) y al análisis filogenético de una única región génica, permitió tener una aproximación a las especies causantes de las EM en los materiales de vivero producidos en el país. No obstante, para conocer con precisión cuáles son las especies causantes de dichas enfermedades fue necesario incorporar el análisis de nuevas regiones génicas. Particularmente, en el caso de Pie Negro se procedió a realizar una caracterización de estos patógenos incluyendo el análisis filogenético de tres regiones génicas, factor de elongación 1-α, beta tubulina e histona (Cabral et al., 2012a; 2012b; Berlanas et al., 2020), además de una descripción detallada de caracteres morfológicos (largo y ancho de micro y macroconidios, presencia de clamidosporas), y la evaluación de la patogenicidad de todas las especies identificadas sobre el portainjerto Gravesac.

En dicha caracterización se incluyeron también aislados obtenidos de plantas prontas con síntomas internos de Pie Negro analizadas en el 2017, procedentes del mismo vivero, lo que dio lugar a una colección de 71 aislados en total. Se constató la presencia de cinco especies pertenecientes a los géneros *Dactylonectria* e *Ilyonectria* como causantes de la enfermedad. La especie encontrada de forma prevalente fue *D. macrodidyma* (n = 31), seguida de *D. novozelandica* (n = 14), *D. torresensis* (n = 10), *I. liriodendri* (n = 9) y *D. palmicola*. Los cuatro aislados restantes, si bien pertenecen al

género *Ilyonectria*, no se agruparon con ninguna especie conocida por lo que concluimos que debe tratarse de una nueva especie. Todas las especies identificadas, incluyendo *Ilyonectria* sp., fueron capaces de reducir la biomasa radicular del portainjerto Gravesac, comparado con el testigo sin inocular, y fueron re-aisladas con éxito confirmando así su patogenicidad.

Las especies *D. macrodidyma* e *I. liriodendri* ya habían sido asociadas al Pie Negro en numerosos países como Argentina (Longone et al., 2022), Brasil (dos Santos et al., 2014; Russi et al., 2010), Canadá (Petit et al., 2011; Úrbez-Torres et al., 2014), España (Alaniz et al., 2007), Portugal (Reis et al., 2013), Suiza (Casieri et al., 2009; Hofstetter et al., 2009), Turquía (Akgül et al., 2022) y Nueva Zelanda (Pathrose et al., 2014; Probst et al., 2019), e incluso ya habían sido encontradas como causantes de Pie Negro en Uruguay (Abreo et al., 2010). *Dactylonectria macrodidyma* no solo resultó ser la especie prevalente, sino que además fue la más virulenta en el ensayo de patogenicidad. Dicho resultado coincide con lo observado en China por Ye y colaboradores (2021) pero contrasta con lo encontrado en otros países como Argelia, España y Turquía, en los que, por ejemplo, *D. novozelandica* y *D. torresensis* fueron las que se comportaron como más agresivas (Aigoun-Mouhous et al., 2019; Berlanas et al., 2020; Akgül et al., 2022).

Dactylonectria novozelandica y *D. torresensis* también se han asociado al Pie Negro en varias regiones (Álvarez et al., 2012; Cabral et al., 2012b; Agustí-Brisach et al., 2013a; Reis et al., 2013; Úrbez-Torres et al., 2014; Carlucci et al., 2017; Aigoun-Mouhous et al., 2019; Ye et al., 2021; Akgül et al., 2022), siendo incluso esta última la especie prevalente en Argelia (Aigoun-Mouhous et al., 2019), España (Berlanas et al., 2017), Italia (Carlucci et al., 2017), Portugal (Reis et al., 2013) y Turquía (Akgül et al., 2022). Con respecto a *D. palmicola*, la especie fue descrita en Ecuador (Gordillo y Decock, 2017), y hasta lo que conocemos, el presente trabajo constituye el primer anuncio de ésta como agente causal del Pie Negro de la vid en el mundo.

Como se mencionó anteriormente, los patógenos causantes de Pie Negro forman parte de la comunidad fúngica que habita en el suelo. El ensayo de evaluación del efecto de diferentes niveles de riego, simulando situaciones de estrés hídrico severo, moderado y ausencia de estrés, sobre plantas del portainjerto SO4, permitió dilucidar que el contenido hídrico del suelo influye significativamente sobre la composición del microbioma fúngico, tanto del suelo como de la rizosfera y raíces de la vid. Se observó un marcado descenso de la diversidad fúngica en los tres compartimentos analizados

(suelo, rizosfera y raíz) en la condición de déficit hídrico severo. Previamente, Liu y Howell (2021) habían observado una fuerte correlación entre el estado hídrico del suelo y la composición del microbioma fúngico asociado al cultivo de la vid, lo cual, junto con lo observado en este trabajo, confirma que la condición hídrica del suelo, y por lo tanto de la planta, influye sobre la composición del microbioma asociado a la misma.

Es sabido que la sequía desencadena una serie de respuestas en las plantas, desde cambios en la morfología radicular a alteraciones metabólicas, que modifican el perfil de exudados radiculares, lo que probablemente influya sobre el microbioma asociado a las raíces y rizosfera (Santos-Medellín et al., 2017; Naylor et al., 2018; Liu y Howell, 2021). Bajo condiciones de sequía, la planta es capaz de atraer y favorecer el establecimiento de microorganismos que le ayudan a tolerar el estrés y continuar con su crecimiento y desarrollo (Marasco et al., 2012; Rolli et al., 2015). En este sentido, los resultados de este trabajo muestran un destacado enriquecimiento del género *Funneliformis,* Basidiomycete perteneciente a la familia Glomeraceae, taxón al cual pertenecen la mayoría de las micorrizas arbusculares asociadas a las vides silvestres y cultivadas (Schreiner y Mihara, 2009; Likar et al., 2013; Massa et al., 2020; Radić et al., 2021), en los compartimentos raíz y rizosfera en la condición de estrés severo. Las micorrizas arbusculares contribuyen con la nutrición y crecimiento de la planta mediante, por ejemplo, la mejora en la absorción de nutrientes y la tolerancia frente a factores de estrés, tanto bióticos como abióticos (Trouvelot et al., 2015). Los resultados obtenidos sugieren que en situaciones de estrés hídrico prologando es esperable que la asociación de la vid con micorrizas aumente. En este sentido, implementar prácticas de manejo del viñedo que contribuyan a conservar la biodiversidad de las micorrizas presentes en el suelo, será esencial para beneficiarse de los servicios ecosistémicos relativos al incremento de la tolerancia a la sequía que brindan las micorrizas a la vid.

Con respecto a los patógenos causantes de Pie Negro, los resultados obtenidos sugieren que la condición de déficit hídrico es desfavorable para estos patógenos. La abundancia relativa de "*Cylindrocarpon*", *Dactylonectria* y *Thelonectria* fue significativamente mayor en las condiciones de mejor irrigación (estrés moderado y ausencia de estrés), en comparación con la situación de déficit severo, en los tres compartimentos analizados. Estos resultados son consistentes con lo indicado en la bibliografía en cuanto a que suelos con alto contenido de humedad y mal drenaje son más favorables para estos patógenos (Halleen et al., 2006). De todas maneras, serán necesarios

estudios de largo plazo para evaluar si la menor presencia de estos patógenos detectada en la condición de déficit severo implica una reducción en la severidad e incidencia de la enfermedad en dicha condición.

Similar comportamiento presentó *Trichoderma*, quien fue más abundante en las condiciones de estrés moderado y ausencia de estrés hídrico, en comparación con la situación de déficit hídrico severo. Muchos trabajos han evaluado la eficacia de *Trichoderma* spp. como controlador biológico de los patógenos de Pie Negro, con resultados variables (Fourie et al., 2001; Berlanas et al., 2018; Berbegal et al., 2020; Martínez-Diz et al., 2021). Lo observado en este trabajo sugiere que sería conveniente evaluar su performance en escenarios de condiciones ambientales desafiantes, como situaciones de muy bajo contenido hídrico del suelo, ya que parecen ser desfavorables para su desarrollo.

Más allá de las observaciones realizadas sobre la variación de la composición de la comunidad fúngica según la condición hídrica del suelo, es importante tener en cuenta que muchos otros factores pueden influenciar la estructura del microbioma. Las características fisicoquímicas del suelo, el genotipo del portainjerto, el estadio fenológico de la planta y algunas prácticas de manejo como el laboreo se han identificado como factores que influyen significativamente sobre la diversidad del microbioma de la rizosfera de la vid (Vink et al., 2021; Zarraonaindia et al., 2015; Marasco et al., 2018; Berlanas et al., 2019; Liu y Howell, 2021). Por lo tanto, se necesitan más estudios que contemplen otros factores como tipos de suelos o diversos portainjertos, para obtener resultados concluyentes sobre cómo la sequía podría alterar la estructura del microbioma fúngico asociado a la vid, y cuáles serían las consecuencias de dichos cambios.

En referencia al Decaimiento por Diaporthe, los resultados obtenidos permitieron confirmar la hipótesis de que la enfermedad está presente en los viñedos comerciales de Uruguay. Se observaron síntomas de cancro y decaimiento general de la vid y se constató la presencia de *D. ampelina* asociada a dichos síntomas. No obstante, la incidencia observada de este patógeno como causante de los síntomas de decaimiento en los viñedos fue extremadamente baja, lo cual sugiere que la importancia de *Diaporthe* como organismo causante de cancros en vides adultas en Uruguay es aún insignificante.

La caracterización realizada de las especies de *Diaporthe* incluyó tanto a los aislados obtenidos de vides adultas como a los obtenidos previamente de los materiales

de vivero. Se configuró así una colección de 59 cepas en total. La identificación de estas cepas se realizó en base al análisis filogenético de tres regiones génicas, factor de elongación 1-α, beta tubulina e ITS (Santos et al., 2017; Lesuthu et al., 2019) y fue respaldada por la caracterización morfológica (largo y ancho de alfa y beta conidios, evaluación de crecimiento micelial a diferentes temperaturas). Se identificaron así cuatro especies de *Diaporthe,* siendo *D. ampelina* la especie encontrada de forma prevalente (n = 51), seguida por *D. foeniculina* (n = 5), *D. eres* (n = 2) y *D. terebinthifolii* (n= 1). Todas las especies fueron capaces de infectar al cultivar Cabernet Sauvignon generando lesiones necróticas en la madera, aunque el tamaño de las lesiones no siempre se diferenció del testigo, mientras que los porcentajes de re-aislamiento oscilaron entre el 14% y 100%.

Diaporthe ampelina, D. foeniculina y *D. eres* ya han sido asociadas a la vid en varias regiones vitícolas del mundo, incluyendo Norteamérica, Europa, Sudáfrica y China (Úrbez-Torres et al., 2009; Kaliterna et al., 2012; Baumgartner et al., 2013; Úrbez-Torres et al. 2013; Dissanayake et al., 2015; Lawrence et al., 2015, Guarnaccia et al., 2018, Lesuthu et al., 2019). En cuanto a la virulencia, *D. ampelina* se comportó como la especie más agresiva en los ensayos de patogenicidad realizados, lo cual coincide con lo encontrado en otros países (Kaliterna et al., 2012; Baumgartner et al., 2013; Úrbez-Torres et al., 2013; Lawrence et al., 2015; Lesuthu et al., 2019). Respecto a *D. foeniculina* y *D. eres*, los resultados de las pruebas de patogenicidad indican que se trata de patógenos débiles de la vid (generaron lesiones que apenas se diferenciaron del testigo), en concordancia con lo indicado previamente por Kaliterna et al. (2012), Úrbez-Torres et al. (2013), Baumgartner et al. (2013) y Lawrence et al. (2015). Con respecto a *D. terebinthifolii*, esta especie fue descrita por Gomes et al. (2013) en Brasil, y hasta nuestro conocimiento, nunca había sido asociada al cultivo de la vid. Si bien fue aislada a partir de material de vivero asintomático, los resultados de los ensayos de patogenicidad mostraron que es capaz de enfermar la vid ya que fue capaz de generar lesiones necróticas en la madera inoculada.

Diaporthe ampelina fue la única especie aislada tanto de plantas adultas con síntomas de cancro y de materiales de vivero, como del interior de sarmientos que mostraban síntomas externos de Excoriosis. La Excoriosis es una enfermedad de la vid asociada estrictamente a los tejidos verdes (hojas, pámpanos, bayas) también causada por *D. ampelina* (Nita et al., 2006). Si bien el Decaimiento por Diaporthe y la Excoriosis son enfermedades causadas por el mismo patógeno, la relación entre ambas no se conoce con

precisión. En este sentido, Baumgartner y colaboradores (2013) observaron una frecuente coocurrencia de ambas enfermedades en vides de Norteamérica, sugiriendo que los síntomas de cancros de la madera producto de la colonización del hongo son el resultado de infecciones iniciadas en los tejidos verdes. El hecho de haber encontrado en este trabajo a *D. ampelina* en el interior de sarmientos con síntomas externos de Excoriosis, sugiere que después de infectar los pámpanos y provocar los síntomas de Excoriosis, *D. ampelina* sería capaz de colonizar el interior del sarmiento y provocar necrosis de la madera.

Por último, si bien la incidencia observada de *Diaporthe* como agente causal de cancros y decaimiento de la vid en viñedos comerciales fue baja, la alta frecuencia con que fue aislada *D. ampelina* a partir de los materiales analizados es preocupante en tanto que demostró ser la especie más agresiva dentro del género. Por otra parte, independientemente de que los resultados de este trabajo sugieren que posiblemente *Diaporthe* colonice la madera a partir de las infecciones producidas sobre los pámpanos, son necesarios nuevos estudios para establecer con exactitud las estrategias de infección que utiliza este patógeno como agente causal del Decaimiento por Diaporthe. En otras regiones se ha comprobado que algunas especies de *Diaporthe* son capaces de infectar la madera a través de heridas de poda (Baumgartner et al., 2013). En este sentido, dilucidar cuáles son las vías de entrada utilizadas por este patógeno en las condiciones locales, permitirá comprender mejor la epidemiología de la enfermedad. Asimismo, evaluar otros aspectos como por ejemplo la susceptibilidad de diferentes cultivares o la eficacia de diferentes fungicidas, resulta esencial para diseñar un programa de manejo que permita prevenir la expansión de la enfermedad.

Para finalizar, este trabajo permitió actualizar el conocimiento sobre la situación sanitaria de la vid en el país con relación a las EM, poniendo el foco en la sanidad del material de vivero. Es un hecho que las plantas de vid producidas en el país están infectadas por patógenos causantes de las EM. También es sabido que los daños que provocan estas enfermedades suelen ser paulatinos, y que generalmente se acentúan cuando la planta está sometida a factores de estrés (Gramaje y Armengol, 2011). En este sentido, es conveniente monitorear el desarrollo de los nuevos viñedos para conocer el estatus sanitario que presentan en relación con las EM. Independientemente de esto, es prioritario comenzar a desarrollar un programa de manejo integrado para reducir la incidencia de estas enfermedades en los materiales de propagación. Quedó demostrado

que parte del material de partida con el que se producen las plantas ya está infectado y que durante el proceso de vivero ocurren nuevas infecciones. Renovar con mayor frecuencia los bloques de plantas madre, incorporar rotaciones en los suelos utilizados para la fase de enraizamiento, así como implementar la termoterapia en los materiales de propagación en alguna etapa del proceso, son algunas de las medidas de manejo que podrían evaluarse.

Una vez implantado el viñedo, los esfuerzos se deben enfocar en prevenir las infecciones que puedan tener lugar en el campo. Para esto, también es necesario diseñar y evaluar medidas de manejo como, por ejemplo, realizar la poda en diferentes momentos considerando las épocas de mayor probabilidad de diseminación de los patógenos en el campo y el uso de fungicidas para pintar los cortes de poda. La utilización de materiales de vivero con menores niveles de incidencia de EM, la implementación de medidas preventivas en el viñedo para evitar nuevas infecciones y el desarrollo de prácticas de manejo del viñedo que contribuyan a fomentar su crecimiento y desarrollo equilibrado, probablemente sean las claves para que la producción de uva siga siendo una actividad sostenible en el país.

CONCLUSIONES

- Las plantas de vid producidas en el país presentan altos niveles de incidencia de enfermedades de madera, por lo que constituyen una importante vía de diseminación de estos patógenos hacia los viñedos comerciales, comprometiendo su productividad y longevidad desde el inicio.
- La presencia de enfermedades de la madera en las plantas de vivero se origina parcialmente en el material madre utilizado y el resto en infecciones ocurridas durante el proceso de producción en el vivero. Por esto es necesario desarrollar un programa de manejo integrado que abarque todo el proceso de producción de las plantas, con el fin de producir plantas de mejor calidad sanitaria.
- En los materiales de propagación es posible encontrar Enfermedad de Petri, Pie Negro, Decaimiento por Botryosphaeria y Decaimiento por Diaporthe, causadas por más de 20 especies de patógenos
- Los patógenos causantes de Pie Negro, una de las principales enfermedades encontradas afectando plantas terminadas, infectan principalmente durante la fase de enraizamiento. Este hallazgo enfatiza la necesidad de priorizar estrategias de manejo enfocadas en dicha etapa, para disminuir la incidencia de esta enfermedad en plantas terminadas.
- Se demostró que el déficit hídrico en el suelo altera la composición del microbioma fúngico asociado a la raíz de la vid y que algunos microorganismos patógenos, como los causantes de Pie Negro, parecen ser desfavorecidos en dicha condición, mientras que lo opuesto ocurre con las micorrizas arbusculares. Estos hallazgos deben ser considerados en futuras investigaciones.
- El Decaimiento por Diaporthe, causado principalmente por *Diaporthe ampelina*, fue detectado en los viñedos nacionales con bajos niveles de incidencia, por lo que esta enfermedad es aún irrelevante en el país. Sin embargo, es conveniente monitorear su avance en las regiones vitícolas del país debido a que su presencia en los materiales de vivero está garantizando su diseminación.

REFERENCIAS BIBLIOGRÁFICAS

Abreo, E. 2011. Comunidad fúngica asociada a las enfermedades del tronco de la vid en Uruguay: composición, diagnóstico molecular y patogenicidad. PhD thesis, Montevideo, PEDECIBA Ciencias Biológicas, Universidad de la República.

Abreo, E., Martínez, S., Bettucci, L., Lupo, S. 2010. Morphological and molecular characterization of *Campylocarpon* and *Cylindrocarpon* spp. associated with black foot disease of grapevines in Uruguay. *Australasian Plant Pathology,* 39, 446-452.

Abreo, E., Martínez, S., Bettucci, L., Lupo, S. 2011. *Phaeomoniella chlamydospora* and *Phaeoacremonium* spp. in grapevines from Uruguay. *Phytopathologia Mediterranea,* 50, 77-85.

Abreo, E., Martínez, S., Bettucci, L., Lupo, S. 2013a. Characterization of *Botryosphaeriaceae* species associated with grapevines in Uruguay. *Australasian Plant Pathology,* 42, 241-249.

Abreo, E., Martínez, S., Navarrete, F., Betucci, L., Lupo, S. 2013b. Detección temprana de organismos causantes de las enfermedades del tronco de la vid. Proyecto FPTA-237. Serie 44 FPTA-INIA, 1-32. Instituto Nacional de Investigación Agropecuaria, Montevideo, Uruguay.

Agustí-Brisach, C., Armengol, J. 2013. Black-foot disease of grapevine: an update on taxonomy, epidemiology and management strategies. *Phytopathologya Mediterranea*, 52, 245-261.

Agustí-Brisach C., Gramaje D., León M., García-Jiménez J., Armengol J., 2011. Evaluation of vineyard weeds as potential hosts of black-foot and Petri disease pathogens. *Plant Disease*, 95, 803-810.

Agustí-Brisach, C., Gramaje, D., García-Jiménez, J., Armengol, J. 2013a. Detection of black-foot disease pathogens in the grapevine nursery propagation process in Spain. *European Journal of Plant Pathology*, 137, 103-112.

Agustí-Brisach, C., Gramaje, D., García-Jiménez, J., Armengol, J. 2013b. Detection of black-foot and Petri disease pathogens in soils of grapevine nurseries and vineyards using bait plants. *Plant Soil*, 364, 5-13.

Agustí-Brisach, C., Mostert, L., Armengol, J. 2014. Detection and quantification of *Ilyonectria* spp. associated with black-foot disease of grapevine in nursery soils using multiplex nested PCR and quantitative PCR. *Plant Pathology*, 63, 316-322.

Aigoun-Mouhous W., Elena G., Cabral A., León M., Sabaou N., Armengol, J., Chaouia, C., Mahamedi, A.E., Berraf-Tebbal, A. 2019. Characterization and pathogenicity of *Cylindrocarpon*-like asexual morphs associated with black foot disease in Algerian grapevine nurseries, with the description of *Pleiocarpon algeriense* sp. Nov. *European Journal of Plant Pathology*, 154, 887-901.

Akgül, D.S., Yıldız, M., Güngör Savaş, N., Bülbül, İ., Özarslandan, M., León, M., Armengol, J. 2022. Occurrence and diversity of black-foot pathogens on asymptomatic nursery-produced grapevines in Turkiye. *European Journal of Plant Pathology*, 164, 21-32.

Alaniz, S., León, M., Vicent, A., García-Jiménez, J., Abad-Campos, P., Armengol, J. 2007. Characterization of *Cylindrocarpon* species associated with black foot disease of grapevine in Spain. *Plant Disease*, 91, 1187-1193.

Álvarez, L.A., Tamayo, D., Castilla, C., Munive, J., Agustí-Brisach, C., Gramaje, D., Armengol J., 2012. Occurrence of grapevine trunk pathogens in nurseries and vineyards in the northern and southern coast of Peru. Abstracts of oral and poster presentations given at the *8th International Workshop on Grapevine Trunk Diseases*, Valencia, 18-21, June 2012. *Phytopathologia Mediterranea*, 51, 410-452.

Armengol, J. 2017. Enfermedades fúngicas de madera de la vid. Una visión general del problema. Enoviticultura, 46, 6-15.

Aroca, A., García-Figueres, F., Bracamonte, L., Luque, J., Raposos, R. 2006. A survey of trunk disease pathogens within rootstocks of grapevines in Spain. *European Journal of Plant Pathology*, 115, 195-202.

Baptista, M.B., Berreta, A. 2005. La temprana vitivinicultura en el Uruguay (1874-1930) ¿Tradición o Innovación? Tesis de Maestría, Facultad de Ciencias Sociales, Universidad de la República. Montevideo, Uruguay.

Barnard, R.L., Osborne, C.A., Firestone, M.K. 2013. Responses of soil bacterial and fungal communities to extreme desiccation and rewetting. *ISME Journal* 7, 2229-2241

Baumgartner, K., Fujiyoshi, P.T., Travadon, R., Castelbury, L.A., Wilcox, W.F., Rolshausen, P.E. 2013. Characterization of species of *Diaporthe* from wood cankers of grape in eastern North American vineyards. *Plant Disease*, 97, 912-920.

Berbegal, M., Ramón-Albalat, A., León, M., Armengol, J. 2020. Evaluation of long-term protection from nursery to vineyard pro-vided by *Trichoderma atroviride* SC1 against fungal grapevine trunk pathogens. Pest Management Science, 76, 967-977.

Berlanas, C., Andrés-Sodupe, M., López-Manzanares, B., Maldonado-González, M.M., Gramaje, D. 2018. Effect of white mustard cover crop residue, soil chemical fumigation and *Trichoderma* spp. root treatment on black-foot disease control in grapevine. *Pest Management Science*, 74, 2864-2873.

Berlanas, C., Berbegal, M., Elena, G., Laidani, M., Cibriain, J.F., Sagües, A., Gramaje, D. 2019. The fungal and bacterial rhizosphere microbiome associated with grapevine rootstock genotypes in mature and young vineyards. *Frontiers in Microbiology*, 10, 1142.

Berlanas, C., López-Manzanares, B., Gramaje, D. 2017. Estimation of viable propagules of black-foot disease pathogens in grapevine cultivated soils and their relation to production systems and soil properties. *Plant Soil*, 417, 467-479.

Berlanas, C., Ojeda, S., López-Manzanares, B., Andrés-Sodupe, M., Bujanda, R., Martínez-Diz, M. P., Díaz-Losada, E., Gramaje, D. 2020. Occurrence and diversity of black-foot disease fungi in symptomless grapevine nursery stock in Spain. *Plant Disease*, 104, 94-104.

Bertsch, C., Ramírez-Suero, M., Magnin-Robert, M., Larignon, P., Chong, J., Abou-Mansour, E., Spagnolo, A., Clément, C. Fontaine, F. 2013. Grapevine trunk diseases: complex and still poorly understood. *Plant Pathology*, 62, 243-265.

Bouasria, A., Mustafa, T., De Bello, F., Zinger, L., Lemperiere, G., Geremia, R.A., Choler, P., 2012. Changes in root-associated mi-crobial communities are determined by species-specific plant growth responses to stress and disturbance. *European Journal of Soil Biology*, 52, 59-66.

Bouskill, N.J., Lim, H.C., Borglin, S., Salve, R., Wood, T.E., Silver, W.L., Brodie, E.L. 2013. Pre-exposure to drought increases the resistance of tropical forest soil bacterial communities to extended drought. *ISME Journal*, 7, 384-394.

Bruez, E., Lecomte, P., Grosman, J., Doublet, B., Bertsch, C., Fontaine, F., Ugaglia, A., Teissedre, P.L., Da Costa, J.P., Guerin-Dubrana, L., Rey, P. 2013. Overview of grapevine trunk diseases in France in the 2000s. *Phytopathologia Mediterranea*, 52, 262-275.

Cabral, A., Groenewald, J.Z., Rego, C., Oliveira, H., Crous, P.W. 2012a. Cylindrocarpon root rot: multi-gene analysis reveals novel species within the *Ilyonectria radicicola* species complex. *Mycological Progress*, 11, 655-688.

Cabral, A., Rego, C., Nascimento, T., Oliveira, H., Johannes, Z., Crous, P.W. 2012b. Multi-gene analysis and morphology reveal novel Ilyonectria species associated with black foot disease of grapevines. *Fungal Biology*, 116, 62-80.

Carlucci, A., Lops, F., Mostert, L., Halleen, F., Raimondo, M. 2017. Occurrence fungi causing black foot on young grapevines and nursery rootstock plants in Italy. *Phytopathologia Mediterranea*, 56, 10-39.

Casieri, L., Hofstetter, V., Viret, O., Gindro, K., 2009. Fungal communities living in the wood of different cultivars of young *Vitis vinifera* plants. *Phytopathologia Mediterranea*, 48, 73-83.

Chaverri, P., Salgado, C., Hirooka, Y., Rossman, A.Y., Samuels, G. J. 2011. Delimitation of *Neonectria* and *Cylindrocarpon* (Nectriceae, Hypocreales, Ascomycota) and related genera *Cylindrocarpon*-like anamorphs. *Studies in Mycology*, 68, 57-78.

De la Fuente, M., Fontaine, F., Gramaje, D., Armengol, J., Smart, R., Nagy, Z.A., Borgo, M., Rego, C., Corio-Costet, M.F. 2016. Grapevine trunk diseases. A Review. OIV publications. 25 pp.

Dissanayake, A.J., Liu, M., Zhang, W., Chen, Z., Udayanga, D., Chukeatirote. Li, X., Yan, J., Hyde, K.D. 2015. Morphological and molecular characterisation of *Diaporthe* species associated with grapevine trunk disease in China. *Fungal Biology*, 119, 5, 283-294.

dos Santos, R.F., Blume, E., Muniz, M.F.B., Heckler, L.I., Finger, G., Maciel, C.G., Harakawa, R., Garrido L.R., 2014. First report of *Ilyonectria macrodidyma* associated with black foot disease of grapevine in Brazil. *Plant Disease*, 98, 156-156

Fourie, P.H., and Halleen, F. 2002. Investigation on the occurrence of *Phaeomoniella chlamydospora* in canes of rootstock mother vines. *Australasian Plant Pathology*, 31, 425-426.

Fourie, P.H., Halleen, F. 2004. Proactive control of Petri disease of grapevine through treatment of propagation material. *Plant Disease*, 88, 1241-1245.

Fourie, P.H., Halleen, F., van der Vyver, J., Schreuder, W. 2001. Effect of *Trichoderma* treatments on the occurrence of decline pathogens in the roots and rootstocks of nursery grapevines. *Phytopathologia Mediterranea*, 40, S473-S478.

Fuchslueger, L., Bahn, M., Hasibeder, R., Kienzl, S., Fritz, K., Schmitt, M., Watzka, M., Richter, A. 2016. Drought history affects grassland plant and microbial carbon turnover during and after a subsequent drought event. *Journal of Ecology*, 104, 1453-1465.

Giménez-Jaime, J., Aroca A., Raposo, R., García-Jiménez, J., Armengol, J. 2006. Occurrence of fungal pathogens associated with grapevine nurseries and the decline of young vines in Spain. *Journal of Phytopathology*, 154, 598-602.

Gomes, R.R., Glienke, C., Videira, S.I.R., Lombard, L., Groenewald, J.Z., Crous, P.W. 2013. *Diaporthe*: a genus of endophytic, saprobic and plant pathogenic fungi. *Persoonia*, 31, 1-41.

Gordillo, A., Decock, C. 2017. *Cylindrocarpon*-like (Ascomycota, Hypocreales) species from the Amazonian rain forests in Ecuador: additions to *Campylocarpon* and *Dactylonectria*. *Cryptogamie, Mycologie*, 38, 409-434.

Gramaje, D., Armengol, J. 2011. Fungal trunk pathogens in the grapevine propagation process: potential inoculum sources, detection, identification, and management strategies. *Plant Disease*, 95, 1040-1055.

Gramaje, D., Úrbez-Torres, J.R., Sosnowski, M. 2018. Managing grapevine trunk diseases with respect to etiology and epidemiology: current strategies and future prospects. *Plant Disease*, 102, 12-39.

Guarnaccia, V., Groenewald, J.Z., Woodhall, J., Armengol, J., Cinelli I.T., Eichmeier, A. Ezra, D., Fontaine, F., Gramaje, D., Gutierrez-Aguirregabiria, A., Kaliterna, J., Kiss, L., Larignon, P., Luque, J., Mugnai, L., Naor, V., Raposo, R., Sándor, E., Váczy, K.Z., Crous, P.W. 2018. *Diaphorte* diversity and pathogenicity revealed from a broad survey of grapevine diseases in Europe. *Persoonia* 40, 135-153.

Halleen, F., Crous, P.W., Petrini, O. 2003. Fungi associated with healthy grapevine cuttings in nurseries, with special reference to pathogens involved in the decline of young vines. *Australasian Plant Pathology*, 32, 47-52.

Halleen, F., Fourie, P.H., Crous, P.W. 2006. A review of black foot disease of grapevine. *Phytopathologia Mediterranea*, 45, 55-67.

Halleen, F., Mostert, L., Crous, P.W. 2007. Pathogenicity testing of lesser-known vascular fungi of grapevines. *Australasian Plant Pathology*, 36, 277-285.

Halleen, F., Schoroers, H., Groenewald, J., Crous, P. 2004. Novels species of *Cylindrocarpon* (Neonectria) and *Campylocarpon* gen. nov. associated with black-foot disease of grapevines (*Vitis* spp.). *Studies in Mycology*, 50, 431-455.

Hofstetter, V., Casieri, L., Viret, O., Gindro, K., 2009. Esca de la vigne et communauté fongique. *Revue Suisse de Viticulture, Arboriculture, Horticulture*, 41, 247-253.

INAVI. 2022. Estadísticas de viñedos 2022, datos nacionales. Instituto Nacional de Vitivinicultura (INAVI), Departamento Registro de Viñedos. Disponible en: https://www.inavi.com.uy/uploads/vinedo/e114169ff8dd5bd2a83547b5a8c60636eb4aebcc.pdf

Kaliterna, J., Miličević, T., Cvjetković, B. 2012. Grapevine trunk diseases associated with fungi from the *Diaporthaceae* family in Croatian vineyards. *Archives of Industrial Hygiene and Toxicology*, 63, 471-479.

Larignon, P., Spagnolo, A.; Bertsch, C., Fontaine, F. 2015. First report of young grapevine decline caused by *Neofusicoccum parvum* in France. *Plant Disease*, 99, 1859.

Lawrence, D.P., Travadon, R., Baumgartner, K. 2015. Diversity of *Diaporthe* species associated with wood cankers of fruit and nut crops in northern California. *Mycologia*, 107, 5, 926-940.

Lesuthu, P., Mostert, L., Spies, C.F.J., Moyo, P., Regnier, T., Halleen, F. 2019. *Diaporthe nebulae* sp. nov. and first report of *D. cynaroidis*, *D. novem*, and *D. serafiniae* on grapevines in South Africa. *Plant Disease*, 103, 5, 808-817.

Likar, M., Hančević, K., Radić, T., Regvar, M. 2013. Distribution and diversity of arbuscular mycorrhizal fungi in grapevines from production vineyards along the eastern Adriatic coast. *Mycorrhiza*, 23, 209-219.

Liu, D., Howell, K. 2021. Community succession of the grapevine fungal microbiome in the annual growth cycle. *Environmental Microbiology*, 23, 1842-1857.

Lombard, L., Van der Merwe, N.A., Groenewald, J.Z., Crous, P.W. 2014. Lineages in Nectriaceae: Re-evaluating the generic status of *Ilyonectria* and allied genera. *Phytopathologia Mediterranea*, 53, 515-532.

Longone, V., Escoriaza, G., Paolinelli, M., Gramaje, D., 2022. First report of *Dactylonectria alcacerensis*, *Dactylonectria macrodidyma*, and *Ilyonectria liriodendri* associated with black foot disease of grapevine in Argentina. *Plant Disease*, 106, 1996.

Lovisolo, C., Perrone, I., Carra, A., Ferrandino, A., Flexas, J., Medrano, H., Schubert, A. 2010. Drought-induced changes in development and function of grapevine (*Vitis* spp.) organs and in their hydraulic and non-hydraulic interactions at the whole-plant level: a physiological and molecular update. *Functional Plant Biology*, 37, 98-116

Luque, J., García-Figueres, F., Legorburu, F.J., Muruamendiaraz, A., Armengol, J., Trouillas, F. 2012. Species of Diatrypaceae associated with grapevine trunk diseases in Eastern Spain. *Phytopathologia Mediterranea*, 51, 528-540.

Maldonado-González, M.M., Martínez-Diz, M.P., Andrés-Sodupe, M., Bujanda, R., Díaz-Losada, E., Gramaje, D. 2020. Quantification of *Cadophora luteo-olivacea* from grapevine nursery stock and vineyard soil using droplet digital PCR. *Plant Disease*, 104, 2269-2274.

Marasco, R., Rolli, E.; Ettoumi, B., Vigani, G., Mapelli, F., Borin, S., Abou-Hadid, A.F., El-Behairy, U.A., Sorlini, C., Cherif, A., Zocchi, G., Daffonchio, D. 2012. A drought resistance-promoting microbiome is selected by root system under desert farming. *PLoS One*, 7, e48479.

Marasco, R., Rolli, E., Fusi, M., Michoud, G., Daffonchio, D. 2018. Grapevine rootstocks shape underground bacterial microbiome and networking but not potential functionality. *Microbiome*, 6, 3.

Martin, M.T., Cobos, R. 2007. ldentification of fungi associated with grapevine decline in Castilla y León (Spain). *Phytopathologia Mediterranea*, 46, 18-25.

Martínez-Diz, M.P., Díaz-Losada, E., Andrés-Sodupe, M., Bujanda, R., Maldonado-González, M.M., Ojeda, S., Yacoub, A., Rey, P., Gramaje, D. 2021. Field evaluation of

biocontrol agents against black-foot and Petri diseases of grapevine. *Pest Management Science*, 77, 697-708.

Massa, N., Bona, E., Novello, G., Todeschini, L., Boatti, F., Mignone, E., Gamalero, G., Lingua, G., Berta, G., Cesaro, P. 2020. AMF communities associated to *Vitis vinifera* in an Italian vineyard subjected to integrated pest management at two different phenological stages. *Scientific Reports*, 10, 9197.

MGAP. 2023. Anuario estadístico agropecuario 2023. Ministerio de Ganadería, Agricultura y Pesca. Estadísticas agropecuarias. Disponible en: https://descargas.mgap.gub.uy/DIEA/Anuarios/Anuario2023/ANUARIO2023WEB.pdf

Mondello, V., Songy, A., Battiston, E., Pinto, C., Coppin, C., Trotel-Aziz, P., Clément, C., Mugnai, L., Fontaine, F. 2018. Grapevine Trunk Diseases: a review of fifteen years of trials for their control with chemicals and biocontrol agents. *Plant Disease*, 102, 1189-1217.

Moreno-Sanz, P., Lucchetta, G., Zanzotto, A., Loureiro, M.D., Suarez, B., Angelini, E. 2013. Fungi associated to grapevine trunk diseases in young plants in Asturias (Northern Spain). *Horticultural Science*, 40, 138-144.

Mostert, L., Halleen, F., Fourie, P., Crous, P.W. 2006. A review of *Phaeoacremonium* species involved in Petri disease and esca of grapevines. *Phytopathologia Mediterranea*, 45, 12-29.

Mugnai, L., Graniti, A., Surico, G. 1999. Esca (black measles) and brown wood-streaking: two old and elusive disease of grapevine. *Plant Disease*, 83, 404-418.

Naylor, D., DeGraaf, S., Purdom, E., Coleman-Derr, D. 2017. Drought and host selection influence bacterial community dynamics in the grass root microbiome. *ISME Journal* 11, 2691-2704

Naylor, D., Coleman-Derr, D. 2018. Drought stress and root-associated bacterial communities. *Frontiers in Plant Science*, 8, 2223.

Nita, M., Ellis, M.A., Wilson, L.L., Madden, L.V. 2006. Evaluation of a disease warning system for Phomopsis Cane and Leaf Spot of Grape: a field study. *Plant Disease,* 90, 9, 1239-1246.

Pathrose, B., Jones, E.E., Jaspers, M.V., Ridgway, H.J. 2014. High genotypic and virulence diversity in *Ilyonectria liriodendri* isolates associated with black foot disease in New Zealand vineyards. *Plant Pathology,* 63, 613-624.

Petit E., Barriault E., Baumgartner K., Wilcox W., Rolshausen P., 2011. *Cylindrocarpon* species associated with black-foot of grapevine in Northeastern United States and Southeastern Canada. *American Journal of Enology and Viticulture*, 62, 177-183.

Pintos, C., Redondo, V., Costas, D., Aguín, O., Mansilla, P. 2018. Fungi associated with grapevine trunk diseases in nursery-produced *Vitis vinifera* plants. *Phytopathologia Mediterranea*, 57, 407-424.

Probst, C.M., Ridgway, H.J., Jaspers, M.V., Jones, E.E. 2019. Pathogenicity of *Ilyonectria liriodendri* and *Dactylonectria macrodidyma* propagules in grapevines. *European Journal of Plant Pathology*, 154, 405-421.

Radić, T., Likar, M., Hančević, K., Regvar, M., Čarija, M., Zdunić, G. 2021. Root-associated community composition and co-occurrence patterns of fungi in wild grapevine. *Fungal Ecology*, 50, 101034.

Rego, C., Carvalho, A., Nascimento, T., Oliveira, H. 2001. First approach on the understanding of inoculum sources of *Cylindrocarpon destructans* and *Phaeomoniella chlamydospora* concerning grapevine rootstocks in Portugal. *IOBC wprs Bulletin*, 24, 67-72.

Rego, C., Nascimento, T., Cabral A., Silva, M.J., Oliveira, H. 2009. Control of grapevine wood fungi in commercial nurseries. *Phytopathologia Mediterranea*, 48, 128-135.

Reis, P., Cabral, A., Nascimento, T., Oliveira, H., Rego, C. 2013. Diversity of *Ilyonectria* species in a young vineyard affected by black foot disease. *Phytopathologia Mediterranea*, 52, 335-346.

Rolli, E., Marasco, R., Vigani, G., Ettoumi, B., Mapelli, F., Deangelis, M.L., Gandolfi, C., Casati, E., Previtali, F., Gerbino, R., Pierotti Cei, F., Borin, S., Sorlini, C., Zocchi, G., Daffonchio, D. 2015. Improved plant resistance to drought is promoted by the root-associated microbiome as a water stress-dependent trait. *Environmental Microbiology*, 17, 316-331.

Russi A., Nalin R., Dequigiovanni G., Gava R., Quecini V., Garrido, L.R., Ritschel P. 2010. Study of the genetic variability of Brazilian populations of *Cylindrocarpon* spp., causal agent of grapevine black foot. Abstracts of oral and poster presentations given at the 7th International Workshop on Grapevine Trunk Diseases, Santa Cruz, Chile, 17–21 January 2010. *Phytopathologia Mediterranea*, 49, 103-133.

Santillán, D., Iglesias, A., La Jeunesse, I., Garrote, L., Sotes, V. 2019. Vineyards in transition: A global assessment of the adaptation needs of grape producing regions under climate change. *Science of the Total Environment*, 657, 839-852.

Santos-Medellín, C., Edwards, J., Liechty, Z., Nguyen, B., Sundaresan V. 2017. Drought stress results in a compartment-specific restructuring of the rice root-associated microbiomes. *mBio*, 8, e00764-17.

Santos, L., Alves, A., Alves, R. 2017. Evaluating multi-locus phylogenies for species boundaries determination in the genus Diaporthe. *PeerJ*, 5, e3120.

Schreiner, R.P., Mihara, K.L. 2009. The diversity of arbuscular mycorrhizal fungi amplified from grapevine roots (*Vitis vinifera* L.) in Oregon vineyards is seasonally stable and influenced by soil and vine age. *Mycologia*, 101, 599-611.

Spagnolo, A., Marchi, G., Peduto, F., Phillips, A.J.L., Surico, G. 2011. Detection of Botryosphaeriaceae species within grapevine woody tissues by nested PCR, with particular emphasis on the *Neofusicoccum parvum*/*N. ribis* complex. *European Journal of Plant Pathology*, 129, 485-500.

Trivedi, P., Leach, J.E., Tringe, S.G., Sa, T., Singh, B.K. 2020. Plant-microbiome interactions: from community assembly to plant health. *Nature Reviews Microbiology*, 18, 607-621.

Trouvelot, S., Bonneau, L., Redecker, D., van Tuinen, D., Adrian, M., Wipf, D. 2015. Arbuscular mycorrhiza symbiosis in viticulture: a review. *Agronomy for Sustainable Development*, 35, 1449-1467.

Úrbez-Torres, J.R., Adams, P., Kamas, J., Gubler, W.D. 2009. Identification, incidence and pathogenicity of fungal species associated with grapevine dieback in Texas. *American Journal of Enology and Viticulture*, 60, 4, 497-507.

Úrbez-Torres, J.R., Haag, P., Bowen, P., O'Gorman, D.T. 2014. Grapevine trunk diseases in British Columbia: Incidence and characterization of the fungal pathogens associated with esca and Petri diseases of grapevine. *Plant Disease*, 98, 469-482.

Úrbez-Torres, J.R., Leavitt, G.M., Voegel, T.M., Gubler, W.D. 2006. Identification and distribution of *Botryosphaeria* spp. associated with grapevine cankers in California. *Plant Disease*, 90, 1490-1503.

Úrbez-Torres, J.R., Peduto, F., Smith, R., Gubler, W. 2013. Phomopsis dieback: A grapevine trunk disease caused by *Phomopsis viticola* in California. *Plant Disease*, 97, 1571-1579.

Vink, S.N., Chrysargyris, A., Tzortzakis, N., Falcão Salles, J. 2021. Bacterial community dynamics varies with soil management and irrigation practices in grapevines (*Vitis vinifera* L.). *Applied Soil Ecology*, 158, 103807.

Whitelaw-Weckert, M.A., Rahman, L., Appleby, L.M., Hall, A., Clark, A.C., Waite, H., Hardie, W.J. 2013. Co-infection by Botryosphaeriaceae and *Ilyonectria* spp. fungi during propagation causes decline of young grafted grapevines. *Plant Pathology*, 62, 1226-1237.

Ye, Q., Zhang, W., Jia, J., Li, X., Zhou, Y., Han, C., Wu, X., Yan, J. 2021. Fungal pathogens associated with black foot of grapevine in China. *Phytopathologia Mediterranea*, 60, 303-319.

Zarraonaindia, I., Owens, S.M., Weisenhorn, P., West, K., Hampton-Marcell, J., Lax, S., Bokulich, N.A., Mills, D.A., Martin, G., Taghavi, S., van der Lelie, D., Gilbert, J.A. 2015. The soil microbiome influences grapevine-associated microbiota. *mBio*, 6, e02527-14.